Alpha-Glucan, Water Dikinase and the Control of Starch Degradation in *Arabidopsis thaliana* Leaves

Alastair William Skeffington

A thesis submitted to the University of East Anglia for the degree of Doctor of Philosophy

John Innes Centre
Norwich
September 2012

Abstract

This thesis examines the role of alpha-glucan, water dikinase (GWD) in the control of starch degradation in *Arabidopsis thaliana* leaves. Starch is degraded at night in Arabidopsis leaves to provide carbon for metabolism and growth. The rate of starch degradation is constant through the night and is precisely regulated such that starch reserves last until dawn. Despite the importance of this regulation for normal plant growth, we do not know which enzymes of the pathway are regulated to modulate flux.

In this work I focus on the first enzyme in the starch degradation pathway, GWD. This enzyme phosphorylates the starch granule surface, thereby stimulating starch degradation by hydrolytic enzymes. It is hypothesised that GWD is important for the control of starch degradation. *GWD* shows large diel oscillations in transcript abundance. The enzyme is redox responsive *in vitro*, and is phosphorylated and SUMOylated *in vivo*.

My work revealed that GWD protein levels are essentially invariant over the diel cycle. Studying plants in which *GWD* transcript was targeted by inducible RNAi and rapidly decreased to low levels revealed that GWD has half life of 2 days and a very low flux control coefficient for starch degradation. Taken together these findings demonstrate that large diel oscillations in GWD transcript abundance are not important for the daily control of starch degradation. Using transgenic plants in which native GWD was replaced with mutant forms of the enzyme, I demonstrate that redox responsive properties and certain SUMOylation and phosphorylation sites of GWD are not of *in vivo* relevance for appropriately timed starch degradation. Finally, I identify a previously unknown role for GWD in starch synthesis and find ROC4 to be a novel, putative GWD interaction partner.

Acknowledgements

First, a massive thank you to my supervisor, Professor Alison Smith, for her constant enthusiasm: making starch (even more) exciting, for attentive supervision and for staying engaged through the more difficult times, before the projects began to bear fruit.

I am grateful to the other members of my supervisory committee, Professor Caroline Dean and Professor Martin Howard for their invaluable advice and direction. I would also like to thank Professor Caroline Dean and Professor Phillip Poole for hosting me in their labs during the rotation year of my PhD. Both rotations were wonderful experiences from which I learnt a lot. Also thanks to Professor Nick Brewin, for his incredible dedication to making the rotation programme as valuable an experience as possible.

Dr Sean Murray and Dr Richard Morris kindly gave their time to discuss the more quantitative aspects of this thesis. Their advice was indispensible.

I am indebted to Professor Sam Zeeman and Professor Wilhelm Gruissem (ETH, Zurich) for allowing me to work in their labs for a month. While I was there I received help from many people, but would especially like to thank Dr Oliver Kötting, David Seung and Leonie Luginbühl for making me so welcome.

Of course, it has been the people I have shared the lab with who have really made the experience over the past three years. In particular, I would like to express my admiration for Dr Marilyn Pike, who posses superhuman patience and irrepressible good cheer. Many thanks also to Doreen Feike, Dr Sam Mugford, Dr Vasilios Andriotis, Dr Cristina Pignocchi, Dr Alistair McCormick, Brendan Fahy, Dr Matilda Crumpton-Taylor, Dr Christian Ruzanski, Dr Sylviane Comparot-Moss, Dr Paul Barratt and Dr Thomas Howard for their help and advice and for making the lab a lovely place to work. Special thanks go to Dr Alex Graf, without whom much of my PhD would not have been possible.

The John Innes Centre has been a great place to be a student, and that is down to the people I have shared my time with while here. In particular I would like to thank Ruth

Bryant, Simon Lloyd, Philippa Borrill as well all the people I have shared 101 City Road with, for their friendship and many happy times.

Where would I be without my friends from Cambridge: Natscis and Notscis? Few are privileged to have such a wonderful and close group of friends. Collectively and individually you have been a constant source of strength and joy and I look forward to many more wonderful times together.

The last year has not always been easy, and to a large extent I owe my sanity to Wiebke Apel. Thank you so much for your incredible friendship, love and support. I have so many treasured memories of our time together already, and I know we have more wonderful times ahead of us.

Finally, but most importantly, I have my family to thank for everything: for their encouragement and support through so many years of education, for their companionship, love and good humour.

Table of Contents

List of Figures

List of Tables

Abbreviations

ΔG	Change in Gibbs free energy
2-CysPrx	2-Cystein peroxiredoxin
3-PGA	3-Phosphoglycerate
ADP	Adenosine diphosphoate
AGPase	ADP-glucose pyrophosphorylase
AMP	Adenosine monophosphate
AtGWD	Arabidopsis alpha-glucan, water dikinase
ATP	Adenosine triphosphate
BAM	Beta-amylase
BE	Branching enzyme
CAH	Carbonic anhydrase
CBM	Carbohydrate binding module
CCA1	Circadian clock-associate 1
cDNA	Complementary DNA
CER	Controlled environment room
Col-0	Columbia-0
dex	dexamethasone
DPE	Disproportionating enzyme
DTT	Dithiothreitol
EDTA	Ethylenediaminetetraacetic acid
EOD	End of day
EON	End of night
ER	Endoplasmic reticulum
ESD4	Early in short day 4
ev	Empty vector
F6P	Fructose 6-phosphate
Fd	Ferredoxin
FNR	Frerredoxin-$NADP^+$ reductase
FTR	Ferredoxin-thioredoxin reductase
G6P	Glucose 6-phsophate
GFP	Green fluoresent protein
GO	Gene ontology
GWD	Alpha-glucan, water dikinase
HEPES	4-(2-hydroxyethyl)-1-piperazineethanesulfonic acid
HFT	Main dichroic beamsplitter
His	Histidine
HPAEC-PAD	High performance anion exchange chromatography with pulsed ampiometric detection
IMAC	Immobilised metal affinity chromatography
ISA	Isoamylase
LB	Lysogeny broth
LC	Liquid chromatography
LDA	Limit dextrinase
LHY1	Late elongated hypocotyl
LSF	Like starch excess four
LTQ-orbitrap	Linear trap quadrupole orbitrap
m/z	Mass/charge
MALDI-TOF	Matrix assisted laser desorption ionisation time of flight
MBP	Maltose binding protein
MES	2-(N-morpholino)ethanesulfonic acid
MEX	Maltose excess
MOPS	3-(N-morpholino)propanesulfonic acid

mRNA	Messenger RNA
MS	Mass spectrometry
MWCO	Molecular weight cut off
NAD+	Nicotinamide adenine dinucleotide (oxidised)
NADH	Nicotinamide adenine dinucleotide (reduced)
NADP+	Nicotinamide adenine dinucleotide phosphate (oxidised)
NADPH	Nicotinamide adenine dinucleotide phosphate (reduced)
NADP-MDH	NADP-dependent malate dehydrogenase
NCBI	National center for biotechnology information
NFT	Secondary dichroic beamsplitter
NMR	Nuclear magnetic resonance
NR	Nitrate reductase
NTRC	NADPH-thioredoxin reductase
OPPP	Oxidative pentose phosphate pathway
PAGE	Polyacrylamide gel electrophoresis
PCNA	Proliferating Cell Nuclear Antigen
PCR	Polymerase chain reaction
PGI	Phosphoglucoisomerase
PHS	Alpha-glucan phosphorylase
PVP	Polyvinylpyrrolidone
PWD	Phosphoglucan, water dikinase
SAE	SUMO-specific E1 activating enzyme
SAT1	Serine acetyl-transferase
SBD	Starch binding domain
SBE	Starch branching enzyme
SDS	Sodium dodecyl sulfate
SEX	Starch excess
SnRK1	Sucrose non-fermenting related kinase 1
SOC	Super optimal broth
SS	Starch synthase
StGWD	*S. tuberosum* alpha-glucan, water dikinase
SUMO	Small ubiquitin like modifier
T6P	Trehalose 6-phosphate
TFA	Trifluoroacetic acid
TPT	Triose phosphate translocator
Trx	Thioredoxin
ULP	Ubiquitin like protease
UTR	Untranslated region
v/v	Volume/volume
w/v	Weight/volume

1 Introduction

1.1 Starch and plant growth

This thesis considers the role of α-glucan, water dikinase in the control of starch degradation in the leaves of *Arabidopsis thaliana*. Starch is the second most abundant carbohydrate on the planet after cellulose and is the major carbohydrate of nutritional importance in the world's staple crops. Most plants accumulate starch as a carbon and energy store at some point in their life cycle, providing reserves which are mobilised when primary photoassimilate is unavailable. For example, endosperm starch in the seeds of cereals is consumed for growth while the photosynthetic tissues are developing. Similarly, starch in tubers, rhizomes and turions provides the carbon required for the regeneration of vegetative tissue after a period of dormancy. This occurs in plants as diverse as *Erica* species in the South African fynbos, regenerating after fire, and the duckweed *Spirodela polyrhiza* in British ponds, regenerating after winter (Ley *et al.*, 1997; Verdaguer and Ojeda, 2002).

Another time at which primary photosynthate is not available is at night. This means that plants must partition some of the carbon assimilated in the day into storage reserves which are mobilised during the subsequent night to support continued metabolism and growth. In many grasses these reserves are provided by sucrose and fructans which accumulate in leaf cell vacuoles (Schnyder, 1993). However, in most vascular plant and green algae species studied, starch constitutes the major leaf storage carbohydrate. Such starch reserves, which accumulate in the chloroplasts of photosynthetic cells during the day prior to mobilisation at night, are known as transitory starch.

The partitioning of assimilated carbon between growth and storage varies depending on the time of day and the external conditions, so a knowledge of leaf starch metabolism is fundamental to our understanding of plant growth (Smith and Stitt, 2007). The role of leaf starch is best understood in the reference organism, Arabidopsis. In controlled growth conditions, Arabidopsis accumulates starch in a linear manner during the day, and by dusk starch makes about 1% of the fresh weight of a leaf. At night, the plant degrades starch, again in a linear manner, such that around 95% of the reserves have been used by dawn. Mutants of Arabidopsis unable to synthesise starch, such as mutants

in phosphoglucomutase (PGM), and ADP-glucose pyrophosphorylase (AGPase), display much reduced growth (Lin *et al.*, 1988; Caspar *et al.*, 1991). Likewise, mutants that cannot properly degrade their starch at night also show pronounced retardation of growth. For example mutants which lack glucan water dikinase, an enzyme essential for starch degradation, contain 40-100 fold more starch at the end of the night than wildtype plants (Niittylä *et al.*, 2006; Kötting *et al.*, 2009) and are severely compromised in growth (Yu *et al.*, 2001). In fact, amongst starch-related mutants, the more starch an Arabidopsis plant retains at the end of the night, the lower its growth rate tends to be (Gebert, L. Smith lab, unpublished data). This relationship extends to wildtype plants. Cross *et al.* (2006) found a highly significant negative correlation between end-of-night starch and biomass in a set of Arabidopsis accessions collected from various parts of Europe (Figure1.1 A). It seems that some accessions grew conservatively, not using all their stored assimilate for growth and metabolism at night, while others grew less conservatively and used all their reserves by dawn.

Starch degradation rates in Arabidopsis are adjusted with exquisite precision depending on the environmental conditions. This ensures efficient use of carbohydrate reserves and makes certain that supplies do not run out before dawn. For example, if plants are subject to sudden changes in night length, starch degradation rates are rapidly adjusted, a phenomenon first described by Lu *et al.* (2005), and later studied by Graf *et al.* (2010). In one experiment, Arabidopsis plants were grown from seed in 12 h light, 12 h dark cycles, and then subject to an unexpected, early night 4 h earlier than usual. Remarkably, starch degradation then proceeded at a much slower rate than the previous night, such that the rate of degradation was still linear and around 95% of reserves were still used by dawn (Figure1.1 B). If degradation had occurred at the same rate as the previous night, starch would have run out four hours before dawn.

The consequences of running out of starch before dawn can be simulated by subjecting plants to an extended night, in which the lights are not switched on at dawn as normal (Figure1.1 C and D). Arabidopsis plants subject to this condition show depleted sugars and a rapid cessation of root growth in under two hours after the anticipated dawn (Usadel *et al.*, 2008; Yazdanbakhsh *et al.*, 2011). Growth does not recover until several hours after return to the light (Smith and Stitt, 2007). Addition of exogenous sucrose greatly slows the decline in root growth during the extended night, indicating that a

carbon shortage is at least partly responsible for growth cessation (Yazdanbakhsh *et al.*, 2011). Plants grown in an extended night also display massive transcriptional reprogramming, including repression of genes involved in anabolic processes such as starch synthesis and nitrate and sulphur assimilation and the upregulation of genes responsible for the catabolism of amino acids, nucleotides and phospholipids (Thimm *et al.*, 2004; Usadel *et al.*, 2008). After 24 h in the dark, there are increases in amino acids, consistent with the catabolism of proteins (Usadel *et al.*, 2008). Thus plants which run out of starch reserves before dawn are likely to starve and stop growing.

The metabolic state of a wildtype plant after an extended night reflects the situation every night in starchless mutants such as *pgm*. Sugars fall to extremely low levels in *pgm* every night (Gibon *et al.*, 2004b; Bläsing *et al.*, 2005), similar to wildtype in an extended night. Transcriptional reprogramming is also qualitatively similar, with an downregulation of genes involved in anabolic processes and an upregulation of genes involved in catabolic processes as described above (Thimm *et al.*, 2004). Thus *pgm* appears to starve every night, and this probably results in the greatly reduced night-time leaf and root extension growth rates observed in this mutant (Wiese *et al.*, 2007; Yazdanbakhsh and Fisahn, 2010; Pantin *et al.*, 2011).

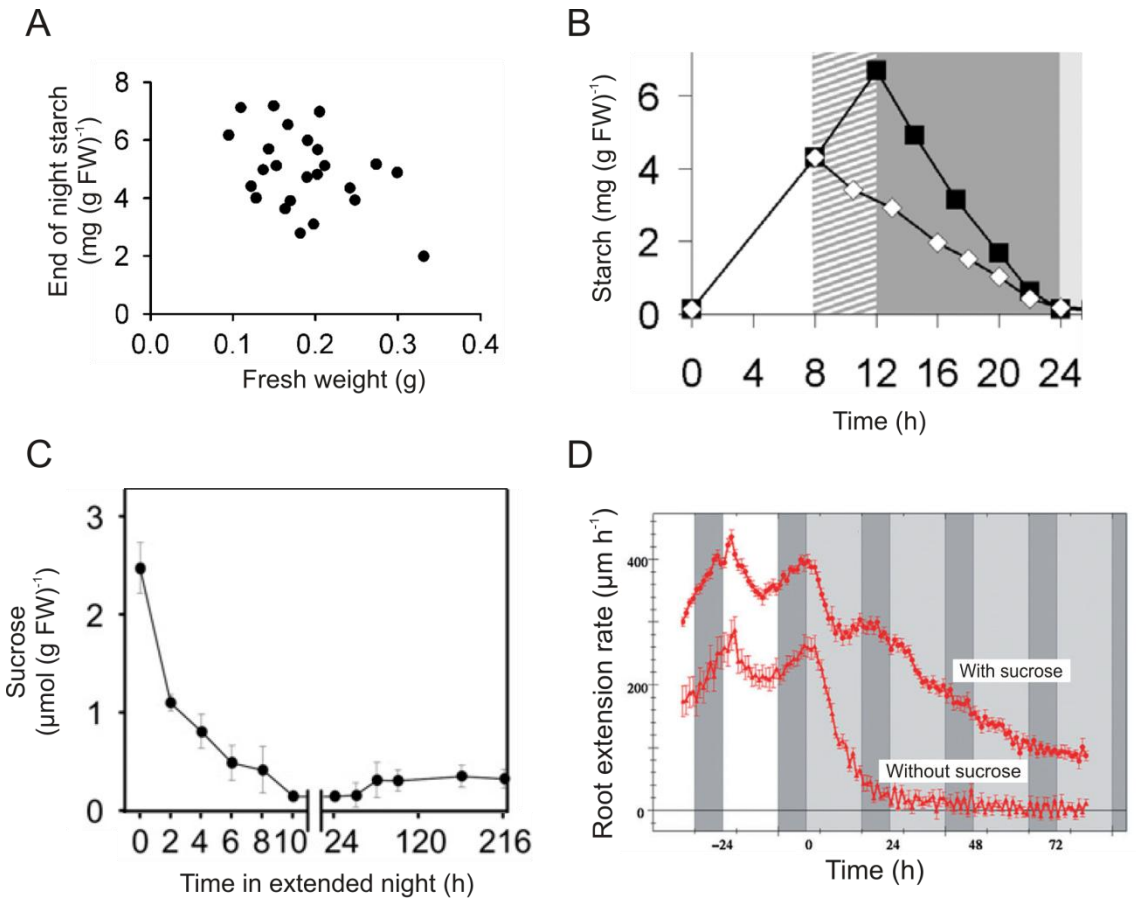

Figure1: Starch degradation and growth. **A** Correlation between end of night starch levels and fresh weight in a set of Arabidopsis accessions. Adapted from Cross *et al.* (2009). **B** Diel starch turnover in a 12 h light, 12 h dark diel cycle (black squares) or in the first night after transfer to an 8 h light, 16 h dark cycle (white diamonds). White background, day; grey background, night; striped background, additional dark period in early night. Modified from Graf *et al.* (2010) **C** Sucrose levels in an extended night. Modified from Usadel *et al.* (2008). **D** Root extension growth in an extended night in the presence and absence of sucrose. White background, day; dark grey background, night; light grey background, subjective day in extended night. Modified from Yazdanbakhsh *et al.* (2011).

The experiments described above combine to suggest that there are mechanisms in an Arabidopsis plant which integrate information about the amount of starch and the time remaining until dawn and set an appropriate degradation rate. These mechanisms ensure that the plant does not run out of starch before dawn and are therefore crucial for normal growth. As I will describe in section 1.4.2.1, we have some knowledge of how the time until dawn is measured, but no idea about how the enzymes of starch degradation are regulated to effect changes in the rate of degradation. This thesis aims to begin to

address this gap in our knowledge with a focused study on the first enzyme of the starch degradation pathway, α-glucan, water dikinase (GWD), which catalyses the phosphorylation of the granule surface. In the remainder of this introduction, I first describe the structure of starch, the enzymes responsible for its synthesis and how these enzymes are regulated. Next I examine our knowledge of the enzymes of starch degradation, with a particular focus on the role of GWD and granule phosphorylation. Subsequently, I discuss in detail the evidence that starch degradation is tightly regulated and summarise the properties of the enzymes of degradation which might be relevant to that regulation. Finally, I conclude that GWD is a good candidate for an enzyme which is regulated to control flux through the pathway, and outline my experimental approach.

1.2 The synthesis of the starch granule

Starch granules are used as a transient carbohydrate store throughout the Archaeplastida (the land plants, red and green algae and the glaucophytes) (Ball *et al.*, 2011). The insoluble semi-crystalline starch granule represents an efficient means of storing carbohydrate while not affecting the water potential of a cell or sub-cellular compartment. In the Chloroplastida starch always accumulates in the plastids, while in other lineages such as the Rhodophyta and the Glaucophyta it accumulates in the cytosol (Ball *et al.*, 2011). Some lineages which evolved through secondary endosymbiosis of the Rhodopyta, such as the dinoflagellates and apicomplexan parasites, have also retained the machinery to synthesise starch granules. Starch is not found beyond the AH/SAR clade of the eukaryotes, although one group of cyanobacteria produces a long chain polyglucan which may be related to amylopectin (Nakamura *et al.*, 2005).

1.2.1 Starch structure

Although starch granules from different species and tissues exhibit a wide variety of shapes and sizes and differ in physical properties, the chemistry underlying granule structure is conserved. Starch is made of two distinct types of glucan polymer. The more abundant polymer is amylopectin, which consists of many short α-1,4 bonded glucan chains linked through α-1,6 branch points (Figure1.2 A). These α-1,6 linkages form 5 – 6% of the glycosidic bonds in amylopectin. The less abundant polymer is

amylose, also an α-1,4 linked glucan, but containing very few branch points (Buléon *et al.*, 1998).

There is good evidence that amylopectin is responsible for the higher order glucan structures which ultimately form the starch granule. The *waxy* mutants of wheat, maize, sorghum, barley and rice lack amylose but retain starch granules of normal appearance in their storage organs (Jeon *et al.*, 2010). The same is true for the *lam* mutants of pea (Denyer *et al.*, 1995) and the *amf* mutants of potato (van der Leij *et al.*, 1991). Indeed, Arabidopsis and rice leaf starch granules only contain 6% and 4% amylose respectively (Taira *et al.*, 1991; Zeeman *et al.*, 2002) compared to 20 - 30% amylose for many cereal storage starches (Buléon *et al.*, 1998). Not all leaf starches contain such low levels of amylose as Arabidopsis. Both tobacco and cotton leaves accumulate leaf starch with 15 – 20% amylose (Chang, 1979; Matheson, 1996), although these starch reserves accumulate through development, so are not entirely comparable with Arabidopsis transitory starch.

Amylopectin crystallises to rigid structures which form the building blocks of a starch granule. X-ray diffraction studies of storage starch have identified the repeating unit cell as chains of 12 glucose residues that form two left handed, parallel double helices (Figure1.2 B). These double helices may crystallise in either an open, hexagonal lattice (B-type starch) or a denser monoclinic lattice (A-type starch) (Imberty *et al.*, 1988; Imberty and Perez, 1988). Diffraction studies of Arabidopsis starch indicates that it is largely organised in a B-type structure (Delvalle *et al.*, 2005; Wattebled *et al.*, 2008). Amylose can also crystallise to A and B type structures *in vitro* (Buléon *et al.*, 1998), but is thought to form single helices *in vivo* (Zeeman *et al.*, 2010). The distribution of amylose in a granule has been defined in corn and potato starches using reagents which cross-link glucan molecules if they are less than 0.4 nm apart (Jane *et al.*, 1992). Amylopectin became highly cross linked, consistent with a dense, crystalline structure. Very little cross linking between amylose molecules was observed, but there was some cross-linking of amylose and amylopectin. These results suggest firstly that amylose is more amorphous than amylopectin and secondly, that amylose molecules are not clustered, but are distributed throughout the amylopectin of the starch granule.

At a larger scale, detailed analysis of the acid hydrolysis products of potato starch provide strong support for a side-chain cluster model for amylopectin (Figure1.2 C) (Robin *et al.*, 1974; Thompson, 2000). In this model, a few long glucan chains are punctuated by clusters of shorter branches, resulting in the bimodal distribution of amylopectin chain lengths which is commonly observed (Hanashiro *et al.*, 1996). Clusters of the tightly packed double helices (described above) tend to align to form crystalline lamellae, while regions high in branch points make up amorphous lamellae. Differences in this organisation seem to correlate with the emergence of an A-type or a B-type crystalline structure. A-type structures tend to have more short side chains, with branch points occurring both in the crystalline and the amorphous layers. In contrast B-type structures contain longer average chain lengths and most branch points occur in the more amorphous layers (Hizukuri, 1985; Jane *et al.*, 1997). The deduced space taken by the crystalline and amorphous layers matches the scale of periodic variations in electron density within the starch (Jenkins *et al.*, 1993; Oostergetel and Vanbruggen, 1993). The repeating unit of the density variations consists of a 5-6 nm, dense (more crystalline) layer and a 3-4 nm, less dense (more amorphous) layer. The resultant 9 nm repeat is highly conserved across storage starches from different species (Jenkins *et al.*, 1993). The above model assumes that amylopectin chains are largely arranged perpendicular to the granule surface. This is corroborated by the fact that starch granules are optically anisotropic and display birefringence consistent with such a radial organisation of amylopectin chains (French, 1984).

Higher order structures are also thought to form within the starch granules. These include an 18 nm wide amylopectin superhelix with a 10 nm pitch, identified through electron tomography and electron diffraction (Figure1.2 D) (Oostergetel and Vanbruggen, 1993). The pitch height of the structure could also potentially relate to the 9 nm periodicity of electron density. At a larger scale still, starch granules contain concentric growth rings observable by light microscopy which appear to represent alternating semi-crystalline and amorphous layers with periodicities of hundreds of nm (Figure1.2 E). Individual layers become visible by scanning electron microscopy after partial acid hydrolysis or α-amylolysis of the granule (Buttrose, 1960; Pilling and Smith, 2003). The altering crystalline and amorphous lamellae associated with the 9 nm repeat are found within the semi-crystalline layers. Electron microscopy of granules after partial α-amylolysis and atomic force microscopy of sectioned starch granules

reveals near-spherical ‘blocklets’ (Figure1.2 F). (Gallant *et al.*, 1997; Ridout *et al.*, 2002). These vary in size between about 20 and 500 nm in diameter and may form layers of larger and smaller blocklets. Precisely how the different higher order structures relate to one another is unclear.

Many of the structures discussed above are observed in the Arabidopsis leaf starch granule. Small angle X-ray scattering data confirm the presence of the 9 nm repeat, and birefringence data the radial orientation of the amylopectin molecules (Zeeman *et al.*, 2002). Diffraction data also indicate that Arabidopsis starch posses a B-type organisation, with helices arranged in a monoclinic lattice (Delvalle *et al.*, 2005; Wattebled *et al.*, 2008). Wildtype Arabidopsis starch granules are thin and disc-like: 1 – 2 μm in diameter and 0.2 – 0.5 μm thick (Figure1.2 G) (Zeeman *et al.*, 2002). Growth rings cannot be observed in fractured wildtype granules but can be seen in the thicker, more spherical granules which accumulate in the *starch excess 4* mutant. In this case, each growth ring is similar in thickness to a wildtype starch granule.

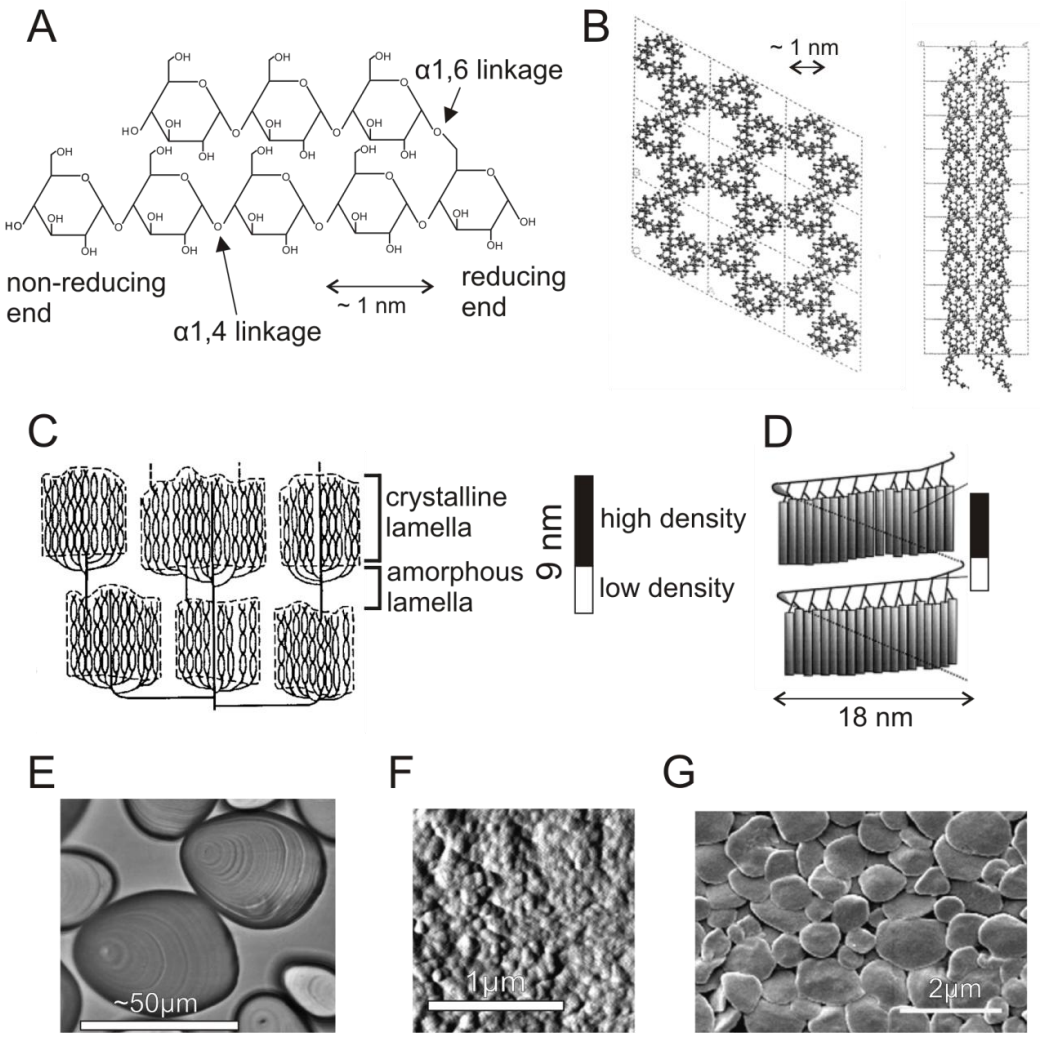

Figure1.2: Levels of organisation within a starch granule. **A** Part of an amylopectin chain showing α-1,4 and α-1,6 linkages. **B** The crystalline organisation of B type starch showing the (001) (left) and the (110) (right) planes. Amylopectin double helices pack in a hexagonal manner. Dotted quadrilaterals show the unit cell. Modified from Waigh *et al.* (2000) **C** Side chain cluster model of amylopectin structure showing amorphous and crystalline lamellae which are thought to correspond to the 9 nm variations in electron density. Modified from Myers *et al.* (2000) **D** Amylopectin superhelix, also hypothesised to relate to 9 nm variations in electron density. Modified from Waigh *et al.* (2000) **E** Optical micrograph of whole potato starch granules showing growth rings. From Ridout *et al.* (2002) **F** Atomic force microscopy image of a sectioned maize starch granule provides evidence for blocklet organisation. From Ridout *et al.* (2002) **G** Scanning electron micrograph of Arabidopsis starch granules isolated at the end of a 12 hour photoperiod. Note the flattened, discoid shape. From Zeeman *et al.* (2002).

The only covalent modifications of starch are phosphate esters which may be present at the C3 and the C6 position of glucose residues within the amylopectin portion of the granule (Blennow and Engelsen, 2010). Starches from tubers and leaves tend to contain much more phosphate than those from cereal grains. The quantity of C6 phosphate esters ranges from undetectable levels in barley grain starches, to more than 1 G6P per 100 glucose residues in the tubers of certain potato varieties (Blennow *et al.*, 2000b) and double that amount in *Curcuma zedoaria* root starch (Blennow *et al.*, 2000a). C3 phosphate is generally much less abundant than C6 phosphate. High phosphate potato starches contain about one C6 phosphate ester per 300 glucose residues. Arabidopsis leaf starch contains only about 1 C6 phosphate ester for every 2000 glucose residues and about 5 times more C6 phosphate than C3 phosphate (Yu *et al.*, 2001; Ritte *et al.*, 2006; Haebel *et al.*, 2008).

In potato starches, phosphate esters have been found to be enriched in the more amorphous components of the amylopectin (Muhrbeck *et al.*, 1991; Blennow *et al.*, 2000a). It has also been found that longer chain amylopectin molecules tend to contain more phosphate esters (Blennow *et al.*, 2005b; Wischmann *et al.*, 2005). The phosphorylation of starch has structural consequences that affect important industrial properties such as gel elasticity and viscosity (Blennow *et al.*, 2005b). The physiological importance of starch phosphorylation and the nature of the enzymes responsible for phosphorylation are explored further in section 1.3.

1.2.2 The enzymes of starch synthesis in chloroplasts

The substrate for starch synthesis in chloroplasts is ADP-glucose, derived from fructose 6-phosphate, a Calvin-Benson cycle intermediate, via glucose 6-phosphate and glucose-1-phosphate in reactions catalysed by phosphoglucoisomerase (PGI), phosphoglucomutase (PGM) and ADP-glucose pyrophosphorylase (AGPase). Loss of any of these enzymes essentially abolishes leaf starch synthesis (Smith, 2012). The conversion of glucose 1-phosphate to ADP-glucose is the first committed step in starch synthesis and is made irreversible by the action of plastidial alkaline pyrophosphorylase which hydrolyses the pyrophosphate (PPi) produced by AGPase to Pi (Lin *et al.*, 1988; Stitt and Zeeman, 2012). AGPase is a heteromeric enzyme consisting of two large

subunits and two small subunits, encoded by four (*APL1-APL4*) and two genes (*APS1*, also known as *ADG1* and *APS2*) respectively in Arabidopsis (Haedrich *et al.*, 2012). APS2 is expressed at very low levels and has no detectable catalytic activity *in vitro* (Crevillén *et al.*, 2003; Crevillén *et al.*, 2005).

The *pgi*, *pgm*, and *adg1* mutants of Arabidopsis are nearly, but not quite, starchless (Streb *et al.*, 2009). The residual starch in these mutants (1-3 % of wildtype), combined with a report that AGP-glucose levels are normal in mutants lacking PGM and AGPase, led to the suggestion that ADP-glucose might be produced in the cytosol by sucrose synthase (SuSy) and imported into the chloroplast as a major pathway of starch synthesis in leaves (Munoz *et al.*, 2005). This seems unlikely for several reasons. First, new data are reported to show that ADP-glucose levels are indeed decreased in the leaves of *pgm* relative to wildtype, contradicting the original study (Stitt and Zeeman, 2012). Second, Arabidopsis plants completely lacking SuSy activity in leaf mesophyll cells have normal starch metabolism (Barratt *et al.*, 2009). Third, import of glucose-1-phosphate into the chloroplast (Fettke *et al.*, 2011) could explain the small amount of starch in the *pgi* and *pgm* mutants, while residual AGPase activity, provided by remaining AGPase subunits, could explain the starch in the *adg1* mutant.

Amylopectin is synthesised from ADP-glucose through the action of starch synthases, starch branching enzymes and debranching enzymes. The requirement for these activities is highly conserved, although the dominant isoforms vary with the tissue and the species (Smith, 2012). Below I focus primarily on the enzymes required to synthesise transitory starch in Arabidopsis. The starch synthases involved in amylopectin biosynthesis fall into four classes, which are conserved across taxa (Patron and Keeling, 2005). They act by transferring glucose units from the ADP-glucose donor to the non-reducing ends of the growing α-1,4 linked glucan chain. A large amount of the starch synthase (SS) activity in Arabidopsis leaves is provided by SSI, thought to elongate the shortest chains, but significant contributions are also made by SSII and SSIII which seem to elongate medium and longer chains respectively (Delvalle *et al.*, 2005; Zhang *et al.*, 2008; Szydlowski *et al.*, 2009; Szydlowski *et al.*, 2011).

Starch branching enzymes (BEs) cleave an α-1,4 glucan chain at an internal linkage before forming a new linkage at the C6 position on another glucan chain, thereby

creating a branch point (Zeeman *et al.*, 2010). In Arabidopsis, BE2 and BE3 provide most of the branching enzyme activity and the *be1be2* mutant is starchless. This double mutant also accumulates maltose to high levels in a manner dependent on the presence of AGPase, suggesting that the reason for the lack of starch is that unbranched chains produced by starch synthases are hydrolysed by degradative enzymes as they are produced.

Perhaps counterintuitively, debranching enzymes are also important for the synthesis of starch granules. Debranching enzymes in plants fall into two classes, the isoamylases (ISAs) and the limit dextrinases or pullulanases (LDAs) which have different substrate preferences. The Arabidopsis genome contains four isoamylase genes: *ISA1*, *ISA2*, *ISA3* and *LDA1*. ISA1 and the catalytically inactive ISA2 form a heteromeric enzyme in Arabidopsis leaves, potato leaves and rice endosperm (Hussain *et al.*, 2003; Delatte *et al.*, 2005; Utsumi and Nakamura, 2006), although in rice an ISA1 homomer may be more important than the heteromer (Utsumi *et al.*, 2011). Loss of ISA1 in Arabidopsis results in the accumulation of a highly branched, soluble carbohydrate known as phytoglycogen and a low starch phenotype. Both the *isa2* mutant and the *isa1*/*isa2* mutants show the same phenotype as *isa1*. This is consistent with ISA1 and ISA2 being constituents of the same enzyme (Delatte *et al.*, 2005). Loss of ISA3 in Arabidopsis results in a starch excess phenotype, suggesting that it primarily acts in starch degradation rather than starch synthesis (Wattebled *et al.*, 2005). However, loss of ISA3 in the *isa1* background causes a reduction in starch content relative to *isa1* single mutant, suggesting that ISA3 may contribute a little to starch synthesis (Wattebled *et al.*, 2008). The *lda1* single mutant has normal starch levels and turnover but causes a decrease in starch content in the *isa1*/*isa2*/*isa3* background relative to the triple mutant (Streb *et al.*, 2008).

Analysis of the quadruple branching enzyme mutant *isa1*/*isa2*/*isa3*/*lda1* has shed light on why debranching activities are required for starch synthesis. The quadruple debranching mutant has no starch at all (Streb *et al.*, 2008), supporting the hypothesis that branching activities are necessary to remove 'incorrectly' positioned branches to allow the proper crystallisation of amylopectin. Unexpectedly however, loss of the only chloroplast localised α-amylase, AMY3, in the *isa1*/*isa2*/*isa3*/*lda1* background partially restores starch granule synthesis (Streb *et al.*, 2008). This demonstrates that

debranching activities are not directly necessary for granule synthesis. Instead, it indicates that the branched glucans produced in the *isa1*/*isa2*/*isa3*/*lda1* background are simply degraded by amylolytic activities before they can crystallise. Thus, in the wildtype plant, it seems likely that debranching activities are necessary for rapid and ordered crystallisation of the amylopectin helices before amylolytic activities can begin to degrade the newly synthesised chains.

There is good evidence that starch is phosphorylated during synthesis. Isolated amyloplasts from potato supplied with ^{33}P-labelled glucose-6-phosphate incorporate radioactivity into starch (Wischmann *et al.*, 1999). The same occurs in potato tuber discs, and conditions which prevent starch synthesis also prevent ^{33}P incorporation (Nielsen *et al.*, 1994). When ^{32}P orthophosphate is added to suspension cultures of *Chlamydomonas reinhardtii* in the light, radioactivity is incorporated into starch (Ritte *et al.*, 2004). After a chase period with unlabelled orthophosphate, the amount incorporated plateaus. This implies that starch phosphate is not turned over in the light. The significance of starch phosphorylation for the process of starch synthesis is entirely unknown, although the physical properties of the granule important for industrial processes differ depending on the degree of phosphorylation (Zeeman *et al.*, 2010).

Amylose is synthesised from ADP-glucose through the action of granule bound starch synthase (GBSS). Unlike the other starch synthases, GBSS operates only within the granule matrix and elongates glucan chains in a processive manner. In addition to its role in amylose production, GBSS may be partly responsible for the elongation of very long amylopectin chains (Zeeman *et al.*, 2010).

The number of starch granules in Arabidopsis chloroplasts is remarkably constant per unit chloroplast volume (Crumpton-Taylor *et al.*, 2012). The number of granules also remains relatively constant though the diel cycle, suggesting that starch accumulates during the day through increases in the size of pre-existing granules, rather than the initiation of new granules. However, as cells grow, chloroplasts divide and stromal volume increases, new starch granules must be initiated. The control of starch granule initiation and starch granule number is not well understood. Clues may however be provided by analysis of a mutant of Arabidopsis lacking starch synthase 4 (the *ssiv* mutant). This mutant has apparently no reduction in total starch synthase activity, but

has an average of only one starch granule per chloroplast, compared with about 5 to 6 in wildtype (Roldan *et al.*, 2007; Szydlowski *et al.*, 2009; Crumpton-Taylor *et al.*, 2012). However granule initiation can clearly still occur in the absence of SSIV, even if the number of initiation events is much reduced. The *ssiv*/*ssiii* double mutant in contrast contains no detectable starch (Szydlowski *et al.*, 2009), thus the presence of either SSIV or SSIII activity is a prerequisite for granule formation.

The links between SSIV and starch granule initiation have been strengthened by studies in the green alga, *Ostreococcus tauri.* Electron micrographs indicate that starch granules are cleaved during cell division such that one daughter granule is retained within each of the daughter cells (Ral *et al.*, 2004). Thus in this organism there is no need for a granule initiation system beyond the establishment of an ancestral granule. Intriguingly, *SSIV* has been lost from the *O. tauri* genome. Thus, there is a correlation between the presence of SSIV and the need for starch granule initiation.

Starch granule initiation must occur through the production of glucan precursors on which the starch synthases can act. It is not clear how this might happen in plants. In yeasts and mammals a protein called glycogenin is required for the priming of glycogen synthesis. This protein self glucosylates to produce a short glucan chain which can then be extended by glycogen synthases (Lomako *et al.*, 1988; Roach *et al.*, 2012). However there is no good evidence for such a self glucosylating protein in plants (D'Hulst and Merida, 2010). It has been reported that SSIII will synthesise glucans from ADP-glucose in the absence of any primer, but no other SSs have been shown to do this. The fact that starch metabolism is normal in the SSIII mutant (Szydlowski *et al.*, 2009) implies that the self-priming activity of this protein is not required for starch granule initiation.

ISA1 may also be involved in starch granule initiation. Arabidopsis plants lacking ISA1 display increased numbers of smaller granules relative to wildtype, and the same effect is observed in equivalent mutants of several species (Zeeman *et al.*, 1998; Zeeman *et al.*, 2010). This phenotype could be a secondary effect of the mutation, but may well tell us more about granule initiation if studied further.

The pathway of starch synthesis in leaves is summarised in Figure1.3.

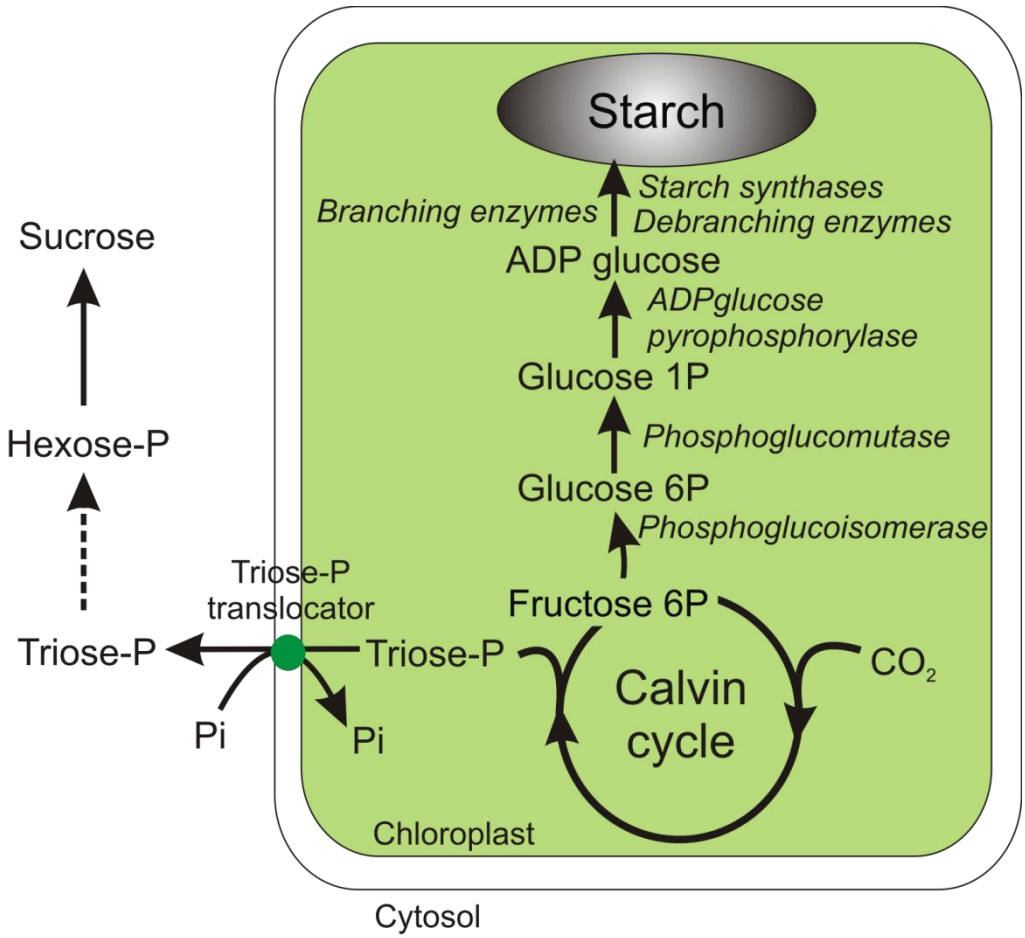

Figure1.3: The pathway of starch synthesis in the Arabidopsis leaf. During the day starch is synthesised from the Calvin cycle intermediate fructose 6-phosphate. Sucrose is synthesised in the cytosol from triose phosphate exported from the chloroplast. P, phosphate; Pi, inorganic phosphate.

1.2.3 The control of starch synthesis

It has become clear that leaf starch does not accumulate simply as a carbon 'overflow' when the supply of photosynthate exceeds demand. Rather, starch synthesis is a highly regulated process which is adjusted to ensure there is sufficient carbon to last the expected length of the night. In general, the shorter the photoperiod the higher the rate of starch synthesis, consistent with the requirement for more starch to provide carbon and energy in the longer nights. The trend of enhanced partitioning of assimilate into storage carbohydrates in short photoperiods is found in leaves many species including pangola, spinach, soybean, maize, sugarbeet, wheat and Arabidopsis (Chatterton and Silvius, 1979; Chatterton and Silvius, 1980; Sicher *et al.*, 1982; Gibon *et al.*, 2004b; Lu *et al.*, 2005; Gibon *et al.*, 2009). As described previously, mutants that are unable to

make or mobilise starch are compromised in growth, as are plants which run out of starch before the end of the night (Lin *et al.*, 1988; Caspar *et al.*, 1991; Graf *et al.*, 2010; Yazdanbakhsh *et al.*, 2011). Thus the control of the partitioning of starch is crucial for normal patterns of diel growth.

In Arabidopsis leaves, a substantial degree of control of starch synthesis resides in AGPase. The flux control coefficient of AGPase with respect to starch synthesis is 0.64 under saturating light conditions for photosynthesis and 0.2 to 0.3 under low light conditions (Neuhaus and Stitt, 1990; Haedrich *et al.*, 2011). AGPase is known to have many regulatory properties. In particular, the enzyme is redox responsive: when oxidised, a disulphide bridge forms between the two small subunits of the tetrameric enzyme resulting in a decrease its sensitivity to allosteric activation by 3-phosphoglycerate (3-PGA) (Fu *et al.*, 1998; Tiessen *et al.*, 2002). Reductive monomerisation, and consequently an increase in 3-PGA sensitivity, is triggered by light and sugars in the leaves of Arabidopsis, pea and potato (Hendriks *et al.*, 2003).

The combined allosteric and redox regulation of AGPase is thought to link the rate of starch synthesis to sucrose levels. Photosynthate is exported from the chloroplast as triose phosphate in exchange for Pi released during sucrose synthesis. Triose phosphates are converted to sucrose in the cytosol by a series of enzymatic steps including the conversion of fructose bisphosphate to fructose 6-phosphate (F6P) by fructose bisphosphate phosphatase (FBPase). An increase in cytosolic sucrose results in an increase in the hexose phosphate intermediates on the pathway of sucrose synthesis, including F6P. A freely reversible reaction converts F6P to the signalling metabolite fructose 2,6-bisphophate which in turn feeds back to inhibit FBPase. Consequent accumulation of cytosolic triose phosphate inhibits triose phosphate export from the chloroplast and Pi import. Thus the 3-PGA : Pi ratio will increase in the stroma, as will the allosteric activation of AGPase, resulting in an increase in starch synthesis.

The signalling pathways that lead to AGPase reduction have not been characterised fully, although three important components have been identified. The first of these is the signalling metabolite, trehalose-6-phosphate (T6P). T6P concentrations in a cell are thought to link carbon availability to variety of processes, from photosynthesis to cell wall deposition to mechanisms of drought tolerance (Paul, 2007). Loss of one isoform

of T6P synthase (*TPS1*) in Arabidopsis leads to an embryo lethal phenotype. Increases in the concentration of T6P in Arabidopsis plants correlated with increased reductive activation of AGPase and increased rates of starch synthesis (Lunn *et al.*, 2006). Indeed when Arabidopsis leaf discs are incubated with exogenous trehalose, or isolated chloroplasts are incubated with T6P, the redox activation of AGPase increases (Kolbe *et al.*, 2005). Plants overexpressing T6P synthase displayed increased redox activation of AGPase, while plants expressing T6P phosphatase displayed decreased activation. Little is understood about how T6P synthesis and degradation are regulated, and the signalling pathway between T6P and AGPase is unknown.

The second component known to influence the AGPase redox status is SnRK1, the plant homologue of the mammalian sensor of cellular energy status, AMP kinase. Over-expression of SnRK1 in Arabidopsis results in a decrease in the glucose-induced monomerisation of AGPase and a decrease in starch content relative to wildtype when grown on glucose (Jossier *et al.*, 2009). The third component is the plastidial NADP-thioredoxin reductase C (NTRC). The Arabidopsis *ntrc* mutant shows a decrease in the redox activation of AGPase in response to light or sucrose compared to wildtype (Michalska *et al.*, 2009). Acceleration of starch synthesis by light and sucrose are also decreased. NTRC can also reduce and activate AGPase *in vitro,* suggesting that it provides a direct link between chloroplast redox status and AGPase activity. How the effects of T6P, SnRK and NTRC on AGPase relate to one another has yet to be discovered.

Despite ample *in vitro* and correlative evidence implying that the redox regulation of AGPase may be important, its *in vivo* relevance has only recently been tested. Hädrich *et al.* (2012) identified a cysteine residue in AGPase necessary for its redox responsive properties. A mutant version of AGPase in which this cysteine had been converted to a serine was transformed into the *adg1* background. The mutant protein restored starch turnover to *adg1*, including the tendency for higher rates of starch synthesis in short days than in long days. In addition, the rate of starch synthesis in short days was significantly greater in the transgenic line than in wildtype, consistent with complete monomerisation of the protein, increasing its sensitivity to 3-PGA activation. Intriguingly, in long day conditions the transgenic lines did not degrade all their starch at night, leading to a starch excess phenotype. This effect on starch degradation is hard

to explain, but the authors suggest that a general perturbation of redox signalling may be responsible. Overall, these results show that the redox responsive properties of AGPase are not required for starch turnover or for the adjustment of starch synthesis rates to changing day lengths. Thus it may be that allosteric regulation of AGPase can provide sufficient control over starch synthesis in the absence of redox regulation, although the latter may still contribute in a wildtype plant.

1.3 The enzymes of starch degradation

The roles of the enzymes of starch degradation are discussed in detail in the following sections, but are outlined in the following paragraph and in Figure1.4. Briefly, glucan water dikinase and phosphoglucan water dikinase phosphorylate glucans at the starch granule surface, thereby increasing the susceptibility of the granule to attack by hydrolytic enzymes. The starch is then degraded by the action of β-amylases, which cleave maltose from the end of the glucan chains, and isoamylase 3, which cleaves the α-1,6 branch points in the amylopectin. A pair of glucan phosphatases remove the phosphate added by the glucan water dikinases. This is necessary for full degradation of the glucans by amylases. The action of β-amylase, isoamylase 3 and a disproportionating enzyme (which transfers glucosyl units between glucan chains) degrades all the glucans to maltose and a small amount of glucose. The maltose and glucose are exported from the chloroplast by specific transporters.

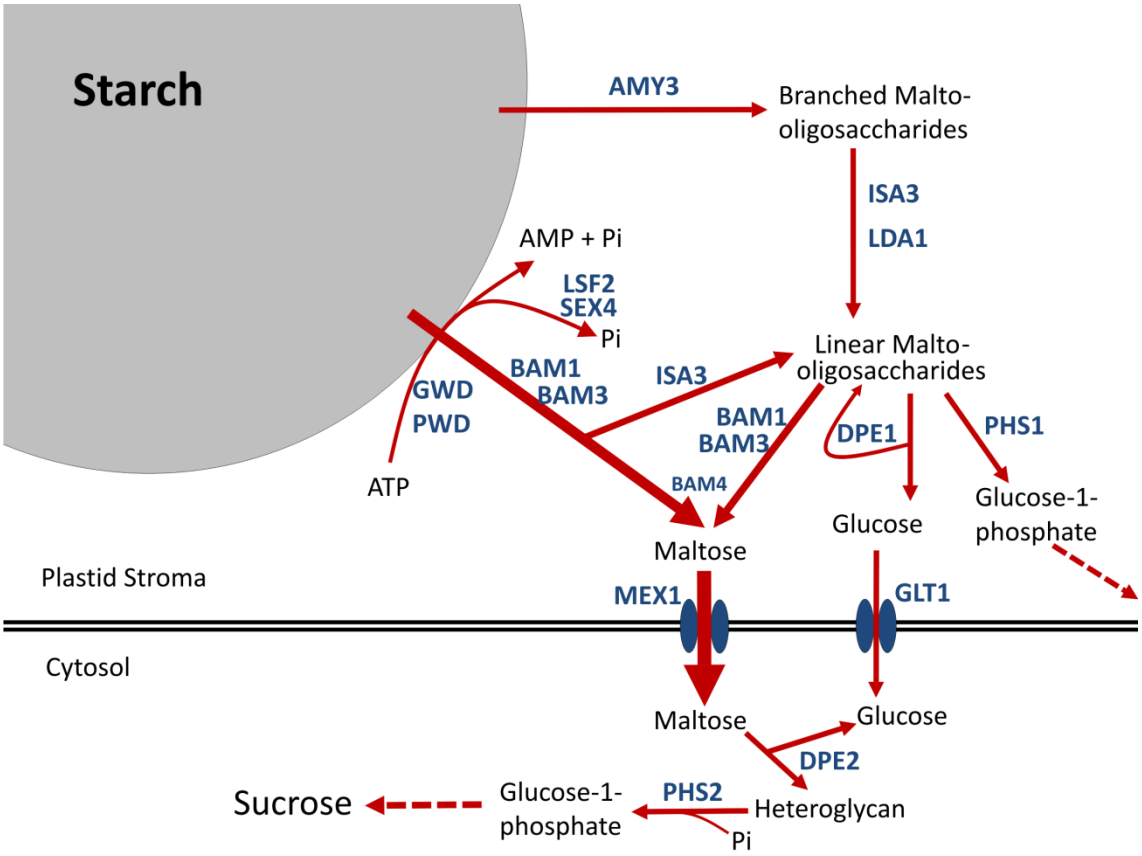

Figure1.4: Conversion of starch to sucrose in the leaves of Arabidopsis. The pathway begins with the phosphorylation of the starch granule surface by glucan water dikinase (GWD) and phosphoglucan water dikinase (PWD), making the granule more susceptible to hydrolytic attack. Starch Excess 4 (SEX4) and Like Sex4 2 (LSF2) dephosphorylate the glucans. Isoamylase 3 (ISA3) and limit dextrinase (LDA1) are largely responsible for the hydrolysis of α-1,6 branch points. β-amylase 1 and 3 (BAM1 and BAM3) cleave maltose units from the ends of glucan chains. Disproportionating enzyme 1 (DPE1) disproportionates maltotriose units to generate maltopentaose and glucose. The glucose is exported from the plastid by a glucose transporter (GLT1) while the maltose is exported via Maltose Excess 1 (MEX1). Some lesser fluxes are also indicated. α-amylase 3 (AMY3) is probably capable of removing branched glucans from the granule. Plastidial glucan phosphorylase (PHS1) may produce a small amount of glucose 1-phosphate by phosphorolytic attack on glucan chains. In the cytosol, maltose is converted to hexose phosphates through the action of the cytosolic disproportionating enzyme (DPE2) which may use a complex heteroglycan as a glucosyl acceptor. Cytosolic glucan phosphorylase (PHS2) probably releases glucose-1 phosphate from the heteroglycan.

1.3.1 Attacking a crystalline granule

Starch granules are dense, semi-crystalline structures. Thus enzymes attacking the granule interact with a complex solid surface, not molecules in solution. This fact has important consequences for the degradation of starch. In particular, the dense crystalline arrays of amylopectin double helices are recalcitrant to degradation by amylases (Edner *et al.*, 2007). The double helices are perpendicular to the granule surface, and the narrow water filled spaces in the hexagonal lattice are too small for enzymes to enter and hydrolyse glycosidic bonds (Imberty and Perez, 1988). Leaf starch degradation in Arabidopsis largely occurs through the action of exo-amylolytic β-amylases which release maltose units (Smith, 2012), but the relevant glycosidic bonds are hidden within the crystalline structure. Therefore, for efficient degradation of the starch granule there must first be a decrease in crystallinity.

There is now considerable evidence to suggest that starch crystallinity is modulated *in vivo* through changes in starch phosphorylation. The existence of phosphate esters in starch has been known for over 100 years (Fernbach, 1904), but their importance for *in vivo* starch metabolism was not appreciated until 1998 with the identification of a starch binding protein of potato tubers known as R1, later designated glucan water dikinase (GWD). Lorberth *et al*. (1998) cloned a cDNA for R1 and knocked down the expression of the gene in potato plants using antisense technology. These plants were deficient in tuber and leaf starch phosphate (~4 times less G6P than wildtype) and displayed a dramatic starch excess phenotype in the leaves. When the cDNA was expressed in *E. coli*, glycogen in the bacterium became highly phosphorylated, suggesting R1 might be an enzyme directly responsible for glucan phosphorylation.

An Arabidopsis mutant with an extreme leaf starch excess phenotype, similar to the potato *R1* antisense plants, was identified by Caspar *et a*. (1991). This mutant, designated *sex1*, still had starch after 84 hours of darkness and displayed a much reduced growth rate compared to wildtype in a 12 h photoperiod, but not in continuous light. Another study found that chloroplasts isolated from *sex1* were less effective at glucose export than chloroplasts of wildtype plants and concluded, based on this and other evidence, that the *sex1* lesion is most likely in a chloroplast hexose transporter (Trethewey and ap Rees, 1994). However, when a chloroplast hexose transporter was cloned the gene could not complement the *sex1* mutant, demonstrating that *sex1* was not

mutated in this hexose transporter gene (Weber *et al.*, 2000). Yu *et al.* (2001) used map based cloning to identify the *sex1* locus and validated their finding by complementing the *sex1* mutant phenotype with the cloned gene. The identified gene had significant homology to the R1 locus of potato, suggesting a function related to starch phosphorylation. Indeed leaf starch from the *sex1* mutant had much reduced G6P levels. Otherwise, the chain length distribution of the mutant starch was similar to wildtype, although the mutant had a higher amylose content. *In vitro* characterisation of the R1 protein finally provided a mechanism for R1 action (Ritte *et al.*, 2002). R1 is an α-glucan, water dikinase (GWD) which hydrolyses ATP, transferring the β-phosphate to a conserved histidine on the protein and the γ-phosphate to water. The β-phosphate is then transferred from the autophosphorylated histidine to the glucan substrate, completing the 'ping-pong' mechanism.

In the rest of this thesis I will refer to the R1/SEX1 enzyme as GWD. When specifically referring the potato enzyme I will use the term StGWD, and when specifically referring to the Arabidopsis enzyme I will use the term AtGWD.

Further *in vitro* analysis of the StGWD revealed that the enzyme only phosphorylates glucans at the C6 position (Ritte *et al.*, 2006). However glucose residues in starch are also phosphorylated at the C3 position, so there must be another enzyme responsible for this reaction. There are two close homologues of AtGWD in the Arabidopsis genome. The first, *GWD2*, has no plastidial targeting sequence and was confirmed to be extrachloroplastic by examining transgenic plants expressing a GWD2::GFP fusion protein with confocal fluorescence microscopy (Glaring *et al.*, 2007). Despite the fact that GWD2 is an active enzyme with α-glucan water dikinase activity, the *gwd2* mutant plant has growth rates and sugar and starch levels almost identical to wildtype. Intriguingly, *GWD2* promoter activity was restricted to phloem companion cells just before senescence (Glaring *et al.*, 2007), suggesting the enzyme might have a specific developmental role in that tissue.

The second GWD homologue, GWD3, was found to be responsible for the phosphorylation of starch at the C3 position. The reaction mechanism is the same as for GWD (Kötting *et al.*, 2005). However for PWD to phosphorylate glucans in the context of a semi-crystalline starch granule, the starch must first have been phosphorylated at

the C6 position by GWD (Baunsgaard *et al.*, 2005; Kötting *et al.*, 2005; Hejazi *et al.*, 2008). Thus GWD3 was renamed Phosphoglucan Water Dikinase (PWD). PWD is specific for C3 phosphorylation and the *pwd* mutant lacks any detectable C3 starch phosphate (Ritte *et al.*, 2006). The *pwd* mutant has a starch excess phenotype, containing about five times as much starch as wildtype at the end of the night (Baunsgaard *et al.*, 2005; Kötting *et al.*, 2005). This phenotype is much milder than that of the *gwd* mutant, which may contain around 40-100 times as much starch as wildtype at the end of the night (Niittylä *et al.*, 2006; Kötting *et al.*, 2009). In addition, *pwd* still has about 75% of wildtype diel starch turnover, whereas *gwd* shows no consistent turnover. Growth is only slightly decreased in the *pwd* mutant, whereas the *gwd* plant is seriously compromised.

The phenotypes of the *gwd* and *pwd* mutants demonstrate that glucan phosphorylation has a large impact on the susceptibility of starch to degradation *in vivo*. Detailed *in vitro* studies provide a structural basis for these effects. A key strategy has been to synthesise parts of an amylopectin chain and examine any changes in bond angles in these molecules on phosphorylation. Such information can then be interpreted in the context of molecular models of amylopectin structure (Blennow and Engelsen, 2010). The simplest study examined the geometry of α-D-glucopyranoside 6-*O*-phosphate (G6P) (Engelsen *et al.*, 2003). When this geometry was extrapolated to an amylopectin double helix, the phosphate group was contained within the helix and so would be unlikely to disrupt the hexagonal packing of the amylopectin.

Another study considered maltose molecules containing phosphate esters at the C3 and the C6 position (Hansen *et al.*, 2008). Phosphorylation at either position restricted the geometry of the α-1,4 glycosidic linkage, and phosphorylation in the C3 position caused a 50° deviance in the Φ bond angle from that of the unphosphorylated maltose. These data were incorporated into the model of amylopectin double helices. C6 phosphorylation has little impact on amylopectin structure but the C3 phosphate protrudes from the side of the helix and would be expected to cause significant disruption to the hexagonal packing of the chains. Starch phosphorylation has also been demonstrated to increase granule hydration. Electron paramagnetic resonance was used to probe the molecular environment of Cu^{2+} ions incorporated into the matrix of starch granules from a variety of sources (Blennow *et al.*, 2006). Hexaaqua Cu^{2+} complexes

were found primarily in high phosphate starches, supporting the idea that phosphate can increase the internal hydration of the granule.

Testing the effects of phosphorylation on real starch granules is made difficult by the huge, and not fully understood, complexities of the granule structure. To circumvent this, Hejazi *et al*. (2008) used an experimental model: crystalline maltodextrin which displays the B-type crystalline structure similar to Arabidopsis starch. Crystalline maltodextrins have the major advantage that solubilisation products do not remain covalently attached to the granule, so the effects of enzymes on granule crystallinity can be readily monitored. Crystalline maltodextrins were efficiently phosphorylated by StGWD in the presence of ATP. In the absence of StGWD, there was no solublisation of maltodextrins from the crystalline granules. However, in the presence of StGWD maltodextrins were progressively released over time. If more StGWD was included in the reaction, a greater phosphate content resulted and solubilisation of maltodextrin chains was more rapid. This suggests that phosphorylation of maltodextrins by StGWD promotes solubilisation. Both neutral and phosphorylated chains were released, implying that the effects of StGWD can extend beyond the phosphorylated chain. PWD will also phosphorylate the crystalline maltodextrins, but only after pre-phosphorylation by GWD (Hejazi *et al.*, 2009). When pre-phosphorylated crystalline maltodextrins and PWD were incubated with β-^{33}P-ATP, then some of the resultant radiolabelled solubilisation products were found to be monophosphorylated. This suggests that the action of PWD is dependent on the disorder introduced by the action of GWD, rather than C6 phosphate esters themselves.

The *in vitro* analysis of the effects of granule phosphorylation by GWD and PWD was extended to real starch granules by Edner *et al.* (2007). The authors extracted starch granules lacking phosphate from the *sex1-3* mutant. The granules were incubated with a recombinant Arabidopsis β-amylase, BAM3, in the presence or absence of StGWD or AtGWD. The presence of GWD resulted in a doubling of the amount of glucan released from the granule compared to BAM3 alone. However a version of AtGWD lacking the histidine essential for catalysis did not stimulate BAM3 activity. This implies that GWD acts through phosphorylation of the granule rather than some other mechanism, for example by interacting directly with BAM3 and recruiting it to the granule surface. The

amount of glucan released by BAM3 and AtGWD was only slightly enhanced by the inclusion of PWD.

Taken together, the experiments described in this section suggest the following model for the action of GWD and PWD. First, GWD phosphorylates surface glucans at the C6 position. This induces sufficient decrease in crystallinity to make the granule more susceptible to amylolytic attack. The decrease in crystallinity also creates an appropriate substrate for PWD, which then phosphorylates glucans at the C3 position. This disrupts the packing of the amylopectin double helices, causes a further decline in crystallinity and a further stimulation of amylolytic activity. However there is still much we do not understand about the action of these enzymes. First, it is not clear how GWD acts on a crystalline substrate. Does the binding of the protein induce local disruption in the amylopectin and thereby reveal the phosphorylation site? Or is the surface of the granule not fully crystalline, but subject to stochastic structural fluctuations which grant temporary access to internal residues? Second, there are discrepancies in the data about the relative importance of C3 versus C6 phosphorylation. Structural evidence suggests that C3 phosphorylation has a much more disruptive effect on the packing of amylopectin double helices than does C6 phosphorylation. However, the *pwd* mutant is much less compromised than the *gwd* mutant. In addition, Edner *et al.* (2007) found that PWD provided little stimulation of β-amylolytic activity beyond that provided by GWD. Third, the current model in which glucan water dikinase activity causes a decrease in granule crystallinity, thereby giving hydrolytic enzymes access to glycosidic bonds, is clearly over-simplistic. This is evident from the report that the activity of barley β-amylase on Arabidopsis starch granules could not be stimulated by the action of AtGWD (Edner *et al.*, 2007). In contrast BAM3 activity is effectively simulated. This suggests that specific, co-evolved interactions between the glucan water dikinases, the amylolytic enzymes and the granule surface determine the rate of degradation, not simply granule crystallinity.

1.3.2 Degrading the granule

Arabidopsis starch granules are principally degraded by amylolytic attack (Smith, 2012). For some time it was thought that degradation might be phosphorolytic, but the *phs1* mutant of Arabidopsis, which lacks plastidial phosphorylase activity, has normal starch metabolism and structure (Zeeman *et al.*, 2004). It seems that PHS1 might have

some role in providing carbon for specific chloroplastic pathways in response to abiotic stress. We now know that hydrolytic degradation is the dominant process releasing carbon from the starch granule. However, a mutant lacking the only chloroplastic isoform of α-amylase (AMY3) displays normal starch metabolism (Yu *et al.*, 2005). Thus starch degradation in leaves differs fundamentally from that in cereal grains, in which the process is dominated by α-amylase. In fact there is now good evidence that transitory starch degradation proceeds by the release of maltose units from the ends of glucan chains by β-amylases, while isoamylases cleave the α-1,6 branch points. The discovery of the molecular identities of these activities has been complicated by a multiplicity of isoforms and associated redundancy.

The first good evidence for the importance of β-amylases in starch degradation came from reports that antisense repression of β-amylases in potato leads to a starch excess phenotype in the leaves (Scheidig *et al.*, 2002). The tractable genetics of Arabidopsis has permitted the detailed characterisation of the *β-AMYLASE* gene family. There are nine *β-AMYLASE* (*BAM*) genes in Arabidopsis, which fall into 4 phylogenetic subfamilies (Fulton *et al.*, 2008). Of these isoforms, BAM1-4 have been confirmed to be chloroplastic (Lao *et al.*, 1999; Sparla *et al.*, 2006; Fulton *et al.*, 2008). The *bam1* mutant has no discernible phenotype except a starch excess in guard cells (Valerio *et al.*, 2011), but the *bam3* mutant has a mild starch excess phenotype. The *bam1bam3* double mutant has a strong starch excess phenotype and is retarded in growth (Fulton *et al.*, 2008). BAM2 has very low activity *in vitro* compared to BAM1 and BAM3 (Fulton et al., 2008), possibly due to low affinity for amylopectin (Li *et al.*, 2009). The *bam2* mutant has no phenotype in any genetic background tested (Fulton *et al.*, 2008). *BAM4* encodes a protein lacking key catalytic residues which are present in other BAMs, and indeed the protein lacks activity *in vitro*. Intriguingly, the *bam4* single mutant has a similarly mild starch excess phenotype to the *bam3* mutant, but the loss of BAM4 in the *bam3* or the *bam1bam3* backgrounds significantly enhances the starch excess phenotype of these mutants (Fulton *et al.*, 2008). Thus it seems that BAM1 and BAM3 provide most of the β-amylase activity in the Arabidopsis chloroplast and BAM4 may have a regulatory or structural role in starch degradation, perhaps modulating the activity of other enzymes.

Similar to BAM4, BAM9 also lacks key catalytic residues and *in vitro* activity (Fulton *et al.*, 2008). No function has yet been assigned to this protein. BAM5 is not predicted to be chloroplastic and appears to localise to phloem sieve elements (Wang *et al.*, 1995; Fulton *et al.*, 2008). The *bam5* mutant has no starch excess phenotype and the function of the protein is unclear. Recombinant BAM7 and BAM8 both have rather low specific β-amylase activity but contain a BRASSINAZOLE RESISTANT 1 type DNA binding domain, and indeed localise to the nucleus (Reinhold *et al.*, 2011). They are able to activate transcription in a protoplast based transactivation assay, and the *bam7/bam8* mutant, and a *BAM8* overexpressor, show widespread changes in gene expression relative to wildtype. This mis-regulated gene set overlaps with a set of brassinosteroid responsive genes. Starch and sugar levels in the double knockout and the BAM8 overexpressor are similar to wildtype.

Debranching enzymes are required to cleave the α-1,6 linkages in the amylopectin. As mentioned above, the *isa3* mutant shows a starch excess phenotype and so probably provides much of the debranching activity for starch degradation (Wattebled *et al.*, 2005). The *lda1* mutant does not show a starch excess phenotype, but the *isa3*/*lda1* double mutant has a phenotype more severe than *isa3* (Delatte *et al.*, 2006; Wattebled *et al.*, 2008). Thus both enzymes may contribute to debranching activity during starch degradation in a wildtype plant. As already discussed, ISA1 and ISA2 in contrast, are primarily involved in starch synthesis (Delatte *et al.*, 2005; Wattebled *et al.*, 2005).

Glucan-phosphate phosphatase activity has been found to be crucial for normal starch degradation. The β-amylase from sweet potato will degrade a linear glucan chain from the non-reducing end, but will not progress past a glucose 6-phosphate residue (Tabata *et al.*, 1978; Takeda and Hizukuri, 1981). Therefore, if other β-amylases behave in the same way, one would expect a glucan-phosphate phosphatase activity to be necessary for the complete degradation of a starch granule. Consistent with this, the *starch excess 4* (*sex4*) mutant is deficient in glucan phosphatase activity and has a starch excess phenotype and reduced growth (Kötting *et al.*, 2009). The SEX4 protein releases phosphate from both the C6 and the C3 position *in vitro* and, unlike the glucan water dikinases, acts efficiently on soluble maltodextrins (Hejazi *et al.*, 2010). The *sex4* mutant accumulates phospho-oligosaccharides at night and it is hypothesised that these inhibit other starch degrading enzymes. *In vitro*, SEX4 stimulates a 50% increase in

glucan release by BAM3, ISA3 and GWD from *sex1-3* starch granules (Kötting *et al.*, 2009). In addition, the presence of SEX4 counteracts the StGWD mediated solubilisation of crystalline maltodextrins *in vitro* (Hejazi *et al.*, 2010). This strongly suggests that the principal role of SEX4 is to generate unphosphorylated substrates for amylases, rather than participating in the remodelling of the granule surface.

Further roles for AMY3 and ISA3 are revealed in the *sex4* background. Mutation of *amy3* or *isa3* enhances the *sex4* starch excess phenotype yet reduces the accumulation of phospho-oligosaccharides at night. This suggests that both ISA3 and AMY3 may have a role in the release of phospho-oligosaccharides from the granule surface, at least in the *sex4* background.

There are two genes similar to *SEX4* in the Arabidopsis genome: *LIKE SEX4 1* and *LIKE SEX4 2* (LSF1 and LSF2), both of which are involved in starch degradation. While SEX4 removes phosphate from both the C3 and the C6 position, LSF2 will only release phosphate from the C3 position (Santelia *et al.*, 2011). The *lsf2* mutant has no starch excess phenotype and does not accumulate phospho-oligosaccharides, but contains elevated C3 starch phosphate. The *lsf2/sex4* double mutant accumulates more starch and grows slower than the *sex4* single mutant. The *lsf1* mutant has a starch excess phenotype, although not as extreme as that of *sex4* (Comparot-Moss *et al.*, 2010). However the phenotype of the *lsf1/sex4* double mutant is more extreme than that of *sex4*. Thus it would seem that LSF1 has some role in starch degradation in the *sex4* background, however *lsf1* starch contains wildtype levels of C3 and C6 phosphate and crude extracts of *lsf1* leaves contain equivalent glucan phosphatase activity to wildtype. These data suggest that LSF1 does not contribute to glucan phosphatase activity in the plant, but still has a role in starch degradation.

The findings discussed above suggest that the starch granule is degraded through a cycle of phosphorylation, hydrolysis, dephosphorylation and more hydrolysis. However there is much about the process we still do not understand. First, positive feedback effects between enzymes can be observed *in vitro*. Edner *et al.* (2007) found β-amylolytic attack stimulated the incorporation of phosphate into starch granules by GWD. This stimulation could be observed if BAM3 was removed before GWD was added, but was especially pronounced when BAM3 and GWD acted simultaneously. In a similar

manner, pre-treatment of starch granules with BAM3 resulted in increased subsequent phosphate release by SEX4 (Kötting *et al.*, 2009). Thus, *in vitro* at least, interactions between enzymes and the physical state of the granule surface are critical for the dynamic process of starch degradation. Developing an improved understanding of these mechanisms will be extremely challenging, as it will require tools to monitor both the dynamics of enzymes at the granule surface and intermediate structures that form at the starch surface as the glucans are degraded. Second, two proteins, LSF1 and BAM4, are clearly important for normal starch degradation and yet are apparently catalytically inactive. It may be that these have a structural role, and facilitate interactions between active enzyme and the granule. Third, some enzymes which are not required for normal starch metabolism in a wildtype background clearly have a role in metabolism in certain mutant backgrounds. For example, mutation of *lda1* makes the phenotype of *isa3* more severe despite the fact that the *lda1* single mutant has normal starch metabolism and growth (Delatte *et al.*, 2006; Wattebled *et al.*, 2008). This makes it difficult to assess the role of *lda1* in a wildtype plant. It is also possible that apparently unimportant enzymes have specific roles under environmental conditions not yet tested in the laboratory.

1.3.3 Further metabolism in the stroma

The principal products of hydrolytic attack on the starch granule are maltose and small amounts of maltotriose (Lu and Sharkey, 2006; Smith, 2012). The maltose is exported from the chloroplast by the specific maltose transporter, MEX1. The *mex1* mutant has a starch excess phenotype and accumulates maltose to high levels in the plastids (Niittylä *et al.*, 2004; Lu and Sharkey, 2006). The maltotriose products of starch degradation cannot be broken down by β-amylase (Lizotte *et al.*, 1990) and are metabolised through the action of a glucanotransferase or disproportionating enzyme, DPE1. The *dpe1* mutant has a starch excess phenotype and accumulates maltotriose at night (Critchley *et al.*, 2001). α-1,4-glucanotransferases such as DPE1 will catalyse the transfer of maltosyl units between glucan chains (Takaha and Smith, 1999). In these reactions, the number of glycosidic bonds is conserved, and the bonds broken and made are approximately equivalent in enthalpy (Goldberg *et al.*, 1991). This means that entropy is the principal driver for disproportionation, and at equilibrium, the frequency distribution of malto-oligosaccharide species is an exponentially decaying function of chain length (Kartal *et al.*, 2011). Thus, as β-amylase degrades long malto-oligosaccharides to maltose, residual maltotriose is disproportionated to longer chains by entropy-driven reactions

catalysed by DPE2. Free glucose produced by the disproportionation of maltotriose is thought to be exported via the chloroplast envelope hexose transporter, GLT1 (also known as pGlcT) (Cho *et al.*, 2011). The export of glucose from the chloroplast at night is clearly not very important in the wildtype plant because the *glt1* mutant displays normal growth and starch turnover. However the *glt1*/*mex1* double mutant has a more severe starch excess phenotype and is much more compromised in growth than the *mex1* single mutant, suggesting that glucose export becomes important when maltose export is compromised.

1.3.4 The fate of maltose in the cytosol

Maltose is metabolised the in the cytosol to hexose phosphates, from which the carbon is principally channelled into sucrose synthesis for export to the phloem, or into glycolysis, the Krebs cycle and associated biosynthetic processes. However the metabolism of cytosolic maltose is not well understood. The first step is known to be catalysed by the glucanotransferase, DPE2. Similar to *mex1*, the *dpe2* mutant accumulates maltose to high levels, and shows a starch excess phenotype and reduced growth (Chia *et al.*, 2004; Lu and Sharkey, 2004). *In vitro,* the DPE2 enzyme can transfer glucosyl units from maltose to soluble polysaccharide acceptors such as glycogen, releasing glucose (Chia et al., 2004). The *in vivo* acceptor substrate of DPE2 is thought to be a complex, cytosolic heteroglycan consisting of a wide variety of sugars and linkages (Fettke *et al.*, 2009). DPE2 will use purified cytosolic heteroglycan as an acceptor substrate *in vitro* (Fettke *et al.*, 2006). Heteroglycan glucosylated by DPE2 can also be donor substrate for recombinant PHS2: the cytosolic glucan phosphorylase (Lu *et al.*, 2006; Fettke *et al.*, 2009). The *phs2* mutant has elevated night time maltose levels, consistent with a role for this enzyme in cytosolic maltose metabolism (Lu and Sharkey, 2006). So it seems that maltose could be converted to glucose and glucose-1-phosphate by the actions of DPE2 and PHS2 using the soluble heteroglycan as an acceptor and a donor substrate respectively. However we have no direct evidence that this is the pathway which operates *in vivo,* and the precise nature and origin of the cytosolic heteroglycan remain unclear.

1.4 The control of starch degradation

It is worth distinguishing two modes of control when considering starch degradation in Arabidopsis at the phenomenological level. First, degradation is initiated every dusk. Second, the rate of degradation is exquisitely regulated such that reserves run out around dawn. These two controls are discussed in detail in the following sections. For each I describe the phenomena concerned, and underlying mechanisms which might operate. It is important to remember that the enzyme activities that are modulated to change the pathway flux might not necessarily be the same for each mode of control. In a subsequent section I discuss the known properties of the enzymes of starch degradation which might be relevant for control of flux and regulation of the pathway. This leads me to the central hypothesis of this thesis: that GWD is an enzyme which is likely to be regulated for flux control.

1.4.1 The initiation of starch degradation

There is good evidence, based on ^{14}C labelling, that starch is not turned over in the day in the leaves of pea, pepper and Arabidopsis (Kruger *et al.*, 1983; Grange, 1984; Zeeman *et al.*, 2002). Therefore starch degradation must be initiated at dusk. The trigger for initiation not known. It could be changes in plastidial redox status causing the thioredoxin pool to become oxidised in the dark, or changes in pH as the thylakoid pH gradient is dissipated after dusk. A transitory decrease in sucrose is often observed on light to dark transition (Chia *et al.*, 2004; Smith *et al.*, 2004; Zeeman *et al.*, 2004; Lu *et al.*, 2005; Comparot-Moss *et al.*, 2010), and this could potentially trigger starch degradation. A further possibility is that the transient increase in stromal free Ca^{2+} observed on light-dark transitions somehow triggers degradation (Sai and Johnson, 2002). This phenomenon is particularly interesting because the magnitude of the Ca^{2+} spike seemed to be related to the length of the proceeding light period, so it is possible that the spike could feed information about day length into starch degradation.

Light-dependent regulation of metabolism has been well studied in several cases. Starch synthesis principally occurs during the day and not at night (Geigenberger, 2011), although there is evidence for small amounts of turnover during degradation (Stitt *et al.*, 1978; Trethewey and ap Rees, 1994; Scott and Kruger, 1995). It is thought that operation of the Calvin cycle and ATP synthesis in the light causes an increase in the 3-PGA:Pi ratio, activating AGPase and hence starch synthesis. Conversely, at night a

decreased 3-PGA:Pi ratio inactivates AGPase and hence inactivates starch synthesis (Geigenberger, 2011). Nitrogen assimilation is also regulated by light (Lillo, 2008). During the day nitrate reductase (NR) (in the cytosol) is in its unphosphorylated, active state, driving conversion of nitrate to nitrite. At night, nitrite reductase no longer has sufficient reducing power from photosystem I to effectively reduce nitrite, so NR must be inactivated to prevent nitrite accumulation and associated toxicity. NR is phosphorylated in the dark, enhancing 14-3-3 protein binding, thereby inactivating the enzyme. Thioredoxins may also act to reduce and activate various plastidial components of the nitrate assimilation system in the light. A classic example of light-regulated metabolism is the Calvin-Benson cycle, which also becomes inactive at night, in part to prevent futile cycling of metabolites (Geiger and Servaites, 1994). The ferredoxin / thioredoxin system uses electrons from photosystem I in the light to reduce and activate four enzymes of the Calvin cycle. In the dark the enzymes rapidly become oxidised and inactive. Given these examples, it seems reasonable that signalling pathways involving allosteric regulation by metabolites, phosphorylation or redox regulation could all potentially be involved in the initiation of starch degradation.

The fact that starch is degraded on the darkening of leaves is well documented (Geiger and Batey, 1967; Zeeman *et al.*, 2010). However there are other conditions which lead to the initiation of starch degradation. First, one might expect starch degradation to initiate when the light levels drop below the light compensation point for photosynthesis. This is supported by experiments in which plants were grown in sinusoidal light regimes (Fondy *et al.*, 1989; Servaites *et al.*, 1989). When light levels became sufficiently low, starch degradation was initiated, even though darkness had not yet arrived. Second, starch is degraded in the light when CO_2 levels are sufficiently low. When Arabidopsis plants are incubated in the light in an atmosphere lacking CO_2 starch is degraded (Weise *et al.*, 2006). Fox and Geiger (1984) found that sugar beet leaves would degrade starch in the light when CO_2 levels are dropped to the CO_2 compensation point of photosynthesis. Interestingly, net starch synthesis was restored in the low CO_2 condition on petiole girdling. This might suggest that carbon availability signals override light signals in the control of starch synthesis and degradation.

Finally, starch degradation is induced in the light when the export of triose phosphate from the chloroplast is restricted. In tobacco plants expressing an antisense construct

targeted at the triose phosphate translocator, starch content decreased towards the end of the day (Hausler *et al.*, 1998). A study of Arabidopsis plants lacking almost all triose phosphate translocator activity (the *tpt-1* mutant) also reported starch turnover in the light, although the data were not shown (Schneider *et al.*, 2002). The *tpt-1* mutant was not compromised in photosynthesis and growth but the *tpt-1*/*adg1* double mutant showed photosynthetic and growth phenotypes much more severe than the *adg1* mutant alone, demonstrating that starch is required for normal growth in the absence of *tpt-1*. Interestingly, the *tpt-1*/*sex1-1* mutant was only slightly more compromised than *sex1-1* alone, indicating that it is the starch synthetic process, rather than carbon made available through the degradation of starch, which is important for growth of the *tpt-1* mutant. This would be consistent with the idea that reduced export of triose phosphate in *tpt-1* causes Pi limitation of photosynthesis and ATP synthesis. This limitation could be relieved to a certain extent by the starch synthetic pathway. Further evidence for this hypothesis was provided by the finding that growth of *tpt-1* under high light resulted in decreased photosynthesis and growth relative to wildtype (Walters *et al.*, 2004). Moreover, the authors demonstrated unambiguously that starch was degraded at the same time as synthesis was occuring in the light under these conditions. An increase in non-photochemical quenching in the mutant suggested an increased thylakoid pH gradient, consistent with a constraint on ATP synthesis. This was probably due to Pi limitation and not NADPH limitation, because NADPH-dependent malate dehydrogenase (the activation state of which is dependent on NADPH levels) displayed wildtype or increased activity in the mutant. Measurements of chlorophyll fluorescence also suggested that the plastoquinone pool was more reduced in the mutant.

The above data give some clues about the signals which control the initiation of starch degradation, although one should remember that the signals may be different under different conditions. First, starch degradation can clearly initiate in the light and the dark, so direct light regulation is not likely. However, as work on the *tpt*-1 mutant readily demonstrates, stromal triose phosphate accumulation can also affect the redox status of components of the electron transport chain, so it is hard to separate the effects of light and carbon on putative redox signalling pathways. Second, low light or low CO_2 in the light will both result in decreasing sugar levels which may in turn stimulate starch degradation. Conversely, the supply of exogenous sucrose to Arabidopsis leaf discs inhibits starch degradation in the dark (my data, unpublished). Third, the onset of starch

degradation in the light in the *tpt*-1 mutant correlates with a more reduced plastoquinone pool, an increased thylakoid pH gradient and lower sugar levels than wildtype. A combination of these factors may trigger starch degradation. Fourth, signals from the cytosol might be particularly important. The evidence for this is that the *tpt-1* mutant activates starch degradation even though it presumably accumulates triose phosphate in the stroma. Plants grown in the presence of sucrose are also expected to accumulate triose phosphate in the stroma (Geigenberger, 2011), and yet starch degradation is inhibited. Thus, it is low cytosolic sugar status, not low stromal sugar status, which correlates with the initiation of starch degradation. These data suggest that cytoplasmic carbon status may be of greater consequence for the control of starch degradation than is stromal carbon status. How cytosolic carbon status might regulate the enzymes of starch degradation is not clear.

There are indications that the initiation of starch degradation might be under the control of an endogenous timing mechanism. First, when spinach or pea plants are transferred to continuous light, leaf starch content has been observed to decrease substantially towards the end of the 24 hour period (Pongratz and Beck, 1978; Kruger *et al.*, 1983). Second, two studies from one research group found that Arabidopsis plants transferred to continuous light tended to accumulate maltose to higher levels in the subjective night than in the subjective day (Lu *et al.*, 2005; Weise *et al.*, 2006). In addition they found that rates of starch synthesis were greater in the subjective day than in the subjective night (Weise *et al.*, 2006). The role of endogenous timers in the control of starch degradation is discussed further in section 1.4.2.1. The properties of the enzymes of starch degradation which might be relevant for the initiation of starch degradation are discussed in section 1.5.2.

1.4.2 Regulation of starch degradation rates

As discussed previously, starch degradation in Arabidopsis is exquisitely regulated such that reserves run out around dawn. If starch degradation rates are too fast and reserves run out before dawn, the plant exhibits symptoms of starvation and growth ceases. If starch degradation rates are too slow, such that there is significant starch remaining at dawn, then the plant has not optimised use of its carbon supply and might be at a competitive disadvantage in conditions conducive to rapid growth. As discussed earlier, starch degradation rates adjust in response to an unexpectedly early night (Figure1.5 A)

(Lu *et al.*, 2005; Graf *et al.*, 2010). Starch degradation rates also adjust to an unexpectedly late night (Figure1.5 B). If plants are grown from seed in 12 hours light, 12 hours dark cycles and then are subject to a single 14 hour light, 8 hour dark cycle the starch degradation rate is increased relative to the previous night.

Many environmental parameters affect the photosynthetic performance of a plant during the day and thus the amount of starch synthesised will vary from day to day. Therefore starch degradation rates must also adjust depending on the amount of starch accumulated at dusk if night time starvation is to be avoided. For example, if plants are grown from seed at a high light intensity and are then transferred for a single day to a low light intensity, they make less starch that day than previous days. Consequently, the rate of degradation is reduced that night compared to previous nights, such that the plant does not exhaust its starch reserves before dawn (Figure 1.3 C). Recently it has been shown that starch degradation rates are compensated against changes in temperature when grown in short days (Pyl *et al.*, 2012). Plants grown from seed at a constant 24°C were transferred to 12°C for a single night. The transferred plants displayed the same rate of starch degradation as plants which remained in 24°C conditions (Figure1.5 D). Rate constants of chemical reactions are inversely related to temperature, so one would expect a decrease in night time temperature to result in a decrease in the rate of starch degradation. The fact that no decrease is observed indicates that the enzymes of starch degradation are regulated to maintain flux through the pathway at the lower temperature.

The above data strongly suggest that the rate of starch degradation is set by a division calculation. The amount of starch at the end of the day is divided by the time remaining until dawn to yield an appropriate rate of degradation. This means there must be mechanisms to predict the amount of time until dawn, measure the amount of starch, perform the division calculation and appropriately regulate the enzymes of starch degradation. Our knowledge of each of these mechanisms is discussed in subsequent sections.

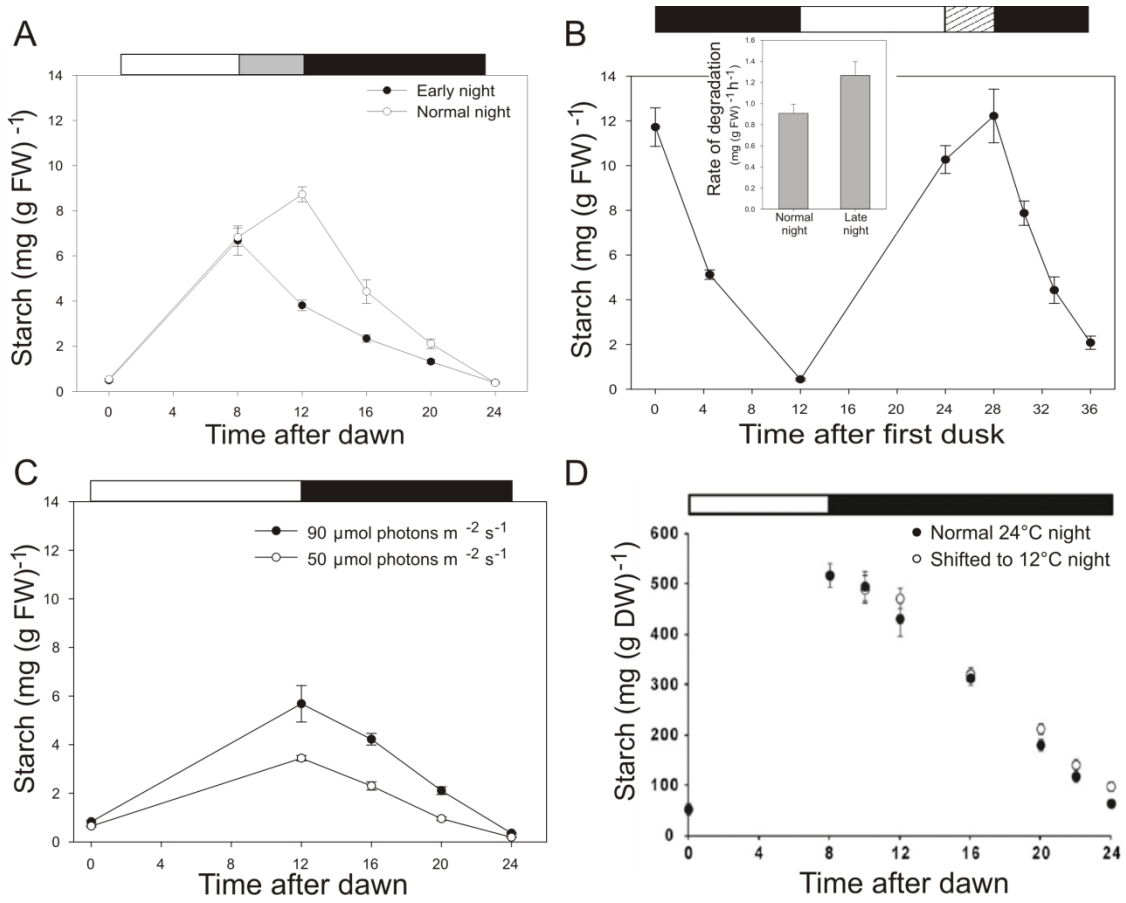

Figure1.5: Starch degradation rates in Arabidopsis adjust with changes in the external environment. A-C are my data. **A** Starch degradation rates adjust to an early night. Plants grown in 12 h light, 12 h dark (12L:12D) cycles were either maintained in that condition (normal night, open symbols) or shifted to a 4 h early night (early night, closed symbols). Grey bar is additional dark period in early night. **B** Starch degradation rates adjust to a late night. Plants were grown in 12L:12D cycles (first dark period, normal night) and then transferred to a 16L:8D cycle (second dark period, late night). Hatched bar is additional light period before late onset of darkness. **C** Starch degradation rates adjust depending on the amount of starch made the previous day. Plants were grown in 90 µmol photons m^{-2} s^{-1} were either maintained in those conditions (filled symbols) or were transferred for one day to 50 µmol photons m^{-2} s^{-1} (open symbols). n=4-8 rosettes and error bars are ±SE **D** Starch degradation rates are temperature compensated in short days. Plants grown at a constant 24°C were either maintained in that condition (filled symbols) or transferred to 12°C for one night (open symbols). Data from Pyl *et al.* (2012). n=4 pools of 5 plants. Error bars are ±SD. Black bars above plots represent dark periods, white bars light periods.

1.4.2.1 Predicting the time until dawn

There is good evidence that the time information for the calculation of starch degradation rates in Arabidopsis originates from an endogenous biological clock. Endogenous biological timers known as circadian clocks have been identified in many organisms, from cyanobacteria to mammals to higher plants (Bell-Pedersen *et al.*, 2005). A simple indication of clock control is that some regular change in an organism over a diel cycle persists in the absence of diel changes in external stimuli such as light or temperature. Much effort has been invested in the characterisation of circadian clocks over the last decade, and it has been concluded that clocks of divergent organisms are often based on common design principles, although the exact nature of the components differs (Bell-Pedersen *et al.*, 2005; Novak and Tyson, 2008). Most circadian clocks are based on systems of interlocking feedback loops incorporating sufficient delay such that the system oscillates with a period of approximately 24 hours. The clock is re-set each day by regular external stimuli, thereby keeping it synchronous with the external environment. In Arabidopsis, it has been shown that the fitness of a plant is compromised if the period of its endogenous oscillator does not match the period of diel cycle in which the plant is grown (Dodd *et al.*, 2005). We now know that this effect is probably largely attributable to the role of the clock in the proper timing of starch degradation.

Graf *et al.* provided strong evidence that starch degradation is regulated by the circadian clock (Graf *et al.*, 2010). First, they showed that plants grown from seed in 14 hour light, 14 hour dark cycles, degrade their starch too fast and reserves run out before dawn. In fact, the plants degrade their starch so that it runs out 24 hours after the previous dawn, even though these plants have never lived in 24 hour light-dark cycles. This suggests that starch degradation is controlled by an endogenous timer that predicts that dawn will be 24 hours after the previous dawn. Further evidence for the role of the clock in starch degradation came from analysis of clock mutants. Mutations in core circadian clock genes often result in plants which display an altered periodicity of circadian outputs in free running (ie continuous light, constant temperature) conditions. For example, in continuous light the *cca1/lyh* double mutant shows patterns of leaf movement and patterns of gene expression which oscillate with a shorter period than the 24 hour periodicity observed in wildtype plants (Alabadi *et al.*, 2001; Mizoguchi *et al.*, 2002). In particular, transcripts which show peak abundance at dawn in wildtype, show

peak abundance some 4 hours before dawn in the *cca1/lhy* mutant. Graf *et al.* (2010), hypothesised that these plants would misanticipate dawn, affecting the timing of starch degradation if it was a circadian clock regulated process. Indeed, starch degradation is mis-timed in the *cca1*/*lhy* mutant and the plant runs out of starch several hours before dawn. The time at which starch is exhausted in the mutant corresponds to peak expression of clock genes which normally peak at dawn. This suggests that the time information used for the calculation of starch degradation rates is provided by the circadian clock.

The data described above also provide an explanation for the slow growth phenotype of the *cca1*/*lhy* mutant. In wildtype plants, transcripts of sugar repressed genes only increase when the night is artificially extended, whereas in *cca1/lyh* they increase some 3 h before the end of a normal night, approximately when the plant runs out of starch (Graf *et al.*, 2010). This indicates that the plant is experiencing carbon starvation at the end of the night, which will have a negative impact on growth.

Evidence that starvation at night and reduced growth can be caused by a mistiming of starch degradation was provided by experiments in which wildtype plants were grown in 14 h light, 14 h dark cycles in the presence of exogenous sugars. Plants grown without sugars in these conditions run out of starch before dawn and are retarded in growth relative to plants grown in 12 h light, 12 h dark cycles. However the addition of exogenous sugars abolished differences in growth between the 12/12 and the 14/14 conditions (Graf *et al.*, 2010).

1.4.2.2 Measuring starch

The mechanism by which the amount of starch in the chloroplast is measured is not known. How the mass of a solid object might be sensed is an intriguing problem, since proteins are generally responsive to concentrations of molecules, not the amount or mass of a substance. One way to resolve the problem would be to represent the mass information in the concentration of a stromal molecule which could then allosterically regulate the enzymes of starch degradation. For example a molecule could become sequestered into the starch granule as it grows, such that its concentration in the stroma is inversely proportional to the amount of starch. Alternatively, one of the enzymes of starch synthesis could produce regulatory molecules in proportion to the flux through

the starch synthesis pathway. For instance, AGPase might make GDP-glucose at a low frequency, proportional to the amount of ADP-glucose. The concentration of GDP-glucose in the stroma would then be proportional to the amount of starch. GDP-glucose is found in plants and incorporated into cell wall polysaccharides (Barber and Hassid, 1964; Piro *et al.*, 1993), but whether it is found in the plastid is unknown. A mechanism to degrade the GDP-glucose at night would also be required. Some enzymes of nucleotide sugar metabolism have already been shown to catalyse reactions using several alternative substrates. VTC2, for example, is a cytosolic enzyme of ascorbate biosynthesis whose primary role is to generate L-galctose-1-phophate from GDP-L-galactose but also produces GDP-mannose from D-mannose-1-phosphate as part of the reaction (Linster and Clarke, 2008). The enzymes has low affinity for other sugar phosphate substrates substrates, with the exception of glucose-1-phosphate, which it may use to produce GDP-glucose at appreciable rates (Linster *et al.*, 2007). Similarly, a VTC2 homologue from *Caenorhabditis elegans* has a primary role as a GDP-D-mannose pyrophosphorylase, but can also accept glucose-1-phosphate as a substrate, producing GDP-glucose in an aberrant side reaction (Adler *et al.*, 2011).

There is no evidence for or against the sequestration hypothesis, but there is some evidence against the idea that starch quantity is sensed by the accumulation of a by-product of synthesis. The Arabidopsis *isa1*and *isa2* mutants accumulate a large amount of soluble glucan (phytoglycogen) over the diurnal cycle, but also some starch. Similar to a wildtype plant, the *isa* mutants degrade starch in a linear fashion such that reserves run out at dawn (Delatte *et al.*, 2005; Streb *et al.*, 2008). If a by-product of a starch synthetic enzyme contributed to setting the rate of degradation then one would expect the *isa* mutant to ‘overestimate’ the amount of starch and set a degradation rate which is too fast.

Starch could potentially be measured more directly, for example by proteins which sense the curvature of the granule. Even in the case of the flattened granules of Arabidopsis leaves, the maximum curvature of the granule surface should decrease through the day. There are a few examples of proteins which are sensitive to curvature. The *Bacillus subtillis* membrane protein SpoVM localises specifically to membranes with a convex curvature (Ramamurthi *et al.*, 2009). It is thought that SpoVM may have to act in large oligomers to effectively sense curvature on such large scale relative to the

size of the protein. Other studies have found Golgi associated proteins in yeast which associate with vesicles in a curvature dependent manner (Bigay *et al.*, 2005). These proteins may sense defects in structure that become more pronounced on more tightly curved surfaces.

Starch volume could also be measured indirectly by mechanosensitive ion channels sensing membrane distortion caused by starch accumulation. Mechanosensitive ion channels have been characterised from the inner chloroplast envelope and Arabidopsis mutants in the genes concerned have severely altered plastid morphology (Haswell and Meyerowitz, 2006). Further characterisation of these mutants might provide clues as to how starch is measured. Alternatively, the starch might interact with a hypothetical 'plastoskeleton', formed by orthologues of the bacterial cyctoskeletal element FtsZ. This putative mechanism is broadly analogous to a mechanism by which statolithic amyloplasts are thought to operate in gravitropic responses. As amyloplasts follow the gravity vector, they interact with the F-actin cytoskeleton via the J-domain protein ALTERED RESPONSE TO GRAVITY 1 which then may initiate further signalling (Morita, 2010). However mutants altered in hypothetical plastoskeletal components do not show alterations in starch turnover (Crumpton-Taylor *et al.*, 2012).

1.4.2.3 Performing arithmetic division

A mechanism must exist to divide the amount of starch by the amount of time remaining until dawn such that an appropriate rate of degradation can be calculated. There are two lines of evidence to suggest that such a calculation is likely to be post-translational. First, starch degradation rates become correctly adjusted within two hours of an early dusk (Graf *et al.*, 2010), so the division calculation must happen within this period, and probably occurs much faster. Second, where protein levels for enzymes of starch degradation have been measured over the diel cycle, only very slight changes in abundance are detected (Chia *et al.*, 2004; Smith *et al.*, 2004; Lu *et al.*, 2005; Yu *et al.*, 2005).

Arithmetic division could potentially be implemented at a post-translational level through chemical kinetics (Scialdone, A. Mugford, S. Skeffington, A. Borrill, P. Graf, A. Pullen, N. Morris, R. Smith, A.M. Howard M. Submitted). An example of such a model is as follows (courtesy of Antonio Scialdone and Martin Howard). Consider a

molecule T, whose concentration is proportional to the time remaining until dawn and a molecule S, whose concentration is proportional to the amount of starch present. Both S and T will bind a third molecule M. When S is bound to M, the action of the resulting SM complex degrades the starch granule. However S, T and TM will not degrade the granule. Thus, as the amount of starch increases, the concentration of SM increases and the granule is degraded at a faster rate. As the amount of T increases, the concentration of TM increases and M is titrated away from the SM complex. This results in a lower concentration of SM and lower rates of starch degradation. Thus the rate of starch degradation is proportional to S divided by T, so arithmetic division is effectively implemented.

1.5 Regulating the enzymes of starch degradation

Information about the amount of starch and the time until dawn must ultimately feed into the regulation of the enzymes of starch degradation, such that an appropriate rate can be set. At present there is no evidence beyond the circumstantial as to which enzymes in the pathway might be regulated to change flux. The clues that we do have are summarised in the subsequent sections. These include known properties of enzymes in the pathway which could used for regulation *in vivo*, as well as arguments based on the phenotypes of mutant plants and the thermodynamic structure of the pathway. I shall argue that GWD is a good candidate for an enzyme which might be regulated to influence flux.

Throughout the discussion below, it is worth remembering that the control of pathway flux may well be distributed amongst many of the enzymes of starch degradation. Theoretical development combined with experimental validation over the past 40 years has established the concept of distributed control as the paradigm for the organisation of metabolic systems (Kacser and Burns, 1973; Stitt *et al.*, 2010). Parallel activation of enzymes to achieve changes in flux may have several advantages over regulation of a single “rate limiting” enzyme . First, changes in flux are achieved without large changes in the size of metabolic pools. Indeed empirical studies support this view. For example, the onset of thermogenesis in the spadix of *Arum maculatum* was accompanied by a 50 fold increase in glycolytic flux with no detectable changes in the concentrations of any glycolytic intermediates except fructose-1,6-bisphosphate (ap Rees *et al.*, 1977).

Likewise, the concentrations of Calvin cycle intermediates are quite independent of the net rate of photosynthesis (Arrivault *et al.*, 2009). Second, the potential dynamic range of pathway flux will be greater than could be achieved by modulating a single enzyme. If the V_{max} of a single enzyme is increased, then its control of the pathway will, in most cases, decrease, thereby attenuating any further increases in flux on further enhancement of V_{max}. Third, if a single enzyme has high control over flux, then the concentrations of other enzymes in the pathway could be decreased without affecting flux. Thus shared control represents a parsimonious use of resources (Brown, 2010). In either the shared control case or the rate limiting step case, rapid increases in flux are possible through post-transcriptional regulation as long as there is sufficient capacity in the pathway.

It should be noted that parallel activation does not mean that each enzyme must be the target of a signalling pathway external to the metabolic pathway. The velocities of reactions operating close to equilibrium are extremely sensitive to changes in the concentrations of reactants and products. Thus if the pathway flux upstream increases, leading to an accumulation of reactants, the rate of reaction will increase to restore equilibrium without the need for external regulation.

1.5.1 Properties of the genes and enzymes of starch degradation which might be relevant for control of the pathway

Below I summarise the known features of the genes and enzymes involved in leaf starch degradation which might have relevance for regulation.

1.5.1.1 Transcriptional regulation

Many of the starch degradation genes are co-regulated, with peak transcript abundance at dusk. The genes in this co-regulated set are: *GWD1, PWD, SEX4, ISA3, AMY3, DPE1, DPE2, PHS1, PHS2* and *SBE3* (Smith *et al.*, 2004). It is surprising to see *SBE3* in this set, because it is not normally thought to function in starch degradation. One could speculate that the pattern of transcript abundance reflects a need for increased abundances of the enzymes at dusk for the initiation of starch degradation. However, immunoblotting has been used to show that protein levels of AtGWD, AMY3 and DPE2 do not change substantially over a diel cycle (Yu *et al.*, 2001; Smith *et al.*, 2004; Lu *et al.*, 2005; Yu *et al.*, 2005). These changes in transcription could still have significance for regulation on a daily basis if the proteins are subject to rapid turnover or

if flux is sensitive to small changes in the amount of enzyme. The role of transcriptional regulation is explored further in chapter 3.

1.5.1.2 Redox regulation

Redox regulation is a pervasive theme in chloroplast metabolism. The redox sensitivity of proteins is normally dependent on disulphide linkages in the protein structure which may be reduced to free thiols, thereby modulating enzyme properties (Koenig *et al.*, 2012). Electrons for protein reduction in chloroplasts come ultimately from either ferredoxin reduced by photosystem I or from NADPH in the stroma. Downstream, ferredoxin dependent thioredoxin reductase (FTR) or NADPH dependent thioredoxin reductase (FNR) then reduce small redox transmitter proteins, thioredoxins (Trxs). There are tens of Trxs in Arabidopsis, which reduce specific target proteins. Disulphides in proteins can also be reduced by glutaredoxins, which gain electrons from the tripeptide redox buffer glutathione, and ultimately from NADPH (Rouhier *et al.*, 2008). Reactive oxygen species such as H_2O_2 then reoxidise the target thiols in reactions catalysed by peroxidases. These redox systems affect many different pathways. I have already discussed that both the Calvin cycle and starch synthesis may be activated by the reduction of disulphides in enzymes. Another example, is the activation of the maltate valve for dissipation of excess reducing power from the plastid. Reducing conditions in the stroma are signalled through the Fd/FTR/Trx system to NADP dependent malate dehydrogenase (MDH) resulting in reductive activation of the enzyme (Taniguchi and Miyake, 2012). NADP-MDH then catalyses the reduction of oxaloacetate to malate which is exported from the plastid, effectively transferring reducing equivalents from the stroma to the cytosol.

Several of the enzymes of starch degradation are known to have redox responsive properties *in vitro*. StGWD can be reductively activated by the addition of DTT or reduced Trx *f* and Trx *m* (Mikkelsen *et al.*, 2005). Oxidation of StGWD results in formation of a disulphide bridge between C1004 and C1008 close to the catalytic histidine and loss of activity. When C1008 is mutated to a serine the enzyme becomes constitutively active across a range of redox potentials. Similarly, recombinant BAM1 is activated *in vitro* by the addition of reduced Trx *f* or NTRC, and a cysteine involved in the disulphide was identified (Sparla *et al.*, 2006; Valerio *et al.*, 2011). The activity of recombinant SEX4 is also much decreased on oxidation with H_2O_2 (Sokolov *et al.*, 2006). Another study showed that a poplar leaf endoamylase could be reductively

activated by DTT and *E. coli* thioredoxin (Witt and Sauter, 1996). There are several lines of evidence to suggest that limit dextrinase (a debranching enzyme) can be redox responsive. First, overexpression of Trx *h* in barley endosperm leads to an increase in debranching activity (Cho *et al.*, 1999). Second, recombinant wheat limit dextrinase was activated by reduction (Repellin *et al.*, 2008). Third, recombinant limit dextrinase from spinach could be reduced and activated by reduced glutathione (Schindler *et al.*, 2001). Interestingly, reduction also broadened the pH range at which the enzyme is active. In physiological context this means that oxidised limit dextrinase would be inactive in the day (pH 8) but active at night (pH 7) (Werdan *et al.*, 1975) whereas the reduced form would be active across the physiological pH range.

Given the above data, proteomic screens for Trx interactors have identified surprisingly few proteins related to starch metabolism. For example, as far as I am aware, GWD has not been identified in any proteomic screen for Trx interactors (Lindahl and Kieselbach, 2009). Of course, if GWD only interacts with Trx when it is bound to the starch granule surface, it would probably not be identified by these approaches. A screen for Trx interactors in the spinach stroma pulled out BAM1 (TR-BAMY) as a potential target (Balmer *et al.*, 2003), providing some *in vivo* support for the *in vitro* data.

A recent study made a more comprehensive survey of the redox sensitivities of the enzymes of Arabidopsis starch metabolism (Glaring *et al.*, 2012). Gel based assays on crude protein extracts across a range of redox potentials demonstrated reductive activation for β-amylase, isoamylase, α-amylase and limit dextrinase as well as SS1, SS3 and BE2. Assays on extracts of mutant plants established that AMY3 provided the redox sensitive α-amylase activity, while BAM1 and BAM3 provided the redox sensitive β-amylase activity. BAM5 and DPE1 were redox insensitive. Enzyme assays of protein extracts demonstrated that PHS1 was irreversibly inactivated by oxidation with $CuCl_2$.

The relevance of redox regulation for starch degradation *in vitro* has yet to be established. It is noticeable that all the redox responsive enzymes in starch degradation are reductively activated. Given that starch degradation is active at night, when the chloroplast is in its most oxidised state, the relevance of reductive activation is not obvious. StGWD has a very positive redox mid-potential (-310 mV at pH 7.9, approx -

255 mV at pH7.0) (Mikkelsen *et al.*, 2005) so is perhaps less likely to be reduced *in vivo* than BAM1 which has a more negative redox mid-potential (-302 mV at pH 7.0) (Sparla *et al.*, 2006). Of course the chloroplast is not a uniform redox environment: electrons are channelled to particular targets in a highly specific manner dependent on protein-protein interaction. Thus, at night it may be that electrons from NADPH generated through the oxidative pentose phosphate pathway are used to specifically reduce and activate the enzymes of starch degradation. If this flow of reductant was regulated, it could provide a means to control the rate of starch degradation.

1.5.1.3 Other post-translational modifications

Protein phosphorylation is known to be crucial for the regulation of several chloroplast processes. For example, state transitions which control the relative excitation of photosystem I and photosystem II are dependent on the phosphorylation and dephosphorylation of light harvesting complex II by a specific kinase and a specific phosphatase (Tikkanen *et al.*, 2011; Samol *et al.*, 2012). A bioinformatics analysis in Arabidopsis identified 45 putative chloroplast protein kinases and 21 putative phosphatases (Schliebner *et al.*, 2008). Several attempts have been made to identify members of the plastidial phosphoproteome and these are compiled in the PhosPhAt database (Heazlewood *et al.*, 2008). GWD, GWD2, DPE2, AMY3, GLT1 and MEX1 are all phosphorylated according to mass spectrometry data recorded in this database. Although the database contains very recent studies, it omits the phosphoproteomic study of Lohrig *et al*. (2009), which finds that BAM3 and LDA are also phosphoproteins. The phosphorylated serine in GWD is within starch binding domain 1 (SBD1), pointing to a possible role in the regulation of starch binding.

The fact that a protein is phosphorylated does not mean that the phosphorylation status changes *in vivo*, or that changes in phosphorylation have any regulatory consequences. Reiland *et al*. (2009) began to address this point by quantitatively comparing the phosphoproteome one hour before dusk and one hour before dawn. Interestingly there were very few differences between these two time points, with the exception of the chloroplast ATPase β-subunit, which was exclusively phosphorylated at the end of the night. However no starch degradation related phosphoproteins were identified in their dataset. It should also be noted that the reproducibility of phosphoproteomic results between labs is at present doubtful. One study made use of stringent filters to select

high probability chloroplast phosphoproteins from three different experiments from different laboratories (Baginsky and Gruissem, 2009). The resulting lists contained 142, 49 and 54 chloroplastic phosphoproteins for the respective studies, but only 4 proteins were common between the lists.

Unique among proteins involved in starch metabolism, AtGWD is confirmed to be SUMOylated (Elrouby and Coupland, 2010). SUMO is a small (100 amino acid), ubiquitin-like peptide modifier which is known to have diverse roles in the regulation of cellular processes (Gareau and Lima, 2010). AtGWD has nine predicted SUMOylation sites (more than any other chloroplastic protein) and interacts with a SUMO ligase in yeast two hybrid screens. In addition it is SUMOylated by components of the Arabidopsis SUMOylation system when reconstituted in *E. coli* (Elrouby and Coupland, 2010). The function of GWD SUMOylation is completely unknown, and its relevance is explored further in chapter 5.

1.5.1.4 Regulation of protein localisation

Diel changes in sub-chloroplastic protein localisation have been observed for StGWD and for SEX4. In one experiment potato leaves or pea plants were incubated in either the light or the dark for several hours and starch was then isolated and dried (Ritte *et al.*, 2000). Starch granule associated GWD was defined as the amount of GWD released when isolated starch granules were heated in denaturing buffer. Interestingly, starch associated GWD was only detectable by immunoblotting if the starch was extracted from darkened leaves. Moreover, recombinant StGWD binds to starch granules isolated from darkened leaves more effectively than to granules isolated from illuminated leaves. This implies that changes in GWD binding are substantially due to changes in the granule at dusk rather than changes in GWD. Of course, changes in the granule at dusk could be mediated by GWD, creating a better substrate for GWD binding such that the effects of a small change in GWD become amplified.

Mikkelsen *et al.*(2005) suggest that changes in GWD localisation are primarily due to changes in the enzyme, rather than changes in the starch. Specifically they claim a relationship between the StGWD redox status and its starch binding capacity. Starch granules were isolated from illuminated or darkened potato leaves and incubated in 100 mM HEPES pH 7 alone or in the presence of either reduced Trx *f* or $CuCl_2$. After a

period of 30 min, samples were taken from the solution to measure GWD activity using a radioactive assay. The maximal catalytic activity (ie. in the presence of Trx *f*) was greater from granules extracted in the dark than in the light, consistent with the findings of Ritte *et al.* (2000). Addition of Trx *f* to the dark-isolated starch resulted in a large increase in activity as compared to the HEPES only control. For both light and dark isolated granules, oxidation with $CuCl_2$ caused a small decrease in activity (which was already low) in relation to the HEPES only control. The authors interpret these data to mean that starch associated GWD is mainly in the oxidised, inactive form in the dark. However their assumption that the activity they assay in the HEPES only condition reflects the activity of GWD when bound to potato starch granules *in vivo* is fanciful. Thus their conclusion, that redox status affects the affinity of GWD for starch, is not substantiated by their data.

SEX4 localisation is also reported to change through the diel cycle (Sokolov *et al.*, 2006). Soluble extracts or purified starch were subject to SDS-PAGE and immunoblotting at different times of day. In the day, SEX4 was exclusively found in the starch bound fraction, whereas during the night, SEX4 was exclusively found in the soluble fraction. Given that SEX4 is thought to function in starch degradation (Niittylä *et al.*, 2006; Kötting *et al.*, 2009), this result is hard to interpret. *In vitro* binding of recombinant SEX4 to corn starch seemed to require the protein to be in the reduced state (Sokolov *et al.*, 2006). When oxidised with H_2O_2 or oxidised glutathione, most of the protein remained in the soluble fraction. Although consistent with the daytime starch binding data, this result is again hard to reconcile with a principal function for SEX4 in starch degradation at night. SEX4 binding to starch in the light also does not fit with the fact (discussed in section 1.22) that turnover of *Chlamydomonas reinhardtii* starch phosphate only occurs in the dark (Ritte *et al.*, 2004). It might be that decreased steady state binding masks an increase in the number of transient, catalytic interactions SEX4 makes with the granule per unit time. Alternatively, it may be that the experiments described above do not reflect the *in vivo* situation.

1.5.1.5 Feedback regulation

There is mounting evidence that feedback regulation may operate at multiple points in the starch degradation pathway. First, the binding of StGWD and PWD to isolated *sex1-3* starch granules was enhanced by pre-phosphorylation of the granules by StGWD

(Kötting *et al.*, 2005). This suggests that a positive feedback loop may operate. Indeed starch granules isolated from Arabidopsis leaves become progressively better substrates for recombinant StGWD the further into the night they are harvested (Ritte *et al.*, 2004), although these experiments lacked controls for the expected increase in surface area to volume ratio. Positive feedback may also originate from mutual stimulation of enzyme activities. Granule phosphorylation by GWD *in vitro* stimulates granule degradation by BAM3 and vice versa (Edner *et al.*, 2007). The mutual stimulation effects operate if the enzymes act sequentially, but are enhanced if they act simultaneously. Positive feedbacks could serve to make the initiation of degradation more switch-like, such that reserves can be rapidly mobilised when they are required

Some of the enzymes also have characteristics that could result in feedback regulation. StGWD and SEX4 are inhibited *in vitro* by soluble, linear maltodextrins (Hejazi *et al.*, 2009; Hejazi *et al.*, 2010) . In addition, it has been found that pea epicotyl β-amylase is inhibited by maltose (Lizotte *et al.*, 1990). High maltose levels in the *mex1* and the *dpe2* mutants are also associated with starch accumulation (Chia *et al.*, 2004; Lu and Sharkey, 2004; Niittylä *et al.*, 2004), suggesting some form of feedback regulation. Thus end product accumulation may inhibit starch degradation if demand for carbon is decreased.

1.5.1.6 Protein- protein interactions

There is as yet no direct evidence for physical interactions between the enzymes of starch degradation. However, as previously discussed, there are two non-catalytic proteins known to be necessary for normal starch degradation: BAM4 and LSF1 (Fulton *et al.*, 2008; Comparot-Moss *et al.*, 2010). It is quite possible that these mediate interactions between the enzymes of starch degradation and /or the granule and thus could potentially have a regulatory role. In addition, both AtGWD and AMY3 are predicted to contain coiled-coil domains (Lohmeier-Vogel *et al.*, 2008), which are frequently associated with protein-protein interactions. The protein encoded by At5g39790 also contains both coiled coil domains and carbohydrate binding modules and appears to be chloroplast localised (Lohmeier-Vogel *et al.*, 2008). It is a protein of unknown function and will bind to starch *in vitro* so is an interesting candidate for a regulatory protein. Unfortunately there has been no *in vivo* characterisation of its function.

There is some evidence that GWD may be a target of 14-3-3 proteins. AtGWD was pulled down in a tandem affinity purification protocol aimed at identifying 14-3-3 protein interactors (Chang *et al.*, 2009). 14-3-3 proteins are phosphothreonine/phosphoserine binding proteins found throughout the Eukarya and regulate diverse cellular processes. For example, I have already described how 14-3-3 protein binding to phosphorylated nitrate reductase leads to inactivation of the enzyme in the dark (Lillo, 2008). Specifically, AtGWD was shown to interact with 14-3-3ω. Immunogold electron microscopy suggests that 14-3-3 proteins are present in the chloroplast (Sehnke *et al.*, 2000; Sehnke *et al.*, 2001), however 14-3-3ω is not predicted to have a transit peptide (using ChloroP), so how it might enter the chloroplast is unclear. Antisense reduction of the ε subgroup of 14-3-3 proteins in Arabidopsis was reported to lead to starch accumulation relative to wildtype, although this was only assessed by iodine staining of plants grown in continuous light (Sehnke *et al.*, 2001).

1.5.2 Other evidence pertinent to the regulation of starch degradation

1.5.2.1 Evidence for the role of granule phosphorylation in the regulation of starch degradation

The phenotypes of the *gwd*, *pwd* and *sex4* mutants clearly demonstrate the importance of the cycle of granule phosphorylation and dephosphorylation for normal starch degradation. There is also some circumstantial evidence that this cycle could be regulated to modulate flux through the pathway. First, as described in section 1.2.2, starch phosphate is only turned over in the dark in *C. reinhardtii* (Ritte et al., 2004). Thus the operation of the cycle of phosphorylation and dephosphorylation correlates with the operation of starch degradation. Second, starch surface phosphate increases on the light to dark transition. This was discovered by studying the phosphate content of glucans released from starch granules by a short isoamylase treatment. Potato leaf starch granules isolated at the end of the day contained barely detectable amounts of C6 phosphate, but the amount increased rapidly in the first hour of the night (Ritte *et al.*, 2004).

Further clues have come from the study of the turions (overwintering organs) of the duckweed *Spirodella polyrhiza*. Red light induces rapid starch degradation which supports germination of non-dormant turions (Appenroth and Ziegler, 2008). Interestingly, the amount of GWD bound to the turion starch declines rapidly on the

initiation of degradation and is accompanied by an increase in the autophosphorylation state of GWD (Reimann *et al.*, 2004). Thus, once again, a change in the properties of the starch phosphorylation system accompanies the onset of starch degradation.

1.5.2.2 The requirement for a starch granule

The proper regulation of storage glucan degradation in Arabidopsis seems to require the presence of a starch granule. Evidence for this comes from the *isa1* mutant which accumulates soluble glucans (phytoglycogen) during the day with only a small amount of starch. The phytoglycogen is broken down in an exponential manner, as would be expected for a reaction dependent on (limited by) the amount of substrate (Delatte *et al.*, 2005; Streb *et al.*, 2008). As the amount of substrate decreases, so does the rate of reaction. However, in *isa1*, starch is degraded in a linear fashion throughout the night. This implies that the structure of the starch granule is required for the normal regulation of storage glucan degradation. As previously discussed, the cycle of phosphorylation and dephosphorylation is thought to cause changes in granule structure, so the above data suggest that GWD, PWD and SEX4 may be important for the regulation of starch degradation.

The simplest explanation for the observed linear starch degradation pattern is that granule surface area does not limit the rate of degradation. Thus the rate of degradation must be largely limited by enzyme activity. However, from the exponential decrease in soluble glucans through the night in *isa1* it is probable that substrate availability (not enzyme activity) limits the rate of glucan degradation in this mutant. This is despite the presence of an accessible glucan pool much larger than that found in a wildtype chloroplast. Therefore one would also expect the hydrolytic enzymes of starch degradation to be substrate limited in a wildtype plant. Glucan degradation in *isa1* probably does not require the cycle of phosphorylation and dephosphorylation, since GWD has a very strong preference for crystalline substrates (Hejazi *et al.*, 2008). To summarise the above: starch degradation is probably enzyme limited in wildype, but the hydrolytic reactions probably do not limit the rate. Thus it seems likely that that most of the control of starch degradation lies with the enzymes responsible for phosphorylation and remodelling of the granule surface.

1.5.2.3 Thermodynamics

It is not possible to calculate precisely the thermodynamic driving force for a reaction in the cell without a knowledge of the concentrations of reactant and products and participating ions, pH and ionic strength. However, we can make reasonable judgements as to the sign and magnitude of free energy changes of relevant reactions. The first stage of starch granule breakdown can be summarised in two simplified steps:

$$\text{Glucan} + \text{ATP} \longrightarrow \text{AMP} + \text{Pi} + \text{P-glucan} \quad (1)$$

$$\text{Glucan}_{\text{crystalline}} \longrightarrow \text{Glucan}_{\text{hydrated}} \quad (2)$$

The free energy change of the reaction: glucose + ATP → ADP + glucose-6 phosphate is -21 kJ mol^{-1} at 25°C, pH 7, 3 mM Mg^{2+} and an ionic strength of 0.25 M (Alberty and Goldberg, 1992). Given that reaction (1) also involves the hydrolysis of ADP (for which $\Delta_r G'^{\circ}$ = -33 kJ mol^{-1}), it is likely that it will have a free energy change of the order of -50 kJ mol^{-1} under the standard conditions described. The thermodynamics of glucan hydration processes (2) have not been fully investigated. However, the free energy of solvation of α-D-glucose by water is known to be -95 kJ mol^{-1} (Dashnau *et al.*, 2005). Clearly the free energy of solvation will be rather different for an α-1,4 linked glucan which has fewer free hydroxyl groups, but one might still expect it to be large and negative. The free energy change of the decrease in glucan crystallinity would also have to be taken into account. In summary, although we cannot know the precise value, the free energy change of granule phosphorylation and hydration is likely to be large and negative.

The free energy change of hydrolysis of the glucose-glucose α-1,4 linkage in maltose has been estimated variously between -13 kJ mol^{-1} and -16 kJ mol^{-1} at 25°C (Tewari *et al.*, 2008). Enthalpies of hydrolysis of oligosaccharides can be estimated in an additive manner based on the enthalpies of hydrolysis of disaccharide units (Goldberg *et al.*, 1991). Thus the free energy change of hydrolytic release of a maltose unit from the end of a long glucan chain may be similar in sign and magnitude to the free energy of hydrolysis of maltose. Therefore one might expect a significant negative free energy change for the hydrolytic degradation of the starch granule, but not as large as the free energy change for granule phosphorylation and hydration.

As discussed previously, the disproportionation reactions in the stroma are believed to be driven almost entirely by entropy changes. At equilibrium, the concentration of malto-oligosaccharide products is a decreasing exponential function of chain length (Kartal *et al.*, 2011). In wildtype Arabidopsis plants at night there is more maltose than maltotriose and more maltotriose than maltoheptaose (Chia *et al.*, 2004). This might suggest that the disproportionation reactions are close to equilibrium in a wildtype plant.

The thermodynamic driving force for a reaction in a pathway and the degree displacement of a step from equilibrium are not directly relevant to the question of whether or not that step has any control over the pathway flux. However they may provide information about the likelihood of a step to be the subject of regulatory mechanisms. Specifically, the large and negative free energy change associated with granule phosphorylation and hydration means that if this reaction went to equilibrium the starch surface glucans would become extremely phosphorylated. It has been shown that restriction of ATP import into Arabidopsis chloroplasts leads to slow growth and necrotic lesions under short day conditions (Reinhold *et al.*, 2007). Thus, unregulated depletion of chloroplastic ATP at night could lead to similar problems. I would argue that the phosphorylation steps must be regulated to prevent this scenario. Howevere flux control and sites of regulation may still be distributed amongst enzymes of the pathway.

1.5.3 AtGWD as a candidate for an enzyme regulated to modulate flux

The properties of genes and proteins discussed above which might have relevance for the control of starch degradation are collated in Table 1.1. From this summary it is clear that AtGWD is associated with a great many properties which have regulatory potential.

Enzyme	Diel oscillations in transcript abundance	Redox responsive	SUMOylated	Phosphorylated	Evidence for feedback (negative or positive)	Interacts with other proteins?	Diel changes in protein localisation	Acts in cycle of granule phosphorylation	Essential for starch degradation?
GWD	✓	✓	✓	✓	✓	✓	✓	✓	✓
PWD	✓				✓			✓	
SEX4	✓	✓					✓	✓	
LSF1									
LSF2									
BAM1		✓							
BAM3		✓		✓	✓				
ISA3	✓	✓							
LDA1		✓		✓					
AMY3	✓	✓		✓					
DPE1	✓								
DPE2	✓			✓					
PHS1	✓								
PHS2	✓								
MEX1				✓					
GLT1				✓					

Table 1.1: Summary of the properties of the enzymes of starch degradation which might have regulatory relevance.

Based on the above discussion, I believe that AtGWD is likely to be one of the enzymes regulated for the control of flux through starch degradation, be this at the level of degradation initiation, the setting of the rate or both. First, it is clear that AtGWD is absolutely required for normal starch degradation: the mutant displays almost no decrease in starch content through the night. Second, in common with many of enzymes of starch degradation *AtGWD* displays large diurnal variation in transcript abundance which may have regulatory consequences. Third, the starch granule structure is required for the normal regulation of starch degradation, and AtGWD is a key part of the system which is thought to modulate that structure. Fourth, AtGWD catalyses granule phosphorylation, and the amount of surface phosphate on the granule increases as starch degradation is initiated. Fifth, the phosphorylation and hydration of the granule is probably associated with a large and negative free energy change, meaning that this step may be regulated for ATP homeostasis. Sixth, the granule association of GWD is

increased in the dark. Seventh, the GWD protein has numerous properties often associated with regulation. These include redox responsiveness in vitro, phosphorylation, SUMOylation, potential for feedback inhibition, feedforward interactions with other enzymes, confirmed interactions with 14-3-3 proteins and strongly predicted coiled coil domains hinting at physical interactions with other proteins.

Thus, although control may be distributed throughout the pathway, AtGWD is highly likely to be one of the enzymes regulated for the control of flux. The remainder of this thesis is dedicated to an investigation of the *in vivo* relevance of putative regulatory mechanisms acting on AtGWD.

1.6 Outline of experimental approach

In this thesis, I begin by examining the role of transcriptional regulation of *AtGWD* in the control of starch degradation. In chapter 3 I present a detailed analysis of plants expressing an inducible silencing construct targeted at *AtGWD*. This allows me to deduce the half life of the protein, its flux control coefficient and ultimately the importance of transcriptional regulation of AtGWD for the daily control of starch degradation. In addition, this approach provides new insights into the function of AtGWD in starch metabolism which are not evident from analysis of the full mutant. To study the post-translational regulation of AtGWD I first had to clone the gene and purify the protein. This was not trivial, and is presented in chapter 4. To assess the importance of known post-translational modifications of *AtGWD in vivo* I create versions of the gene which cannot be modified at key sites by redox regulation, phosphorylation and SUMOylation. These altered versions of *AtGWD* are expressed in the *gwd* mutant background to see if wildtype starch metabolism can be restored. In this manner, I deduce the *in vivo* importance of these post-translational modifications of AtGWD. The generation and analysis of these transgenic lines is described in chapter 5.

2 Materials and Methods

2.1 Supplier details

Suppliers for reagents and equipment are referred to by name only in the main text of this chapter. For contact details please refer to Table 2.1.

Company	Address	Website
3M Health Care	Neuss, Germany	http://solutions.3m.co.uk/
Agilent Technologies	Wokingham, Berkshire, UK	www.agilent.com/chem/uk
Applied Biosystems	Carlsbad, CA, USA	www.appliedbiosystems.com
BD Diagnostics	Oxford, UK	www.bd.com/uk/
Bearing Supplies Norwich Ltd	Norwich, UK	www.bearing-supplies.co.uk/
Bio-rad	Hemel Hempstead, Hertfordshire, UK	www.bio-rad.com
Corning Life Sciences	Amsterdam, The Netherlands	www.corning.com
Duchefa Biochemie	Ipswich, Suffolk, UK	www.duchefa.com
Eppendorf	Stevenage, Hertfordshire, UK	www.eppendorf.co.uk
Eurogentec	Seraing, Belgium	www.eurogentec.com
GE Healthcare	Little Chalfont, Bucks., UK	www.gehealthcare.com
GE silicones	Friendly, WV, USA	www.siliconeforbuilding.com
Geneflow Ltd	Fradley, Staffordshire, UK	www.geneflow.cuk
Jeyes	Thetford, Norfolk, UK	www.jeyes.com
Levington Horticulture	Ipswich, Suffolk, UK	N/A
Matrix Science	London, UK	www.matrixscience.com
MEGAzyme	Wicklow, Ireland	www.megazyme.com
Melford	Ipswich, Suffolk, UK	www.melford.c.o.uk
Millipore	Billerica, MA, USA	www.millipore.com
Molecular Devices	Wokingham, Berks, UK	www.moleculardevices.com
New England Biolabs	Hitchin, Hertfordshire, UK	www.neb.com
Nonlinear Dynamics	Newcastle, UK	www.nonlinear.com
Proteome Software Inc.	Portland, OR, USA	www.proteomesoftware.com
Qiagen Ltd	Crawley, UK	www.qiagen.com/
Roche	Basel, Switzerland	www.roche.co.uk/
SANYO	Watford, Hertfordshire, UK	http://uk.sanyo.com/

Sigma-Aldrich	Gillingham, Dorset, UK	http://www.sigmaaldrich.com
SPEX SamplePrep	Stanmore, London, UK	www.spexsampleprep.com
TECAN	Männedorf, Switzerland	www.tecan.com
Thermo Fisher Scientific Inc	Waltham, MA, USA	www.thermofisher.com

Table 2.1: Supplier details

2.2 Chemicals

Unless otherwise stated all chemicals were obtained from SIGMA or Melford.

2.3 Enzymes

All enzymes were ordered from SIGMA, Roche or MEGAzyme.

Enzyme	**Company**	**Catalogue Ref**	**Source**	**Concentration**
Amyloglucosidase	Roche	11202332001	*Aspergillus niger*	6 U mg^{-1}; 100 mg in 10 ml
α-amylase	Roche	10102814001	Pig pancreas	1000 U mg^{-1}; 50 mg ml^{-1}
Pullulanase	Roche	Discontinued	*Klebsiella pneumoniae*	720 U ml^{-1}
Hexokinase	Roche	11426362001	Yeast overproducer	1500 U ml^{-1}
Glucose 6-phosphate dehydrogenase	Roche	10165875001	*Leuconostoc mesenteroides*	1000 U ml^{-1}
Diaphorase	Sigma-Aldrich	D5540	*Clostridium kluyveri*	3 – 20 U mg^{-1}
Platinum™ Taq DNA polymerase high fidelity	Invitrogen	11304	N/A	5 U μl^{-1}
Taq DNA polymerase	Invitrogen	11508	N/A	5 U μl^{-1}
SuperScript® reverse transcriptase	Invitrogen	18080	N/A	200 U μl^{-1}
LR Clonase® II	Invitrogen	11791	N/A	2.5 U μl^{-1}
Restriction enzymes	Roche	N/A	N/A	N/A
RQ1 DNase 1	Promega	M610A	Bovine pancreas	1 U μl^{-1}

Table 2.2: Sources of Enzymes

2.4 Plant material

Throughout this thesis, the Columbia (Col-0; N1093) accession of *Arabidopsis thaliana* L. (Heynh) is referred to as wild-type. This line was originally provided by the Nottingham Arabidopsis Stock Centre (NASC) (University of Nottingham, UK).

The *glucan water dikinase* (*gwd*) / s*tarch excess 1* (*sex 1*) mutant used throughout this work, unless otherwise stated, was SALK_077211, which carries a T-DNA insertion in intron 11 of At1g10760. This line was originally obtained from Nottingham Arabidopsis Stock Centre (NASC) (University of Nottingham, UK) and homozygous lines were isolated by previous workers in the Smith lab.

2.5 Homogenisation of plant material

Unless otherwise stated, plant material for analysis was ground to a fine powder in 2 ml centrifuge tubes containing a 4 mm diameter stainless steel ball (Bearing Supplies) using a Geno/Grinder^{TM} 2000 (SPEX SamplePrep) at 500 strokes min^{-1} for 35 s. Samples were kept frozen during this process by packing the grinding blocks with dry ice.

2.6 Growth conditions

2.6.1 Media and selection

The media used for seedling and bacterial growth are described in Table 2.3

Medium	**Use**	**Ingredients**
Murashige and Skoog (MS) medium	For seed germination and seedling growth	Half strength Murashige and Skoog plant salt mixture (Duchefa Biochemie), 50 mg l^{-1} *myo*-inositol, 0.5 mg l^{-1} thiamine, 0.25 mg l^{-1} pyridoxine, 0.25 mg l^{-1} nicotinic acid, 0.25 g l^{-1} 2-[N-morpholino]-ethanesulphonic acid (MES), 0.8% (w/v) Bacto agar (Difco™; BD Diagnostics), pH 5.7 (KOH). No sucrose was added.
Luria-Bertani Broth (LB)	For bacterial growth	10 g l^{-1} Bacto-tryptone, 5 g l^{-1} bacto-yeast extract, 10 g l^{-1} NaCl, pH 7.0. For solid medium Bacto agar (Difco) was added to a final concentration of 1.5% (w/v)
Super Optimal broth with Catabolite repression (SOC)	For bacterial growth	20 g l^{-1} Bacto-tryptone, 5 g l^{-1} bacto-yeast extract, 0.5 g l^{-1} NaCl, 0.186 g l^{-1} KCl, pH 7.0, medium was autoclaved prior to addition of glucose to a final concentration of 20 mM and $MgCl_2$ to a final concentration of 2 mM.

Table 2.3: Media used for plants and bacteria.

The selective agents and antibiotics used to select bacterial strains and plant lines of interest are detailed in Table 2.4.

Selective agent	Final concentration	Solvent	Targets and mode of action
Ampicillin	100 μg ml^{-1}	dH_2O	Gram-negative bacteria. Inhibits transpeptidase and cell wall synthesis.
Gentamycin	50 μg ml^{-1}	dH_2O	Gram-negative bacteria. Inhibits ribosome function.
Rifampicin	10 μg ml^{-1}	methanol	Bacteria. Inhibits DNA dependent RNA Polymerase.
Spectinomycin	100 μg ml^{-1}	dH_2O	Bacteria. Inhibits translation initiation.
Hygromycin	50 μg ml^{-1}	dH_2O	Bacteria, fungi and plants. Inhibits translation.
Kanamycin	50 μg ml^{-1} (*E.coli*)	dH_2O	Bacteria, fungi and plants. Inhibits translation initiation.
Chloramphenicol	34 μg ml^{-1}	dH_2O	Bacteria. Inhibits translation elongation.
Phosphinothricin (Glufosinate ; BASTA)	100 μg ml^{-1}	dH_2O	Plants. Glutamine synthetase inhibitor.

Table 2.4: Antibiotic concentrations in selective media

2.6.2 Growth on plates

Dry seed was sterilised overnight in a vacuum desiccator filled with chlorine gas generated by adding 8 ml concentrated HCl (12 M) to 200 ml of thick bleach (Parazone, Jeyes). Sterile seed was left in open paper bags in a laminar flow hood for 30 min to dissipate the chlorine gas.

Seed was subsequently sown on MS agar plates, sealed with microporus tape (3M Health Care) and grown under a 16 h light, 8 h dark regime at 200 μmol photons m^{-2} s^{-1} for 10 days until the effects of selection were evident. Selected plants were transferred to soil.

2.6.3 Growth on soil

All plants used for phenotypic characterisation were germinated and grown on soil. Seeds were planted in trays (21 by 35 cm) containing 24, 40 or 60 cells filled with compost (Levington's F2, Levington Horticulture). Trays were covered in clear plastic

lids and kept at 4 ^{o}C in the dark for two days to allow the seed to stratify. Subsequently, trays were moved to either a growth cabinet (SANYO) or a controlled environment room (CER). The clear plastic lids were removed after 10 days.

CERs were kept at a constant 20 ^{o}C, 75% relative humidity with a 12 h photoperiod and 180 µmol photons m^{-2} s^{-1}. SANYO cabinets were run with the same conditions except the light intensity was 160 µmol photons m^{-2} s^{-1}. Where conditions differed from the above, they are described with each individual experiment.

Unless otherwise stated, leaf tissue was harvested at 21 days, equivalent to growth stage 3.50 - 3.70 according to Boyes *et al.* (2001).

Plants for seed production were grown in glasshouses under ambient light conditions, with supplementary lighting as required to provide a 16 h photoperiod. Seeds were harvested by bagging inflorescences as the siliques developed and then allowing the plants to dry completely for at least two weeks.

Unless otherwise stated, leaf tissue for analysis was harvested 21 days post germination, frozen immediately in liquid nitrogen and stored at -80°C.

2.7 Bacterial strains

2.7.1 Strains used in work

Plasmid propagation and manipulation was largely carried out in *E. coli* strain DH5-α, with the exception of empty GATEWAY™ vectors still carrying the ccd lethality cassette, which were maintained in strain DB3.1. This strain has a DNA gyrase mutation (*gyrA462)* rendering it resistant to the *CcdB* lethal effect (Salmon *et al.*, 1994). Large plasmids containing *AtGWD* which had been subject to site directed mutagenesis were propagated in high transformation efficiency XL-10 Gold cells (Stratagene, Agilent Technologies). *A. tumefaciens* strain GV3101 was used for transient expression of proteins in tobacco leaves, and for floral dipping of Arabidopsis.

Strain	**Antibiotic resistance**	**Genotype and properties**	**Source / reference**
Escherichia coli			
Library efficiency DH5-α	None	F- φ80*lac*ZΔM15 Δ (*lac*ZYA-*arg*F)U169 *rec*A1 *end*A1 *hsd*R17(rk-, mk+) *pho*A *sup*E44 *thi*-1 *gyr*A96 *rel*A1	Invitrogen (Hanahan, 1983)
TOP10	Streptomycin	F- *mcrA* (*mrr-hsdRMS-mcrBC*) *80lacZM15 lacX74 recA1 ara139* (ara-leu)7697 *galU galK rpsL* (Str^R) *endA1 nupG*	Invitrogen (Hanahan, 1983)
DB3.1	Streptomycin	F- *gyrA462 endA1* D*(sr1-recA) mcrB mrrhsdS20* (rB-, mB-) *SupE44 ara14 galK2 lacY1proA2 rpsL20 xyl5 _leu mtl*	Invitrogen (Hanahan, 1983)
XL-10 Gold	Tetracyclin	Δ*(mcrA)183* Δ*(mcrCB-hsdSMR-mrr)173 endA1 supE44 thi-1 recA1 gyrA96 relA1 lac* Hte [F' *proAB lacIqZΔM15 Tn10* Amy]	Stratagene / Agilent Technologies
Agrobacterium tumefaciens			
GV3101	Rifampicin (on chromosome), Gentamycin (on helper plasmid)	pMP90 (pTiC58ΔT-DNA), genes for nopaline biosynthesis	Van Larebeke *et al.* (1973)

Table 2.5: Bacterial strains.

2.8 Plasmids

Vectors used for cloning are described in Table 2.6.

Gateway Vector	Resistance	Description	Source
pCR8/GW/TOPO TA	Spectinomycin	Vector for cloning DNA fragments with terminal 3' A-overhangs	Invitrogen
pCR2.1	Kanamycin Ampicillin	TOPO TA entry vector for the cloning of DNA fragments with 3' A-overhangs. Insertion disrupts *LacZ* to allow colony selection by β-galactosidase assay.	Invitrogen
pGreenII	Kanamycin	Binary vector for restriction cloning and plant transformation.	Dr Mark Smedley (JIC) (Hellens *et al.*, 2000)
pGW:LUC	Kanamycin BASTA (in plants)	Binary vector for the production of promoter luciferase fusions.	Dr Hailong An (JIC)
pOpoff2Hyg	Hygromycin	Vector system for the production of dexamethasone-inducible RNAi lines. LhGR transcription factor is constitutively expressed but activates transcription from the pOp6 promoter only when dexamethasone is present. pOp6 promoter drives expression of a hairpin RNA cassette.	(Wielopolska *et al.*, 2005) Craft *et al.* (2005b)
pB7FWG2	Spectinomycin BASTA (in plants)	Gateway binary vector for the expression of proteins in plants under control of the cauliflower mosaic virus 35S promoter. Provides a C-terminal GFP tag.	Dr Christine Faulkner (JIC) http://gateway.psb.ugent.be/search
pB7WG	Spectinomycin BASTA (in plants)	Gateway binary vector for the expression of proteins in plants. Vector provides no promoter. Adds a C-terminal GFP tag.	http://gateway.psb.ugent.be/search

Table 2.6: Cloning vectors

2.9 Oligonucleotides

All oligonucleotide primers used in this study are detailed in Table 2.7 and were ordered from Sigma-Aldrich. The ID number refers to the Alison Smith Lab primer database.

ID	Purpose	Sequence (5'-3')
	Sequencing primers	
1	*GWD* sequencing primer	TCAGTGACAAGAAAGCATGAG
2	*GWD* sequencing primer	ACCAGAATCTGCATCTAAATC
3	*GWD* sequencing primer	CTTTCTTATTTTCCATGTCAG
4	*GWD* sequencing primer	TAACAAACACCTATTTAGAGG
5	*GWD* sequencing primer	TGGTATATTGGACTGATCAGC
6	*GWD* sequencing primer	GATTGAGCATAAAACTGACCG
7	*GWD* sequencing primer	TGTTTGTTACTAAACTTTCCG
8	*GWD* sequencing primer	CGGAAGTAAAATCTTTTACAG
9	*GWD* sequencing primer	CGGTCAGTTTTATGCTCAATC
10	*GWD* sequencing primer	GTATAGCCGACTCAAGGTCTG
11	*GWD* sequencing primer	CTGTAAAAGATTTTACTTCCG
12	*GWD* sequencing primer	CATTGTCATCTGAAGAGAGGG
13	*GWD* sequencing primer	CAGACCTTGAGTCGGCTATAC
14	*GWD* sequencing primer	CACAACAATGACATATCCGAC
15	*GWD* sequencing primer	CCCTCTCTTCAGATGACAATG
16	*GWD* sequencing primer	CGGGAAAGTAAGAATCCAATA
17	*GWD* sequencing primer	GTCGGATATGTCATTGTTGTG
18	*GWD* sequencing primer	GTGTCTCAAGGTTCTCACGAC
19	*GWD* sequencing primer	TGACTTGGTTAGTGTGTAATG
20	*GWD* sequencing primer	CCGACCGGGATATGCTCCTAC
21	*GWD* sequencing primer	GTCGTGAGAACCTTGAGACAC
22	*GWD* sequencing primer	AGAATTTGATCACACTTGTGG
23	*GWD* sequencing primer	CTGACATGGAAAATAAGAAAG
24	*GWD* sequencing primer	GTAGGAGCATATCCCGGTCGG
353	Sequencing out of *AtGWD* promoter	GGGTTCAAGAAAGGAGAATGG
382	M13 F	CGACGTTGTAAAACGACGGCCAGT
383	M13 R	CACACAGGAAACAGCTATGACCATG
192	pCR8/GW/TOPO Sequencing primer GW1	GTTGCAACAAATTGATGAGCAATGC
193	pCR8/GW/TOPO Sequencing primer GW2	GTTGCAACAAATTGATGAGCAATTA
	Mutagenic primers	
615	Adding 6*His tag and stop codon to *pCR8::AtGWD* F	CAGACACGACCACAAGTGCGACATCACCATCACCA TCACTGATCGAAGGGCGAATTCGACCCAGC
626	Adding 6*His tag and stop codon to *pCR8::AtGWD* R	GCTGGGTCGAATTCGCCCTTTCAGTGATGGTGATGG TGATGCACTTGTGGTCGTGTCTG
773	Adding 6*His tag and stop codon to *pCR8::AtGWD* (native Promoter) F	GACACGACCACAAGTGCATCACCATCACCATCACT GATCAAATTCTCTGACC
774	Adding 6*His tag and stop codon to *pCR8::AtGWD* (native promoter) R	GGTCAGAGAATTTGATCAGTGATGGTGATGGTGAT GCACTTGTGGTCGTGTC
527	His1004-Arg (catalytic mutant) F	CATGCCGGATGTACTATCTCGTGTTTCTGTTCGAGC AAG
528	His1004-Arg (catalytic mutant) R	CTTGCTCGAACAGAAACACGAGATAGTACATCCGG CATG
531	Cys1019 – Ser (redox mutant) F	GAAAGATCTGCTTTGCCACATCTTTTGATTCTGGTA TCTTATCTGAC
532	Cys1019 – Ser (redox mutant) R	GTCAGATAAGATACCAGAATCAAAAGATGTGGCAA AGCAGATCTTTC
579	Ser161-Ala SBD1 F	GTGAAATCCGGTGGCAATGCACACCTTAAACTAGA

		G
580	Ser161-Ala in SBD1 R	CTCTAGTTTAAGGTGTGCATTGCCACCGGATTTCAC
636	Deletion W132 in SBD1 F	ATTTTCCATGTCAGAAATGTTCTACCTTCTCGCTCTC CG
637	Deletion W132 in SBD1 R	CGGAGAGCGAGAAGGTAGAACATTTCTGACATGGA AAAT
638	Deletion W405 in SBD2 F	TGTCTCAAAAGGGTGGAGAATTGGTAAGATAATTC TTC
639	Deletion W405 in SBD2 R	GAAGAATTATCTTACCAATTCTCCACCCTTTTGAGA CA
646	K164-R (SUMO mutant) F	GTGGCAATTCTCACCTTAGACTAGAGATAGATGATC CTGCC
647	K164-R (SUMO mutant) R	GGCAGGATCATCTATCTCTAGTCTAAGGTGAGAATT GCCAC
622	Insert an A to correct *AtGWD* promoter sequence	TTTTCCCAGGATCCATAACAAAAAAATATCTTTGAG AAAA
623	G-A to correct *AtGWD* promoter sequence	GGATATAATTGACATGATTGAACAAGTGGGCTT
624	T-C to correct *AtGWD* promoter sequence	TTTACCTTCAATTTCGATTGCTTTCGGTGTTTTTG
753	Adding TEV site before 6His *GWD* F	CAGACACGACCACAAGTGGAGAACCTTTACTTCCA GTCACATCACCATCACCATCAC
754	Adding TEV site before 6His *GWD* F	GTGATGGTGATGGTGATGTGACTGGAAGTAAAGGT TCTCCACTTGTGGTCGTGTCTG
	PCR primers	
305	Amplifying *AtGWD* promoter F	AATTTGCCGATAGAAATGTTTTC
306	Amplifying *AtGWD* promoter R	GCTTTCTTGTCACTGAATCAAACTT
356	Amplifying *AtGWD* genomic DNA with promoter F	GTGACAAAGACAAACACAAACT
366	Amplifying *AtGWD* genomic with 3'UTR R	AGTTTTCAGTTGCACTCAACTT
373	Amplifying *AtGWD* genomic with 3'UTR R	TTTTGATCTGCCAATCTTGCCAA
379	Amplifying *AtGWD* coding region genomic and cDNA F	ATGAGTAACTCTGTAGTGCATAAC
380	Amplifying *AtGWD* CDS or cDNA no stop codon R	CACTTGTGGTCGTGTCTGGAC
610	Left flanking primer *gwd* salk_077211	TCCGGTATGACAAGTCGAATC
611	Right flanking primer *gwd* salk_077211	GTCAGTCTATCCTGCGCTTTG
714	SALK T-DNA left border primer LB1.3 F	ATTTTGCCGATTTCGGAAC
10	R in *GWD* for use with border primer LB1.3	GTA TAG CCG ACT CAA GGT CTG
	cDNA Synthesis	
	Oligo dT	TTTTTTTTTTTTTTT
	QPCR primers	
696	At1g13320 PP2A subunit PDF2	TAACGTGGCCAAAATGATGC
697	At1g13320 PP2A subunit PDF2	GTTCTCCACAACCGCTTGGT

698	At4g26410 unknown protein	GAGCTGAAGTGGCTTCCATGAC
699	At4g26410 unknown protein	GGTCCGACATACCCATGATCC
700	At5g08290 mitosis protein YLS8	TTACTGTTTCGGTTGTTCTCCATTT
701	At5g08290 mitosis protein YLS8	CACTGAATCATGTTCGAAGCAAGT
702	At5g46630 clathrin adaptor complex subunit	AAGACAGTGAAGGTGCAACCTTACT
703	At5g46630 clathrin adaptor complex subunit	AGTTTTTGAGTTGTATTTGTCAGAGAAAG
285	Ubiquitin F	GGCTTGTATAATCCCTGATGAATAAG
286	Ubiquitin R	AAAGAGATAACAGGAACGAAACATAGT
297	*GWD* F	ACAACCTTGATTCGCCTCTG
298	*GWD* R	CGTCCATTGGTACACTGTCG

Table 2.7: Oligonucleotides used in this study. F, forward primers; R, reverse primers.

2.10 Molecular methods

2.10.1 DNA isolation from plants

Approximately 50 mg of ground plant material were extracted at 40°C in 250 µl of DNA extraction buffer (200 mM Tris-HCl (pH 9.0), 400 mM LiCl, 25 mM EDTA, 1% (w/v) SDS). Cell debris was pelleted by centrifugation at 20,000 g for 5 min. One volume of isopropanol was added to the supernatant with mixing by inversion. DNA was pelleted by centrifugation at 20,000 g for 10 min. The pellet was washed with 500 µl of 70% (v/v) ethanol, and subsequently centrifuged at 20,000 g for 2 min. The pellet was air dried and dissolved in 50 µl dH_2O.

2.10.2 DNA isolation from bacteria

Plasmid DNA from bacterial cultures grown overnight at 37°C in a shaking incubator was isolated with the QIAprep Spin Miniprep Kit according to the manufacturer's instructions (Qiagen).

2.10.3 PCR

Standard PCR reactions were performed using Taq DNA polymerase (Qiagen) in a final volume of 20 µl. PCR reaction components are described in Table 2.8 and cycling conditions are detailed in Table 2.9. PCR amplifications were performed in DYAD or DNA engine thermal cyclers (BioRad). For amplification of some problematic products, 3 % (v/v) DMSO and up to 3 mM $MgCl_2$ (final concentration) was added to the reaction. A negative and a positive control sample were included with each reaction.

High fidelity polymerase (Platinum™ High Fidelity Taq, Invotrogen) was used to amplify products for cloning.

Component		**Final Concentration**
Template DNA	Genomic	50 ng – 500 ng
	Plasmid	1 pg – 50 ng
DNA polymerase buffer with $MgCl_2$		1 x
Deoxyribonucleotides		250 – 500 µM
Each oligonucleotide primer		0.4 µM
Taq polymerase	Standard	0.1 U
	Platinum™ high fidelity	0.05 U

Table 2.8 Standard PCR composition

Step	**Temperature (°C)**		**Time (s)**	
	Taq	Platinum HF Taq	Taq	Platinum HF Taq
1	95	94	60	60
2	95	94	30	30
3	T_m - 5	T_m - 5	30	20
4	72	68	60 / kb	20 / kb
5	Repeat steps 2 – 4, 32 times			
6	72	68	120	120
7	Cool to 12°C			

Table 2.9 PCR cycle conditions

For colony PCR, part of a bacterial colony was added with a pipette tip to a standard PCR mix as described above. An additional 10 min lysis and denaturation step was performed at 95°C at the beginning of the reaction cycles.

2.10.4 Plasmid digests

Restriction digestion of plasmids was used as a diagnostic tool during cloning and mutagenesis to check plasmid identity and insert orientation. Approximately 250 ng of DNA were added to a 10 µl reaction containing 1 U of enzyme. Bovine serum albumin (BSA) and buffer were used at 1x concentration, according to the manufacturer's instructions (NewEngland Biolabs, Invitrogen or Roche). Reactions were carried out at 37°C for 2 h.

2.10.5 Agarose gel electrophoresis

PCR products (1 – 5 µl) were mixed with 5 x loading dye (50% (v/v) glycerol, 0.05% (w/v) Orange G) and loaded onto a 1% agarose gel, prepared using 1 x TAE buffer (40 mM Tris, 20 mM acetic acid, 1 mM EDTA, pH 8.0) and containing 0.01% (v/v) ethidium bromide. If the anticipated product was greater than 8 kb, 0.8% gels were used if less than 200 bp, 1.5% gels were used. DNA was visualised through fluorescence of the ethidium-DNA complex when exposed to ultraviolet (UV) light from a transilluminator. Gels were photographed using a Gel Doc 1000 system (Bio-Rad).

2.10.6 GATEWAY® cloning

The Gateway system was used as a fast and efficient means of transferring clones in the correct orientation between entry vectors and destination vectors (Walhout *et al.*, 2000).

2.10.6.1 Cloning into pCR8/GW/TOPO/TA

PCR products were generated with Platinum™ high fidelity polymerase (Invitrogen) which leaves 3'-A overhangs, so no additional A-tailing reaction was necessary. TOPO vectors such as pCR8 (Invitrogen) have DNA topoisomerase I covalently attached to each 3' end of the linearised plasmid. Initial annealing occurs between the 5' T-overhangs of the vector and the 3' A-overhangs of the PCR product before topoisomerase I acts to repair the double strand break. The TOPO TA reaction was carried out at 25°C for 1 h with components present as described in Table 2.10. Products of the reaction were transformed into *E. coli* strain DH5-α (Table 2.5) which was then plated on selective medium containing spectinomycin (Table 2.3).

Component	Amount
PCR product	1 µl
pCR8 Vector	0.5 µl
Salt solution (1.2 M NaCl, 60 mM $MgCl_2$)	0.5 µl
dH_20	2 µl

Table 2.10: Components of TOPO/TA cloning reaction

2.10.6.2 PvuI digestion of pCR8 entry clone

In cases in which pCR8 and the chosen destination vector shared the same selective marker it was necessary to cleave the vector containing the entry clone within the spectinomycin resistance gene. This was achieved by digesting for 2 h with the Pvu1 restriction enzyme (Invitrogen) at 37°C with reaction components as described in Table 2.11. The reaction was stopped by heating at 80°C for 10 min.

Component	Amount
pCR8 entry clone	2 µl (approx. 400 ng)
PvuI enzyme (Invitrogen)	2 µl
Buffer K (Invitrogen)	1 µl
dH_2O	5 µl

Table 2.11: Components of a *PvuI* digest

2.10.6.3 LR reactions

Clones in pCR8 were transferred to destination vectors through recombination reactions between the attL-sites in pCR8 and the attR-sites in the entry clone. The reaction was catalysed by LR clonase (Invitrogen) and carried out for 16 h at 25°C. Reaction components are described in Table 2.12.

Component	Amount
PvuI digested pCR8 entry clone	1 µl (approx. 80 ng)
Destination vector	1 µl (approx. 80 ng)
LR clonase	0.5 µl
TE buffer (10 mM Tris-HCl, 0.1 mM EDTA, pH 8.0)	2.5 µl

Table 2.12: Components of LR reactions

2.10.7 Site directed mutagenesis

Site directed mutagenesis was carried out using the XL single site kit (Stratagene, Agilent Technologies) according to the manufacturer's instructions. Briefly, mutagenic primers were used to amplify the entry clone for mutagenesis resulting in a mutagenised and non-methylated, single stranded copy of the plasmid. Next, the old strand was digested with DpnI which specifically cleaves methylated DNA. The single stranded, mutagenised plasmid was then transformed into *E. coli* for further amplification. Mutations were confirmed by sequencing (section 2.10.8).

2.10.8 DNA Sequencing

Sequencing reactions were performed using the ABI prism BigDye terminator kit v3.1 (Applied Biosystems) according to the manufacturers' instructions. Reactions contained approximately 100 ng of template DNA, 1 µl of 2 µM sequencing primer, 2 µl Big Dye sequencing buffer and 2 µl BigDye version 3.1 sequencing mix (Applied Biosystems). Extension conditions were as described in Table 2.13. Capillary sequencing and fluorescence detection of the reaction products was performed by the John Innes Centre Genome Laboratory on AbiPrism 3730XL and 3730 capillary sequencers (Applied Biosystems). DNA sequences were analysed using the Vector NTI Advance Suite 11 (Invitrogen)

Step	Temperature	Time
1	96°C	10 s
2	55°C	5 s
3	60°C	4 min
4	Repeat steps 1 to 3, 25 times	
5	Cool to 8^{o}C, store at -80 ^{o}C	

Table 2.13: Sequencing reaction conditions

2.11 Transformation of organisms

2.11.1 Transformation of *E.coli*

E. coli were transformed by the heat shock method. Frozen competent cells (20 – 40 µl) were thawed on ice and mixed with 2 µl of LR reaction products (section 2.10.6.3) or 1 – 4 µl of pure plasmid DNA (section 2.10.2) and incubated on ice for 30 min. The cells were then heat shocked at 42°C for 30 s and returned to ice for 2 min. One ml of SOC medium (Table 2.3) was added and the cells incubated at 30°C with gentle agitation for one h. Cells were plated on LB agar medium containing appropriate antibiotics and the plates incubated at 30°C for 2 days or until colonies appeared. Colonies were screened using colony PCR (section 2.10.3) or with diagnostic digests after plasmid preparation (section 2.10.4).

2.11.2 Transformation of *Agrobacterium tumefaciens*

To generate electrocompetent *A. tumefaciens,* cells of strain GV3101 were grown to an OD_{600} of 0.8 and washed 4 times in cold dH_2O, re-suspended in 10% glycerol, aliquoted and stored at -80°C. To transform the cells, approximately 100 ng of plasmid DNA were added to 40 µl of cells. The mixture was then placed in an electroporation cuvette (Geneflow Ltd) shocked at 200 Ω delivering a total of 2.5 V. One ml of SOC medium was added to the cells, which were then incubated with gentle agitation at 28°C for 4 h. Subsequently, cells were plated on LB-agar medium containing appropriate antibiotics and incubated at 28°C for 2 – 3 days, or until colonies appeared. Colonies were screened using colony PCR (section 2.10.3) or with diagnostic digests after plasmid preparation (section 2.10.2).

2.11.3 Stable transformation of Arabidopsis

Arabidopsis plants were grown in CER or glasshouse conditions until flowering. The first inflorescence was removed and plants grown for a further 8 to 10 days to encourage the production of secondary inflorescences. *Agrobacterium* strains transformed with the appropriate plasmid were grown in 200 ml LB medium containing the appropriate antibiotics at 28°C with vigorous agitation to an OD_{600} of 1. Cells were pelleted by centrifugation at 2,500 *g* for 15 min at 20°C and then resuspended in 200 ml of infiltration medium (5% (w/v) sucrose, 0.05% Silwet® L-77 (GE silicones) 0.1 mM acetosyringone, 3 mM MES pH 5.5, (Clough and Bent, 1998)). Cultures were left to

gain virulence for one h at room temperature in the dark. Infloresences were dipped into beakers containing the cell suspensions and gently agitated for one to two min. The infiltrated plants were placed in clear plastic bags and kept shaded for 24 h before being returned to the glasshouse to set seed.

2.11.4 Transient expression in *Nicotiana benthamiana*

Agrobacterium strains containing the plasmid of interest were grown in 200 ml LB medium containing the appropriate antibiotics at 28ºC with vigorous agitation to an OD_{600} of 1. Cells were pelleted by centrifugation at 2,500 *g* for 15 min at 20°C and then resuspended in 200 ml 50 mM MES pH 5.5, 10 mM $MgCl_2$, 0.1 mM acetosyringone. The culture containing the plasmid of interest and the culture containing the P19 suppressor of silencing (Voinnet *et al.*, 2003) were diluted to OD 0.8 and then mixed in a 1:1 (v/v) ratio and left in the dark for two to three h to gain virulence. The mixture was then infiltrated into the intracellular space of an *N. benthamiana* leaf using a syringe pressed against a shallow scratch in the abaxial side of the leaf. Leaves were examined under the confocal microscope 3 – 5 days post infiltration, or harvested for protein extraction 9 days post infiltration.

2.12 SDS PAGE

Sodium dodecylsulphate polyacrylamide gel electrophoresis (SDS PAGE) was used in combination with immunoblotting for the analysis of purified proteins and for characterising transformants.

2.12.1 Preparation of extracts

Plant material was placed in a tube with a 4mm diameter steel ball and ground by shaking at 500 strokes per minute for 35 seconds in a Genogrinder (www.spexsampleprep.com). Samples were kept on dry ice during grinding. A known amount of ground plant material was mixed vigorously with a 1:5 ratio (m/v) of protein extraction buffer (100 mM HEPES pH 7.0, 33 µl ml^{-1} plant protease inhibitor (Sigma), 20 mg PVP) then centrifuged at 20,000 *g* for 10 min at 4°C. The supernatant was removed and diluted 1:1 (v/v) in 2 × Laemmli sample buffer (120 mM Tris HCl pH 6.8, 3.4% SDS, 12% w/v glycerol, 200 mM DTT, 0.04% (m/v) bromophenol blue). The samples were incubated at 80°C for 10 min and allowed to cool before 12 µl were loaded onto the SDS-polyacrylamide gel.

2.12.2 Gels and running conditions

Protein samples were run on either laboratory-prepared SDS-polyacrylamide gels (Table 2.14) with trs-glycine running buffer (125 mM Tris-HCl pH 8.3, 960 mM glycine, 5% w/v SDS), or on pre-cast NuPAGE® 4 – 12% Bis-Tris gels (Invitrogen) according to the manufacturer's instructions with a MES SDS running buffer. Gels were run at 100 V for 30 min and then at 200 V until the required separation was achieved. Prestained protein markers (10 – 230 kDa, New England Biolabs) were used for protein size estimation. Gels were either used for immunoblotting or stained with InstantBlue™ (New England Biolabs) to visualise bands.

Component	Stacking Gel	Separating Gel
Tris HCl	pH 6.8; 125 mM	pH 8.8; 375 mM
SDS	0.1% (w/v)	0.1% (w/v)
Acrylamide : bis acrylamide (37.5:1)	3.9 % (w/v)	7.5 % (w/v)
Ammonium persulphate	0.05 % (w/v)	0.05 % (w/v)
TEMED	0.1 % (v/v)	0.1 % (v/v)

Table 2.14 Components of SDS polyacrylamide gels

2.13 Immunoblotting

Proteins were transferred from SDS gels to nitrocellulose using Trans-Blot SD transfer apparatus (Bio-Rad) according to the manufacturer's instructions. Blotting was carried out at 4°C and 100 V for 1 h. After blocking for 1 h with 3% (w/v) BSA and 2% (w/v) dried milk powder, blots were incubated with the primary antibody at a 1:1000 dilution at 4°C overnight. The blots were then developed similar to Blake *et al.* (1984) using a secondary antibody conjugated to alkaline phosphatase and the SIGMAFAST™ BCIP®/NBT reagent.

2.14 Protein band identification by mass spectrometry

Protein bands were excised from Coomassie-Blue stained gels and sent to the JIC proteomics service, run by Dr Gerhard Saalbach, for identification. As a first step, tryptic digests of samples were run on a matrix assisted laser desorption ionisation time

of flight (MALDI-TOF) mass spectrometer (Brucker Reflex III) and the resulting MS spectra compared to a database compiled from predicted digests of all predicted proteins in TAIR. Subsequently all samples were run on an LTQ-Orbitrap^{TM} mass spectrometer (Thermo Fisher Scientific) generating MS/MS data which were searched against the TAIR database. Scaffold viewer (version Scaffold_2_04_00, Proteome Software) was used to validate MS/MS based peptide and protein identifications and to view the data.

2.15 GWD quantification by mass spectrometry

Plant material was placed in a tube with a 4mm diameter steel ball and ground by shaking at 500 strokes per minute for 35 seconds in a Genogrinder (www.spexsampleprep.com). Sampes were kept on dry ice while grinding. The remainder of the work described in this section was carried out in the lab of Professor Wilhelm Gruissem (ETH, Zurich) under the supervision of Dr Alexander Graf. Frozen, ground plant leaf material (5 to 100 mg) was suspended in 200 µl of SDS extraction buffer (4% w/v SDS, 40 mM Tris, 60 µl ml^{-1} protease inhibitor cocktail (Roche)) and mixed vigorously to solubilise proteins. Cell debris were removed by centrifugation for 10 min at 16,000 g. The supernatant was further centrifuged at 100,000 g for 45 min in a Beckman ultracentrifuge (rotor: TLA 120.1). A small aliquot of the supernatant from ultracentrifugation was used for total protein determination using the bicinchoninic acid reagent according to the manufacturer's instructions (Pierce reagent, Thermo Scientific). The remaining supernatant was stored at -80°C.

Protein samples were diluted 1:1 (v/v) in Laemmli sample buffer and incubated at 65°C for 20 mins. Approximately 105 µl of total protein was loaded on a 10% SDS-polyacrlamide gel (using Protean II^{TM} gel apparatus, Bio-rad) which was run at 50 V overnight such that the 100 kDa marker had moved approximately 2 cm into the gel. Gels were stained for 45 min in Coommassie Blue solution (20% methanol, 10% acetic acid, 0.1 % Coomassie Brillinat Blue R) and then incubated in destaining solution A (50% methanol, 10 % acetic acid) for 2 h at room temperature. A 2 cm gel slice was cut from the top of each lane, including all the separating gel above the 100 kDa marker, and transferred to a 96 well, 1.2 ml storage plate (Fischer Scientific). The gel slices were washed 3 times with 1 ml of destaining solution B (50% methanol, 100 mM ammonium bicarbonate), incubating each time for 1 h at 37 °C. The washed slices were stored at -20°C.

The gel slices were washed once with 1 ml of water and then dehydrated by washing 3 times with 1 ml 50% acetonitrile, for 15 min each time, followed by drying for 2 h in a vacuum evaporator. Proteins were reduced by the addition of 1 ml of 10 mM dithiothreitol (DTT), 5 mM ammonium bicarbonate (pH 8.0) and incubating at 50°C for 45 min. The DTT solution was removed before alkylating free cysteines with 0.75 ml of 50 mM iodoacetamide, 50 mM ammonium bicarbonate (pH 8.0) for 90 min in the dark at room temperature. After removing the iodoacetamide, gel slices were again dehydrated by washing 3 times with 1 ml 50% acetonitrile for 15 min each time, and then drying for 2 h in a vacuum evaporator. Subsequently, 0.75 ml of 50 mM ammonium bicarbonate (pH 8.0) containing 3.6 mg trypsin was added, and the gel pieces allowed to re-swell at 4°C for 45 min before 0.25 ml of 50 mM ammonium bicarbonate solution were added to cover the gel slices completely. The tryptic digest was incubated overnight at 30°C.

The liquid from each digest was transferred to a 2 ml tube containing 20 µl 10% trifluoroacetic acid (TFA) and then centrifuged at 45°C under vacuum until the volume was reduced to approximately 0.2 ml. The gel slices were incubated with elution solution (5% formic acid, 50% acetonitrile) for 60 min at room temperature and then centrifuged at 5,200 g for 3 min. The supernatant was combined with the remaining supernatant from the tryptic digest and the tube returned to the vacuum centrifuge. This elution process was repeated 4 times and ended with a 60 min incubation at 45°C in the vacuum centrifuge to ensure that all acetonitrile had evaporated.

Finistere SPE columns (1 ml bed volume, packed with 100 mg C18; TR-F034000/10, WICOM International AG, 7304 Maienfeld, Switzerland) were wetted with 0.8 ml 100% methanol, followed by 0.8 ml SepPack elution buffer (60% acetonitrile, 0.1% TFA), then equilibrated by washing three times with 0.8 ml of 0.1% TFA. Twenty µl of 10% TFA were added to each sample before loading onto the column. Each sample tube was washed with 0.8 ml of 0.1% TFA and the washings also loaded on the column. The column was subsequently washed three times with 0.8 ml of 0.1% TFA before elution in 0.8µl of elution buffer. Eluate was collected in 2 ml centrifuge tubes and dried down completely at 45°C in the vacuum centrifuge. Peptides were stored at -80°C.

Peptides were resuspended by vigorous mixing in 40 µl of 3% acetonitrile, 0.1% formic acid, and centrifuged briefly. Measurements were performed on a LTQ-Orbitrap XL ETD (Thermo Scientific) coupled with a Probot autosampler system (LC-Packings/Dionex) and an UltiMate HPLC-system (LC-Packings/Dionex). The samples were loaded onto a laboratory made capillary column (75 µm inner diameter, 8 cm length, packed with Magic C18 AQ beads, 5 µm, 100 Å (Microm)) for 16 min at a flow rate of 0.5 µl min^{-1} in 3% acetonitrile, 0.2% formic acid. The peptides were eluted from the column by an acetonitrile concentration gradient from 5% acetonitrile, 0.2% formic acid to 40% acetonitrile, 0.2% formic acid over 70 min, followed by an increase to 80% acetonitrile, 0.2% formic acid over the subsequent 10 min at a flow rate of 0.25 µl min^{-1}. Peptide ions were detected in a full scan from 300 to 2000 m/z. MS/MS scans were performed for five peptides with the highest MS signal (minimal signal strength 500 hits, isolation width 3 m/z, relative collision energy 35 %). Peptides for which MS/MS spectra had been recorded were excluded from further MS/MS scans for 2 min.

Quantitative analysis of the MS/MS measurements was performed using Progenesis LCMS software (Nonlinear Dynamics). The RAW data files were imported into Progenesis LCMS and the pick picking time limited to between 20 min and 80 min of the LCMS run, while the full m/z range was imported. One run was selected as a standard and 15 vectors were placed manually on prominent peaks for each run before running the automatic alignment function of Progenesis which places 200 – 500 more vectors per run. Each run is manually curated to check for gaps before implementing the automatic peak picking function of Progenesis which collates relevant MS spectra for subsequent export to Mascot. Peak picking 'refinement' functions were not used. The Progenesis calculated normalisation factors, all between 0.8 and 1.2, were applied across the runs. Following this, the best 6 spectra for each peak are exported to Mascot as an MFG file for identification.

Mascot search parameters were set as follows: *A. thaliana* TAIR10 genome annotation, requirement for tryptic ends, one missed cleavage allowed, fixed modification: carbamidomethylation (cysteine), variable modification: oxidation (methionine), peptide mass tolerance = ± 1.2 Da, MS/MS tolerance = ± 0.6 Da, allowed peptide charges of +2 and +3. Additional modifications were not included so as to maximise the number of identifications. Spectra were also searched against a decoy database of the Arabidopsis

proteome in reverse amino acid sequences. This allows estimation of the false positive rate. A filter (created by Jonas Grossmann, Functional Genomics Centre Zurich, University of Zurich) was applied to the mascot search results to remove ambiguous identifications and all mascot identifications below rank one and the filtered XML file is exported to Progenesis. Peptides with a Mascot ion score below 25 were deleted. Peaks were then assigned identities in Progenesis and quantitative peak area information extracted, combined for a given protein and exported to Microsoft Excel for further analysis.

2.16 Measuring starch in Arabidopsis leaves

Starch was extracted from leaves using the perchloric acid method of Hargreaves and ap Rees (1988), modified for high throughput of samples in a 96 well format. The starch was then digested to free glucose and glucose phosphates and glucose determined with a coupled enzyme assay.

2.16.1 Starch extraction

Approximately 20 – 200 mg of ground Arabidopsis leaf tissue was mixed vigorously in 1 ml of 0.7 M perchloric acid. Aliquots of 400 µl were transferred two replicate 96 well 1.2 ml storage plates (Thermoscientific) and 300 µl of 100% ethanol was added to each aliquot. Samples were centrifuged at 3,000 *g* for 10 min to pellet the starch. The starch pellet was washed twice more in 600 µl of 80% ethanol and then incubated for 15 min at 95°C in 150 µl of dH_2O to gelatinise the starch. Once cool, 600 µl of 80% ethanol were added to the water and the plates centrifuged at 3,000 *g* for 10 min. The supernatant was removed and the pellet air dried for 20 min in a laminar flow hood. The pellet was re-suspended in 200 µl of dH_2O and stored at -20°C.

2.16.2 Starch digestion

The resuspended, gelatinised starch was made up to 390 µl with 0.2 M sodium acetate pH 4.8. To samples in one plate, 10 µl of a 9:1 (v/v) mixture of amyloglucosidase:α-amylase was added, while 10 µl of water was added to sample in the other plate. Samples were incubated overnight at 37°C and then used for glucose determination or stored at -20°C.

2.16.3 Glucose assay

Samples were mixed before centrifuging at 4500 g for 10 min. Glucose in the supernatant was assayed enzymatically according to Hargreaves and ap Rees (1988). Briefly, all the glucose was converted to glucose 6-phosphate with hexokinase and a blank reading was taken at 340 nm using a plate reader (SPECTRAmax 340PC, Molecular Devices), then glucose 6-phosphate dehydrogenase was added to each sample in the presence of NAD^+. The oxidation of glucose 6-phosphate was thus stoichiometrically coupled to the production of of NADH, which was detected by absorbance at 340 nm in a plate reader.

2.17 Iodine staining of Arabidopsis leaves

Arabidopsis rosette material was harvested into 80% (v/v) ethanol and heated at 60°C to remove all chlorophyll. The ethanol was removed and the decolourised tissue incubated with 50% (v/v) Lugol's solution (iodine/potassium iodide solution, Sigma Aldrich) for 10 min and then in dH_2O for 20 min to remove excess stain.

2.18 Measuring starch (surface) phosphate

The most used method for the quantification of starch phosphate (which relies on the reaction of orthophosphate with malachite green (Werner *et al.*, 2005; Kötting *et al.*, 2009)) lacks sensitivity, so large amounts of plant material are required to make measurements. Other methods based on NMR (Haebel *et al.*, 2008) or mass spectrometry (Ritte *et al.*, 2006) are expensive, slow and limit the numbers of samples that can be analysed. In this section I describe the use of a sensitive enzymatic method for the analysis of starch phosphate which circumvents the disadvantages of the other methods. This assay has not previously been used for the measurement of starch phosphate.

2.18.1 Purification of starch granules

Arabidopsis leaf material (2 – 10 g) was homogenised with a glass homogeniser in starch extraction buffer (20 mM HEPES (pH 8.0), 0.2 mM EDTA, 0.5% v/v Triton X 100) at 1:5 sample weight to buffer volume. The homogenate was filtered through a 100 μm nylon net before centrifugation for 5 min at 1,500 g. The starch pellet was re-suspended in 10 ml of starch extraction buffer and filtered successively through nylon meshes of pore size 60 μm, 30 μm and 15 μm. This filtered starch suspension was overlayed on a 10 ml Percoll cushion and centrifuged at 2,500 g for 15 min. After

carefully removing the supernatant, the starch pellet was re-suspended in 1 ml of 0.5% SDS and mixed vigorously before centrifugation at 20,000 g for 1 min. The supernatant was removed and 5 further washes with 0.5% SDS performed. Each time, before discarding the supernatant, the surface layer of the starch pellet was gently re-suspended with a pipette tip and discarded with the supernatant until the starch pellet was completely clean. Starch was stored at room temperature in 0.5% aqueous SDS (w/v).

2.18.2 Partial starch digests

Purified starch granules were washed in 1 ml of digest buffer (50 mM sodium acetate pH 4.8) and centrifuged at 20,000 g for 1 min before discarding the supernatant. This wash was repeated 6 times to remove all residual SDS. After the final centrifugation step, the wet mass of the starch pellet was measured. For each sample, a digest cocktail was made in 100 µl of digest buffer that contained 1.2×10^{-3} U amyloglucosidase and 0.05 U pullulanase for each mg of starch wet weight. The digest reaction was started by the addition of the starch suspension to the enzyme mix and then the reaction was incubated with vigorous shaking at 30°C for 30 min. The reaction was terminated by centrifugation at 20,000 g and 4°C for 4 minutes. The supernatant containing surface glucans was transferred to a fresh tube, and the starch pellet re-suspended in 100 µl of digest buffer.

2.18.3 Complete hydrolysis of starch and glucans

The re-suspended starch pellet was gelatinised by heating at 99°C for 30 min. Twenty µl of a 10: 1 (v/v) mixture of amyloglucosidase to α-amylase was added to the starch suspension, and the mixture incubated at 37°C overnight. To ensure complete hydrolysis to glucose and glucose phosphates, 46 µl of 4 M hydrochloric acid were added to the mixture which was then incubated at 99°C for 3 h. The samples were neutralised with 4 M sodium hydroxide.

2.18.4 Assay for glucose 6-phosphate

Glucose 6-phosphate (G6P) was measured exactly according to the fluorescence assay of Zhu *et al.* (2009), except that 50 mM HEPES was used instead of 50 mM triethanolamine. Briefly, all the G6P in the sample is used to reduce $NADP^+$, producing stoichiometric quantities of NADPH which is used by diaphorase to reduce resazurin to the fluorescent compound, resorufin (figure 2.1). The assay was started by the addition of the sample or standard to the assay cocktail in a flat bottomed, black 96 well plate

(Corning, Amsterdam, The Netherlands) and incubated at room temperature for 30 min. Fluorescence emission was recorded at 590 nm with excitation at 530 nm, using an Infinite M1000 plate reader (Tecan, Männedorf, Switzerland) operated with Megellan 7.1 software (Tecan) (one s linear shake 30 s before read, power at 302 W, band width 5 nm).

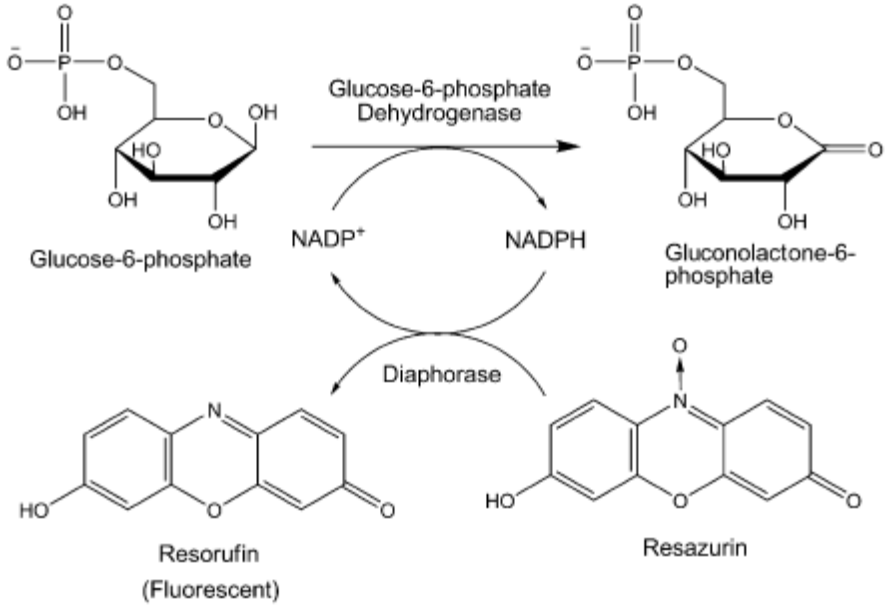

Figure 2.1: Mechanism of fluorescence based glucose 6-phosphate assay. Taken from Zhu *et al.* (2009).

2.19 Chromatographic methods

All automated purification procedures were carried out on ÄKTA® FPLC chromatographic system (GE Healthcare). The entire system was refrigerated at 4°C.

2.19.1 Nickel affinity chromatography

N. benthamiana tissue expressing AtGWD (see section 2.11.4) was ground in a glass homogeniser in extraction buffer (100 mM HEPES (pH 7.0), 25 mM imidazole, 250 mM NaCl, 33 µl ml^{-1} plant protease inhibitor (Sigma)) at a 1:4 ratio of sample weight to buffer volume. The extract was centrifuged for 15 min at 18,000 g and 4°C, and the supernatant was centrifuged again for 30 min at 30,000 g and 4°C. The supernatant was filtered through a 0.2 µm syringe filter (Millipore).

Sixteen ml of the extract was loaded at 0.5 ml min^{-1} onto a 1 ml Ni-sepharose HisTrap™ HP column (GE Healthcare) already equilibrated in extraction buffer (without protease inhibitor). After loading, the column was washed with 5 ml of 100 mM HEPES (pH 7.0), 25 mM imidazole, 250 mM NaCl, then eluted by increasing the imidazole concentration to 500 mM in a single step. The column was regenerated by washing with 8 ml of 500 mM imidazole buffer and then with 5 ml of extraction buffer.

2.19.2 Cobalt affinity chromatography

Co^{2+} affinity chromatography was performed as for Ni^{2+} affinity chromatography except 1 ml Co^{2+}-agarose HisPur Cobalt Spin Columns (Thermo Scientific) were used. The ÄKTA® FPLC was not used; instead, sample or buffer was forced over the column by centrifugation at 700 g.

2.19.3 Dextrin affinity chromatography

Protein eluted from the Ni-column was dialysed overnight against buffer A (40 mM MOPS pH7.4) at 4°C with stirring, against 1000 times the volume of the protein sample. One ml MBPTrap™ HP columns were equilibrated with 8 column volumes of buffer A before loading the sample. The column was washed with 4 column volumes of buffer A. Protein was eluted with 10 mg ml^{-1} β-cyclodextrin (Sigma) in buffer A. Fractions eluted were incubated at 80°C for 10 min after the addition of 1 vol of Laemmli sample buffer and analysed by SDS-PAGE (section 2.13)

2.19.4 Blue-Sepharose affinity chromatography

A 1 ml Blue (CL6B) Sepharose (Pharmacia, Uppsala, Sweden) gravity flow column was prepared and washed with buffer D (40 mM MES pH7.5, 10 mM $MgCl_2$, 2 mM DTT). Protein (equivalent to 4 g of *N. benthamiana* tissue) eluted from the Ni-column was loaded on the Blue column and then washed 3 times with 2 column volumes of buffer B. Bound protein was eluted first with 1 column volume of buffer E (40 mM MOPS pH 7.0) then with buffer E with 1 mM ATP and finally with buffer E with the addition of 1 M NaCl. Eluted proteins were concentrated on a 10 kDa MWCO Amicon Ultra filter (Millipore), stored at -80°C or diluted 1:1 (v/v) in Laemmli sample buffer, heated at 80°C for 10 min, then analysed by SDS-PAGE (see section 2.13).

2.19.5 Amylose affinity chromatography

Protein eluted from the Ni-column was dialysed overnight against buffer A (40 mM MOPS pH7.4) at 4°C, with stirring, against 1000 times the volume of the protein

sample. Amylose resin (high flow, New England Biolabs) was equilibrated by repeated washing in buffer A, and then poured to make a 1 ml gravity flow column. Protein recovered from dialysis was loaded onto the amylose resin column, washed with 4 column volumes (cv) of buffer A, before elution with 2 cv of buffer A containing 5 mg ml^{-1} potato dextrin (type IV, Sigma). Eluate was either concentrated on a 10 kDa MWCO centrifugal filter (Millipore), then flash frozen and stored at -80°C or diluted 1:1 (v/v) in Laemmli sample buffer, heated at 80°C for 10 min, then analysed by SDS-PAGE (see section 2.13).

2.20 Selective protein precipitation

Selective protein precipitation was carried out with either ammonium sulphate or acetone. Protein extract eluted from a Ni column, (section 2.19.1), was mixed with saturating ammonium sulphate or 100% acetone to reach a desired final concentration according the following formulae: where V_0 is the original volume of the sample; V_{sat} is the volume of saturating solution to be added to achieve the desired proportion of saturation P_F; and P_0 is the original proportion of saturation:

$$V_{sat} = \frac{V_0(P_0 - P_F)}{P_F - 1}$$

Immediately after addition of the saturating solution, the mixture was mixed vigorously and incubated for 15 min before centrifugation at 20,000 g for 10 min to collect precipitated proteins. During precipitation by ammonium sulphate the samples were kept at 4°C, and during precipitation by acetone samples were kept below 0°C by use of an ice/water/salt bath. Precipitated protein was resuspended in 50 µl of 40 mM HEPES (pH 7.0), diluted 1:1 (v/v) in Laemmli sample buffer and incubated at 80°C for 10 min then analysed by SDS-PAGE (see section 2.13)

2.21 Antibody preparation

Purified AtGWD protein (150 µg) was sent to Eurogentec for a 28-day rat immunisation programme. The crude serum from the terminal bleed was used directly for immunoblotting at a dilution of 1:500.

2.22 Quantifying gene expression

Gene expression was measured using reverse transcriptase (RT) quantitative polymerase chain reaction (Q-PCR).

2.22.1 RNA extraction

RNA was extracted from leaf tissue using the plant RNeasy^{TM} minikit (Quiagen) according the manufacturer's instructions.

2.22.2 cDNA synthesis

RNA was treated with DNase before cDNA synthesis. This reaction, as detailed in Table 1.15, was carried out for 20 min at 37°C before adding 1 µl of DNase STOP solution (Promega) and incubating for 10 min at 65°C.

Component	**Volume**
RNA (400 ng)	1 – 8 µl
10 × DNase buffer (Promega)	1 µl
DNase (Promega)	1 µl
dH_2O	To 10 µl

Table 2.15: Components of DNase treatment reaction

For cDNA synthesis, 2 µl of 50 ng µl^{-1} Oligo dT (16mer) primers were added to the stopped DNase reaction, and the mixture incubated at 70°C for 5 min. Subsequently, components of the cDNA synthesis reaction detailed in Table 2.16 were added, and the reaction incubated at 47°C for 60 min, then stopped by incubating at 75°C for 10 min. cDNA was stored at -20°C.

Component	**Volume**
5 × 1st strand buffer (Invitrogen)	4 µl
dNTPs (10 mM)	1 µl
DTT (100 mM)	1 µl
SuperScript® III reverse transcriptase (Invitrogen)	1 µl

Table 2.16: Components of cDNA synthesis reaction

2.22.3 Quantitative PCR

Q-PCR primers were designed to amplify a 250 bp – 400 bp region near the 3' end of a cDNA molecule, and if possible to overlap exon – exon boundaries. All primers were tested for linearity with respect to cDNA concentration, and only primers with close to 100% amplification efficiency were used. Reference genes (see Table 2.17) were chosen according to the detailed analysis of Czechowski *et al.* (2005), as genes especially stable over developmental and diurnal time courses. The primers for these genes are detailed in section 2.9.

TAIR ID	Gene function
At1g13320	PP2A subunit PDF2
At4g26410	Unknown protein
At5g08290	Mitosis protein YLS8
At5g46630	Clathrin adaptor complex subunit

Table 2.17: Reference genes chosen for Q-PCR

Q-PCR reactions contained 4 µl of 0.2 µM primer mix (forward and reverse), 5 µl of SYBR Green (Invitrogen) and 1 µl of cDNA. Cycle conditions are described in Table 2.18.

Step	Temperature	Time
1	95°C	2 min
2	95°C	30 s
3	60°C	1 min
4	Plate Read	
5	Repeat steps 2 – 4 34 times	
6	95°C	10 min
7	Melting curve: 65°C - 95°C in 0.5°C increments, holding for 5 s and reading between steps	

Table 2.18: Q-PCR reaction programme

Data were analysed by the ΔCT method (Hellemans *et al.*, 2007), except where multiple reference genes were used. In such cases a normalisation factor was calculated as the

geometric mean of CT values for all reference genes (Vandesompele *et al.*, 2002), where the CT values had been (arithmetic) mean-centred to prevent the introduction of bias due to missing data points. The resulting normalisation factor was then used in the same way as the raw reference gene CT values in the standard ΔCT method.

2.23 Confocal microscopy

Confocal microscopy was carried out using a Zeiss LSM 510 Meta system with the following settings: Excitation was at 10% power with a 458 nm argon laser and a 633 nm helium/neon laser. The main band pass filter was HFT 488 and the dichronic beam splitters 1, 2 and 3 were set at NFT 565, NFT 490 and plate respectively. Chlorophyll fluorescence was captured through a 636 nm – 754 nm band pass filter and a 10 μm pinhole, while GFP fluorescence was viewed through a 505 nm – 500 nm band pass filter with a 53 μm pinhole.

2.24 Statistical methods

Arithmetic means were compared using Student's unpaired, two tailed, two sample t-test with Bonferroni correction in the case of multiple comparisons.

Rates were compared by fitting the following linear model to the combined data from both treatments or genotypes in Genstat (12th edition):

$$Response\ variate = Time + Treatment\ A + Treatment\ B + Treatment\ A \times Treatment\ B$$

A p value < 0.05 for the interaction term indicated a significant difference between the gradients.

The standard error of the ratio of two means was calculated as follows (Rieu and Powers, 2009), where $\bar{x}_c$ is the control mean and $\bar{x}_T$ is the treatment mean:

$$Se\left(\frac{\bar{x}_T}{\bar{x}_C}\right) = \left[\frac{\bar{x}_T^2}{\bar{x}_C^2}\left(\frac{Se(\bar{x}_T)^2}{\bar{x}_T^2} + \frac{Se(\bar{x}_C)^2}{\bar{x}_C^2}\right)\right]^{\frac{1}{2}}$$

2.25 Software tools

Sequences were aligned and analysed using the Contig Express feature of the Vector NTY Advance Suite 11 (Invitrogen). Graphs were drawn in Sigma Plot and figures

made in the Corel Draw graphics suite. Tanagra (Rakotomala, 2005) was used for clustering analyses.

2.26 Band quantification

Bands from immunoblots or Coomassie Blue stained gels were quantified using Adobe Photoshop. Images were converted to greyscale and light and dark regions inverted before the perimeter of bands was outlined using the lasso tool. This region was selected as a new layer by copy, and the histogram display was used to find the pixel number and mean pixel intensity for the selection. These two quantities were multiplied and compared against a standard curve.

2.27 Measuring plant growth

Plant growth was measured as fresh weight of above ground biomass after a defined growth period, usually 21 days. Comparisons were always between plants grown in identical conditions.

3 The role of AtGWD transcript oscillations and protein turnover in daily starch metabolism

3.1 Introduction

In chapter 1, putative mechanisms for the regulation of starch degradation were discussed, and I concluded that AtGWD is a good candidate enzyme which might be regulated in the plant to change the rate of starch degradation. In this chapter I investigate the relevance of the large daily changes in *AtGWD* transcript abundance for starch degradation. In addition, I quantify the importance of transcriptional regulation and changes in AtGWD protein abundance to the regulation of starch degradation. A detailed analysis of a timecourse of inducible knockdown of *AtGWD* has been used to achieve these aims.

3.1.1 Daily patterns in *AtGWD* transcript and protein abundance

Some 89% of Arabidopsis transcripts show rhythmic changes in abundance under certain conditions (Michael *et al.*, 2008), while 31 – 41 % display genuine circadian regulation (Covington *et al.*, 2008), meaning that rhythms in transcript abundance will persist in the absence of changing external stimuli. Large transcriptomic experiments have shown that genes involved in the same biological process are often transcriptionally co-regulated under a variety of conditions, including over the diel cycle (Gachon *et al.*, 2005; Monnier *et al.*, 2010). This is true of starch degradation in Arabidopsis (figure 3.1), in which nine known enzymes of the pathway, including *AtGWD*, display large amplitude coordinated daily changes in transcript abundance with a peak at dusk (Smith *et al.*, 2004). Indeed, a search for genes with similar daily transcriptional patterns to the originally identified co-regulated set aided the identification of a new component of the starch degradation pathway, the glucan-phosphate phosphatase, SEX4 (Niittylä *et al.*, 2006).

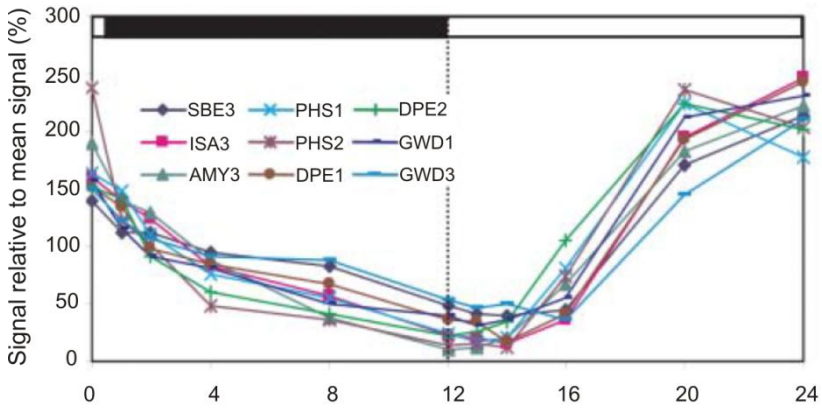

Figure 3.1: Diel patterns of transcript abundance for nine genes involved in starch metabolism. Modified from Smith *et al.,* (2004). Black bar indicates dark period, white bar indicates light period.

It is tempting to speculate from such results that co-regulation of starch degradation genes may be necessary for the daily regulation of starch degradation, especially since the peak expression of the set is at dusk, the time at which the starch degradation pathway becomes active. For some Arabidopsis genes it has been found that large daily oscillations in transcript abundance correlate with large daily oscillations in protein abundance. For example the day length sensor CONSTANS shows large daily changes in protein abundance in Arabidopsis (Imaizumi and Kay, 2006) as does Granule Bound Starch Synthase (GBSS) in sweet potato leaves (Wang *et al.*, 2001) and in Arabidopsis (Smith *et al.*, 2004). Conversely, there is evidence, based on immunoblotting, that AtGWD protein levels do not change dramatically over a diel cycle (Yu *et al.*, 2001; Lu *et al.*, 2005) despite the large changes in *AtGWD* transcript. This conclusion has been extended to *DPE2*, (Smith *et al.*, 2004; Lu *et al.*, 2005) and to *AMY3* (Yu *et al.*, 2005), again through immunoblotting. The generality of such relationships is hard to assess because there is a paucity of quantitative data on protein abundance over the day relative to the vast quantities of available transcript data.

3.1.2 Methods to study AtGWD protein over 24 hours

Although the existing immunoblots of AtGWD protein over 24 hours are sufficient to conclude that there are no drastic daily changes in abundance, immunoblotting is not sufficiently quantitative to reveal small but potentially significant changes in abundance. For example, if AtGWD were to have a high flux control coefficient for starch degradation, then a small change in protein amount would result in a large change

in flux. In this chapter I wanted to precisely quantify AtGWD over 24 hours to discover if there are changes in protein levels over a diel cycle or whether they are essentially constant.

Immunoblotting can be quantitative (Gassmann *et al.*, 2009), but is limited in dynamic range and the data obtained are sensitive to many steps in the protocol including total protein quantification, gel loading and band boundary definition, all of which introduce error. To avoid such pitfalls, I wanted to make use of quantitative proteomics to examine AtGWD levels. Original quantitative proteomic technologies were based on 2D polyacrylamide gel electrophoresis. Mass spectrometry is used to identify protein spots on the 2D gels, and quantification is achieved through comparison of spot intensities. This method suffers from similar pitfalls to those discussed for immunoblotting and at best only a few hundred proteins can be studied (Turck *et al.*, 2007) , so increasingly mass spectrometry (MS) data are being used for quantification. Typically, proteins are digested with trypsin, and then fractionated by liquid chromatography before injection into the mass spectrometer. In MS, the peptides are ionised and separated in an electromagnetic field in a manner dependent on their mass to charge (m/z) ratio. After an initial MS scan across the m/z range, peptides of interest can be selected within the magnetic field and fragmented by collisional activation. The the m/z of the resultant fragments is then used to deduce the sequence of the peptide (Domon and Aebersold, 2010). MS based quantification can be absolute if appropriate internal standards are used, but this is only possible for small numbers of proteins, so more commonly quantification is relative between samples. In practice this means that the area of a peak recorded for a given peptide is compared between samples. The signals from different peptides can never be compared because each peptide has a unique set of physiochemical properties which determine the mass spectrometric response (Bantscheff *et al.*, 2007).

There are two classes of methods for MS based protein quantification: label dependent and label free. Label dependent methods make use of the fact that stable iostopes can be incorporated into proteins or peptides resulting in a shift in mass without affecting the flight properties of the peptide. Labels can be introduced during growth of the organism by labelling of the carbon or nitrogen source, during digestion of the proteins through ^{18}O incorporation, or after digestion by chemically attaching isotope tags to the peptides

(Bantscheff *et al.*, 2007). Before MS, the labelled peptides (from one experimental treatment) are mixed with the unlabelled peptides (from another experimental treatment) so that resultant chromatogram shows two peaks for a given peptide, one for each treatment, separated by a small mass difference. Peak areas are then calculated and provide relative quantitation. However such methods are limited in the numbers of samples which can be compared (a maximum of eight at present using iTRAQ technology) and labelling can be expensive.

Label-free quantification strategies typically have larger dynamic range than label dependent ones and there are no theoretical limits to the number of samples which can be compared (Bantscheff *et al.*, 2007). There are two available strategies for label-free quantification. The first method simply counts the number of spectra matched to a given protein. An index based on the spectral count is strongly correlated with protein abundance (Ishihama *et al.*, 2005), although it is not suitable for proteins for which only a few spectra are collected. In addition, for any given protein, the index is not necessarily linear with protein abundance and the useful dynamic range may differ between proteins (Bantscheff *et al.*, 2007). The second method compares peak areas for peptides between samples, providing a more direct measure of relative protein abundance (Domon and Aebersold, 2010). Identifying equivalent peaks in different LC-MS runs is computationally intensive, but the results for individual proteins are much more reliable than those generated by spectral counting. In this chapter I use this label-free peak area based method for the quantification of AtGWD. It is more suitable than spectral counting because the quantification for an individual protein is reliable, particularly if it is an abundant protein like AtGWD for which multiple peptides can be detected. The chosen method also permits the comparison of many different timepoints which is crucial for my experiments. It would also be possible to focus the assay specifically on AtGWD using a process called selected reaction monitoring. In this method preliminary experiments are used to identify consistently observable peptides from the protein of interest and the elution time and m/z of those peptides (Domon and Aebersold, 2010). This information is then used to focus measurement time on the peptides of interest, resulting in a lower limit of detection. However peptides not included on a list defined by prior information will not be measured. In the experiments presented here, it was useful to measure other proteins beside AtGWD for validation of

the dataset and perhaps to provide useful new information, so the use of such a selective method was not appropriate.

3.1.3 Inducible RNAi as a tool to study AtGWD

Using the method outlined above it should be possible to precisely determine AtGWD protein levels over 24 hours. To understand the significance of any changes in protein abundance, it is necessary to know the flux control coefficient of the enzyme: how much the flux through starch degradation changes on a small change in AtGWD protein levels. For a better description of the system, the half life of the AtGWD protein should also be measured. This is because the transcriptional oscillations could be driving large daily changes in AtGWD protein turnover, perhaps with regulatory consequences. Such dynamics would not be revealed by measurements of steady state protein levels. In this chapter I make use of Arabidopsis plants expressing an inducible silencing (RNAi) construct targeted at *AtGWD* to address the above points. This line was made by Alex Graf when a PhD student in the Smith lab. I follow *AtGWD* transcript and protein levels, in addition to starch content over a timecourse of induction of the silencing construct. Protein levels are followed using the label free MS method described in secion 3.1.2. The resulting data allow me to quantitatively determine the half life of the protein and the flux control coefficient of the enzyme.

In general, inducible RNAi lines are an extremely useful tool with which to study the function of a gene. In a full knock out line, in contrast, the mutation is present throughout the life cycle of the plant so it is impossible or very difficult to distinguish primary and secondary effects of the mutation. A good example of this comes from the study of chloroplastic disproportionating enzyme, DPE1. Disproportionating enzymes transfer maltosyl units from one glucan chain to another (Takaha and Smith, 1999), and the Arabidopsis *dpe1*mutant has a starch excess phenotype (Critchley *et al.*, 2001). Starch from the mutant also contains more amylose than starch from a wildtype plant. However, from these data one cannot tell whether DPE1 has a direct role in amylose synthesis or whether the changed amylose content is a secondary effect of altered starch degradation. Likewise it could be that DPE1 has a primary role in starch synthesis, and the mutation has secondary consequences for starch degradation. To resolve these issues, *dpe1* and wildtype plants were ‘destarched’ by keeping them in the dark for 36 hours. Starch synthesis could then be compared in the mutant and wildtype, without

confounding by any alterations in metabolism the previous night. Starch synthesis proceeded at the same rate in *dpe1* and wildtype and there were no differences in amylose content, demonstrating that the primary role of DPE1 is in starch degradation, not starch synthesis (Critchley *et al.*, 2001). Of course, experiments like this are not possible if the phenotype of the mutant is more severe. For example, starch degradation is so strongly inhibited in the *gwd* mutant that it cannot be destarched with several days of darkness (Caspar *et al.*, 1991), so it is impossible to distinguish the role of AtGWD at different times of day from analysis of the mutant.

Inducible RNAi lines have the advantage that the transcript is abolished only in the presence of the inducer, so knock-down can be effectively achieved in an otherwise wild-type plant. By comparing the relative timing of phenotypic changes and the decreases in protein abundance, primary and secondary effects can be more easily distinguished. In this chapter I make use of a well characterised, dexamethasone inducible RNAi system called pOpOff (Craft *et al.*, 2005a; Wielopolska *et al.*, 2005). This system constitutively expresses a chimeric transcription factor in which the ligand binding domain of a rat glutocorticoid receptor is fused to the DNA binding region of a mutant LacI repressor and the transcription activation domain of Gal4. In the presence of dexamethosone the transcription factor will bind to 6 Lac operators and activate transcription from a minimal 35S promoter thus driving expression of the RNAi cassette. Dexamethasone is a good choice of inducer because it is foreign to plants and has been shown to be benign to Arabidopsis (Moore *et al.*, 2006). The pOpOff system has been successfully used by several other studies. For example it was successfully used to knock-down *γ-TUBULIN* transcript levels (Binarova *et al.*, 2006), while a construct targeted at *RETINOBLASTOMA-RELATED1* resulted in much reduced transcript levels only 24 hours post induction (Kuwabara *et al.*, 2011).

Two classes of methods for the study of protein half lives can be distinguished. The first is based on some form of pulse chase analysis. Traditionally this meant a transient radiolabelling of proteins, for example with ^{35}S-methionine, and then removing the labelling agent and following the decay of a particular protein over time by SDS-PAGE combined with autoradiography (Schimke and Doyle, 1970). This method has been highly successful and is still used (Maitrejean *et al.*, 2011), but it must be possible to efficiently deliver the labelling agent into the relevant cells. Recently, proteome scale

experiments assessing protein stability have made use of the pulse-chase concept. One study on mammalian cells used a stable isotope pulse (Schwanhausser *et al.,* 2011), while another on human cells used the decay of bleached subpopulations of fluorescently tagged proteins to calculate half lives (Eden *et al.,* 2012). The second class of method involves inhibiting protein production and following the decay of the protein of interest. This is most commonly achieved with global protein synthesis inhibitors such as cycloheximide (Belle *et al.,* 2006), although these will have many secondary consequences for a cell and so half lives calculated in this way cannot be considered wholly reliable. An alternative would be to specifically inhibit the production of the protein of interest, for example with RNAi; the approach used in this chapter to determine the AtGWD half life. RNAi has not been widely used to examine protein half lives, possibly because it is hard to determine when and if translation has been completely arrested. However if transcript abundance drops to very low levels, it seems reasonable that protein abundance data collected after this point can be used obtain a very good estimate of the half life.

There are two further ways in which the RNAi line could be used to study the relative importance of *AtGWD* transcript and protein. First it could be used to engineer a situation in which the *AtGWD* transcript is abolished but the protein remains at nearly wild-type levels. This situation would occur in a timecourse of knock down if AtGWD turned out to have a long half life. Analysis of starch degradation in these circumstances would provide sufficient data to infer the importance of transcriptional regulation in the daily control of starch degradation. Secondly, it is possible that the RNAi could improve our understanding of the time of day at which the AtGWD protein is required for normal starch degradation. As discussed in chapter 1, there is some evidence that AtGWD is active in the day. Firstly, Arabidopsis leaf starch is phosphorylated at the end of the day (Yu *et al.*, 2001), so presumably AtGWD is active during the light period as well as in the dark. Secondly, Mikkelsen *et al.* (2005) suggest AtGWD is reduced by thioredoxins, which are themselves reduced by electrons originating from photosystem I. These data could be interpreted to mean that AtGWD should be more active in the day than in the night. There is also evidence supporting the role of AtGWD activity at night. Firstly, *gwd* mutant plants are clearly defective in starch degradation (Yu *et al.*, 2001). Secondly, there is more GWD associated with starch at night than during the day in pea and potato leaves (Ritte *et al.,* 2000). Further work has shown that there is an

increase in starch surface phosphorylation on the transition to darkness (Ritte *et al.*, 2004). Therefore it is not at present clear at which times of day the AtGWD protein is required for normal starch metabolism. If the half life of the AtGWD protein is sufficiently short, then the *AtGWD* RNAi could be used to substantially reduce the amount of protein at a certain time of day and thus investigate when in the diel cycle the protein is really necessary.

There has been one previous study based on the inducible knock-down of *AtGWD* using RNAi (Weise *et al.*, 2012). Using an ethanol inducible system, *AtGWD* transcript levels were decreased by approximately 50%, resulting in a 3 to 7 fold increase in end of night starch content. However the authors were interested in starch accumulation for biotechnological reasons, and did not use the system to further our understanding of the starch degradation pathway. In contrast, the detailed analyses presented in this chapter provide new biological insight, essential for the proper understanding of the role of AtGWD in Arabidopsis leaf starch degradation.

3.2 Results

3.2.1 Diel patterns of *AtGWD* transcript and protein abundance

Several studies have shown that *AtGWD* transcript varies in abundance over 24 hours with peak expression at dusk (Smith *et al.*, 2004) and that this is a circadian rhythm that persists in continuous light (Harmer *et al.*, 2000; Edwards *et al.*, 2006; Covington and Harmer, 2007; Michael *et al.*, 2008). This transcriptional pattern is shared with many of the other enzymes of starch degradation, although analysis of the promoters of these genes failed to identify the *cis* regulatory element responsible for the pattern (Smith *et al.*, 2004). However, when the *AtGWD* promoter element is inspected with the PLACE tool (http://www.dna.affrc.go.jp/PLACE/signalscan.html), *AtGWD* is seen to have 490 recognisable promoter elements, 97 of which are 6 bp or longer. These include three evening elements (figure 3.2). Evening elements are known to cause maximum gene expression at dusk by recruiting the CCA1 and LHY Myb-family transcription factors (Hazen *et al.*, 2005). Evening elements have previously been identified in the promoters of *GWD*, *DPE2* and *PHS2* (Lu *et al.*, 2005). When I extended the analysis to *PWD*, *DPE1* and *ISA3*, I found that these also contain at least one evening element in their promoters. The *AtGWD* promoter contains multiple additional characterised promoter elements consistent with regulation by plant hormones (abscisic acid, gibberellin and ethylene response elements), carbon status (Amybox 1 and 2 and the TATCCA element), environmental factors (low temperature response element, G-box) and with the binding of both Myb and bZip type transcription factors. Interestingly there are four copies of a box identified as necessary for transcription of the plastidial atpb gene by the nuclear encoded plastidial RNA polymerase (Kapoor and Sugiura, 1999). This may be a relic of the time when *AtGWD* was in the plastid genome. Thus the AtGWD promoter is complex, and although not all elements will recruit partners, it may be responsive to many environmental and endogenous signals which likely combine to cause the large diel changes in transcript abundance observed.

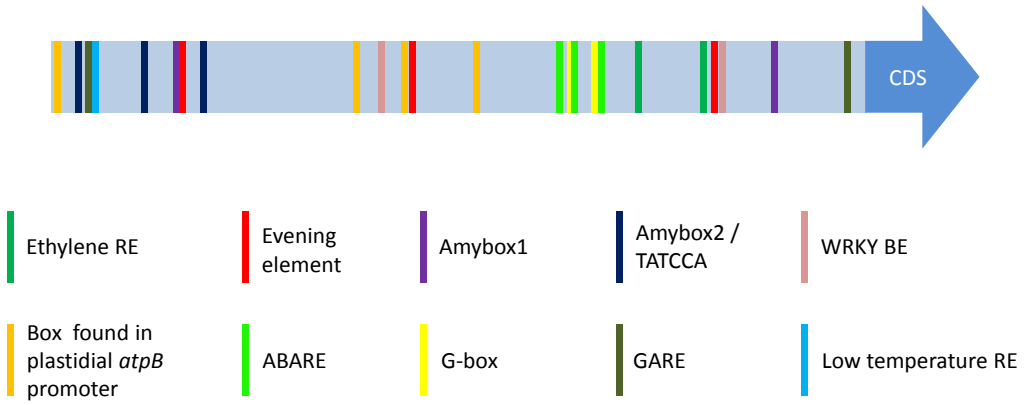

Figure 3.2: The structure of the *AtGWD* promoter. The entire 1600 bp intergenic region up stream of the *AtGWD* coding sequence (CDS) is displayed. A subset of the promoter elements identified with the PLACE tool are indicated by coloured bars. Elements were selected to illustrate the diversity of signals potentially affecting AtGWD transcription. Dark green, ethylene response element (RE); red, evening element (EE); dark blue, amybox / TATCCA element; pink, WRKY binding element (BE); dark yellow, box from plastidial atpb gene; light green, abscisic acid response element (ABARE); light yellow, G-box; brown, gibberellin response element (RE); light blue, low temperature response element (RE).

I wanted to investigate whether the daily oscillations in transcript abundance resulted in oscillations in AtGWD protein abundance. The only previous studies of AtGWD protein levels over 24 hours are based on the qualitative inspection of western blots (Yu *et al.*, 2001; Smith *et al.*, 2004). Although there were no major changes over a diel cycle, I wished to quantitatively examine AtGWD protein levels with sufficient sensitivity to detect small changes. A label-free, peak area based method was chosen to measure AtGWD protein levels for reasons described in the introduction to this chapter. The execution of such methods is not straightforward, especially if large numbers of proteins are to be quantified as was desirable here for validation of the results. Indeed studies which have provided known protein mixtures (of only tens of proteins) to different laboratories have found considerable variation in the resulting quantifications (Turck *et al.*, 2007; Bell *et al.*, 2009). To ensure successful implementation of the method I worked with Alex Graf (ETH, Zurich) in a highly specialised proteomics laboratory.

Soluble protein was extracted from the Arabidopsis leaf tissue harvested over 24 hours. Before proceeding with tryptic digestion and LC-MS/MS, the samples were run on an SDS polyacrylamide gel. The slice of gel above the 100 kDa marker, which should include the 156kDa AtGWD, was taken for tryptic digestion and purification of peptides. This fractionation step was necessary to reduce sample complexity and thus increase the dynamic range of the assay. Complexity is negatively correlated with dynamic range because of the way the MS procedure operates. In each cycle an initial MS scan over the entire m/z range of the instrument identifies the 5 most abundant peptides. These are then selected for collision activated dissociation and MS/MS spectra are recorded for each individual peptide. The MS/MS spectra allow the identification of the peptide, while the peak for the intact peptide from the initial m/z scan is used for quantification. The 5 peptides measured are then excluded from MS/MS scans for the next two minutes, so that less abundant peptides eluting at a similar time from the liquid chromatography column can be measured. Thus only the most abundant proteins eluting at a given time are measured by the mass spectrometer, so the greater the sample complexity, the lower the probability that any particular protein is measured. AtGWD is an abundant protein, so only a crude gel based fractionation step was necessary to ensure it could be identified and quantified with a good dynamic range.

Quantitative analysis of the data was performed using the Progenesis software (Nonlinear Dynamics). First all MS spectra are aligned such that peaks detected at a certain m/z and elution time in one sample can be matched with the equivalent peak from another sample. Consequently a peptide only needs to be selected for MS/MS scans in one sample for it to be correctly identified in all samples. Next the data are normalised to account for variation between samples due to factors such as differences in protein loading on the mass spectrometer or differences in ionisation between runs. This normalisation is achieved by assuming that the majority of proteins do not change between samples, setting one sample as a reference and then calculating the deviation in peak area between each peptide. Extreme values are excluded and the ratio of peak areas for each peptide is calculated between the reference sample and every other sample. These ratios are log transformed such that peaks with areas greater than the reference and those with ratios less than the reference have equal weight. The median of the log ratios for all peptides in a sample is antilogged and used as a scaling factor to be applied globally across peptides in that sample. Peak areas can then be reliably

compared to generate quantitative data on relative protein abundance between samples. The peak list is also searched against a *in silico* reverse transcribed version of the Arabidopsis genome. Any matches to this 'REV' genome are definitely false and so give an indication of the false discovery rate.

AtGWD protein levels were measured over 24 hours in a 12 hours light, 12 hours dark cycle, by the above method. RAW and processed data can be found in appendices II and III. The false discovery rate was 0.16 %. AtGWD protein abundance was found not to vary over a diel cycle (figure 3.3), the maximum fold change being less than 1.1 (ANOVA: p=0.14). Of the set of starch degradation genes showing coordinated daily expression, only 3 were found in the protein data set. These were SBE3, AMY3 and DPE2. They displayed maximum fold changes of 1.14, 1.10 and 1.18 over the diel cycle respectively (ANOVA: p = 0.04, 0.6, 0.001). Thus, as for GWD, protein levels for these enzymes varied remarkably little over the diel cycle despite large changes in transcript abundance. Other aspects of this dataset are discussed in section 3.2.6.

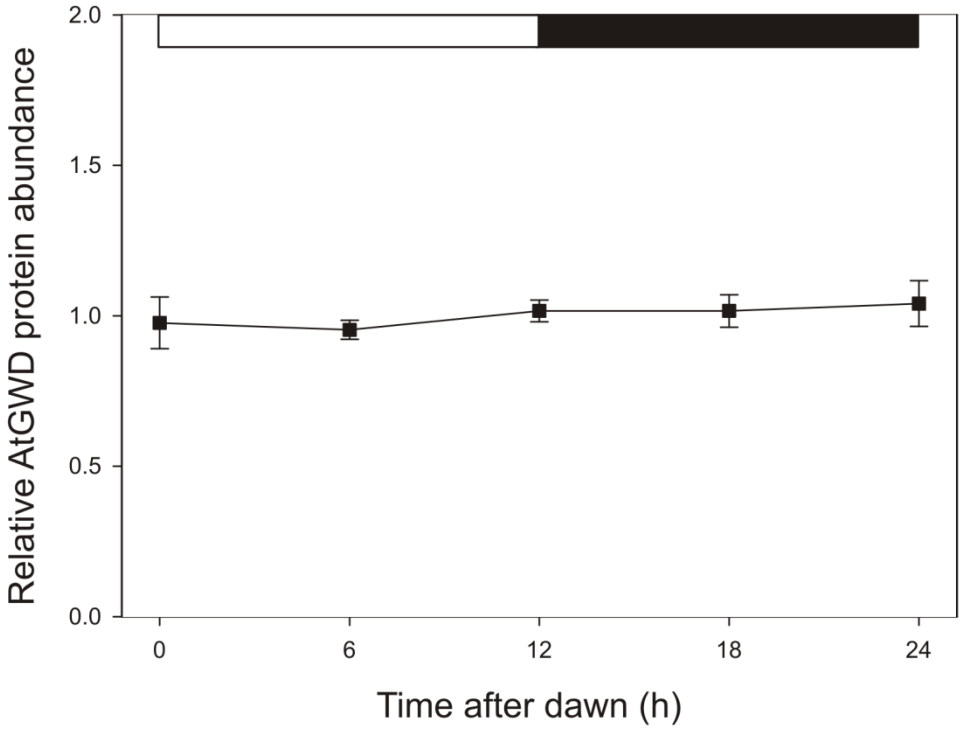

Figure 3.3: AtGWD protein levels over 24 hours measured using quantitative proteomics. White bar shows light period, black bar shows dark period. Values are relative to the geometric mean of all AtGWD data for the timecourse. Error bars are SEM and n = 8, 4, 7, 7 and 8 individual rosettes for timepoints 0, 6, 12, 18 and 24 respectively.

3.2.2 Inducible silencing of AtGWD

Plants expressing an RNAi construct targeted at *AtGWD* were generated by Alex Graf while a PhD student in the Smith lab, JIC, Norwich. The construct contains a section of the cDNA from 984 to1476 bp after the transcription start site (amplified using primers 15 and 17 – see section 2.9) in forward and reverse orientation so as to form a hairpin when expression is induced from a dexamethasone (dex) inducible promoter.

I induced expression from the RNAi construct by spraying plants with dexamethasone just after dawn and repeated this 2, 4 and 6 days later. I harvested leaf tissue at the end of the day (EOD) and the end of the night (EON) until nine days after the first dex spray. Whole rosettes of four plants were pooled to make each biological replicate and

the homogenised tissue then subsampled for different analyses. The EOD samples were analysed for starch content and *AtGWD* transcript and protein levels. The EON samples were analysed for starch content. A line expressing a T-DNA from the empty pOpOff vector was included in the experiment and treated and analysed in an identical manner to the *AtGWD* RNAi line. This provided a control to demonstrate that effects in the RNAi line were due to repression of *AtGWD* and not due to other effects of the T-DNA or the transformation process.

AtGWD transcript abundance at the end of the day declined in the RNAi line to 25% of the control only 1.5 days after the first dex spray (figure 3.4 A) and plateaued at 8% of control levels by 2.5 days after the first dex spray. There was evidence of partial recovery of transcript levels 8.5 days after the first dex spray (and 2.5 days after the last dex spray). AtGWD protein levels decreased at a slower rate (figure 3.4 B), reaching 50% of control levels at 3 days, 20% of control levels 5 days then continuing to decrease to 11% of control levels 9 days after the first spray. Starch at the end of the day stayed fairly constant throughout (Figure 3.4 C), averaging over the timecourse at 6 mg $(g\ FW)^{-1}$ with a standard deviation of just 0.7. Starch began to accumulate at the end of the night 5 days after the first spray. By 9 days the RNAi line contained more than 16 times as much starch as the empty vector control (Figure 3.4 D). Iodine staining showed that the starch at the end of the night in the RNAi line was high throughout the rosette (Figure 3.4 E). In the empty vector control none of the variables measured showed any obvious or consistent variation over the timecourse. These data are summarised on one graph in Figure 3.5.

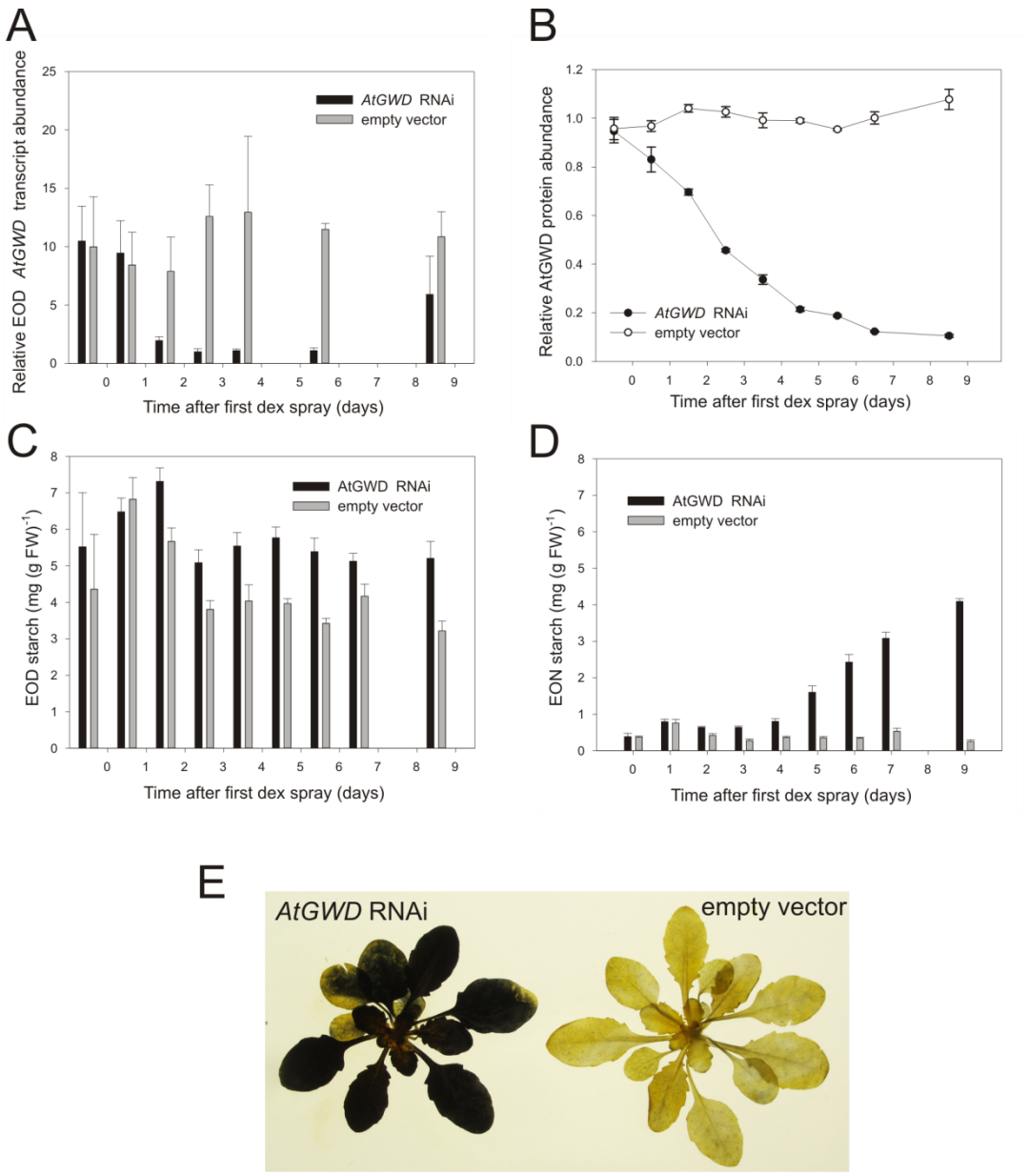

Figure 3.4: Timecourse of *AtGWD* knock-down. In all cases black symbols or bars represent the *AtGWD* inducible RNAi line and white symbols or bars represent the empty vector control. **A** *AtGWD* transcript abundance at the end of the day (EOD) measured with q-PCR, normalised to the smallest value (RNAi line, day 2). **B** AtGWD protein abundance measured by proteomics, normalised to the geometric mean of all empty vector control data. **C** Starch measured at the end of the day (EOD). **D** Starch measured at the end of the night (EON). **E** Iodine stained rosettes 10 days after first dex spray. For all measurements n = 4 pools of 4 plants each and error bars are ± SEM.

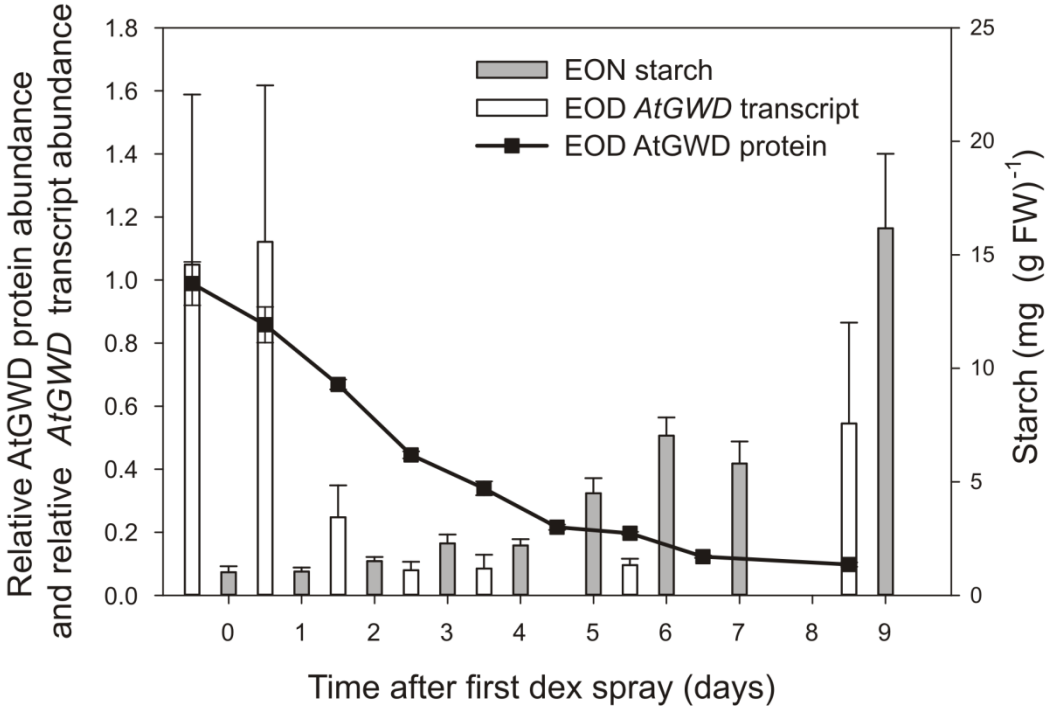

Figure 3.5: Combined data from timecourse of inducible knockdown of *AtGWD*. Data are the same as in Figure 3.4. Grey bars, starch at the end of the night (EON) in *AtGWD* RNAi line. White bars, *AtGWD* transcript abundance relative to empty vector control. Black line and squares, AtGWD protein abundance relative to geometric mean of empty vector control values. For all measurements n=4 pools of 4 plants and error bars are SEM or standard error of the ratio of means.

Four important features of these data are as follows. Firstly, two days after the first dex spray there is only a small amount of transcript remaining and yet starch degradation proceeds essentially normally. This observation strongly suggests that the transcript and the daily oscillations in transcript abundance are not necessary for the daily control of starch degradation. Secondly, the slow decay of AtGWD protein levels demonstrates that AtGWD protein molecules are stable for several days. Thirdly, it is possible to remove around 60% of the protein without an effect on starch degradation and fourthly, starch synthesis rates decrease through the time course. The latter three points are addressed quantitatively in the following sections.

3.2.3 Half life of the AtGWD protein

AtGWD protein abundance data between two and seven days after the first dex spray (see section 3.2.2) were used to calculate the half life of the AtGWD protein, assuming that AtGWD protein synthesis was negligible in this period due to the very low transcript levels. An exponential decay curve was fitted to the data using non-linear regression in Genstat. Equation (1) shows the form of the model, where G is AtGWD protein level, t is time and A, B and C are constants. Given the data, it was reasonable to set A to 0 and constrain C to values less than 1 during the fitting process.

$$G = A + B \cdot C^t \quad (1)$$

The fit to the data was excellent ($R^2 = 0.98$) and data and curve are plotted in Figure 3.6. The parameter B was estimated at 1.17... ± 0.04 (se) and C at 0.69... ± 0.008 (se). The half life of the protein ($t_{\frac{1}{2}}$) can then be calculated as:

$$t_{\frac{1}{2}} = log_c(0.5) \quad (2)$$

Substituting the fitted value of C into (2) yields a half life of 1.93 days (46 hours) for AtGWD. The 95% confidence interval is 1.81 to 2.06 days.

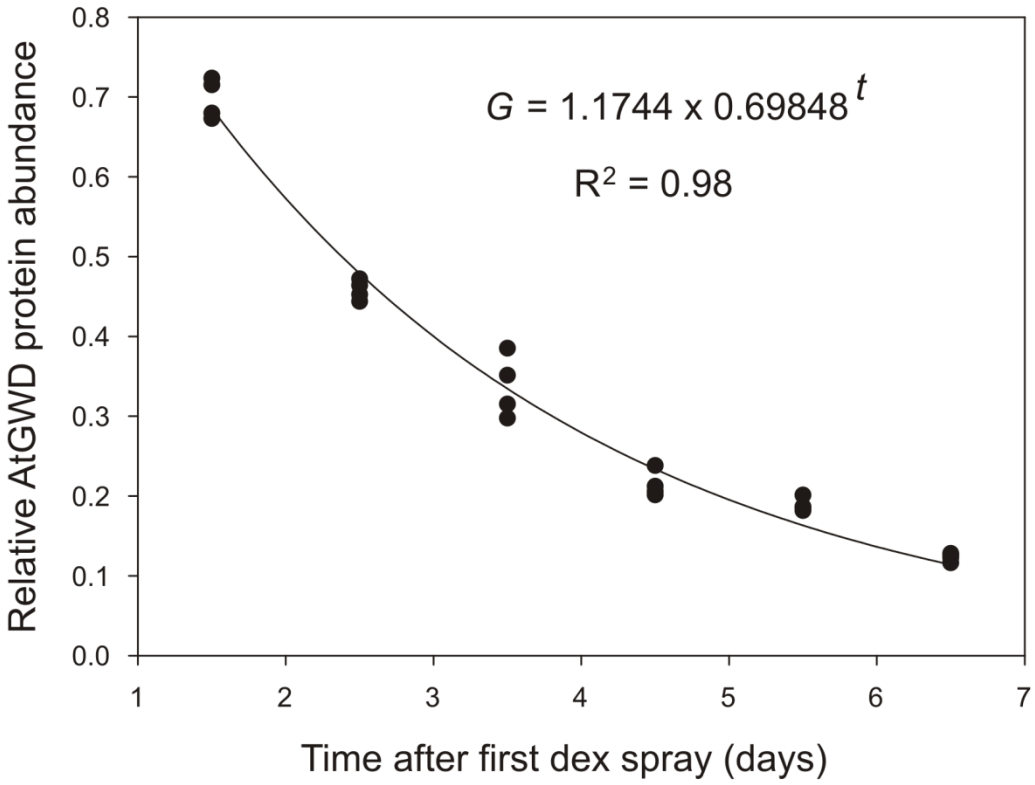

Figure 3.6: AtGWD protein abundance during the portion of the inducible knock down of *AtGWD* timecourse in which *AtGWD* transcript was at low levels. Data are normalised to the geometric mean of all protein values from the empty vector control over the timecourse. Each data point is the value measured from a pool of 4 plants and data are the same as those presented in Figure 3.4. The equation for the fitted exponential decay curve (black curve) is shown on the plot.

It should be noted that this half life only applies to plants in the exponential growth phase (as plants in this experiment were: being at growth stage 3.5 – 3.7 according to Boyes *et al.* (2001), and having plenty of space and nutrients to grow more). This is because protein abundance decays in a cell by two processes: destruction of protein molecules and by dilution due to cell expansion growth. Throughout the exponential growth phase the relative growth rate of the plant and thus the dilution by growth of the protein should be constant. However, when growth slows as resources become limiting the dilution of the protein by growth will decrease and therefore the half life of the protein will effectively increase on these multi-day timescales. The half life presented

may also not be appropriate on short timescales over which cells do not expand significantly (ie. within the G_0 period of a single cell). This is because the dilution of the protein due to growth is no longer relevant and the only contributor to protein decay is the destruction of protein molecules. To calculate the half life in a no-growth situation I would need information about relative growth rates, not available for this experiment. However we could assume a typical relative growth rates for Arabidopsis grown on soil in the exponential phase, in 12 hours light 12 hours dark cycles of 0.15 day^{-1} (Piques *et al.*, 2009) and assume that the total protein : fresh weight ratio remains constant. Under these conditions the half life with only dilution due to growth (no protein decay) is ln0.5/-0.15 = 4.62 days. The no growth degradation rate equals the measured decay rate minus the contribution of the dilution to growth: -0.336 – 0.15 = -0.186, yielding a no growth half life of ln0.5/-0.186 = 3.72 days.

3.2.4 A flux control coefficient for AtGWD with respect to starch degradation

The combined data on protein levels and starch degradation were used to calculate an approximate flux control coefficient for AtGWD. The flux through starch degradation was approximated as the proportion of starch remaining at the EOD which is degraded by the EON. This measure is only a true representation of the flux at any given time in the night if the degradation rate is linear through the night, but this has consistently been found to be the case in many experiments on both wildtype plants and those starch excess mutants which still turn over some starch (Kötting *et al.*, 2005; Kötting *et al.*, 2009; Comparot-Moss *et al.*, 2010). Flux control theory (Kacser and Burns, 1973) requires that protein levels and the metabolic system are at steady state when flux and protein levels are measured for the determination of a flux control coefficient. Clearly this is not the case in this experiment because protein levels are changing throughout the timecourse. However the protein levels do not change by more than 5 – 10% over a single night and we know the starch degradation system reaches steady state rapidly after a perturbation (Graf *et al.*, 2010; Pyl *et al.*, 2012), so analysis of these data should provide a good approximation of the flux control coefficient.

The flux control coefficient was determined by fitting the hyperbolic function described by equation (3) to the flux estimate versus AtGWD protein levels at the beginning of the night (Figure 3.7). This is a equivalent to the method recommended by Small and

Kacser (1993). J is the flux, G is amount of AtGWD enzyme and a, b and d are constants.

$$J = a + \frac{b}{1 + d \cdot G} \tag{3}$$

The function provided a good fit to the data ($R^2 = 0.966$, Figure 3.7). Equation (3) was differentiated with respect to G to yield the following:

$$\frac{dJ}{dG} = \frac{-b \cdot d}{(1 + d \cdot G)^2} \tag{4}$$

Values for the constants, generated in Genstat, were substituted into equation (4) yielding a flux control coefficient of 0.058 at wildtype protein levels ($G = 1$). It should be noted that a good fit could not be achieved if the origin was constrained (ie. $a = -b$), as would normally be the case when dealing with systems of enzymes acting on soluble substrates (Small and Kacser, 1993). I think it is reasonable not to constrain the origin to zero in this case because we do not know the exact effects of AtGWD activity on starch structure and its susceptibility to degradation by hydrolytic enzymes. For example, it may be that a certain minimum density of phosphate is required before there are sufficient changes in starch structure to affect degradation.

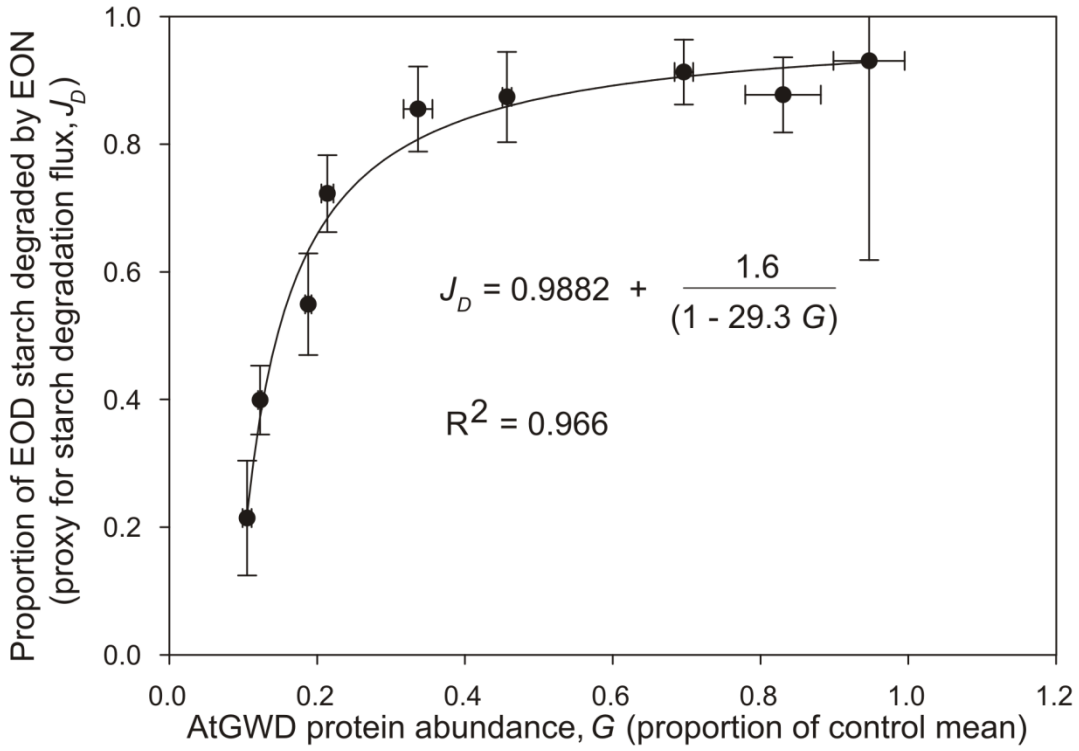

Figure 3.7: Flux through starch degradation, J_D (estimated as the proportion of end of day (EOD) starch remaining at the end of the night (EON)) as a function of AtGWD protein abundance, *G*. For all data n=4 pools of 4 plants each. Data are the same as those presented in Figure 3.4 Error bars on starch values are ± the standard error of the ratio of means and error bars on protein values are ± SEM. The fitted curve is a hyperbola described by the equation displayed on the plot.

3.2.5 A role for AtGWD in starch synthesis

Although EON starch increases over the timecourse of *AtGWD* knock-down, EOD starch remains comparatively constant. Thus rates of starch synthesis decrease as AtGWD protein levels decrease to a level at which starch degradation is inhibited. This is an interesting and unexpected result, since a role for AtGWD in starch synthesis has not been previously recognised. As presented above for starch degradation, it is possible to calculate an approximate flux control coefficient of AtGWD with respect to starch synthesis. The flux through starch synthesis was estimated as the amount of starch made during the day in the RNAi line expressed as a proportion of that made in the empty vector control. Using the ratio of RNAi to control starch levels, removed some small variations in EOD starch which obviously covaried between the RNAi line and the

control. However at many timepoints, the RNAi line had about 30% more EOD starch than the control (Figure 3.4). It is possible that this reflects tray to tray variation in the experiment, as genotypes were not randomised between trays. I do not think that the broad conclusions presented here are invalidated by this anomaly. The first protein data point (-0.5 days) could not be used in the analysis because starch data for the previous night were not available. This is also strictly true of the last protein data point (8.5 days) but I decided to include it in the analysis, using EON starch data from the subsequent night as a proxy for EON starch the previous night. Although only an estimation of the true EON starch value, the inclusion of this data point significantly strengthens the conclusions that can be drawn. The difference between EON and EOD starch is only a true representation of the flux through starch at any given time if the rate of synthesis is linear through the day. This has been consistently true in Arabidopsis plants making starch at different rates (Gibon *et al.*, 2004b), and in many mutants with elevated starch (Kötting *et al.*, 2005; Kötting *et al.*, 2009; Comparot-Moss *et al.*, 2010). It is probable that the system is near steady state, as discussed in section 3.2.4.

The hyperbola described by equation (3) was fitted to a plot of the estimate flux through starch synthesis, J_S, versus AtGWD protein abundance (Figure 3.8). The hyperbola was a good fit to the data, although it only accounted for 69% of the variation. The R^2 value was lower than the equivalent for the starch degradation data because of variation in the amount of starch synthesised in the RNAi line relative to the control at high levels of AtGWD protein. Values for the constants in equation 3 were generated using Genstat and substituted into equation (4), yielding a flux control coefficient for AtGWD with respect to starch synthesis of 0.019.

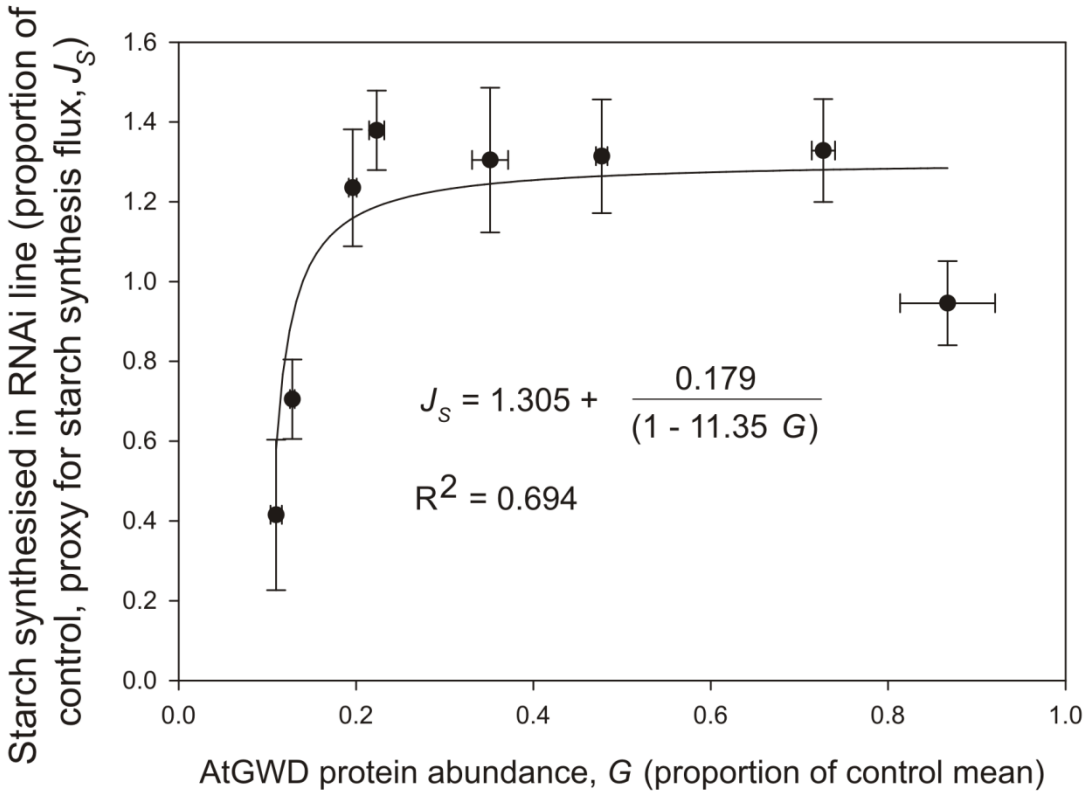

Figure 3.8: Flux through starch synthesis, J_s (estimated as the amount of starch made during the day in the RNAi line as a proportion of that made in the control) as a function of AtGWD protein abundance, *G*. For all data points n=4 pools of 4 plants each. data are the same as those presented in Figure 3.4. Error bars on starch values are ± the standard error of the ratio of differences of means. Error bars on protein values are ± SEM. The fitted curve is a hyperbola described by the equation displayed on the plot.

It is tempting to compare the flux control coefficients here calculated for starch synthesis and starch degradation, but there are two reasons why this should not be done. First, error in the data can easily account for such a small difference between the coefficients (0.04). Second, starch degradation rates for a given night were combined with AtGWD protein measurement from the beginning of that night, whereas starch synthesis rates for a given day were combined with protein measurements from the end of that day. However AtGWD protein levels are decreasing throughout the timecourse, so for each starch synthesis rate the equivalent protein levels are underestimated, and for each starch degradation rate the equivalent protein levels are overestimated. It would be possible to calculate the area under the protein decay curve for a given time interval and thus estimate more suitable protein abundance values. However this assumes that the

relative decay rate is constant throughout the diurnal cycle, and we do not know if this is the case. Thus I think it is best to use the actual data collected rather than interpolated protein abundance values. The effect on the calculated flux control coefficient will be very small, and certainly will not change the conclusions drawn from the analysis.

3.2.6 Other proteins affected by the inducible knock down of *AtGWD*

Quantitative protein abundance data were collected for many proteins besides AtGWD over the RNAi timecourse and were used for two purposes. First, they were used to validate the specificity of the silencing construct. If the RNAi system is truely specific to AtGWD then most proteins should not change in abundance. Secondly, they were used to search for any interesting and unexpected changes in the abundance of proteins other than AtGWD. Any such changes could provide new insights into the enzymology of starch metabolism or its downstream consequences. Details of peptides used for quantification can be found in the Progenesis reports in appendix II. The RAW MGF files are in appendix 3. The false discovery rate for the dataset was below 0.14%.

The AtGWD RNAi proteomic data set contains data for 666 proteins beside AtGWD. These are all large proteins, greater than 100 kDa because they were all extracted from a slice from the top of an SDS polyacrylamide gel. Only one of these proteins changed substantially in abundance in the RNAi line over the timecourse, and this was ROC4 (also called Cyp 20-3; At3g62030) (Figure 3.9 A), a very abundant stromal cyclophilin involved in responses to oxidative stress and photosystem II repair (Peltier *et al.*, 2006; Cai *et al.*, 2008; Dominguez-Solis *et al.*, 2008). The kinetics of decay of the protein are remarkably similar to those of AtGWD (Figure 3.9 B), except that there is a slight lag relative to AtGWD at the beginning of the timecourse and that ROC4 protein levels plateau at around 40% of wildtype levels compared to around 10% for AtGWD. Attempts to quantify ROC4 transcript levels over the timecourse by q-PCR were not successful. No section of the *AtGWD* fragment used in the RNAi construct shares any identity with the unprocessed *ROC4* mRNA sequence.

There is considerable discrepancy between the predicted molecular mass for ROC4 (without its transit peptide) of 19.9 kDa and its migration position when subject to reducing SDS-PAGE. All proteins quantified in the experiment migrated slower than the 100 kDa marker so at least a subfraction ROC4 protein must migrate anomalously

for its size. This suggests the presence of a covalent interaction between ROC4 and some other entity.

It should be noted that the ROC4 protein abundance data are based on a single peptide: IVMGLFGEVVPK. According to the data in TAIR 10 this ROC4 peptide is unique to the ROC4 protein, however it is always possible that it belongs to a protein or splice variant which is not annotated in TAIR 10. ROC4 is regularly identified in proteomic experiments in the Gruissem laboratory sometimes with 35 peptides (A. Graf, personal communication). When ROC4 is detected, the peptide identified in my study is always found. The fact that high confidence ROC4 identification is always associated with this peptide strenghthened the identification of ROC4 in my study. ROC4 may display this anomalous migration because it is covalently attached to some large modifier.

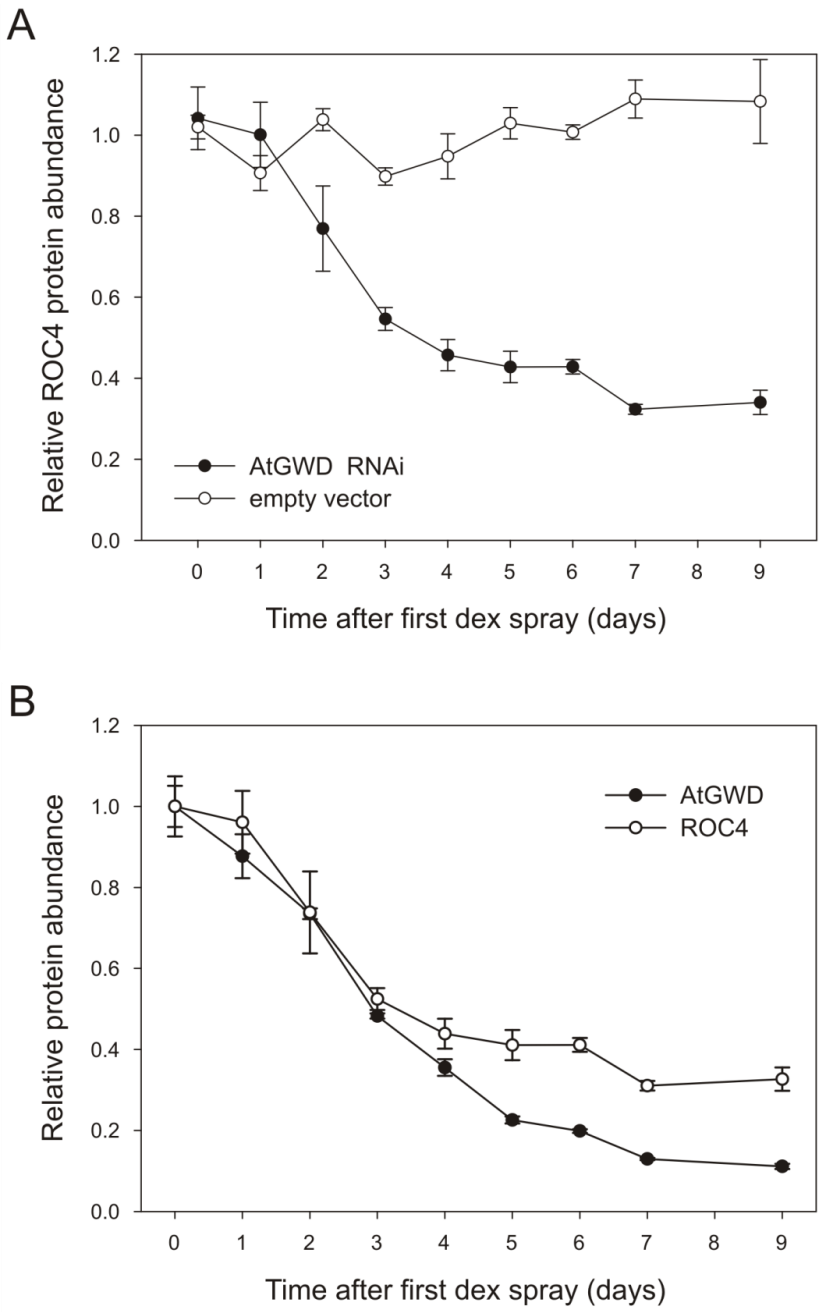

Figure 3.9: ROC4 protein dynamics during a timecourse of the inducible knockdown of *AtGWD*. **A** ROC4 protein abundance in the *AtGWD* RNAi line (filled circles) and in the empty vector control (open circles). Values are relative to the geometric mean of empty vector control values over the entire timecourse. **B** ROC4 (open circles) and AtGWD (closed circles) protein dynamic. For both proteins, values are normalised to the first data point in the timecourse. For all data points n=4 pools of 4 plants each. Error bars are ± SEM.

Although no other protein in the data set displayed as marked a change as ROC4 over the timecourse, I wished to see if there were small but potentially informative changes elsewhere in the data. First, proteins were pre-selected based on there being no greater than a 1.25 fold difference, and no statistically significant difference (p=0.05) in the abundance of the protein between the control and RNAi lines at the beginning of the timecourse. This subset was searched for proteins for which the slope of a linear regression model was significantly different between the control and the RNAi lines. Twenty seven proteins met this criteria at p = 0.05 and 14 proteins at p = 0.01. None of the 27 proteins displayed a greater than 1.24 fold change over the timecourse. Only two of the set of 27 proteins have a known role in carbohydrate metabolism, and these are disproportionating enzyme 2 (DPE2) and alpha-glucan phosphorylase 1 (PHS1). Both proteins met the criteria at the p=0.01 level and showed small but significant increases over the timecourse (Figure 3.10). Of course such an analysis could miss proteins with interesting non-linear dynamics such as a sudden decrease at the beginning of the timecourse. However further exploratory analysis of the data did not identify any proteins which displayed such dynamics.

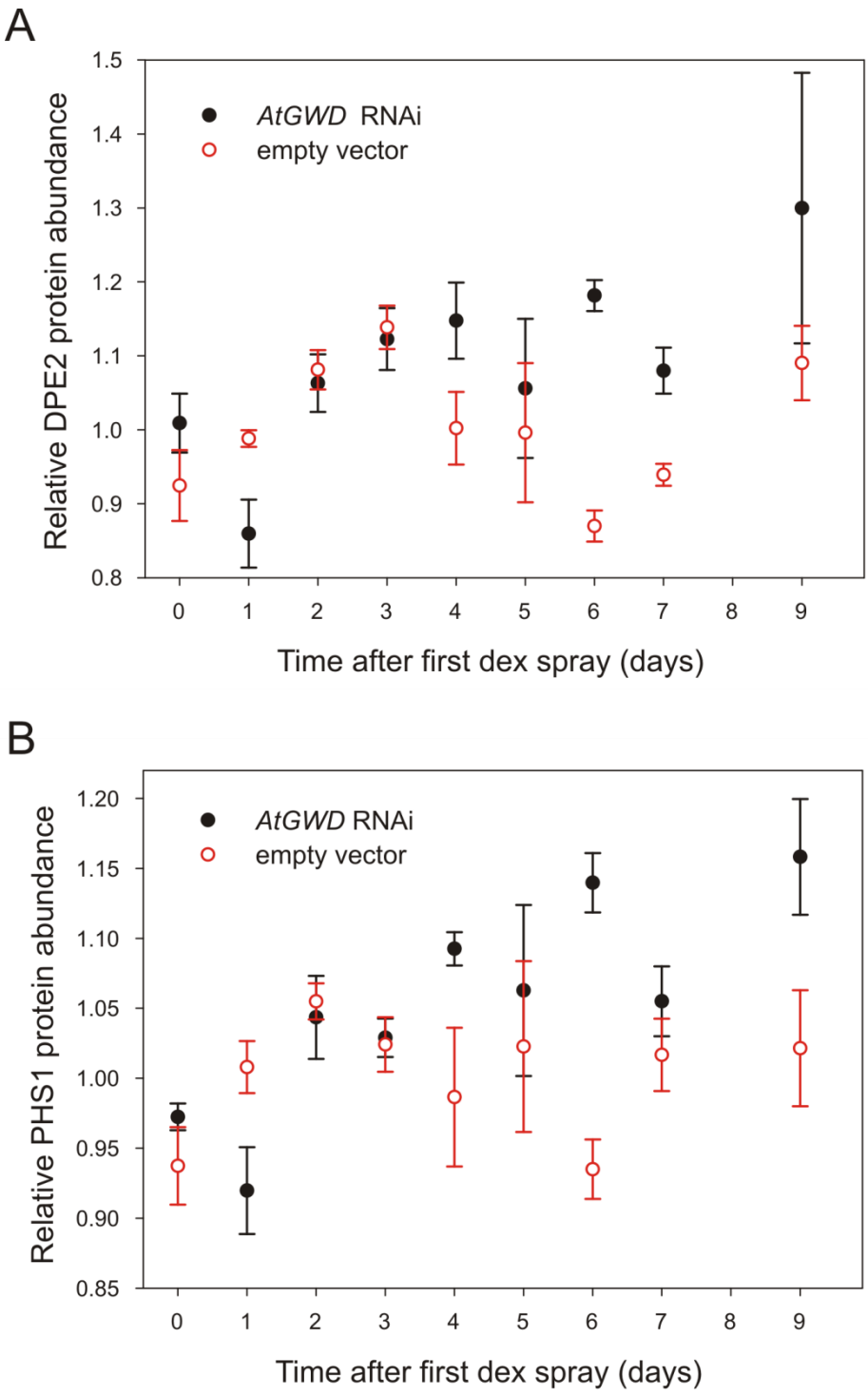

Figure 3.10: Abundance of DPE2 and PHS1 proteins during a timecourse of the inducible knockdown of *AtGWD*. **A** DPE2 protein abundance in *AtGWD* RNAi line (black, filled symbols) and empty vector control (red, open symbols). **B** PHS1 protein abundance in *AtGWD* RNAi line (black, filled symbols) and empty vector control (red, open symbols). For all data points n=4 pools of 4 plants each. Error bars are ± SEM. Trend lines are omitted for clarity.

3.2.7 Further analysis of 24 hour protein data

Data presented in section 3.2.1 demonstrate that large oscillations in *AtGWD* transcript abundance over the diel cycle do not result in changes in AtGWD protein levels on the same timescale. This observation raises some more general questions. Given an oscillating transcript, do protein levels in general tend to be constant or to oscillate? If they oscillate, how do the properties of the transcript oscillations relate to the properties of the protein oscillations? And in general, how much can be inferred from daily transcript data about protein abundance? These questions can be addressed by integrating the 24 hour proteomic data set with a 24 hour transcriptional data set. I chose to use publicly available transcriptional data from the Mark Stitt group (Bläsing *et al.*, 2005) because the plants were grown in very similar conditions to those used for the protein data set: mature plants grown on soil in 12 hours dark, 12 hours light cycles at 20°C. The transcript data were sourced from the NCBI GEO data browser (www.ncbi.nlm.nih.gov/gds) and the record number is GDS1757.

3.2.7.1 Defining the dataset

The protein data were first filtered for quality by removing proteins which differed significantly (t-test, p=0.05) or which showed a greater than 1.5 fold change between the between the 0 and 24 hour timepoints. The resulting data set contained 387 proteins. No such filtering was possible with the transcript data because there was no 24 hour timepoint. Although 387 proteins/transcripts only represent a very small fraction of the proteome/transcriptome, no equivalent quantitative analysis of the proteome over 24 hours is currently available. Thus analysis of this data set can provide valuable new insights despite its limitations. It should be noted that the protein data were obtained through quantitative proteomic analysis of a slice from the top of an SDS polyacrylamide gel, taking all proteins above the 100 kDa marker. Thus the set is highly biased towards large proteins, as well as towards abundant proteins which are most readily detectable by mass spectrometry. To gain a better picture of any additional biases in the data set, the gene ontology (GO) classifications (from www.arabidopsis.org) for the 387 genes in the data set were analysed, and the size of the resultant groups compared to equivalent annotations for the whole genome (Figure 3.11). This analysis revealed an enrichment for genes of known function in the data set

relative to the whole genome, which may be because of the bias towards abundant proteins, which have traditionally been amenable to study. There is also an enrichment for proteins of general metabolic function over proteins involved in nucleic acid binding or transcription. This enrichment may relate to the bias towards abundant proteins, as transcription factors are often very low abundance (Baerenfaller *et al.*, 2008).

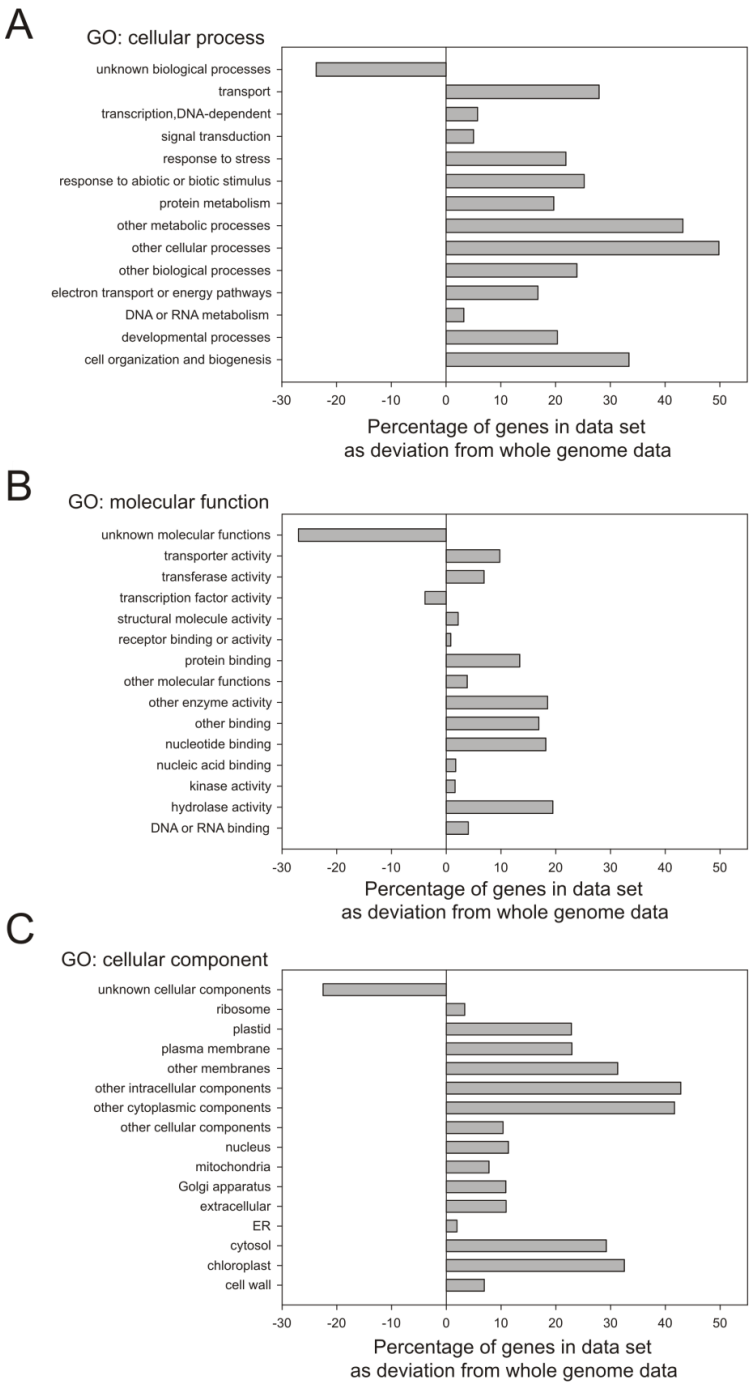

Figure 3.11: Gene ontology (GO) classifications of members of the 24 hour protein and transcript data set. The relative enrichment of a category compared to the whole Arabidopsis genome is expressed as the deviation between the percentage of genes assigned to that category in the whole genome and the percentage of genes assigned to that category in the data set.

3.2.7.2 Transcript rhythmicity as a predictor of protein rhythmicity

I investigated whether *AtGWD* was exceptional in displaying strong daily transcript oscillation but no protein oscillations, or whether this phenomenon is common. To do this I classified proteins and transcripts as rhythmic or non rhythmic based on two different criteria. The first was statistical and defined rhythmicity based on whether the maximum and minimum abundance of the transcript or protein over 24 hours was significantly different at $p = 0.05$. However this method reflects data quality as well as rhythmicity, so I also defined rhythmicity based on an arbitrary fold change cut-off of 1.2. These methods gave similar results which are presented as Venn diagrams in Figure 3.12 A and B. They show that AtGWD is in no way unusual: in 60% of cases in which transcripts are rhythmic, proteins are not rhythmic. It is also noticeable that there are few rhythmic proteins without a rhythmic transcript.

It is possible to broadly classify the members of the data set according to whether they are metabolic enzymes or are involved in other cellular processes and repeat the above analysis for these two categories (Figure 3.12 C, D). The two groups had similar relationships between transcript and protein rhythmicity when compared to each other or the whole dataset.

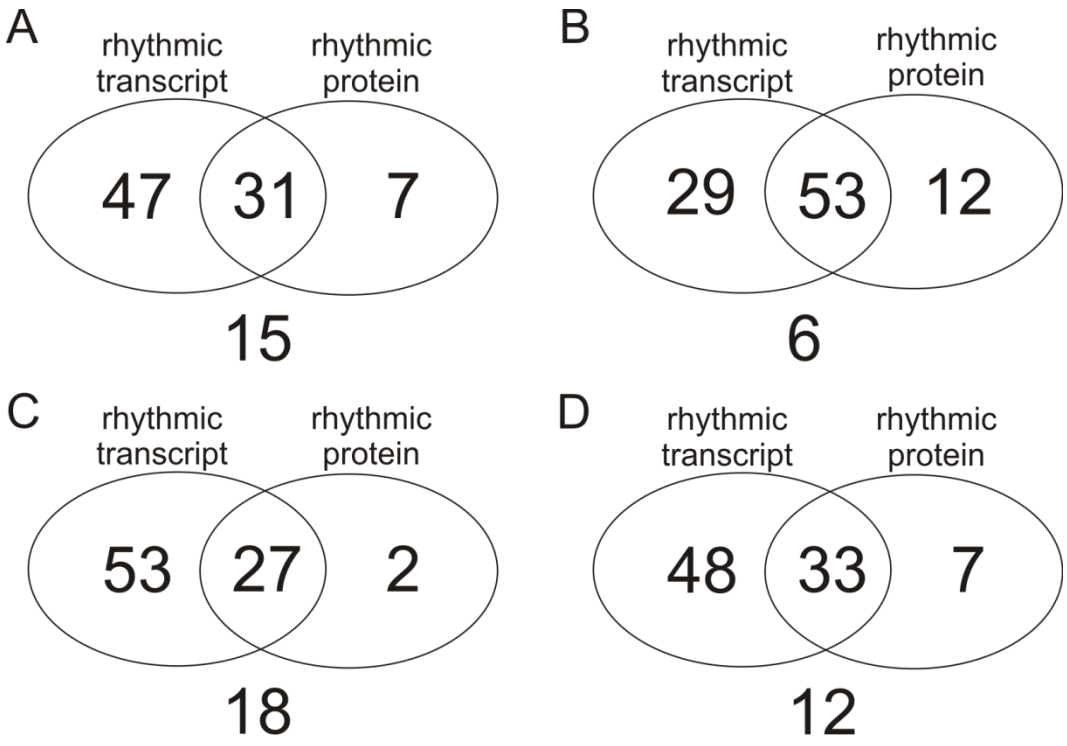

Figure 3.12: Venn diagrams displaying the percentage of genes in the data set for which only transcripts are rhythmic (left circle), only proteins are rhythmic (right circle), both are rhythmic (overlap) or neither are rhythmic (below circles). **A** Rhythmicity is defined by a statistically significant (at p=0.05) difference between the minimum and maximum values in the diel cycle. **B** Rhythmicity is defined by more than a 1.2 fold change in abundance over the diel cycle. **C** The statistical definition of rhythmicity applied only to metabolic enzymes. **D** The statistical definition of rhythmicity applied to proteins other than metabolic enzymes.

I examined data for specific examples for the different categories represented in each Venn diagram in Figure 3.12. In cases where both transcript and protein oscillate it is notable that the protein often oscillates with a much lower amplitude (based on fold change) than the transcript. An exception to this trend is AGPase, which shows a larger fold change in protein levels over the diel cycle than in transcript levels (Figure 3.13 A). This result is consistent with previous findings (Gibon *et al.*, 2004a). In addition, the times of peak abundance for proteins and transcripts do not necessarily match, such that the phase of the protein oscillation may either match or be opposed to that of the

transcript (Figure 3.13). There are many examples besides AtGWD in which the transcript oscillates with a very large amplitude but there is no oscillation in the protein (Figure 3.14). The very small changes sometimes observed in protein abundance in these cases (as in Figure 3.14 B), again do not necessarily match the pattern of transcript oscillations. Cases in which the protein oscillates but the transcripts do not were much rarer, and this classification could be explained as a function of data quality in many cases, for example especially variable transcript data resulting in a non-rhythmic transcript classification (Figure 3.15 A, B). Amongst such examples there were cases in which the transcript and protein showed a similar pattern, but the protein a larger amplitude (Figure 3.15 A). However some examples seemed to genuinely merit this classification because transcript was constant and yet the protein oscillated (Figure 3.15 C).

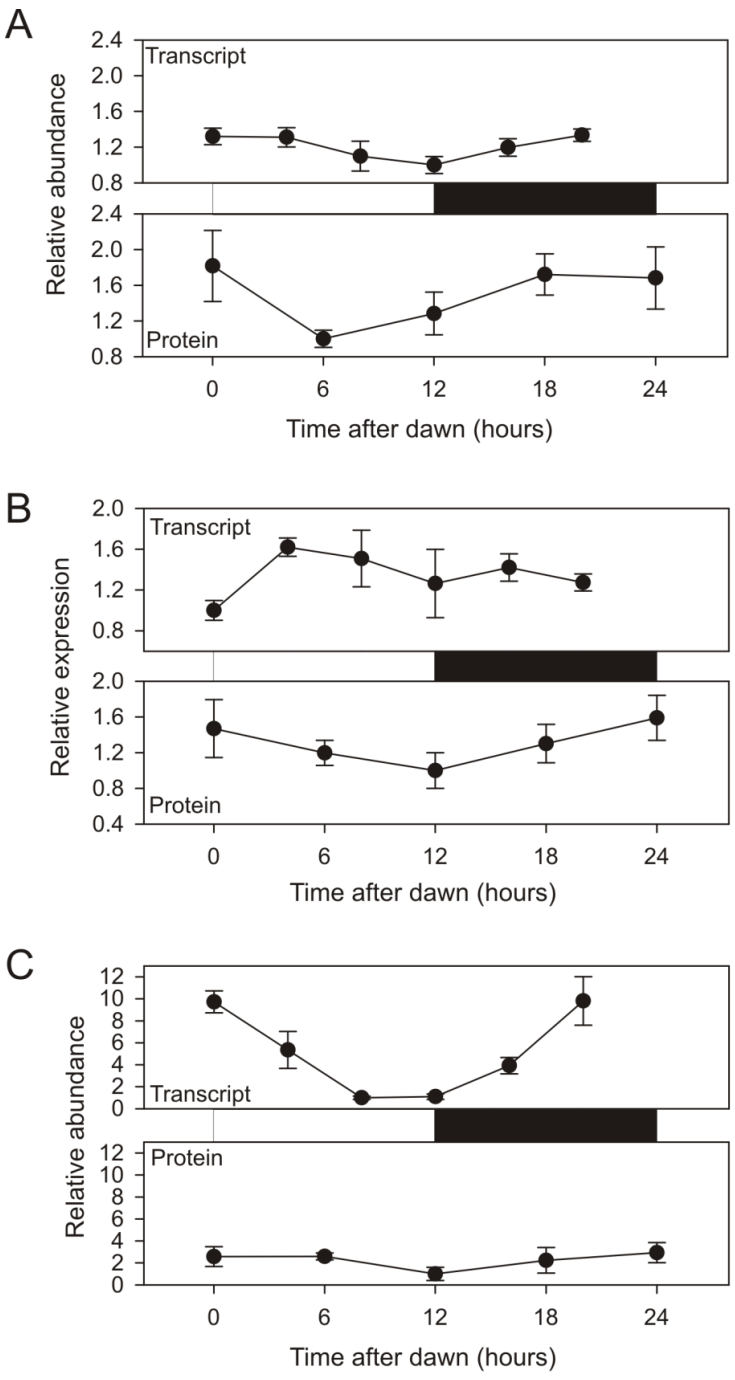

Figure 3.13: Daily patterns in transcript and protein abundance for cases in which both transcript and protein are rhythmic. Each value is relative to the smallest value in that time-series. **A** ADP-glucose pyrophosphorylase small subunit 1 (ADG1, At5g48300) **B** Phototropin 1 (At3g45780) **C** Nitrate reductase 1 (At1g77760). Black bars represent dark period, white bars represent light period. For protein data, n=4 pools of 4 plants each. For transcript data, n=3 individual plants. Error bars are ± SEM.

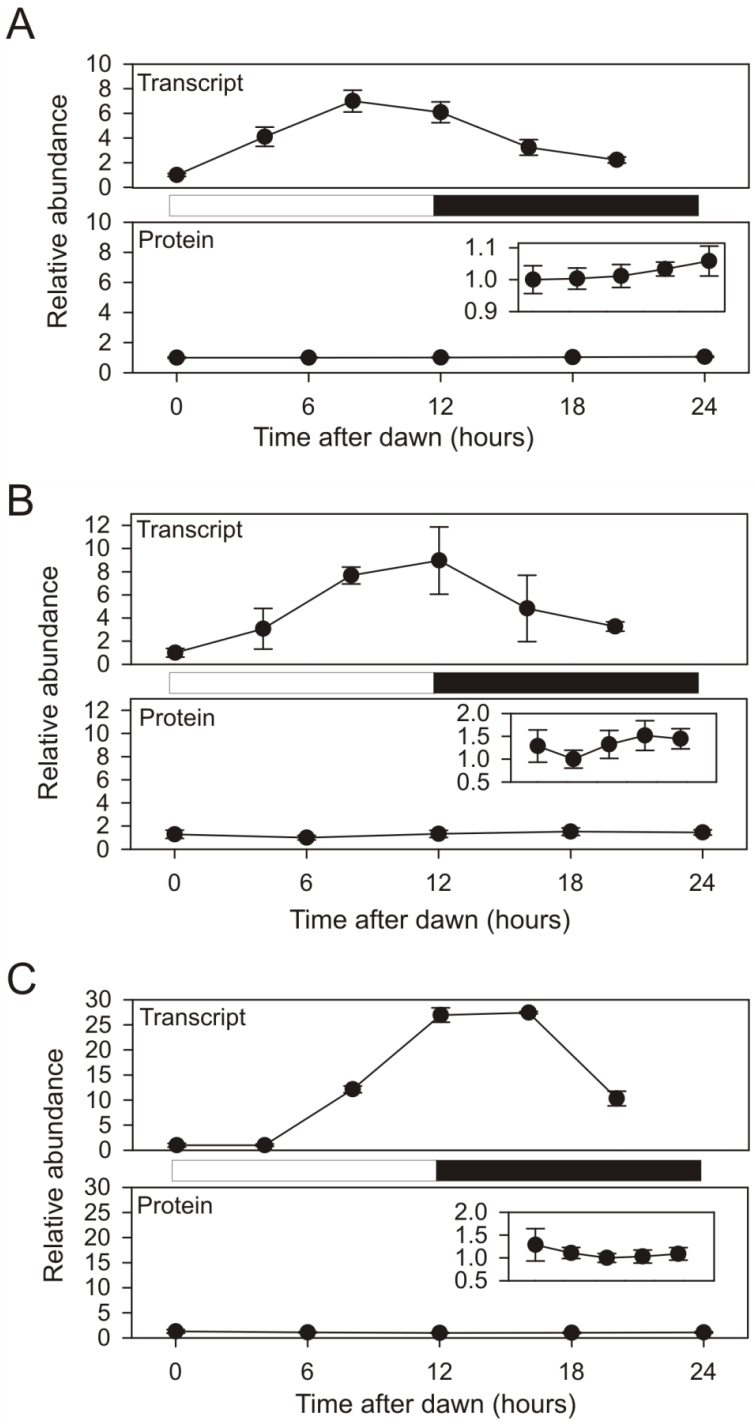

Figure 3.14: Daily patterns in transcript and protein abundance for cases in which only the transcript is rhythmic. Each value is relative to the smallest value in that time-series. The inserts show the protein data at an expanded y-axis scale. **A** Alpha-glucan phosphorylase 1 (PHS1, At3g29320) **B** Copper amine oxidase family protein (At4g12290) **C** Alpha amylase 3 (AMY3, At1g69830). Black bars represent dark period, white bars represent light period. For protein data, n=4 pools of 4 plants each. For transcript data, n=3 individual plants. Error bars are ± SEM.

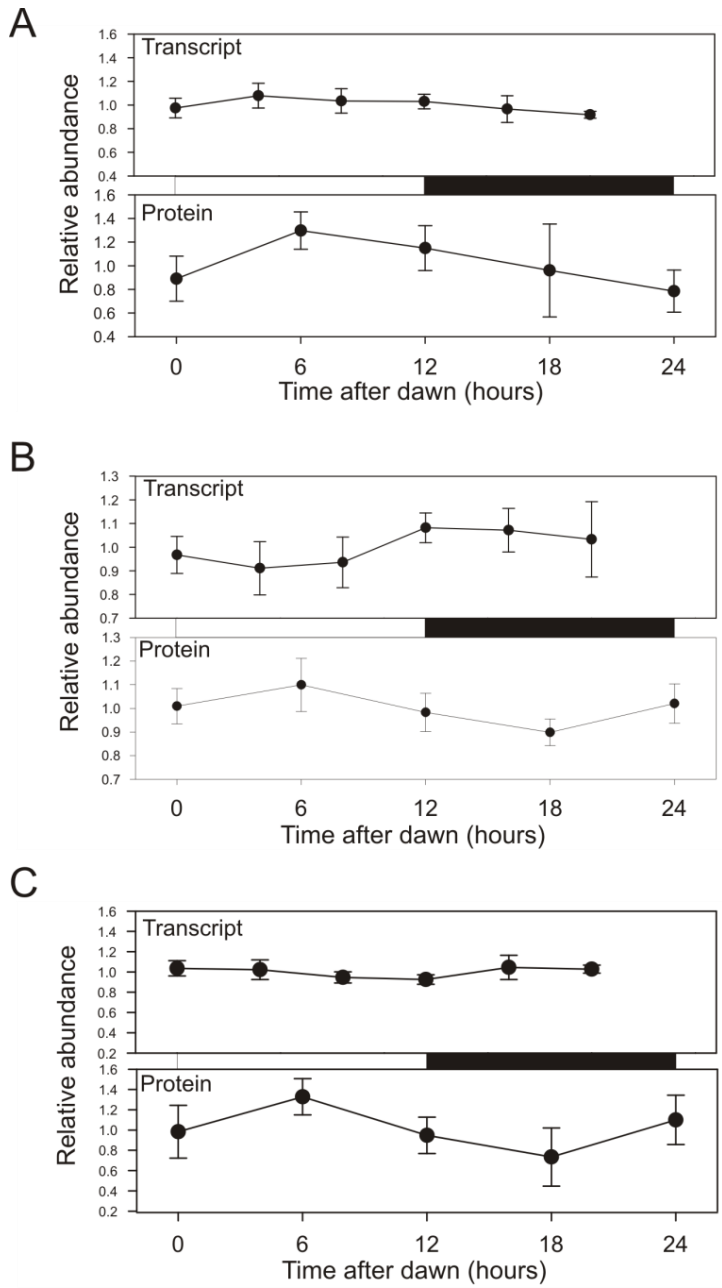

Figure 3.15: Daily patterns in transcript and protein abundance for cases in which only the protein is rhythmic. Each value is relative to the smallest value in that time-series. **A** RNA helicase (At1g59760) **B** Polyribonucleotide nucleotidyltransferase (At3g03710) **C** Tetratricopeptide repeat-like superfamily protein (At5g28740). Black bars represent dark period, white bars represent light period. For protein data, n=4 pools of 4 plants each. For transcript data, n=3 individual plants. Error bars are ± SEM.

\

3.2.7.3 Daily patterns of transcript abundance as predictors of daily patterns in protein abundance

To further investigate the extent to which patterns of transcript abundance over 24 hours can be used to predict patterns of protein abundance I performed an unbiased analysis of the data set. First, the transcript and protein data were reduced to pattern data where a value of 0 was assigned if a data point was lower than the previous data point in the timecourse, and a value of 1 if it was higher. Next, expectation-maximisation (EM) clustering (in Tanagra (Rakotomala, 2005)) was used to separately cluster the transcript and the protein data. The Akaike information criterion (AIC), a measure of model fit (Bozdogan, 1987), was used to decide the number of clusters. For both transcript and protein data there was a clear AIC minimum at 2 clusters (Figure 3.16 A, B). The transcript clusters separated transcripts with a dusk peak from those with a dawn peak (Figure 3.16 B, C) while the protein clusters seemed to separate those with a mid-day peak from those with a mid-day trough (Figure 3.16 D, E). Given that each gene in the dataset had been assigned a transcript cluster and a protein cluster, a contingency table could be drawn to represent the distribution of cluster membership (Figure 3.16 F). A chi squared test shows there is only a 2% chance that this distribution is generated under the null hypothesis of random distribution amongst the classes. Specifically, this supports the notion that if a transcript has a dawn peak, there is more likely to be a mid-day peak in protein abundance than a mid-day trough. Beyond this, patterns of transcript abundance over 24 hours seem to have little predictive power to explain patterns of protein abundance.

Figure 3.16: Unbiased analysis of the relationship between daily changes in abundance of transcripts and proteins within the data set. **A** Akaike information criterion (AIC) for different cluster numbers generated by expectation maximisation clustering applied to transcript data. **B** As for A, but for protein data. **C** Box and whisker plot for all transcript data in transcript cluster 1. **D** Box and whisker plot for all transcript data in transcript cluster 2. **E** Box and whisker plot for all protein data in protein cluster 1. **F** Box and whisker plot for all protein data in protein cluster 2. In each case the box bounds the 25^{th} and 75^{th} percentiles and the middle line is the median of the data. The whiskers denote the 90^{th} and 10^{th} percentiles and outlying data points are displayed as closed circles. Data for each protein or transcript have been normalised to the geometric mean of all data for that protein or transcript in the timecourse. Black bars represent dark period, white bars represent light period. **G** Contingency table for transcript versus protein cluster membership. The *p*-value displayed is the probability of this distribution under the null hypothesis of random cluster membership if the data are from a Chi squared distribution.

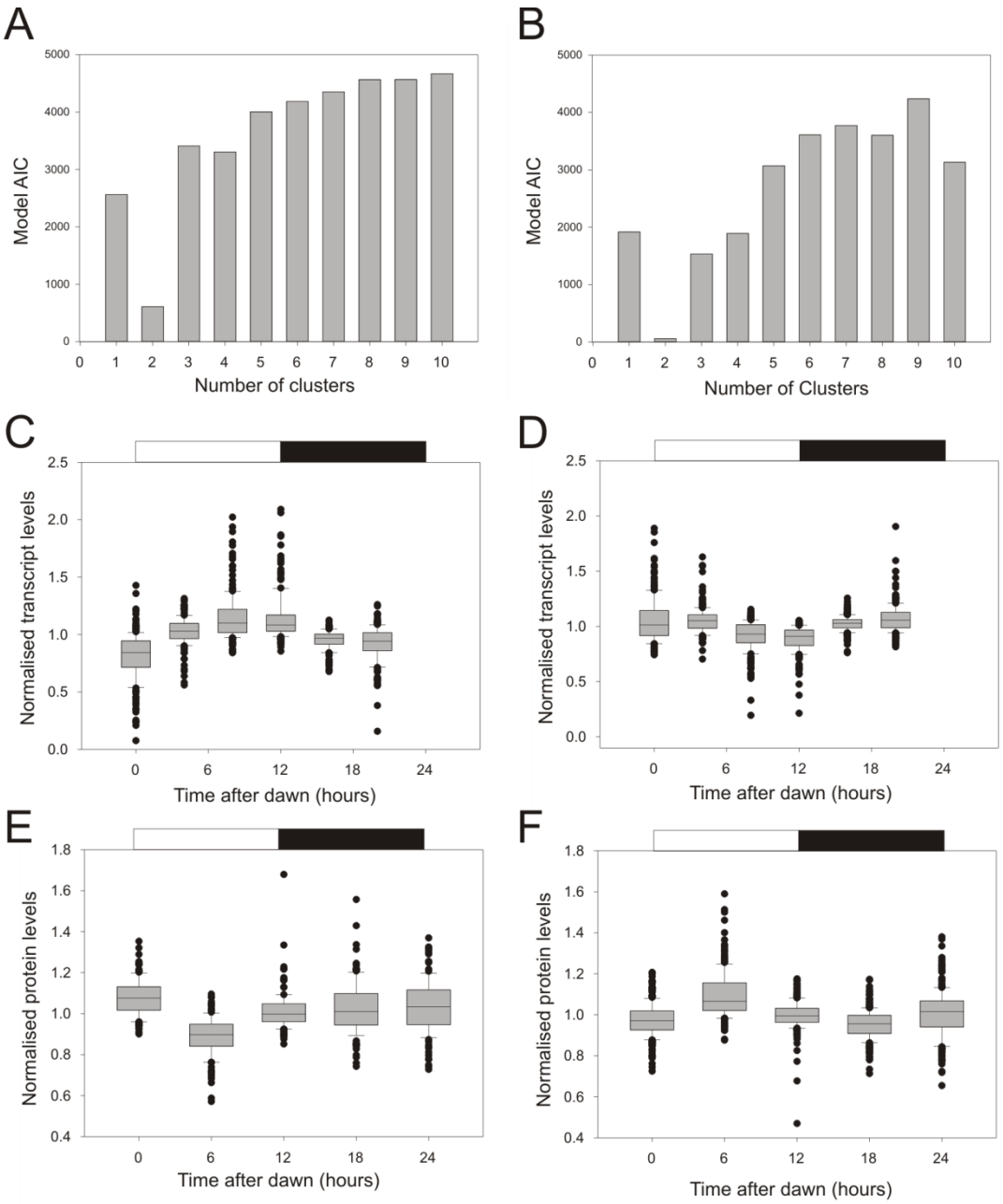

G

p = 0.021

Transcript cluster	Protein cluster 1	Protein cluster 2
1	51	77
2	73	186

3.2.7.4 Summary of analyses

The three major outcomes from the set of analyses described in this section are as follows. First, whether or not a particular transcript shows daily rhythms in abundance is a poor predictor of whether the associated protein shows daily rhythms in abundance. Second, it is rare for a protein to be rhythmic when transcript is not. Thirdly, daily patterns of change in protein abundance are often not a direct reflection of the pattern of change in transcript abundance. If there is a dawn peak in protein abundance there is more likely to be a mid-day peak in protein abundance, but in any particular case it is impossible to predict diel patens of protein abundance from diel patterns of transcript abundance.

3.3 Discussion

In this chapter, the use of label free mass spectrometry based proteomics to measure protein levels has been essential in providing quantitative information in two major experiments. Firstly I measured the abundances of 666 proteins, including AtGWD, over 24 hours and used these data to investigate the relationships between diel patterns of transcript and protein abundance both in general and for AtGWD. Secondly, I have made use of an inducible RNAi construct targeted at *AtGWD* to successfully knockdown the *AtGWD* transcript and hence protein to a small fraction of wild-type levels, thereby recapitulating the high starch phenotype of *gwd* mutant plants. A detailed timecourse of starch content and *AtGWD* transcript and protein levels during the process of knockdown has been information rich, improving our understanding of the relationship between the *AtGWD* transcript and protein and their respective functions in the control of starch degradation.

3.3.1 The role of the *AtGWD* transcript and oscillations in *AtGWD* transcript abundance in starch degradation

In section 3.2.1 I show that the abundance of the AtGWD protein changes less than 1.1 fold over a diel cycle. As discussed in the introduction to this chapter, the *AtGWD* transcript displays high amplitude daily oscillations in abundance with a peak at dusk (Smith *et al.*, 2004), but clearly this does not result in oscillations in protein abundance. Our previous knowledge of AtGWD protein abundance over 24 hours was based on the qualitative inspection of immunoblots (Yu *et al.*, 2001; Lu *et al.*, 2005). Although it was clear from the immunoblots that were no extreme changes in protein abundance, it remained possible that there were small but functionally significant changes. The data presented here clearly show that the role of the large oscillations in *AtGWD* transcript abundance is not to generate oscillations in protein abundance.

Analysis of the timecourse of knockdown of *AtGWD* demonstrated that there are no large changes in protein turnover during the diel cycle for which the large amplitude transcript oscillations could be compensating. During the timecourse of knockdown, *AtGWD* transcripts dropped to a low level within 36 hours of the first dex spray, but protein levels took much longer to decrease. By assuming that AtGWD protein production had essentially stopped two days after the first dex spray, I calculated that the protein has a half life of approximately 2 days. This means that there cannot be any large changes in protein turnover masked by constant steady state protein levels.

The timecourse data also demonstrate that the presence of the transcript, and the oscillations in transcript abundance, are not required for the normal daily control of starch degradation. On the second and third day of the timecourse, *AtGWD* transcript had dropped to very low levels and yet starch degradation was still essentially normal.

3.3.2 General relationships between patterns of transcript and protein abundance

AtGWD protein abundance does not follow changing transcript abundance over the diel cycle, but there are little data in the literature which allows us to assess whether AtGWD is exceptional in this behaviour or whether it is a common phenomenon. Some of the only data available comes from the Stitt group (Max Planck Institute, Golm) who have made detailed studies of transcript and protein levels over 24 hours for 23 enzymes of central metabolism. They found that diel changes in transcripts were generally larger in amplitude than diel changes in enzyme activities (Gibon *et al.*, 2004a). In cases where transcripts showed large diel changes, some enzymes showed no diel change in maximal activity (eg fumarase, and ferredoxin-dependent glutamate synthase) while other showed large changes in maximal activity (nitrate reductase and ADP-glucose pyrophosphorylase). In a further study they demonstrated that changes in protein abundance for these 23 enzymes were always much delayed and damped relative to changes in transcript levels (Gibon *et al.*, 2006). These results suggest that the behaviour of AtGWD is not entirely unusual, but much larger data sets are necessary to assess fully the generality of this conclusion.

A large amount of 24 hour transcript data is publicly available from numerous experiments, but there has been no systematic study of the Arabidopsis proteome over a 24 hour cycle. While making proteomic measurements of AtGWD over a diel cycle, I also measured some 600 other proteins present in the same SDS polyacrylamide gel slice. This slice included all proteins migrating slower than the 100 kDa marker on the gel. After filtering for data quality (ensuring 0 h and 24 h data matched) this left a set of diel abundance data for 387 proteins. These data were combined with published diel transcriptomic data from the Stitt group (Max Planck Institute, Golm) to assess the generality of the *AtGWD*-type relationship between transcript and protein. When drawing conclusions from these data it should be remembered that this is a highly

biased dataset, containing only abundant proteins over 100 kDa identifiable by mass spectrometry. Analysis of the GO classification frequencies within the data set showed it to be enriched for proteins of known function and depleted in functions relating to transcription when compared to the whole genome. However the data are still of considerable interest, especially in the absence of a larger scale study.

On interrogating the data, I found that *AtGWD* is in no way exceptional: in 60% of cases in which the transcript could be classified as rhythmic, the protein displayed no significant change over the diel cycle. It was rare for a protein to be rhythmic in the absence of transcript rhythms, and in only 15% of cases were both transcript and protein invariant over 24 hours. It was notable that the proteins generally oscillated with a somewhat lower amplitude than the transcript (in terms of fold change) as has been found in other studies (Gibon *et al.*, 2004a). These data are consistent with most protein half lives being rather longer that most mRNA half lives, as has been found in non-plant systems (Vogel and Marcotte, 2012).

To what extent can patterns of protein abundance over 24 hours be inferred from patterns of transcript abundance? The crudest level at which to examine this question is simply to compare the mean relative abundance of proteins and transcripts over 24 hours. However this was not possible in my dataset, because the methods I used are suitable only for comparing individual proteins between samples, not for protein-protein comparisons within a sample. However it has been found in mouse, humans and yeast (Vogel and Marcotte, 2012) as well as in Arabidopsis (Piques *et al.*, 2009), that transcript abundance is a poor predictor of protein abundance. This is perhaps not surprising as many factors beyond mRNA abundance are known to affect protein levels. Piques *et al.* (2009) measured the abundance of specific transcripts in polysomes, and ribosome densities per translating transcript. By multiplying these two quantities they could calculate the ribosome occupancies of specific mRNAs, which are related to the translation rate. When ribosome occupancy was compared to absolute mRNA concentration for specific transcripts, they found that mRNA concentrations only accounted for at most 10% of variation in ribosome occupancy. These data suggest that translation rates may depend more on individual features of transcripts than on their abundance.

To see whether the pattern of change in the transcript over 24 hours was at all predictive of the pattern of change in the protein, I took an unbiased cluster based approach. Cluster analysis based on the pattern of change in abundance over 24 hours grouped both the transcript and the protein data sets into two clusters with high confidence. For the transcripts, this clearly separated those with a dawn peak in expression from those with a dusk peak in expression, whereas for the proteins it separated those with a mid-day peak from those with a mid-day trough. The Chi squared statistic for the resultant contingency table of protein cluster membership versus transcript cluster membership suggested a significant (p=0.021) deviation from a random distribution among clusters. This suggests that genes with a transcript peak at dawn are more likely to have a protein peak at mid-day than those genes with a transcript peak at dusk. However for any specific protein, it is impossible to predict the pattern of protein abundance from the pattern of transcript abundance with any confidence. Often, the protein was observed to peak at a different time of day to the transcript, and sometimes they were completely opposed in phase.

From a mechanistic point of view, why is it so common for proteins, including AtGWD not to oscillate when the transcript does? A study in Arabidopsis concluded that the synthesis rates of most proteins are too small to allow very high rates of protein turnover (Piques *et al.*, 2009). Indeed they calculated that for most enzymes it would take about four days to synthesise the entire complement of that protein in the rosette. However the calculations on which this conclusion are based are highly dependent on assumed and unmeasured mRNA translation progression rates and could easily be out by a factor of four or more. Thus there is likely to be sufficient synthetic capacity to generate a 10%-40% increase in abundance of many proteins in a day if there is no protein degradation. If the system is at steady state, then there will of course be no net increase in protein abundance during the day, but depending on the relative timing of protein synthesis and degradation measurable oscillations are possible.

In a particular case, if we know the half life of the protein and we know the amplitude of the transcript oscillations (as we do for AtGWD), it should be possible to predict the expected amplitude of any oscillations in the protein. The concentration of transcript can be described by an oscillatory function of time, and I will assume that the rate of transcription and translation is dependent only on the concentration of transcript. This

assumption is often used in systems biology modelling (Szallasi *et al.*, 2006), and although grossly simplistic, allows essential features of the system to be discerned. The exponential decay of the AtGWD protein shown in Figure 3.15 supports a density dependent protein decay function, indicating an active degradation mechanism involving cellular machinery rather than a passive disintegration. The rate of change of the amount of AtGWD protein, *G*, can be described by the following differential equation, where t is time, ε is the translation rate, α is the amplitude of transcript oscillation, ω is the angular frequency of the oscillations (included for completeness: the period will always be 24 h in plant), β is the centre of the transcript oscillation and γ is the protein degradation rate:

$$\frac{dG}{dt} = \varepsilon(\alpha \sin(\omega t) + \beta) - \gamma G \tag{5}$$

This can be integrated (see appendix 1 for working) to yield:

$$G(t) = \frac{\varepsilon\alpha}{\omega^2 + \gamma^2}(\gamma \sin(\omega t) - \omega \cos(\omega t)) + \frac{\beta\varepsilon}{\gamma} + Ce^{-\gamma t} \tag{6}$$

Where C is the constant of integration. This solution has some features we would expect from the equation (5). For example, protein amounts are increased by increasing translation rates (ε), increasing the 'average' amount of transcript (β) or decreasing degradation rates (γ). However, there are also some features of the solution less obvious from equation (5). First, as the protein decay rate (γ) increases, then the absolute amplitude of the protein oscillations decreases. In other words, the longer the protein half life, the more the oscillations in transcript abundance are reflected at the protein level in terms of absolute amplitude. However, a longer protein half life also means that the stable state protein abundance will be greater, and thus the fold change of the protein oscillations becomes smaller. Second, as the frequency of the transcript oscillations (ω) increases, the amplitude of the protein oscillations decreases. Thus, if the frequency of transcript oscillations varied in the plant, the system has a built-in noise filter meaning that the higher the frequency of the transcript oscillations, the more damped they will be at the protein level. However this is highly unlikely to be relevant in a real plants, which exist in a world dominated by 24 h rhythms.

The combined transcript and protein diel abundance data show that it is common for a protein to oscillate with low fold change, when the transcript oscillates with high fold change. Equation (6) can be used to explore the conditions in which this scenario might arise. Clearly, decreasing the translation rate (ε) or the amplitude of the transcriptional oscillations (α) decreases the amplitude of protein oscillations, but also of the transcript oscillations. Increasing the frequency of the transcript oscillations (ω) damps the amplitude of the protein oscillations. However, there is no good evidence for oscillations with periods other than 24 hours in the transcript data set used in my analysis, so changes in ω are unlikely to explain differences in protein behaviour. The remaining parameter which affects the amplitude of protein oscillations is the protein stability. The slower the degradation rate, the more abundant the protein and the smaller the fold chnage in protein abundance. Therefore, one might predict that proteins with longer half lives are less likely to oscillate with a large fold change. There has been no proteome wide determination of protein half life in Arabidopsis, but Piques *et al.* (2009) estimate a related quantity for over 100 proteins: the half time for synthesis of the enitre rosette complement of each protein. Unfortunately, there is an overlap of only 20 proteins between the Piques data set and my data set, and most of these have only very low amplitude transcript oscillations. However, inconsistent with my hypothesis, those proteins with shorter half lives tended to have a greater diel fold change in protein levels relative to the fold change of the transcript (see appendix 1). Much larger data sets will be needed for a rigorous assessment of these relationships.

It should be remembered that the model described above entirely neglects the massive complexity of both the translational and the protein degradation machinery. For example there is good evidence that polysome occupancy and translation rates are much greater during the day than during the night in Arabidopsis (Piques *et al.*, 2009). In the chloroplast there is a great diversity of protein degradation machinery, with more than 50 genes encoding plastidial proteases (Sakamoto, 2006). However, there is experimental evidence to support density dependent degradation for much of the proteome in non-plant systems such as human cell lines (Eden *et al.*, 2012), so the detailed mechanics of protein degradation may not be important when assessing global trends.

Although regular diel changes in protein abundance can be explained minimally by an oscillating transcript and appropriate degradation rates, in well studied examples it is clear that may other diverse factors may also have a role. In the case of nitrate reductase (NIA), a model has been proposed which can account for daily oscillations in *NIA* mRNA abundance, protein levels and enzyme activity (Yang and Midmore, 2005), although the experimental basis for some aspects of the model is debatable. In this model nitrate stimulates production of the NIA protein, which then catalyses the reduction of nitrate to nitrite, thereby removing the stimulus. This central feedback is coupled to several other feedbacks involving post-translational modification, protein degradation and external inputs, which combine to generate sufficient non-linearity for a stable, self regulating system displaying limit-cycle oscillations. In other examples, protein instability coupled with periodic stabilisation seems to play a key role in the generation of oscillations. For example, granule bound starch synthase (GBSS) is never detectable in the soluble fraction in Arabidopsis leaves, but is found in starch at all times of day (Smith *et al.*, 2004). The plant contains very low GBSS levels at dawn, but the protein rapidly accumulates in starch granules in the first few hours in the light. Presumably, as the starch is degraded at night GBSS is released from the granule and is rapidly degraded in the the cytosol. Thus periodic stabilisation of GBSS by starch could explain the large daily changes in GBSS protein abundance. In an analogous manner large diurnal changes in abundance of the day length sensor CONSTANS require time of day dependent protein stabilisation (Imaizumi and Kay, 2006). In long days phytochrome dependent signals act to stabilise the CO protein towards the end of the day, leading to increase in protein abundance. However even for this well-studied system, a full mathematical description is not available.

3.3.3 The role of transcript oscillations

Why do transcripts of such a large fraction of the genome oscillate in abundance over a diel cycle when this often does not result in oscillations in the protein abundance? This phenomenon has been studied in great detail and at a large scale by the Mark Stitt group (Max Planck Institute, Golm). Gibon *et al.* (2004a) studied patterns of transcript abundance and maximal activities (as a proxy for protein amount) of 23 enzymes of central metabolism over a diel cycle and in response to an extended night. They also found that transcripts typically show much larger amplitude changes in abundance than proteins over a diel cycle, and that the extreme changes in transcript observed in an

extended night only begin to be reflected in protein levels after about 48 hours. From this they conclude that transcript levels provide an immediate readout of the metabolic status of the plant. Proteins tend to have longer half lives, so changes in protein abundance will only occur there is a sustained perturbation in metabolic status, resulting in sustained changes in transcript levels. The synthesis of mRNA is thought to be much less energetically expensive than the synthesis of protein (Piques *et al.*, 2009). Therefore this system has an obvious advantage as a noise filter: transient changes in environmental conditions will not result in energetically expensive changes in protein levels, and yet proteins will change in abundance if those conditions persist. Such adjustments have been observed through analysis of the starchless *pgm* mutant, which suffers from carbon starvation every night. Hundreds of transcripts are altered in *pgm* relative to Col-0 every night. Genes involved in photosynthetic and anabolic processes are downregulated while many genes involved in catabolic processes are induced (Thimm *et al.*, 2004). These changes occur every night for the entire life of the plant and so become reflected in the respective enzyme activities (Gibon *et al.*, 2004a; Gibon *et al.*, 2004b). In contrast, Col-0 subject to a single extended night of just a few hours shows a very similar transcriptional profile to that of *pgm* in the night, but no changes in enzyme activities are observed because this represents a single, transient change in the environment (Gibon *et al.*, 2004a; Thimm *et al.*, 2004; Bläsing *et al.*, 2005). When Col-0 is left in the dark for several days, then enzyme activities shift to resemble those of *pgm* in the dark.

Further studies have focused in more detail how daily changes in expression arise. Usadel *et al.* (2008) were able to generate models explaining daily patterns in transcript abundance based on how a particular gene responds to changing carbon status, light or the circadian clock. Using this approach they could predict which factors were important for the expression of different groups of genes at different times of day. For example, transcripts identified as being carbon repressed (ie abundance decreased in carbon replete conditions such as the addition of exogenous sugars) and which were regulated by the circadian clock tended to peak in the subjective light period in free-running (continuous light) conditions. However in daily conditions, rising sugars in the day tended to attenuate the clock induced increase in abundance. This insight can then be used to explain the rapid increase in transcript levels of some members of this class of genes in an extended night. In such conditions the clock is promoting expression of

the gene at the beginning of the day, while carbon depletion also releases repression, leading to especially high transcription. Several genes involved in sugar signalling display this behaviour. These include genes (*TPS8-11*) encoding enzymes responsible for the synthesis of the signalling metabolite, trehalose-6-phosphate.

The expression pattern of the co-regulated set of starch degradation genes (*PHS1*, *PHS2*, *ISA3*, *DPE1*, *DPE2*, *AtGWD*, *PWD* and *SEX4*) can also be explained through this approach (Usadel *et al.*, 2008). All of these genes display transcript oscillations with a peak at subjective dusk in free running conditions, but importantly their expression is also induced by light and / or carbon replete conditions. This means that carbon signalling acts in the same direction as the clock through the day and so the transcript pattern observed in free running conditions is maintained in daily conditions. In an extended night, falling carbon status overrides the signal from the clock and so transcript levels drop rapidly. In general low carbon conditions will cause decreases in mean transcript levels for enzymes of starch degradation and, if low carbon conditions are sustained, then a decrease in protein levels will also result.

The above observations indicate that oscillations in transcription simply reflect the fact that plants live in changing, rhythmic environments and that signals therefore arrive at different times of day. The endogenous transcriptional/translational/post-translational network is closely tuned to that rhythmic environment, so endogenous signals also arrive at particular times of day. The *AtGWD* promoter, in common with the promoters of many other starch degradation related genes, contains *cis*-elements which could confer responsiveness to many diverse environmental and endogenous signals. mRNAs tend to have half lives of the order of a few hours (Vogel and Marcotte, 2012), therefore the transcript abundance of these genes probably represents an integration of the relative strengths of the various input signals over the previous few hours. The identities, quantity and spatial arrangement of *cis*-elements within the promoter could determine for each gene the extent to which each signal drives expression and how interactions between siganls are resolved. The damping behaviour caused by density dependent protein degradation means that transcript oscillations are not reflected at the protein level. In addition, the long half lives of proteins relative to transcripts mean that only transcriptional changes sustained over several days become reflected in protein abundance.

In general, in line with ideas from the Stitt lab, I suggest daily patterns in transcription probably have little to do with the diel regulation of protein abundance, and rather represent a sophisticated mechanism for three important processes:

1. Responding to multiple signals
2. Integration of those signals according to gene-set specific circuits and rules
3. Optimisation of cellular protein abundances in a sensitive manner while being robust to short term environmental fluctuations and noise.

3.3.4 A flux control coefficient for AtGWD with respect to starch degradation

The timecourse of knockdown of *AtGWD* provided data on the rate of starch degradation through the night at various known levels of AtGWD protein. This information is sufficient to calculate a flux control coefficient for the enzyme: the fractional change in flux resulting from a fraction change in enzyme amount (Kacser and Burns, 1973). There are three essential preconditions for an experiment measuring a flux control coefficient (Araujo *et al.*, 2012). Firstly, the system must be close to steady state. Clearly the inducible knockdown system is not in steady state on a day to day timescale; in fact no biological system is, even in the absence of an experimental manipulation. However we know that starch degradation will reach a new steady rate, withing at least to hours, in response to changes in the timing of dusk and hence night length. (Lu *et al.*, 2005; Graf *et al.*, 2010). I suggest that the timescale of protein change in this experiment is slow enough relative to the rate of adjustment of degradation that the system may be considered in pseudo steady state. Secondly, the enzyme must catalyse only one reaction, which is the case for AtGWD as far as we are aware (Ritte *et al.*, 2002), although it has recently been shown that the enzyme can use ATP or ADP to phosphorylate AMP and ADP in the absence of alpha-glucans (Hejazi *et al.*, 2012), but the significance of these reactions *in vivo* are unknown. Thirdly, only one enzyme should be changed by the experimental manipulation. The proteomic data largely support this conjecture, showing that, at least for proteins migrating above the 100 kDa marker in SDS-PAGE, only AtGWD and one other protein (ROC4) show any large or consistent changes through the timecourse.

The flux control coefficient for AtGWD was calculated to be 0.06 at wildtype protein levels. Thus AtGWD has very low control over the flux: protein levels have to be decreased to approximately 40% of wildtype levels before there is any effect on the

pathway flux. Given that the half life of the protein is 2 days, this means it would be impossible for starch degradation rates to be adjusted *in planta* after sudden changes in night length by the modulation of AtGWD protein levels. It should be remembered that the magnitude of a flux control coefficient has no bearing on the question of whether amounts of an enzyme ever change in the plant without external intervention, or on whether an enzyme is subject to regulation for flux control or concentration control. For example a low flux control coefficient would be measured if the activity of the enzyme was regulated *in planta* for flux control, and as protein levels decreased due to external intervention, feedbacks in the plant acted to increase the proportion of the enzyme in the active state, thereby maintaining flux through the pathway until protein levels decreased to the point that 100% of the enzyme is in the active state.

It may be that some enzyme other than AtGWD has a high flux control coefficient for starch degradation. If so, then this enzyme would be an interesting subject for detailed study because any regulatory change at this point is likely to affect the flux. Alternatively, it is possible that control may be distributed among the enzymes of the starch degradation pathway as proposed in general terms by Kacser and Burns (1981). To distinguish these possibilities, it would be necessary to measure flux control coefficients for all enzymes in the pathway. This is clearly not feasible, especially since we may not know all the enzymes involved. Starch synthesis in potato tubers is under control of the adenylate transporter which is not directly involved the linear pathway of starch synthesis (Geigenberger *et al.*, 2004). By analogy, it could be that control of starch degradation resides mostly in an enzyme not directly involved in the pathway. Even if no enzyme in the pathway has a large flux control coefficient, then regulation of flux through the pathway *in planta* could still reside largely with one enzyme, or a subset of enzymes. Thus the measurement of flux control coefficients for the other enzymes of the pathway is probably not a priority for future work.

3.3.5 An unexpected role for AtGWD in starch synthesis

Intriguingly, the timecourse of knockdown of *AtGWD* suggests that the AtGWD enzyme has a role in starch synthesis. As AtGWD protein levels decrease, the amount of starch at the end of the night increases, yet the amount of starch at the end of the day remains the same. Therefore each day less starch is synthesised. The flux control

coefficient of AtGWD with respect to starch synthesis is 0.08, so there must be a very substantial decrease in AtGWD protein before an effect on starch synthesis is observed.

There are several possible explanations for these data, but by far the simplest and most plausible is that AtGWD has a direct role in starch synthesis. There is certainly no reason why high end of night starch levels in the RNAi line towards the end of the timecourse should inhibit starch synthesis the next day. The full *gwd* mutant accumulates starch to end of the night levels ten times greater (see chapter 5) than those observed in the RNAi lines. In addition, many starch excess mutants, with more starch at the end of the night than accumulated in the RNAi line, still synthesise a considerable amount of starch each day (Kötting *et al.*, 2005; Kötting *et al.*, 2009; Comparot-Moss *et al.*, 2010). Although the data in this chapter support the involvement of AtGWD in starch synthesis, it is clear that AtGWD is not absolutely required for this process because the full *gwd* mutant accumulates starch to extremely high levels. If the RNAi line were examined over a longer timecourse of knockdown, it is likely that degradation would halt completely, while synthesis would drop to the rate of synthesis in the full *gwd* mutant. Thus starch at the end of the day would begin to accumulate and may eventually reach levels equivalent to those in *gwd*.

There are no previous reports supporting the involvement of AtGWD in starch synthesis, but it is known that starch is phosphorylated during synthesis. In Arabidopsis, starch is already phosphorylated by the end of the day (Yu *et al.*, 2001). If *Chlamydomonas reinhardtii* is supplied with exogenous ^{32}P in the light, then incorporation of radioactivity into starch is observed to proceed at a constant rate (Ritte *et al.*, 2004), demonstrating that starch is phosphorylated in the light. It is thought that starch phosphorylation may disrupt the crystallinity of amylopectin, making it more accessible to enzymes (Kötting *et al.*, 2010). One can imagine a situation in which over-crystallisation of the amylopectin blocks the access of starch synthases to the glucan chains and thus inhibits starch synthesis. Then AtGWD might act to relieve this inhibition by phosphorylating the amylopectin chains, causing a decrease in crystallinity and allowing starch synthases to access the glucan chains.

There are already examples of enzyme activities involved in both starch synthesis and degradation. The isoamylase (ISA) 1 activity, provided by the ISA1 and the ISA2

proteins, cleaves glucan chains at α-1,6 branch points and is necessary for the synthesis of normal amylopectin (Delatte *et al.*, 2005; Streb *et al.*, 2008). There are two other debranching enzymes in Arabidopsis, ISA3 and limit dextrinase (LDA) (Wattebled *et al.*, 2005). The *isa3* mutant has a starch excess phenotype which is enhanced by an *lda* mutation, so it is likely that both ISA3 and LDA are involved in starch degradation (Delatte *et al.*, 2006). In the *isa1/isa2* double mutant there is still a small amount of starch synthesis, but this is abolished in the *isa1*/*isa2*/*isa3*/*lda* quadruple mutant, indicating that ISA3 and LDA can also act in starch synthesis, at least in the *isa1*/*isa2* mutant background (Streb *et al.*, 2008). It has been suggested that debranching activates are necessary for normal starch synthesis because they remove misplaced or excessive side chains which prevent the proper crystallisation of the amylopectin (Myers *et al.*, 2000; Streb *et al.*, 2008).

Further experiments could be performed to confirm the involvement of AtGWD in starch synthesis. For example, the silencing construct could be induced in the RNAi line for long enough that AtGWD levels fall significantly, but starch degradation is not yet perturbed. Then the RNAi line and the empty vector control would be transferred to darkness for several days to completely de-starch the plants. Meanwhile, dex spraying would continue so that AtGWD levels drop to 10% of wildtype or less in the RNAi line. Next, the plants would be transferred to continuous light and rates of starch synthesis monitored. If AtGWD is involved in starch synthesis then the rate of synthesis should be slower in the RNAi line compared to the control.

More direct experiments could be envisaged to explore the role of AtGWD at different times of day if there was a method for the rapid and controllable inhibition of the enzyme *in vivo*. The use of inducible RNAi is clearly not a suitable strategy to achieve rapid inhibition given the long half life of AtGWD. In general, tools to abolish the activity of particular enzymes *in vivo* at particular times of day are going to be essential for a good understanding of the daily regulation of plant metabolism. One possible approach is an inducible protein degradation system such as that already developed in *E. coli* (McGinness *et al.*, 2006). In this system proteins carrying a certain peptide tag are degraded to undetectable levels within 30 mins of the induction of expression of a protein which targets the tagged protein to the protease. A converse strategy has been used in mouse cells, whereby a synthetic small molecule can be used to artificially

stabilise proteins carrying a particular tag (Rodriguez and Wolfgang, 2012). However similar systems have not yet been developed in plants. Another possibility is the use of camelid antibodies. These are single (heavy) chain antibodies which have been successfully employed as enzyme inhibitors (Lauwereys *et al.*, 1998) and have potential in a variety of biotechnological applications (de Marco, 2011). The single polypeptide nature of these antibodies is particularly useful as it means the domains responsible for antigen recognition can be cloned and identified (Verheesen *et al.*, 2006) and expressed recombinantly (Teh and Kavanagh, 2010). In one study, llama antibody fragments which bound to potato starch branching enzyme 1 (StSBE1) were isolated by phage display (Jobling *et al.*, 2003). Several of these fragments were found to inhibit StSBE1 *in vitro*, and when expressed in transgenic potato lines resulted in very large reductions in SBE activity and high amylose tuber starch. Such systems could be used to generate highly specific, genetically encodable enzyme inhibitors for many enzymes. Expression under an inducible promoter could be used to inhibit enzymes in particular cellular compartments, tissues or organs at particular times of day.

3.3.6 ROC4: a new line of investigation

Only one protein identified in the proteomic data from the inducible knockdown of *AtGWD* showed any marked change over the timecourse. This was ROC4 (CYP20-3), a cyclophilin and peptidyl prolyl isomerase (Lippuner *et al.*, 1994; Laxa *et al.*, 2007). ROC4 showed decay kinetics remarkably similar to AtGWD except that protein levels plateaued at around 40% of wildtype levels as compared with 10% of wild-type for AtGWD. It seems unlikely that decreases in ROC4 were due to decreases in *ROC4* transcript for two reasons. Firstly, the region of AtGWD used to construct the silencing construct has no identity with any part of the *ROC4* sequence. Secondly, I analysed microarray data (NCBI GEO accession: GSE19260) of Col-0 versus the *sex1-3* mutant which lacks the AtGWD protein. Plants analysed in these microarrays were harvested at the end of the night, and at this timepoint there is no significant difference (p=0.43) in *ROC4* transcript abundance between Col-0 and *sex1-3*. In the diel transcript abundance data set used in previous sections (Stitt group, Max Planck Institute, Golm) the *ROC4* transcript does not vary over 24 hours, so it is probable that there is no difference in *ROC4* transcript abundance between Col-0 and *sex1-3* at any time of day. Despite trying multiple primer pairs, levels of *ROC4* transcript could not be confirmed by q-PCR in the RNAi line at the beginning versus the end of the timecourse. However RT-PCR has

been used successfully to establish the presence or absence of *ROC4* transcript (Romano *et al.*, 2004; Cai *et al.*, 2008; Dominguez-Solis *et al.*, 2008), so a q-PCR strategy may be worth pursuing further. The kinetics of ROC4 decay might suggest a physical interaction between the AtGWD and ROC4 proteins, with AtGWD acting to stabilise ROC4. Alternatively, ROC4 may be stabilised by some factor depending on proper night time starch metabolism. However the fact that ROC4 decreases with AtGWD over the first few days of the timecourse when starch degradation is still normal would argue against this possibility.

One of the most intruiging features of the ROC4 data is the fact that the protein is present in the data set at all. Monomeric ROC4 without its transit peptide is predicted to be 20 kDa, whereas all proteins analysed migrated slower than the 100 kDa marker on the reducing SDS polyacrylamide gel. There many possible explanations for this anomaly, but all assume that ROC4 is covalently attached to some entity or entities, greatly increasing the apparent molecular mass. It may be that ROC4 was still attached to intereacting partners (forming a homomultimeric or heteromultimeric complex) via disulphide bridges, if these were not fully reduced prior to loading the gel. Alternatively, ROC4 could be attached to partners through non-disulphide covalent interactions, for example by isopeptide bonding which attaches peptide modifiers such as Ubiquitin or SUMO to lysine residues in a protein. If ROC4 was modified with ten ubiquitin units then it would have a theoretical mass greater than 100 kDa and so would appear in the data set. Thus the measured abundance of ROC4 in the data set may not reflect absolute ROC4 protein levels, but rather the fraction of ROC4 in larger, modified or complexed form. The fact that the amount of ROC4 at this molecular mass decreases over the timecourse still suggests some interactions with the AtGWD protein, which would stabilise this form of ROC4.

ROC4, in common with many members of the cyclophilin family, has peptidyl prolyl *cis trans* isomerase (PPIase) activity (Lippuner *et al.*, 1994). PPIases are needed for efficient protein folding because of otherwise slow isomerisation around Xaa-Pro bonds (Lang *et al.*, 1987). *ROC4* is only expressed in photosynthetic tissues and its localisation to the chloroplast stroma has been confirmed by enzyme assays, immunoblotting (Lippuner *et al.*, 1994) and fluorescence microscopy (Muthuramalingam *et al.*, 2009). A study combining 2D native/SDS PAGE with

proteomics identified ROC4 as the sixth most abundant protein in the Arabidopsis chloroplast stroma (Peltier *et al.*, 2006). They found ROC4 predominantly in a 110 kDa complex. This would argue against most of the protein being in a complex with the 156 kDa AtGWD.

An interesting feature of *ROC4* is that the transcript becomes undetectable in 6 day old, continuous light grown seedlings when they are transferred to the dark for 24 hours (Chou and Gasser, 1997). This down-regulation in starvation conditions is similar to the behaviour observed in the co-regulated starch degradation gene set when plants are subject to an extended night (Usadel *et al.*, 2008).

There are also intriguing links between ROC4 and chloroplast redox biology. Thioredoxin *m* will bind, reduce and activate ROC4 *in vitro* while oxidation with $CuCl_2$ abolishes PPIase activity (Motohashi *et al.*, 2001; Motohashi *et al.*, 2003). In correlation networks extracted from the ATTED II database (http://atted.jp/) *ROC4* gene expression is very highly correlated with the expression of chloroplastic 2-cysteine peroxiredoxin A (2-CysPrxA, At3g11630). In fact there is evidence that ROC4 and 2-CysPrxs may physically interact. 2-CysPrxs are able to protect DNA from DTT/Fe^{3+} induced cleavage if a protein is present to re-reduce the 2-CysPrx after its oxidation. 2-CysPrxA and 2-CysPrxB are both able to protect DNA from cleavage in the presence of ROC4 in a manner dependent upon the presence of key cysteine residues in the ROC4 protein (Laxa *et al.*, 2007). This shows that ROC4 can reduce and activate both 2-CysPrxA and 2-CysPrxB. Analysis of redox mid-potentials suggests that these interactions may have relevance *in vivo*, since 2-CysPrxA has an E_m value more negative than ROC4 and 2-CysPrxB has an E_m value only slightly more positive (Laxa *et al.*, 2007). Alternatively these redox couples could operate in the opposite direction *in* vivo, depending upon the precise stromal conditions. A further link to redox is provided by data from yeast-two hybrid and *in vitro* immunoprecipitation experiments demonstrating that ROC4 physically interacts with serine acetyltransferase 1 (SAT1) (Dominguez-Solis *et al.*, 2008). SAT1 is known to catalyse a key step in cysteine biosynthesis (Leustek *et al.*, 2000). An increase in SAT activity and total protein thiol content is observed in high salt conditions in wild-type plants, and may help protect the plant against oxidative stress (Dominguez-Solis *et al.*, 2008). This response is attenuated in the *roc4* mutant, so it is possible that ROC4 acts to stabilise SAT1 under oxidative stress conditions.

However this is rather inconsistent with the knowledge that ROC4 is activated by reduction (Motohashi *et al.*, 2003; Laxa *et al.*, 2007).

In a putative interaction with AtGWD, ROC4 could either act on AtGWD through its PPIase activity thereby affecting protein folding, or it might directly reduce and activate AtGWD. The redox mid potential of AtGWD is much more positive than that of ROC4 (Mikkelsen *et al.*, 2005; Dominguez-Solis *et al.*, 2008), so it is possible the two enzymes form a redox couple *in vivo*. The connections between AtGWD, ROC4 and 2-CysPrxs are especially intriguing because they provide a possible mechanism by which AtGWD could be reduced and activated at night using reducing equivalents generated through the oxidative pentose phosphate pathway. NADPH-dependent thioredoxin reductase C (NTRC) can use NADPH to reduce 2-CysPrxs which could in turn reduce AtGWD directly or via ROC4. In the future it would be interesting to see if interactions between AtGWD and ROC4 can be confirmed *in vivo* using a system such as split-YFP, and to see whether ROC4 or 2-CysPrxs are capable of reducing AtGWD *in vitro*.

3.3.7 Summary

Results presented in this chapter show that AtGWD protein abundance does not change over the diel cycle despite large amplitude oscillations in transcript abundance. This relationship is not restricted to AtGWD. Analysis of diel protein and transcript data shows that in approximately 60% of cases in which the transcript oscillates, the protein shows no change in abundance over the diel cycle. I have proposed a mechanism to explain this behaviour: when protein degradation rates are sufficiently slow relative to other parameters, the fold change of protein oscillations will be damped relative to the fold change of oscillations in the transcript. However it should be noted that absolute amplitude shows the opposite relationship.

Some general trends can be observed relating transcript expression patterns and protein expression patterns. However in any particular case it is impossible to predict daily patterns of protein abundance from daily patterns in transcript abundance. Evidence from the literature suggests that the abundance of a given transcript integrates the environmental and endogenous signals converging on that gene in the previous few hours. Proteins tend to have much longer half lives, so only sustained changes in

transcription become apparent at the protein level. Thus the transcript / protein system effectively acts as a signal integrator and a noise filter.

Analysis of a timecourse of knockdown of *AtGWD* has demonstrated that daily oscillations in *AtGWD* transcript abundance are not necessary for the daily regulation of starch degradation. In fact AtGWD has a long half life, of two days, and a near zero flux control coefficient for starch degradation. These data combine to demonstrate that starch degradation could not be regulated *in planta* by the adjustment of AtGWD protein levels on a suitable timescale. Regulation of AtGWD by post-translational means is therefore likely to be more important. The timecourse of knockdown also provides preliminary evidence for a previously unknown role for AtGWD in starch synthesis, which merits future investigation.

Further analysis of proteomic data from the timecourse identified ROC4 as a possible AtGWD interactor. The ROC4 protein measured in the timecourse shows highly anomalous migration in SDS-PAGE, suggesting that it is covalently linked to some other entity. Given the known links between ROC4 and chloroplast redox biology, these data open an interesting avenue for further study.

4 Cloning and Expression of Arabidopsis *GLUCAN WATER DIKINASE*

4.1 Introduction and Aims

The aim of the work described in this chapter was to generate genetic resources that could be used to test hypotheses about the role of AtGWD in the control of starch degradation. In chapter 3 I have already described investigations into transcriptional regulation of *AtGWD*, making use of RNAi lines kindly made available to me by Dr Alex Graf (Smith lab, JIC). To further investigate the importance of transcriptional regulation needed *gwd* plants complemented with *AtGWD* either under the native or the 35S promoter. To investigate post-translational control, my strategy was to clone *AtGWD* and then to mutagenise residues thought to be responsible for particular properties of the enzyme. *gwd* mutant plants were then transformed with these different versions of *AtGWD* and the resulting transgenic lines analysed to determine whether wildtype patterns of starch degradation had been restored (described in chapter 5). I also wished to generate a new anti-GWD antibody to enable the selection of transformed lines expressing consistent levels of AtGWD protein. This necessitated the purification of the AtGWD protein, which also creates potential for future *in vitro* investigations of the properties of the enzyme, to complement the *in vivo* work. These resources and their uses are summarised in Table 4.1.

<table>
<tr><th>Recourse</th><th>Purpose</th></tr>
<tr><td colspan="2">Investigating transcriptional control</td></tr>
<tr><td>Plants expressing a dexamethasone inducible RNAi line targeted at AtGWD</td><td>For determining the relative contribution of the transcript and the protein to the daily control of starch degradation. Made by Dr Alex Graf (Smith lab, JIC) and available to me at the beginning of the project.</td></tr>
<tr><td>AtGWD expressed in the gwd mutant background under the 35S or the native promoter</td><td>For investigating the contribution of transcriptional regulation to the daily control of starch degradation.</td></tr>
<tr><td colspan="2">Investigating post translational control</td></tr>
<tr><td>Mutated versions of AtGWD expressed in the gwd mutant background. Mutations are intended to abolish:</td><td rowspan="5">If a given mutant version of AtGWD with altered properties cannot fully complement the gwd mutant plant phenotype, this implies that those properties are of importance for the regulation of starch degradation.</td></tr>
<tr><td>Catalytic and autophosphorylation activity of AtGWD</td></tr>
<tr><td>Formation of a disulphide bridge and redox responsive properties</td></tr>
<tr><td>SUMOylation in the first SBD</td></tr>
<tr><td>Phosphorylation in the first SBD</td></tr>
<tr><td>Starch binding capacity of SBDs</td></tr>
<tr><td>Purified AtGWD protein: wildtype and mutated version</td><td>For the generation of a new antibody and also for in vitro activity and binding assays to aid the interpretation of the phenotypes of the complemented Arabidopsis lines.</td></tr>
<tr><td>A GWD antibody</td><td>For the screening of transformed Arabidopsis lines.</td></tr>
</table>

Table 4.1: Resources required for this study

4.2 Cloning Arabidopsis GWD

The cloning of *AtGWD* was necessary to generate the resources described in Table 4.1. However, even with modern cloning technology, this proved very difficult.

4.2.1 Previously published clones

Most previous work on the properties of GWD has been carried out using the gene cloned from *Solanum tuberosum* (*StGWD*). Starch degradation in potato leaves and tubers is challenging to study, and for that reason the properties of this enzyme have largely been interpreted in the framework of our understanding of starch degradation in Arabidopsis. This is despite the fact that StGWD and AtGWD only share 63% identity at the amino acid level, with substantial divergence in the nucleotide binding region, as well as in the *N*-terminal half of the protein containing the SBDs. In this study I use the Arabidopsis gene. This is particularly important for the *in vivo* work, ensuring that the enzyme is studied in its proper biological context.

There are three previously published clones of *AtGWD*. After map based cloning of the *sex1* locus, Yu *et al.* (2001) isolated a genomic clone of *AtGWD* from a phage library and used this to complement the mutant plant. This complementation was repeated using a cDNA clone in a study focused on freezing tolerance in the *gwd* mutant (Yano *et al.*, 2005) and the same cDNA clone was subsequently used for an *in vitro* study by Edner *et al.* (2007). The third clone is a partial cDNA clone used by Elrouby and Coupland (2010) to study AtGWD SUMOylation in *E.coli*. For this study they cloned 240 cDNAs for different proteins and it was only for *AtGWD* that they could not recover a full length clone. None of these clones were available for my work.

4.2.2 Approach to cloning

Several scientists in research groups across Europe have tried to clone the *AtGWD* cDNA, but without success (personal communications). I also attempted to clone the cDNA, but could never recover colonies containing anything other than fragments of the gene. I reasoned that a full length genomic clone might be more stable, because *E.coli* should be completely unable to produce a functional protein from such a clone, so any detrimental effects on bacterial growth (eg. perturbation of extracellular polysaccharide synthesis due to aberrant phosphorylation of carbohydrates) should be eliminated. However when the full length genomic PCR product (10.5 kb, amplified with a high fidelity polymerase) was reacted with GATEWAY® compatible entry vector, pCR8, I still could not recover colonies containing a clone. Different vector systems for GATEWAY® and restriction cloning, (pCR2.1 (Invitrogen) and pGreenII

(Hellens *et al.*, 2000)) and different cell types (TOP10 (Invitrogen), DH5-α, XL-10 Gold (Stratagene)) were trialled, but without success.

4.2.3 Successful strategy

Successful clones were eventually isolated in pCR8 by the simple strategies of reducing the growth temperature of *E.coli* from 37°C to 32°C, and optimising the relative concentrations of the PCR product and vector DNA in the TOPO reaction. Decreasing the amount of vector DNA in the reaction from 10 ng to 2 ng resulted in a greater colony density, and a higher proportion of clones contained *AtGWD* sequence.

Clones were generated using PCR products including or excluding the promoter region, and including or excluding the stop codon and 3' UTR.

4.2.4 Confirming correct clones

Plasmids were prepared from cultures derived from 120 bacterial colonies which were screened with diagnostic restriction digests yielding 23 strains containing the insert in the correct orientation. This includes clones with and without the stop codon and with and without the promoter. All of these clones were sequenced at 1 times coverage with 14 sequencing primers and the 8 clones that appeared to contain the least errors were then re-sequenced at 4 – 6 times coverage using 27 sequencing primers. This allowed clones with only 1 – 3 deviations from the published sequence to be obtained. None of these deviations were consistent across clones, so they were corrected back to the published sequence by site directed mutagenesis. The native promoter of *AtGWD* seemed to be particularly prone to rearrangements, and it took several rounds of mutagenesis to generate a version that did not differ from the published sequence near any recognisable promoter elements.

4.2.5 Generation of destination clones

A major advantage of the GATEWAY® cloning system is its flexibility. There are a large number of binary destination vectors available which will add a variety of promoters, N –terminal or C-terminal tags to the gene of interest. Recombination reactions between *GWD* entry clones and GATEWAY® destination vectors were mostly of very low efficiency. Indeed, I was unable to recover destination clones containing *GWD* using the pEAQ vectors (Sainsbury *et al.*, 2009) or using a variety of vectors from

the pGWB series (Nakagawa *et al.*, 2009) and the pEarleyGate series (Earley *et al.*, 2006). A vector series developed at VIB, Gent (Karimi *et al.*, 2005), proved more successful, such that I could construct 3' *GFP* and *RFP* fusions with *GWD*. Unfortunately this vector series lacks vectors for affinity tagging, so I added a 3' 6 times polyhistidine tag (His-tag) through site-directed mutagenesis.

4.2.6 Mutagenesis programme

The mutant versions of *AtGWD* summarised in Table 4.1 were generated through site directed mutagenesis of the entry clone. A detailed justification of the choice of sites for mutagenesis can be found in the introduction to Chapter 5. Five mutant versions of *AtGWD* were successfully generated and transformed into Col-0 and *gwd* plants. The series of mutated versions of *AtGWD* were made in clones without the native promoter and were transformed into plants under the control of the 35S promoter. This was because the native promoter is large and highly repetitive, prone to rearrangements and difficult to work with.

For each mutated clone, the product had to be extensively re-sequenced to check for errors introduced during the mutagenesis process. This was because the *AtGWD* clones appeared to be intrinsically unstable, and rearrangements, deletions and primer insertions were common (Figure 4.1). The region of the protein containing the SBDs seemed to be particularly unstable and it took a long time to isolate clones with the correct mutations. Despite careful checks, plants were transformed with a SBD mutant (ΔW132; ΔW405) clone which was later discovered to contain a 1bp deletion in SBD2 that arose during the mutagenesis reactions, just beyond the termination of the original sequence data. This resulted in a frame shift and change in amino acid sequence. Although these plants contain a version of *AtGWD* correctly mutated in the W132 of SDB1, their phenotypes are difficult to interpret because of the substantial changes of sequence in SDB2. Interpretation of the role of the starch binding properties of AtGWD in the regulation of starch degradation will have to await new lines containing the correct clone, experiments which are beyond the scope of this thesis.

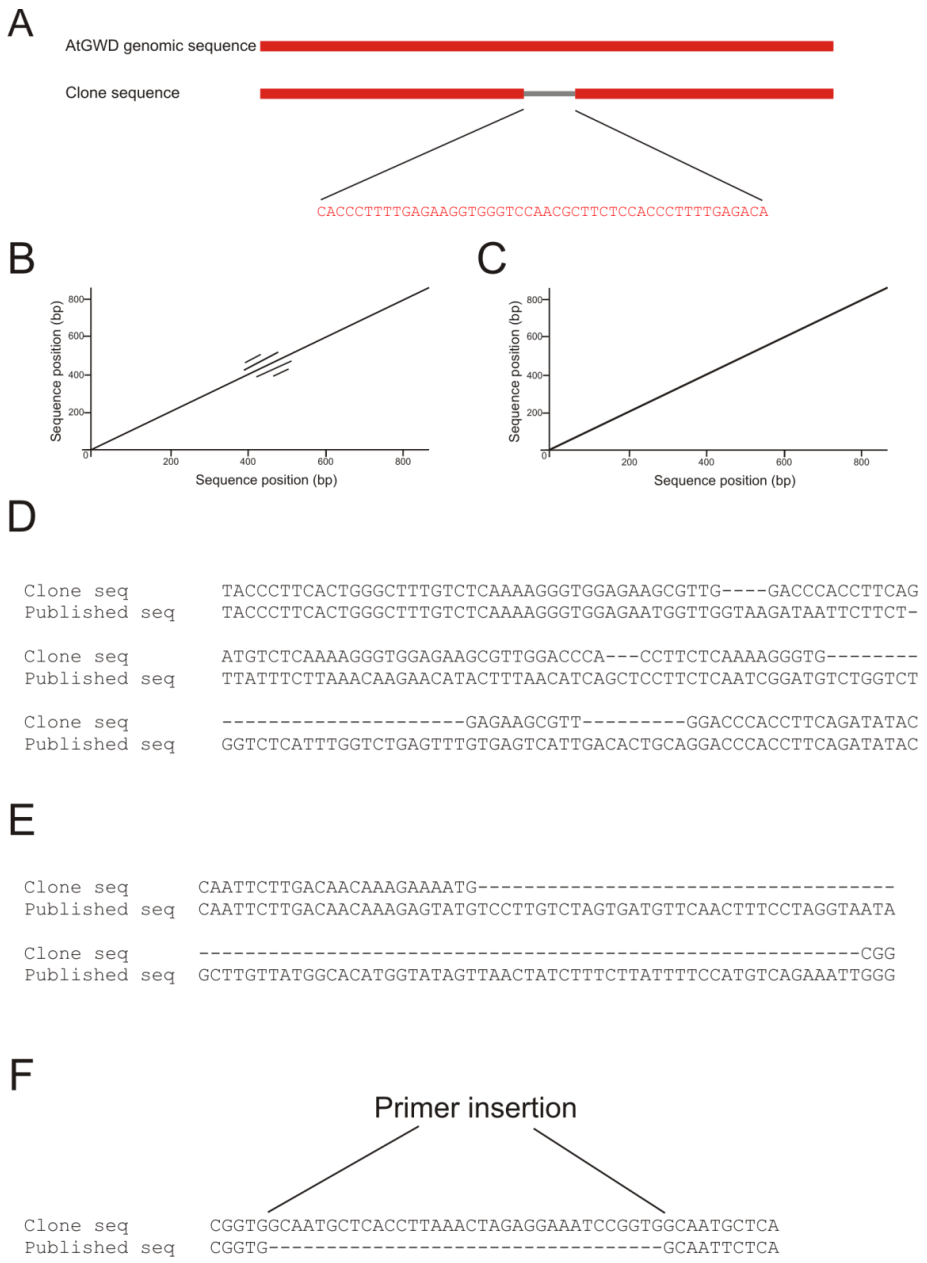

Figure 4.1: Examples of the instability of *AtGWD* clones. **A** An insertion with 100% sequence identity to *AtGWD* . **B** Analysis of clone sequence vs. clone sequence on a dot plot reveals a duplicated region in this clone. **C** Dot plot showing the absence of the duplication in correct sequence from another clone. **D** Rearrangements in clone sequence near a mutagenesis site. **E** A deletion in a clone sequence. **F** Primer sequence inserted adjacent to a mutagenesis site in a clone sequence.

4.2.7 Confirming expression transiently in *Nicotiana benthamiana*

Before continuing with the process of making transgenic Arabidopsis lines, the constructs were transiently expressed in *N. benthamiana* so that the expression and localisation of the GFP tagged protein could be verified by confocal microscopy. Confocal images showing the subcellular distribution of GWD are presented in Figure 3.2. For each construct a GFP signal could be seen in the chloroplast, confirming that the protein could be targeted to its site of action *in vivo*. In the case of constructs containing the wildtype, phosphorylation mutant or the redox mutant versions of *AtGWD*, a substantial signal was also observed in the nuclear-cytoplasmic compartment. This may be an artefact of overexpression of the protein in a heterologous system. In general these data should not be interpreted as direct predictors for localisation of AtGWD in transgenic Arabidopsis lines, but they show that the constructs express the gene, and the targeting signal encoded in the protein sequence operate as it should. The next step was to generate stable, homozygous Arabidopsis transgenics expressing these constructs, a process which is detailed in chapter 5.

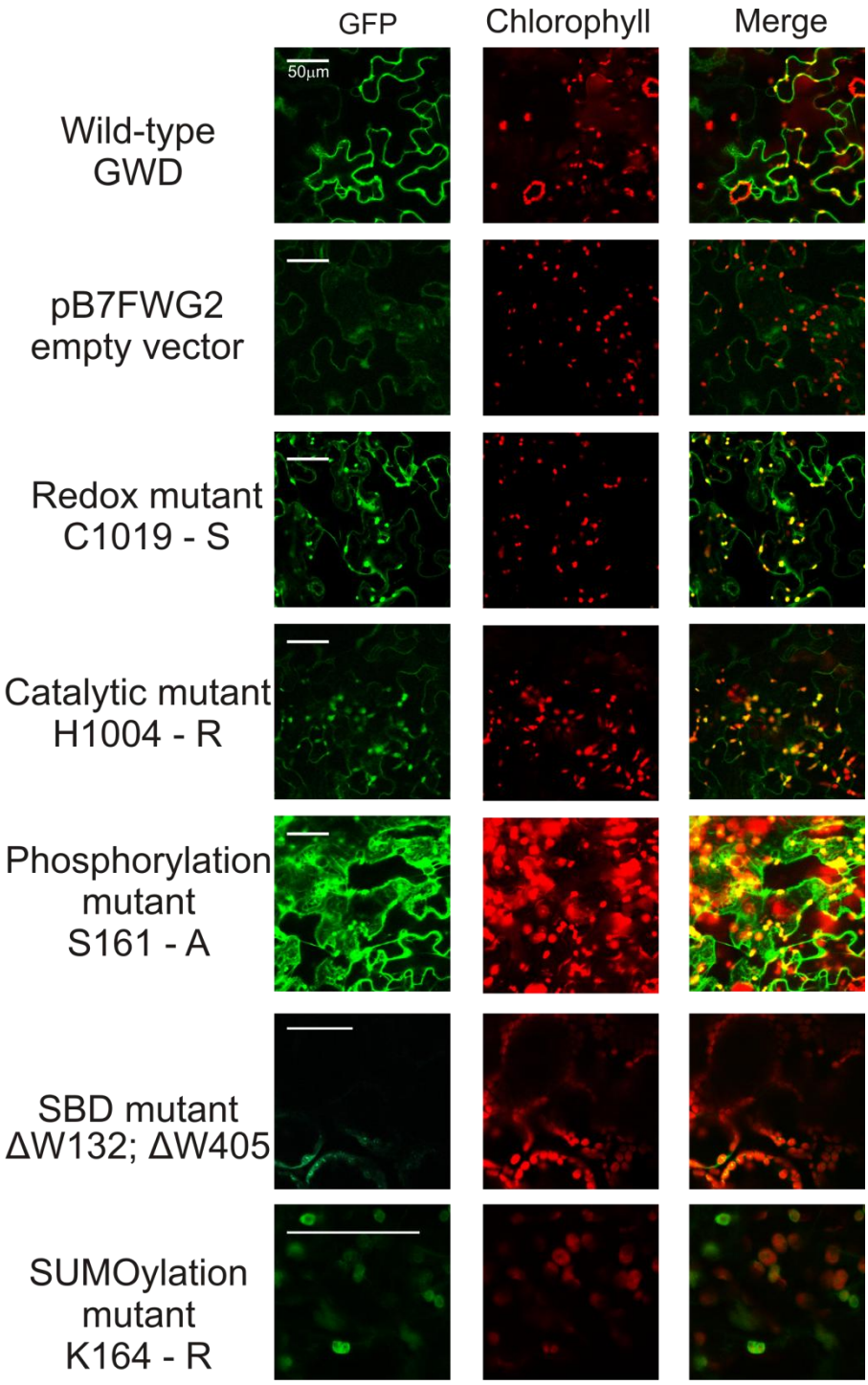

Figure 4.2: Confocal microscopy images showing the subcellular localisation of AtGWD::GFP when transiently expressed in *N. benthamiana* leaves. Left column, GFP signal; middle column, chlorophyll signal; right column, overlay of GFP and chlorophyll. The clone in question is indicated to the left of each image, along with details of any amino acid changes mutated. All scale bars are 50 µm.

4.3 Expression and purification of GWD protein

Once the *AtGWD* gene had been successfully cloned, the purification of the protein was a possibility. This was desirable because stocks of the anti-StGWD antibody (Ritte *et al.*, 2002) were low, and an antibody was required to screen transformed Arabidopsis lines for GWD expression levels. Purifying the protein also provided an opportunity to study the properties of AtGWD and of mutant variants of the protein *in vitro*.

4.3.1 Transient expression system

AtGWD was cloned as a genomic sequence and so could not be expressed in *E. coli*. Instead, *N. benthamiana* was transiently transformed by agroinfiltration for the production of His-tagged AtGWD. *Agrobacterium* containing *AtGWD* within the T-DNA were coinfiltrated with *Agrobacterium* containing the P19 suppressor of gene silencing.

4.3.2 Enrichment on Ni-Sepharose column

The first step towards purifying AtGWD was to load soluble proteins extracted from *N.benthamiana* leaves on a nickel Sepharose column (Ni-column), for which the His-tagged AtGWD was expected to have high affinity. Bound proteins were eluted with imidazole, resulting in good enrichment of AtGWD relative to contaminants (Figure 4.3 A, B). When blots of SDS polyacrylamide gels of the elutate were probed with anti-His antiserum, at least three strong bands in the 150 kDa region were revealed. These are likely to be GWD.

I tried various stratagies to improve the purity and yield of the AtGWD preparation from the Ni-column. First I tried different elution conditions, either eluting by the addition of 500 mM imidazole in a single step, or by applying an increasing gradient of imidazole. However a gradient elution failed to separate out contaminants from GWD and resulted in a low concentration of GWD in the eluate, so a single step elution was used for all subsequent purifications. Secondly, I tried increasing the amount of protein extract I loaded on the column as a strategy to increase yield. However there was no increase in yield when extract from 12 g of infiltrated leaf tissue was loaded when compared with extract from 4 g of tissue, suggesting that the column was already saturated with extract from 4 g of tissue (Figure 4.3 B). Finally, I hypothesized that loading the AtGWD enriched eluate from the Ni-column back onto the column for a second time should result in a greater concentration of AtGWD in the input, thereby

favouring AtGWD binding and perhaps generating greater purity on elution. However in practice this strategy did not seem to be of any value (Figure 4.3 C).

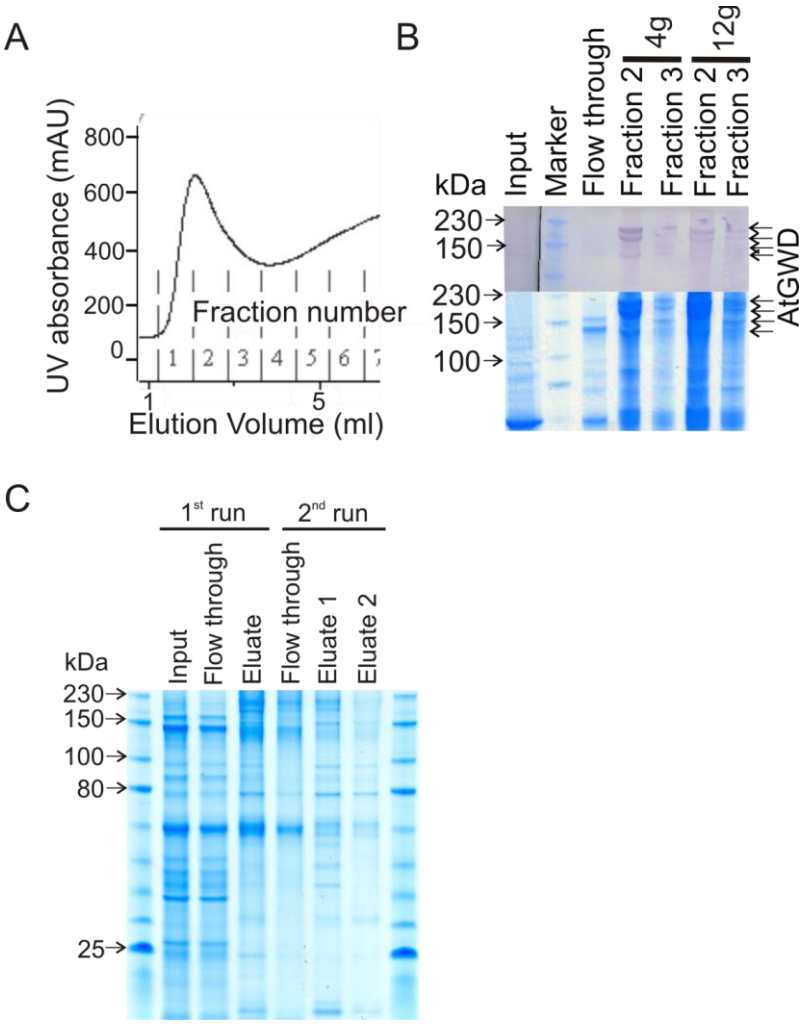

Figure 4.3: Enrichment of AtGWD by Ni affinity chromatography. **A** UV absorbance of fractions collected from the Ni-column after application of 500 mM imidazole (from elution volume = 0). Significant amounts of GWD were only found in fractions (indicated above the x-axis) 1 and 2. **B** Upper panel: SDS polyacrylamide gel (4-12%, stained with Coomassie blue) of the sample loaded onto the Ni colum (Input), the flow through and fractions 1 and 2 (see part A). Lower panel: Immunoblot of equivalent SDS polyacrylamide gel blotted with anti-His antibody. Fractions 1 and 2 are shown for two scenarios: first in which protein extract from 4 g of infiltrated tobacco tissue was loaded onto the column, and second in which extract from 12 g was loaded. **C** SDS polyacrylamide gel of protein input, flowthrough and eluate from Ni-column. The eluate from the 1st run was used as the input for the 2nd run.

4.3.3 Strategies for further enrichment

I explored several strategies, affinity based and chromatographic, for the further purification of AtGWD from extracts of *N. benthamiana* leaves.

4.3.3.1 Cobalt agarose resin

In some purification protocols, Co^{2+} resin has been found to provide better purity than a Ni^{2+} resin when used as an affinity matrix for a His-tagged target (Jiang *et al.*, 2004). I applied *N. benthamiana* extract to Co^{2+}-agarose columns to see if this was true for GWD, but neither GWD or contaminating proteins bound to the matrix.

4.3.3.2 Selective precipitation

Many proteins will precipitate under certain solvent conditions, depending on protein properties such as the degree and arrangement of surface hydrophobicity (Scopes, 1994). I tried two common methods of selective precipitation, making use of increasing concentrations of either organic solvents or salts. There is a weak negative correlation between protein size and the percentage (v/v) of an organic solvent necessary to precipitate it (Scopes, 1994). Since GWD is a relatively large protein, organic solvent precipitation seemed a promising avenue to investigate. Indeed, it appeared AtGWD was enriched compared to contaminants in the fraction of proteins that precipitate between 20% and 30% (v/v) acetone, although with a substantial yield penalty (Figure 4.4 A). Proteins that precipitated between 30% and 40% (of saturation) ammonium sulphate seemed to result in enrichment of AtGWD relative to contaminants but, once again, with a substantial yield penalty (Figure 4.4 B). One difficulty with performing such precipitations in small volumes is that it is hard to ensure proper mixing of the salt/solvent, to prevent locally high concentration causing precipitation; an effect which might explain the observed precipitation of some AtGWD across the range of salt/solvent concentrations.

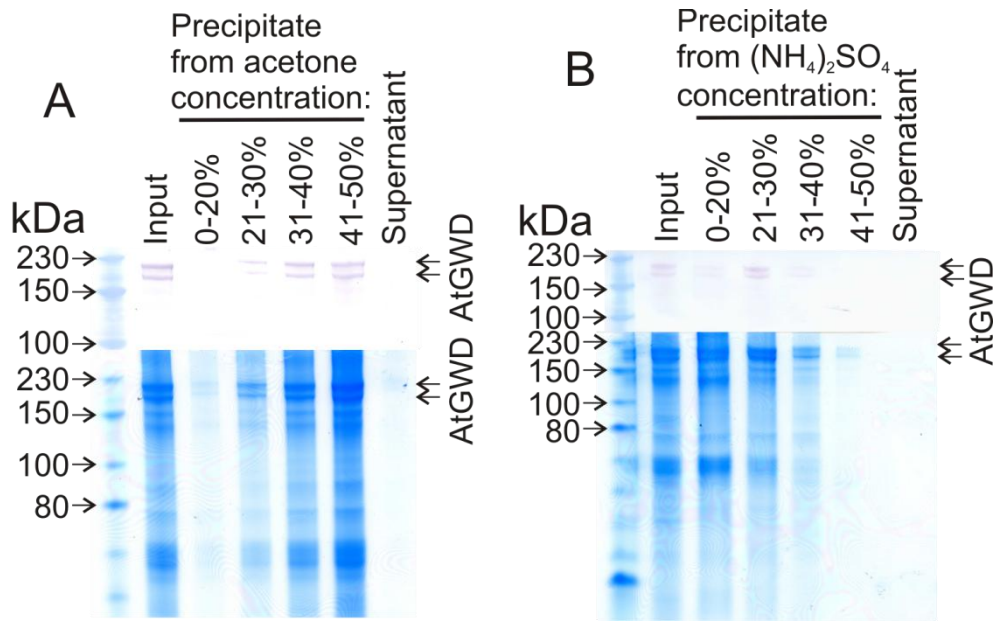

Figure 4.4: SDS polyacrylamide gels (lower panels) of protein precipitated either by increasing concentrations of **A** acetone (percentage, v/v) or **B** ammonium sulphate (percentage of saturation). Input was eluate from the Ni-column and Supernatant is the supernatant of the final precipitation step. Equivalent SDS polyacrylamide gels were analysed by immunoblotting with an anti-His antibody (upper panels).

4.3.3.3 Blue Sepharose affinity chromatography

Cibacron Blue F3G-A is an ADP-ribose mimic (Biellmann *et al.*, 1979) and so can act as an affinity adsorbent for nucleotide binding proteins. StGWD binds ATP, so I reasoned that incubating partially purified AtGWD with Blue-Sepharose beads followed by elution with 1M salt might permit further purification of the enzyme. However AtGWD did not to bind to this matrix (data not shown).

4.3.4 Enrichment on amylose resin

Successful further enrichment of AtGWD was achieved by loading the Ni-column eluate onto an amylose-Sepharose column. The use of a carbohydrate affinity matrix was an obvious strategy to try, given that StGWD is known to be a starch binding protein (Ritte *et al.*, 2000) and StGWD had previously been purified by a multistep protocol making use of a column packed with potato tuber starch granules (Ritte *et al.*, 2002). However I was initially discouraged by the fact that StGWD SBDs have two orders of magnitude lower affinity for carbohydrate substrates than other characterised

SBDs (Glaring *et al.*, 2011), as well as by the difficulties inherent in making a starch granule column with good flow properties. Amylose-Sepharose resin was chosen as a commercially available alternative to a starch column, and was found to significantly retard the flow of AtGWD through the column relative to the contaminants (Figure 4.5 A). Ten mg ml^{-1} cyclodextrin was first trialled as an elution condition (Figure 4.5 B) because StGWD is known to bind this molecule (Glaring *et al.*, 2011). Cyclodextrin was effective, however a high purity AtGWD preparation was also obtained through elution with 5 mg ml^{-1} potato dextrin solution and the latter condition was used for all subsequent purifications.

The AtGWD preparation ran as three major bands on an SDS-PAGE (Figure 4.5 C), all of which were confirmed to be GWD by their reactivity to an anti-His antibody (Figure 4.5 C) and by mass spectrometry (see section 4.4.7). In some preparations a fourth band could be seen (eg Figure 4.5 C), but since this is smaller than the known monomeric size of the protein and only present in some preparations, this is probably a degradation product, or perhaps AtGWD from which the transit peptide has been cleaved. The sizes of the three major GWD bands were estimated by comparing the distance they ran into the gel with the distances run by markers of known sizes. The smallest band is thus be estimated to be 156 kDa, equivalent to the predicted mass of AtGWD and the known mass of monomeric StGWD (Lorberth *et al.*, 1998). The middle and largest bands are estimated to be 186 kDa and 210 kDa respectively.

Purification of AtGWD on amylose resin resulted in substantial losses of AtGWD in the flow through from the column and through partial elution during the washing steps. In an attempt to prevent this, the protocol was carried out either in the presence or absence of ATP (0.5 mM) and DTT (2mM), as reduction state and ATP activation state both have the potential to affect the binding of GWD to its glucan substrate (Mikkelsen and Blennow, 2005; Mikkelsen *et al.*, 2005). However no substantial difference was observed between these two treatments (Figure 4.5 D).

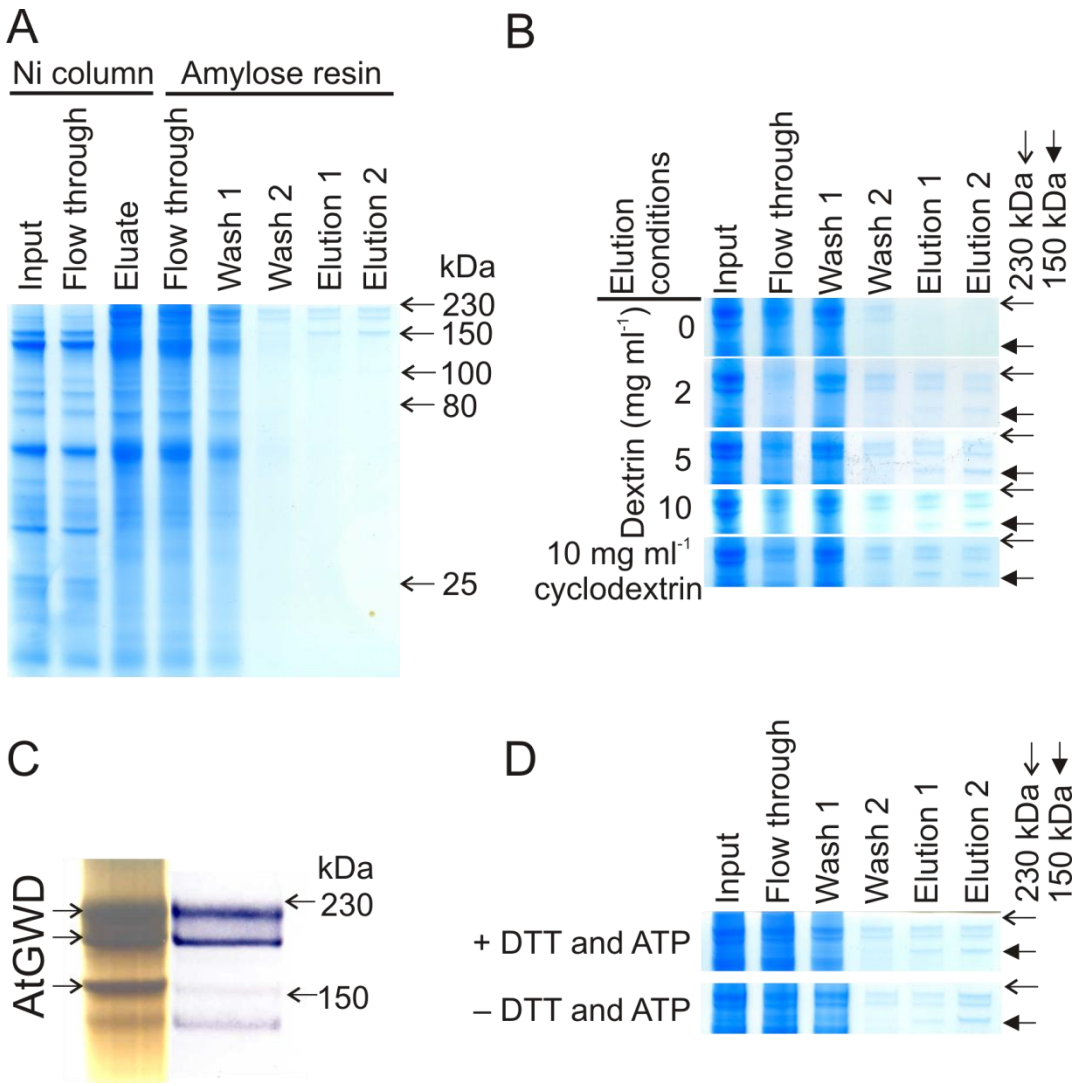

Figure 4.5: Purification of AtGWD using amylose-Sepharose resin. **A** SDS polyacrylamide gel stained with Coomassie Blue and loaded with *N. benthamiana* leaf protein extract (Input), the flow through and eluate from the Ni-column. The eluate from the Ni column was the input for the amylose column. The flow through from the application of this input to the amylose column is loaded, as is the flow through from two subsequent washes of the amylose column with 2.5 cv of binding buffer (wash 1 and wash 2). Two, 2 ml fractions were collected after elution with 5 mg ml^{-1} dextrin and loaded on the gel (elution 1 and 2). **B** Coomassie stained SDS polyacrylamide gels. Lanes are labelled as described in A except Input is elutate from the Ni column. The elution condition is indicated to the left of the gel. **C** Left, portion of silver stained SDS polyacrylamide gel of eluate from amylose resin and right, immunoblot of an identical gel using an anti-His antibody. **D** Coomassie stained SDS polyacrylamide gels labelled as in B. Purification was in the presence of 0.5 mM ATP and 2 mM DTT (top), or their absence (bottom). In B and D arrows indicate the position of 230 kDa (open arrow) and 150 kDa (closed arrow) markers.

4.3.5 Dextrin affinity chromatography

The fact that AtGWD could be eluted from amylose resin with a dextrin solution, strongly suggested that the protein could bind dextrins, and possibly with a greater affinity than it bound amylose. Thus dextrin affinity chromatography represented an alternative to amylose affinity chromatography with potential for increased yields. Dextrin-Sepharose columns are available commercially for the purification of proteins tagged with maltose binding proteins. However, when protein eluted from the Ni-column was loaded onto such a dextrin-Sepharose column, AtGWD did not bind.

4.3.6 Scale up and yield

Once the protocol for AtGWD purification had been established, it was scaled up to produce sufficient protein for antibody production in rat as well as stocks for in vitro work. This involved automating the Ni¯affinity chromatography on the AKTA FPLC. I harvested 215 g of *N. benthamiana* leaf tissue and produced approximately 198 µg of protein as estimated from band area and intensity on a Coomassie stained SDS polyacrylamide gel (Figure 4.6). Thus the yield was 0.92 µg protein per g of *N. Benthamiana* leaf tissue.

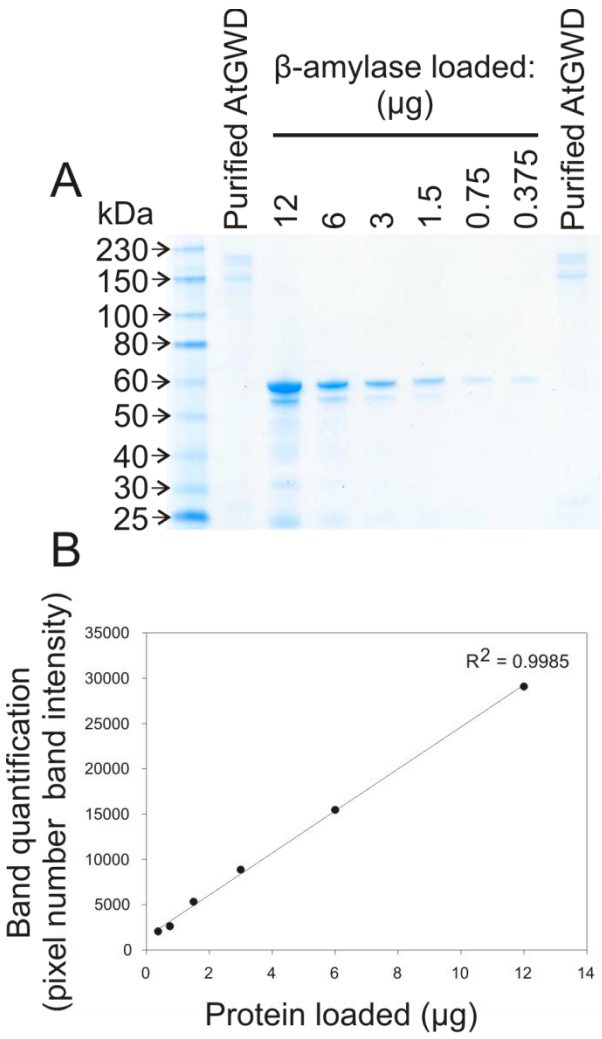

Figure 4.6: Quantification of purified AtGWD. **A**. SDS polyacrylamide gel of purified AtGWD and a dilution series of β-amylase from *Ipomoea batatas*. **B** Standard curve for protein amount constructed by multiplying pixel number and band intensity for β-amylase dilution series.

4.3.7 Analysis of multiple AtGWD bands

I wished to investigate why AtGWD expressed in *N. benthamiana* leaves purifies in three distinct forms with different mobilities when analysed by SDS-PAGE. To probe further into differences between the three AtGWD bands, Orbitrap mass spectrometry (MS/MS) data were collected by the JIC Proteomics Service for each band (figure 4.7). I then used these data to test several hypotheses. Firstly, I speculated that the differences in size could be due to SUMOylation, since AtGWD has been confirmed to be SUMOylated *in vivo* (Elrouby and Coupland, 2010). Potential SUMO sites were identified using data from the Elrouby and Coupland paper, as well as using the SUMOsp SUMO site prediction programme (http://sumosp.biocuckoo.org/). These sites were mapped to the protein, and it was found that each SUMO site happened to fall on a lysine at the end of a peptide identified in the MS data. Trypsin would not cut adjacent to a lysine if it was SUMOylated, so these data demonstrate that none of the predicted or confirmed SUMO sites were 100% SUMOylated in any band. To look for

positive evidence of SUMOylation, I acquired the peptide sequence of all known Arabidopsis or *N. benthamiana* SUMO peptides in the NCBI database and identified the glycine by which each SUMO group is attached to the substrate as well as the nearest tryptic cleavage site to this residue. This information allowed me to calculate, for each SUMO type, the mass of the SUMO derived peptide stem (using the tool at http://web.expasy.org/peptide_mass/) which would remain on a target protein after tryptic digestion. JIC Proteomics Service then created a Mascot (Matrix Science) database of these peptide masses which I used to interrogate the MS/MS data for the different AtGWD forms, searching for the SUMO stem peptides as a variable modification. However no peptides with masses corresponding to SUMO stem modified AtGWD peptides could be found in the data, suggesting that none of the forms of AtGWD purified from *N. benthamiana* are SUMOylated.

A second possibility was that the size differences were due to alternative splicing. To test for this, I generated a list of the tryptic peptides (using the tool at http://web.expasy.org/peptide_mass/) that would be produced if any supposedly intronic *AtGWD* sequence was translated in any frame to form part of the protein. Again, the JIC Proteomics Facility created a Mascot database of these peptides, which I used to interrogate the MS/MS data. However none of these peptides matched the mass spectrometry data, so it seems that the different forms of AtGWD purified here are not different splice variants. It also seems unlikely that the smaller bands are degradation products of the larger bands, because for each AtGWD form there is good peptide coverage near the C and N termini of the mature protein sequence (Figure 4.7). All isoforms are reactive to the anti-His antibody, which also strongly suggests that they are C-terminally intact. The changes in protein size due to degradation which are possible given these data could not account for the 20 – 25 kDa differences in mass observed between the AtGWD forms.

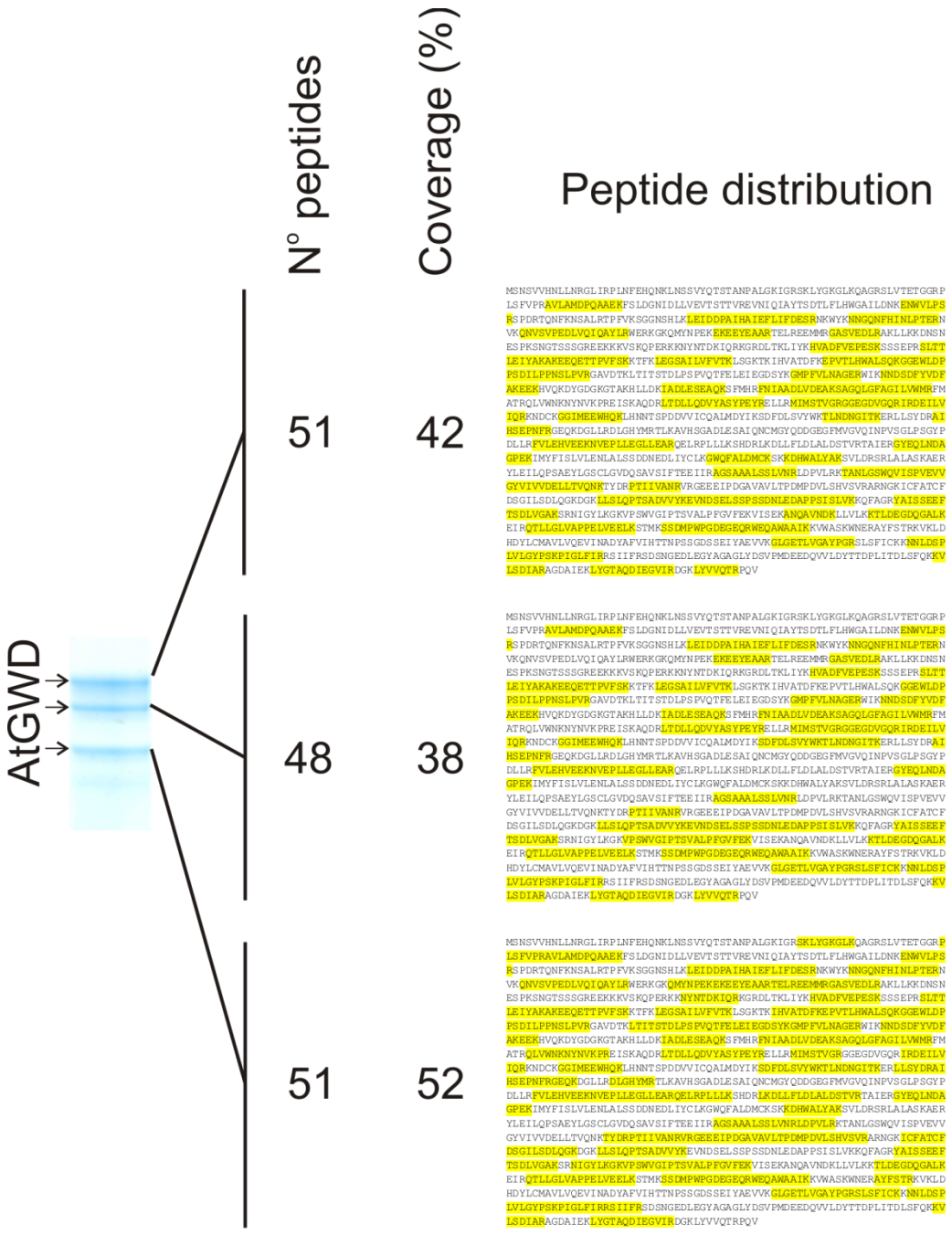

Figure 4.7: Proteomic analysis of three AtGWD bands eluted from the amylose resin. Left, Portion of an SDS polyacrylamide gel stained with Coomassie blue showing the three purified AtGWD bands. For each band the number of peptides identified and the percentage coverage of the protein are shown. The position on the AtGWD amino acid sequence of peptides identified in the MS/MS data is also displayed for each band (right).

The three major forms of the purified protein could not be further separated, either by re-loading the preparation on a Ni-column and eluting with an imidazole gradient or by fractionation by anion exchange chromatography (MonoQ column).

4.4 GWD antibody production

Purified AtGWD (150 μg; a mix of all bands) was used to generate an antiserum in rat (using the Eurogentec 28-day service). The antiserum was tested and compared to the existing StGWD antibody available in my laboratory (Figure 4.8). Both antisera clearly recognised all major bands of the purified AtGWD protein, although the StGWD antibody produced a stronger signal. Neither antiserum recognised a band at 55 kDa in plant extract, corresponding to the highly abundant Rubisco large subunit, suggesting that both antisera were of good specificity. However the AtGWD antiserum did not recognise GWD in protein extract from wild-type (Col-0) plants, except perhaps for a band much bigger than even the largest form of the purified protein, and this was seen only in 2 out of 5 extracts. The StGWD antiserum in contrast, recognised a band of equivalent size to the middle isoform of purified AtGWD in Col-0. As expected, neither antiserum gave a specific signal against AtGWD on the immunoblot of protein extracted from *gwd* mutant plants.

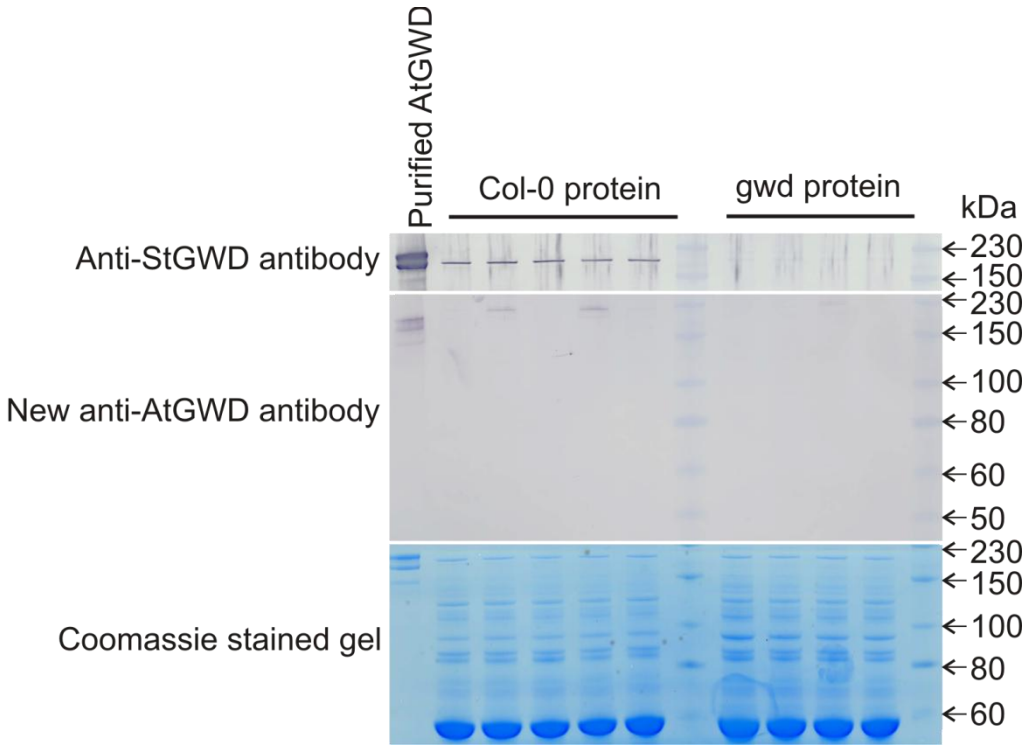

Figure 4.8: Comparison of anti-StGWD and anti-AtGWD antisera. Lower panel: Coomassie stained SDS polyacrylamide gel of purified AtGWD (left lane), soluble protein extract from 5 different Col-0 plants (Col-0 protein) and soluble protein extract from 5 different *gwd* mutant plants (*gwd* protein). Middle panel: Immunoblot of an identical gel developed with the new anti-AtGWD antiserum (1:1000). Top panel: immunoblot of an identical gel developed with existing anti-StGWD serum (1:1000).

4.5 Discussion

In this chapter I describe the successful cloning and manipulation of the *AtGWD* gene and the first purification of the AtGWD protein: both pre-requisites for the rest of the work described in this thesis.

It is now 43 years since Shapiro and colleagues first isolated DNA representing a single, known gene (Shapiro *et al.*, 1969), however despite huge advances in cloning technology, some genes are still difficult to work with because of their particular properties. *AtGWD* has proved problematic in several labs, and I also found its cloning to be technically challenging. One might speculate that these difficulties arise because low expression of the enzyme in *E. coli* could cause phosphorylation of glucans and

disrupt cellular carbohydrate or extracellular polysaccharide metabolism. However, when Lorbeth *et al.* (1998) and coworkers expressed *StGWD* in *E. coli,* they found three fold increased phosphorylation of *E. coli* glycogen, but did not report any decline in cell viability. Indeed other groups have also worked with *StGWD* cDNAs in *E. coli*, apparently without difficulty (Ritte *et al.*, 2002; Kötting *et al.*, 2009). In any case, the *AtGWD* clone used in my work is a genomic sequence, so the protein should not be expressed in *E. coli*, which lacks the necessary splicing machinery to process the immature mRNA. This might suggest that it is something about the AtGWD DNA sequence itself which is unfavourable for *E. coli* viability. Intriguingly, it is the SBD-containing regions of the gene which seem to be most prone to rearrangements, and this is a region which shows significant divergence from the potato homologue. Growing *E. coli* containing *AtGWD* clones at a relatively low temperature of 30°C seems to alleviate the detrimental effects of the gene such that a stable clone can be maintained. This could be explained if, for example, the nature of the *AtGWD* DNA made it difficult to replicate rapidly so lower growth rates would put less pressure on the DNA replication machinery to copy both the introduced plasmid and the rest of the *E.coli* genome.

There are now many affinity based systems available for the purification of tagged recombinant proteins. These include His-tags for metal ion affinity, Strep-tags for biotin affinity, maltose binding protein tags for amylose affinity and epitope tags such as FLAG and HPC for antibody based purification. In general the antibody based affinity tags are best for generating extremely pure protein preparations in a single step (Lichty *et al.*, 2005). Due to the difficulties of working with *AtGWD* clones, I was limited to a single class of destination vectors, which unfortunately didn't contain sequences for the creation of affinity tag fusion proteins. This meant I had to introduce tags by site directed mutagenesis, and thus it was impractical to introduce relatively large tags such as the 3 times FLAG tag. I decided to use a C-terminal His tag, which can be harnessed in a simple immobilised metal affinity chromatography purification (IMAC) procedure using a Ni based affinity matrix.

One limitation of tagging proteins is that the extra amino acids can interfere with normal protein function (Arnau *et al.*, 2006), leading some researchers to add a protease cleavage site between the protein of interest and the tag, such that the tag can be removed after purification. For N-terminal tags, enterokinase will cleave a specific

sequence, leaving only a single lysine as a stem on the original protein (Terpe, 2003). However, for a chloroplast protein, the tag must be C-terminal because an N-terminal tag would be cleaved with the transit peptide unless it can be inserted between the transit peptide and the mature protein. For GWD we do not know the precise position of the transit peptide cleavage site, so a C-terminal tag was the only option. Unfortunately, most available proteases (eg the commonly used TEV protease) cleave towards the C-terminal end of their recognition sequence (Arnau *et al.*, 2006), leaving a stem of 4 – 6 amino acids on the end of the protein. Thus for a histidine tag of only 6 amino acids addition of a cleavage site does not significantly reduce the number of extra amino acids at the C-terminus of the protein. The only scenario in which a cleavage site might be useful is for subtractive IMAC, where the eluate from an initial IMAC run is protease treated and then re-loaded on the metal affinity column, such that the protein of interest now passes through the column while contaminants remain bound to the matrix (Arnau *et al.*, 2006).

Working with a genomic *AtGWD* clone meant that *E. coli* could not be used as an expression system to produce the protein because it lacks the necessary cellular machinery to splice the immature mRNA. So *N. benthamiana* was chosen as the expression system, as this has been successfully used for the production of many proteins (Sainsbury *et al.*, 2009). AtGWD was first partially purified from *N. benthamiana* leaf extract on a Ni-column, as presented in Figure 4.3. However, in addition to AtGWD, large numbers of *N. benthamiana* proteins had some affinity for the Ni-column. Even the presence of 25 mM imidazole and 250 mM NaCl in the loading and washing buffer did not reduce this background binding. This meant that a second purification step was necessary to generate AtGWD of high purity. Amylose-Sepharose resin was a highly effective affinity matrix for the further purification of AtGWD, despite the fact that the individual StGWD SBDs have exceptionally low affinity for carbohydrate ligands when analysed *in vitro* (Glaring *et al.*, 2011). It may be that this information is of relatively little value when considering the tandem pair of SBDs from Arabidopsis in the context of the protein, especially noting the large sequence divergence between the Arabidopsis and the *S. tuberosum* in the SBDs.

It was interesting to find that AtGWD purified from *N. benthamiana* separated into three major forms of different apparent masses. The approximate masses of these forms

were estimated to be 156 kDa, 186 kDa and 210 kDa and all three bands were confirmed to be AtGWD by mass spectrometry and by immunoblotting. These data suggest that there is some form of post-translational modification of AtGWD when expressed transiently in tobacco. It is particularly interesting that the StGWD antibody recognises a band on an immunoblot of protein extracted from wildtype Arabidopsis plants which is equivalent in size to the 186 kDa band purified from tobacco, suggesting that AtGWD may also be in a modified state in Arabidopsis. This encouraged me to investigate the cause of the differences in apparent mass between the bands.

AtGWD is known to be phosphorylated (Heazlewood *et al.*, 2008) and phosphorylation can cause a mobility shift in SDS-PAGE (Mohammadi *et al.*, 2001) because the change in charge on the protein can affect the extent to which it is bound by SDS. However, a single phosphorylation event rarely results in an apparent mass change larger than 10 kDa, so I consider it unlikely that phosphorylation causes the differences in migration observed here for AtGWD.

Another possible modification which could result in a large shift in size is a peptide modification known SUMOylation. Each SUMO group adds about 11 kDa (data from http://www.uniprot.org) to the protein depending on the precise SUMO variant, of which there are eight encoded in the Arabidopsis genome (Miura and Hasegawa, 2010). SUMO1 and SUMO2 are also able to form polySUMO chains on a target protein. SUMOylation is of particular interest in the case of AtGWD, because the enzyme is the most SUMOylated protein detected in the Arabidopsis chloroplast (Elrouby and Coupland, 2010). However there was no evidence of SUMOylation in MS/MS data collected for the different AtGWD protein forms. There was also no evidence of translated intronic sequence, implying that the different forms are not alternative splice variants.

There are several other ways in which AtGWD could be modified. Firstly there are peptide modifications besides the SUMO modifications already discussed. These include ubiquitination and RUBylation, both involved in the targeting of proteins for proteosome dependent degradation. Secondly, AtGWD might be lipid modified through palmitoylation, prenylation or myristoylation (Thompson and Okuyama, 2000).

A third, intruiging possibility is that AtGWD might be glycosylated. Many proteins in eukaryotic cells become glycosylated in the endoplasmic reticulum (ER) and the Golgi apparatus as they travel through the secretory pathway (Van den Steen *et al.*, 1998; Helenius and Aebi, 2004) but chloroplast proteins have traditionally been thought to lack glycosylation because most chloroplast proteins are translated on free ribosomes in the cytosol and directly imported to the plastid (Li and Chiu, 2010). In recent years however, evidence has emerged for the existence of a non-canonical pathway targeting protein for the chloroplast via the secretory pathway. First, an Arabidopsis plastidial carbonic anhydrase (CAH1) was found to contain a signal peptide for ER targeting but no transit peptide for plastidial targeting (Villarejo *et al.*, 2005). CAH1 was also found to be *N*-glycosylated and its transport through the endomembrane system could be inhibited by brefeldin A (which prevents Golgi mediated vesicle trafficking). The glycosylation of this protein also turned out to be crucial for its function in the plastid (Buren *et al.*, 2011). Further examples of proteins targeted to plastids through the secretory pathway soon followed, including the *N*-glycosylated rice plastidial pyrophosphatase / phosphodiesterase (Nanjo *et al.*, 2006) and the plastidial rice α-amylase (Kitajima *et al.*, 2009). A larger scale study indicated that between 14 % and 19 % of known proteins assigned to the chloroplast in the literature lack a predicted transit peptide (Armbruster *et al.*, 2009). AtGWD falls into this category, as it is not predicted to contain a transit peptide at its N-terminus (analysed using ChloroP1.1, www.cbs.dtu.dk/services/ChloroP/), however neither is it predicted to have a signal peptide (determined using SignalP4.0, www.cbs.dtu.dk/services/SignalP/).

Given the above data, it would be fascinating to discover whether or not AtGWD is glycosylated when expressed transiently in tobacco. There are methods to test for glycosylation involving incubation with de-glycosylation enzymes such as PNGase F for most N-glycans, PNGase A for fucosylated N-glycans, and chemical methods such as alkaline β-elimination can be used for the release of O-glycans (Marino *et al.*, 2010). There are also gel based methods of detection (for example the periodic acid – silver stain method (Dubray and Bezard, 1982)). These tools could be used to analyse the different AtGWD variants further.

Throughout any future study of the recombinant protein, it must be remembered that the different modification states found here could simply be an artifact of overproduction in

a heterologous host. Even the fact that the form recognised by the anti-StGWD antibody appears to be equivalent in size to the 186 kDa band in the pure AtGWD preparation does not mean that the modification of the protein is the same in Arabidopsis as it is in *N. benthamiana.*

The purified AtGWD was used to raise an antiserum in rat. The crude serum clearly recognised all forms of the purified protein with good specificity, but failed to recognise AtGWD in Col-0 protein extract. This may well be a problem of sensitivity, which further purification of the antiserum would resolve, creating a useful tool for the future. For the purposes of the remainder of this study, Professor Sam Zeeman (ETH, Zürich) kindly donated sufficient StGWD antiserum (from the same batch used in the rest of this chapter) for the screening and characterisation of the transgenic lines.

5 Post-translational Regulation of AtGWD

5.1 Introduction

From results presented in chapter 3, it seems that transcriptional regulation and the modulation of AtGWD protein abundance are not important for the daily control of starch degradation. Given that AtGWD is an excellent candidate for an enzyme which might be regulated to change the flux through starch degradation (see chapter 1) it is worth pursuing the hypothesis that post-translational regulation of AtGWD is important for the daily control of starch turnover. In this chapter, I begin by examining changes in the extent of starch phosphorylation under different conditions to see if there is any evidence for regulation of the starch phosphorylation cycle. I then make use of genetic resources (the development of which is described in chapter 4) to test the importance of specific post-translational modifications of AtGWD for the control of starch degradation *in vivo*.

5.1.1 Starch phosphorylation as a signature of post-translational regulation of AtGWD

There is strong evidence that AtGWD affects starch degradation via its glucan phosphorylating activity (Ritte *et al.*, 2002; Edner *et al.*, 2007). Therefore, if AtGWD is regulated through the diel cycle, or as night lengths change, one would expect there to be concomitant changes in the rate of starch phosphorylation. However, almost no data are available on the daily changes in the phosphate levels of leaf starch granules. Of course, the starch phosphate content at a given time is dependent not only on the rate of phosphorylation, but also on the rate of dephosphorylation. Thus, if no change in steady state starch phosphate levels is observed experimentally, there could still be functionally significant changes in turnover. However if changes in phosphate levels are observed, this would support the hypothesis that the cycle of granule phosphorylation is regulated, possibly through the modulation of AtGWD activity.

I begin by investigating whether there are changes in starch phosphate that can be correlated with changes in starch degradation. To this end I measure starch phosphate over a diel cycle, including just before and after dusk, in plants grown in 12 hours light, 12 hours dark cycles. As far as we know, AtGWD can only phosphorylate the surface of

a starch granule, so I also decided to measure the phosphate content of surface glucans. Measurement of surface phosphate allows the phosphate added at the start of the night to be distinguished from phosphate within the granule which was added during synthesis.

Studies of starch phosphate are at present hampered by the methods that are used to measure it. All the methods rely on the prior hydrolysis of starch to glucose and glucose phosphates. One of the most used methods is the malachite green assay. First, the phosphate is released from the hydrolysed starch with alkaline phosphatase. Next orthophosphate forms a complex with malachite green and molybdate which can be detected colorimetrically. To make reliable measurements of starch phosphate using this assay, 5 – 10 mg of starch, or approximately 25 – 50 plants, are required (Hostettler *et al.*, 2011). This seriously limits the size of experiments which use this method. Likewise, ^{31}P NMR has very low sensitivity, so an even larger quantity of starting material is required. In addition, measurement times are very lengthy (Muhrbeck and Tellier, 1991; Ritte *et al.*, 2006). High performance anion exchange chromatography with pulsed amperometric detection (HPAEC-PAD) relies on the different retention properties of glucose, glucose 3-P and glucose 6-P on an anion exchange column. Peak area is then used to determine the amount of G6P/G3P (Blennow *et al.*, 1998; Ritte *et al.*, 2006). This method has better sensitivity, but is low throughput. Enzymatic assays for G6P can also be sensitive and have potential for much higher throughput, but such assays cannot be used to measure G3P. Despite this, I thought that an enzymatic method represented the best technique for my study, because it would allow the analysis of multiple samples. Measuring G6P is appropriate in this study because it concerns AtGWD, which catalyses phosphorylation of the C6 position. The most common enzymatic assay for G6P couples oxidation of G6P to NAD^+ reduction. NADH can then be measured via its UV absorbance. However, to minimise the amount of plant material needed, I require better sensitivity than is provided by this method, especially for the measurement of starch surface phosphate. As an alternative, I make use of the fluorometric assay of Zhu (2009) in which NADPH produced by the oxidation of G6P is used for the reduction of reazurin, resulting in production of the highly fluorescent resorufin. The strong fluorescence of this molecule means that it can be detected in the very low nM range, and so provides sufficient sensitivity for my study.

5.1.2 Testing the relevance of post-translational regulation of AtGWD: experimental outline.

In chapter 4 I describe the cloning and mutagenesis of *AtGWD*. The altered genes encode versions of AtGWD which cannot be subject to certain post-translational modifications. In this chapter I describe characterisation of *gwd* mutant plants transformed with the wildtype and mutated forms of *AtGWD*. Examining the extent to which the different constructs restore wildtype starch turnover allows the *in vivo* importance of particular post-translational modifications to be assessed. The broad classes of hypothesis I have addressed are described below. The rationale for the choice of specific sites for mutagenesis is described in detail in subsequent sections.

I decided to focus on four known post-translational modifications of AtGWD, the significance of which for the function of the enzyme *in vivo* is unknown. These modifications are summarised in Figure 5.1. One way in which AtGWD could be regulated at a post-translational level is through direct modulation of the catalytic activity of the enzyme. I wished to test the importance of two modifications relating to this mechanism. The first is phosphorylation of the key histidine residue in the catalytic domain. This residue becomes autophosphorylated as part of the catalytic cycle and is essential for glucan phosphorylating activity. The second is the formation of a disulphide bridge known to confer redox response properties on AtGWD *in vitro*.

Another way in which AtGWD could be regulated at a post-translational level is by modulation of its substrate binding capacity. Evidence to support this idea comes from a study which found that more GWD was associated with starch granules isolated in the dark than those isolated in the light (Ritte *et al.*, 2000). As discussed in chapter 1, pea or potato leaves were harvested either in the light or the dark and starch was purified and dried. Proteins extracted from the starch were analysed by SDS-PAGE and immunoblotted with an anti-StGWD antibody. GWD was always detectable in the soluble fraction, but could only be detected in the starch-associated fraction in samples harvested in the dark. In addition, recombinant StGWD bound more strongly to starch granules extracted from dark adapted potato leaves than granules extracted from light adapted leaves.

These results suggest that there is some regulation of AtGWD localisation through the diel cycle, and it is possible that this could operate through the regulation of starch binding. AtGWD contains two CBM45 family starch binding domains towards the N-terminus of the protein (Mikkelsen *et al.*, 2006). Beyond the GWDs, CBM45s have only been found in the plastidial α-amylases and have not been studied at a structural level in either class of enzyme (Glaring *et al.*, 2011). Starch binding domains of the CBM 20, 21, 25, 26 and 34 classes from microbial glucan hydrolases have been crystallised in complex with β-cyclodextrin or other glucans (Sorimachi *et al.*, 1997; Machovic and Janecek, 2006). These structures indicate that the glucan binding sites are composed of tryptophan residues, the aromatic rings of which probably form stacking interactions with glucose moieties. One can imagine that such delicate interactions could be easily disrupted with regulatory consequences. Thus, if large or charged modifications were added to the starch binding domains, this could interfere with starch binding. SBD1 is known to be both phosphorylated and SUMOylated, so modulation of the proportion of AtGWD proteins containing these modifications could effectively regulate the enzyme.

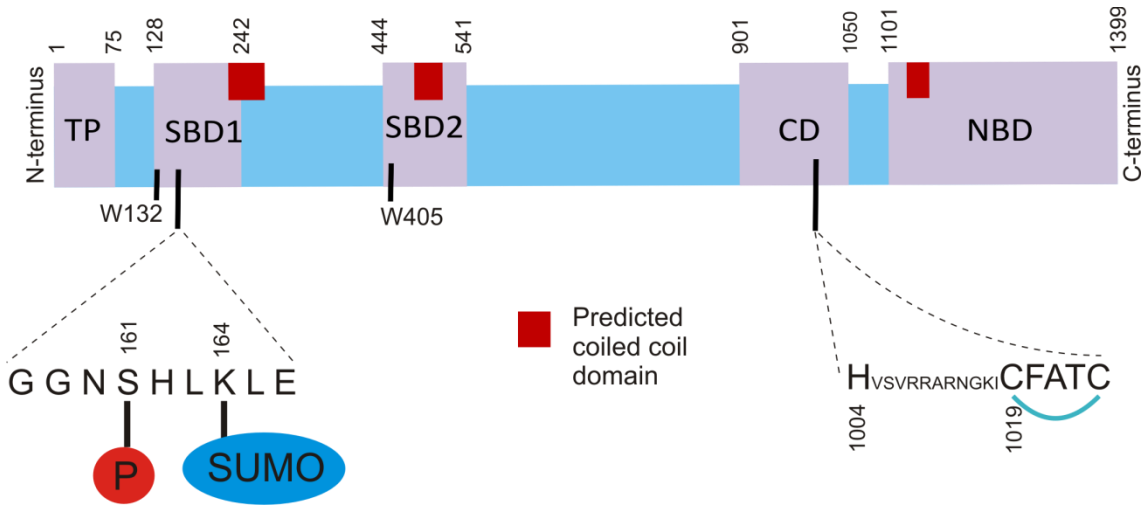

Figure 5.1: Domain organisation and post-translational modifications of AtGWD. The protein is represented from N-terminus to C-terminus, left to right and is 1399 amino acids in length. Amino acid positions of domain boundaries are marked and were derived with reference to Mikkelsen *et al.* (2006). Domains are purple: TP, transit peptide; SBD1, starch binding domain 1; SBD2, starch binding domain 2; CD, catalytic domain; NBD, nucleotide binding domain. Red blocks indicate the position of a predicted coiled coil domain. The positions of W132 and W405 which are important for SBD function are shown in SBD1 and SBD2. Indicated in the diagram and the SUMOylation and phosphorylation sites close to W132 in SBD1 and the redox sensitive disulphide bridge positioned close to the catalytic histidine.

5.1.3 Testing the importance of starch phosphorylation

The *gwd* mutant has an extreme starch excess phenotype and very little starch turnover (Niittylä *et al.*, 2006; Kötting *et al.*, 2009). Although the GWD protein has been characterised as a glucan water dikinase and a decrease in starch phosphate level is observed in the *gwd* mutant, it is still formally possible that the effects of AtGWD on starch degradation are not due to its dikinase activity, but rather some other property of the protein. A version of *AtGWD* mutated in the catalytic histidine should not be able to phosphorylate glucans. By analysing a *gwd* mutant transformed with the catalytic histidine mutant *AtGWD* it should be possible to deduce the importance of the starch phosphorylation activity versus other functions of the protein.

The evidence that GWD affects starch degradation through its dikinase activity comes almost exclusively from *in vitro* studies. It has been shown that phosphorylation by StGWD stimulates the solubilisation of crystalline maltodextrins (Hejazi *et al.*, 2008). This demonstrates that phosphorylation by GWD has the potential to cause a decrease in the crystallinity of the starch granule, thereby making the glucan chains more accessible to hydrolytic enzymes. Another study found that the presence of AtGWD could stimulate the degradation of *sex1-3* starch granules by Arabidopsis BAM3. However when the GWD catalytic histidine was converted to alanine no stimulation was achieved (Edner *et al.*, 2007). Thus, in an *in vitro* setting, dikinase activity is necessary for the stimulation of starch degradation by AtGWD.

Despite the above evidence it remains possible that the effects of GWD on starch degradation *in vivo* are mediated through its binding to the starch granule surface or through interactions with other proteins, and not through its glucan dikinase activity. There is a small amount of evidence that SBDs can have disruptive effects on the starch granule surface. This comes from a study in which the rate of starch degradation catalysed *in vitro* by *Aspergillus niger* glucoamylase was determined in the presence of varying quantities of the purified SBD from the same enzyme (Southall *et al.*, 1999). At high concentrations of the SDB, the rate of degradation by glucoamylase was low due to competition for substrate binding. However at low concentration of SDB, an increase in the rate of degradation was observed as more SDB was added. This suggests that the SDB alone may be able to disrupt the granule surface to some degree, thereby facilitating degradation. However the glucoamylase SBD is a CBM20, and the CBM45s from GWD might not necessarily have the same effect. There are also studies which indicate that SBDs can affect starch architecture *in vivo*. Ji *et al.* (2004) found that expressing a SBD from *Bacillus circulans* in the amylose-free potato mutant, *amf*, resulted in a 50% decrease in tuber starch granule diameter. In contrast, Howitt *et al*. (2006) found that expressing a *Thermoanaerobacterium thermosulfurigenes* SBD in Arabidopsis leaves resulted in an increase in granule size. Other properties of the granule and total starch content were unaffected in both studies. Thus, although SBDs can cause altered granule size *in vivo* there is no evidence they otherwise influence starch metabolism.

To test the necessity for starch phosphorylation during degradation, I created a version of AtGWD in which the catalytic histidine is converted to an arginine; chosen as another polar amino acid with a bulky and basic side chain (see Table 5.1). This protein (GWD^{cat}) should lack autophosphorylation activity, and so should be catalytically inactive. If this version of *AtGWD* partially restores starch degradation to the *gwd* mutant plant, then it would indicate that, *in vivo*, GWD acts by a mechanism in addition to glucan phosphorylation. For example, the SBDs could disrupt the granule surface or the enzyme could recruit other proteins to the granule. If there is no rescue of starch degradation, then it would be probable that GWD mediates its effect through granule phosphorylation. Based on the *in vitro* studies there is a strong expectation that there will be no rescue of starch degradation. Thus, these plants may well serve as a negative control for the other transgenic lines.

5.1.4 Testing the relevance of redox regulation of AtGWD

Redox signals are known to have an extremely important role in the regulation of chloroplast metabolism, especially in response to changes in light intensity. In the day, the photosynthetic electron transport chain actively transfers electrons from water to ferredoxin. Most of this reducing power is then used via ferredoxin-$NADP^+$ reductase to generate metabolic reductant (NADPH). However a small fraction of the electrons is instead used to reduce a disulphide bridge in ferredoxin-thioredoxin reductase (FTR) which will in turn reduce thioredoxin (Trx) (Ruelland and Miginiac-Maslow, 1999; Lemaire *et al.*, 2007). Different thioredoxins can then reduce different target enzymes with regulatory consequences. For example, in the light, the Calvin cycle enzymes glyceraldehyde 3-phosphate dehydrogenase, fructose 1,6-bisphosphate phosphatase, sedoheptulose 1,7-bisphosphate phosphatase and phosphoribulose kinase are all reduced and activated by this mechanism. Glucose 6-phosphate dehydrogenase on the other hand is reduced and inactivated in the light. This inhibits flux through the oxidative pentose phosphate pathway (OPPP) and helps to prevent futile cycling between catabolic and anabolic processes.

Starch degradation is activated at night and inhibited in the day (Zeeman *et al.*, 2002), so it is possible that redox regulation plays a role in control. As described in chapter 1, StGWD is known to have redox-responsive properties *in vitro* (Mikkelsen et al., 2005). The incubation of purified StGWD with a strong oxidising agent ($CuCl_2$) leads to

inactivation of the enzyme. If $CuCl_2$ is subsequently removed, then activity can be regained by the addition of the reducing agent DTT. Addition of purified Trx *m* or Trx *f* from spinach can also reduce and activate the enzyme. An MS analysis of StGWD in the oxidised and the reduced form identified a disulphide bridge between cysteine 1004 and 1008 in the oxidised form only (Figure 5.1). A mutant form of StGWD in which cysteine 1008 was converted to a serine, was constitutively active over a large range of redox conditions, including conditions that entirely inactivate the wildtype form.

The *in vivo* relevance of the above data is questionable for two reasons. Firstly, StGWD displays reductive activation. Therefore if GWD were reduced by Trxs *in vivo* the enzyme would become more active during the day. It is possible that reductive activation reflects the newly identified role for AtGWD in starch synthesis described in chapter 3. However the primary role for AtGWD is probably still in starch degradation, and ^{14}C labelling experiments have demonstrated that leaf starch degradation occurs only during the night (Zeeman *et al.*, 2002). Thus if GWD is regulated for the activation of starch degradation at night, this cannot be via reductive activation by Trxs. Secondly, StGWD has an *Em* at pH 7 of approximately -255 mV (Mikkelsen *et al.*, 2005). This is much more positive than most redox responsive chloroplast enzymes (Schurmann, 2003) and casts doubt on whether a significant proportion of the enzyme would become oxidised and inactivated *in vivo*.

To test the relevance of this putative redox regulation *in vivo*, I recapitulated the StGWD C1008S mutation characterised by Mikkelsen *et al.* (2005) in my *AtGWD* clone (see Table 5.1). This mutated version of AtGWD should be redox unresponsive and will thus be a constitutively active across a wide range of redox conditions. This mutant enzyme is then expressed in the *gwd* mutant plant, to see if it can restore wildtype patterns of starch metabolism.

5.1.5 Testing the relevance of phosphorylation in SBD1

Arabidopsis proteomic MS data (information collated in the PhosPhAt database (Heazlewood *et al.*, 2008)) show that AtGWD is phosphorylated at S161, which lies within SBD1 (Figure 5.1). This residue is only 29 amino acids away from W132, equivalent to a tryptophan residue known to be necessary for the starch binding properties of StGWD SBD1 *in vitro*. As described above, it is thought that SBDs

operate by forming stacking interactions between the aromatic rings of tyrosine residues and the aliphatic rings of glucose units in the starch (Machovic and Janecek, 2006). One can imagine that if a serine close to one of these critical tyrosines becomes phosphorylated, the resulting change in charge could easily destabilise the interaction. Thus regulation of phosphorylation within AtGWD represents a possible mechanism for the regulation of the enzyme.

I have mutated the serine that forms this phosphorylation site to an alanine which cannot be phosphorylated (see Table 5.1). This construct is used to transform the *gwd* mutant plant, and the extent of complementation achieved should provide new information about the importance of this post-translational modification.

5.1.6 Testing the relevance of SUMOylation in SBD1

AtGWD is known to be modified by the small, ubiquitin related modifier, SUMO. The one hundred amino acid SUMO peptides are conjugated to protein substrates through the action of SUMO ligases, and removed by the action of SUMO proteases. The effects of SUMO modification (SUMOylation) are varied and are discussed in more detail below. Elroubly and Coupland (2010) identified AtGWD in a yeast two hybrid screen for SUMO ligase interactors. They also performed a bioinformatic analysis, which predicted AtGWD to be the most SUMOylated protein in the chloroplast. To confirm that the Arabidopsis SUMOylation machinery can SUMOylate AtGWD, the genes encoding three Arabidopsis SUMO ligases were expressed in *E. coli* concomitant with a partial *AtGWD* cDNA. The region of *AtGWD* expressed was not reported. The partial AtGWD protein was successfully SUMOylated by this system. One of the predicted SUMOylated lysines is found in SBD1, 32 resides from a tryptophan residue thought to be critical for SBD function. Given the precise alignment required for SBDs to interact with glucan chains (Machovic and Janecek, 2006), one can imagine that the addition of a large peptide group in the vicinity could disrupt binding. Thus GWD substrate binding could conceivably be regulated by changing its SUMOylation state.

It is not entirely clear how AtGWD would become SUMOylated within the chloroplast, because none of the known SUMO-ligases are predicted to be plastid localised (SAE1, SAE2, SCE1, SIZ1, MMS21, examined with ChloroP). However, there is no experimental evidence for the subcellular localisation of these proteins, and it may be

that one or more of them are imported to the chloroplast by a non-canonical pathway. Interestingly, two Arabidopsis SUMO proteases, ULP1b and ESD4, are both predicted to have transit peptides (ChloroP). Indeed, ULP1b was identified as a chloroplast protein in a proteomics study (Kleffmann *et al.*, 2004). The confirmed presence of SUMO proteases in the chloroplast strengthens the possibility that the entire SUMOylation system operates in this compartment.

The role of SUMOylation in plants is not well understood. In fact there are only half a dozen instances in which a role for SUMOylation has been properly defined. For example, ABA INSENSITIVE 5 is stabilised by SUMOylation, thereby negatively regulating ABA signalling (Miura and Hasegawa, 2010). SUMOylation represses the FLOWERING LOCUS C histone deacetylation activity of FLOWERING LOCUS D, thereby negatively regulating the autonomous (temperature independent) pathway for flowering (Murtas *et al.*, 2003; Jin *et al.*, 2008). The functions of SUMOylation have been better studied in other systems such as the budding yeast, *Saccharomyces cereviscae*. Often, it seems that SUMOylation is involved in switching proteins between different states and functions. This is possible because SUMO modifiers compete for their lysine attachment sites with other modifications, such as acetylation or ubiquitination (Gareau and Lima, 2010). For example PROLIFERATING CELL NUCLEAR ANTIGEN (PCNA) recruits different partners in yeast depending on whether the protein is mono-ubiquitinated, polyubiquitinated or SUMOylated at a key lysine. The complex PCNA formed then determines whether it participates in translesion synthesis, error-free DNA repair or recombination inhibition (Hoege *et al.*, 2002; Pfander *et al.*, 2005; Ulrich, 2009). Phosphorylation can act in concert with SUMOylation to determine subsequent protein function. The mammalian transcription factor MEF2A up regulates genes responsible for synapse disassembly when in it is acetylated at a key lysine. However phosphorylation at a nearby serine promotes SUMOylation of that lysine, resulting in inhibition of MEF2A function and synapse maturation (Shalizi *et al.*, 2006; Shalizi *et al.*, 2007).

In this study, I am interested in how starch degradation is switched between an active and an inactive state, as well as how AtGWD switches between its granule-associated and stromal forms. Given the above precedents, it is quite possible that SUMOylation plays a role in this switching behaviour and it may be that there are important

interactions between the SUMOylation site and the nearby phosphorylation site. Specifically, the SUMOylation state of AtGWD could be regulated to modulate the starch binding affinity of the enzyme. To test this hypothesis, I have made a mutant version of *AtGWD* lacking the SUMOylated lysine (K164) (see Table 5.1). The importance of SUMOylation at this site is assessed in this chapter by examining the extent of complementation achieved when a *gwd* mutant plant is transformed with AtGWD in which K164 has been converted to an argenine.

5.1.7 Testing the relevance of starch binding domain function

The hypothesis that AtGWD could be regulated *in vivo* by modulating the affinity of SBDs for starch assumes that the SBDs are critical for normal AtGWD function. If the SBDs are not important for the normal functioning of the enzyme, then regulation by this mechanism would be highly unlikely. There is in fact some doubt about the role of the GWD SBDs *in vivo*. This is largely because the CBM45 family SBDs contained within GWD have exceptionally low affinity for carbohydrates. The purified SBD1 from StGWD binds cyclodextrins with 100 times lower affinity than most other starch binding domains (Glaring *et al.*, 2011).

The affinity of the StGWD SBD1 for starch can be abolished by the mutation to an alanine of either one of two tryptophan residues, W62 and W117 (Mikkelsen *et al.*, 2006). Although the N-terminal regions of StGWD and AtGWD are divergent, the Arabidopsis equivalents of the StGWD SBD W62 residue can be identified as W132 in SBD1 and W405 in SBD2. I have mutated these resides to an alanine (see Table 5.1). However, as noted previously in chapter 4, plants expressing this construct are not yet ready for analysis. Analysis of the SBD 1 and 2 mutant is thus beyond the scope of this thesis. If, when expressed in the *gwd* mutant plant, the double SBD1/2 mutant version of AtGWD can fully restore wildtype starch degradation then this would indicate that the SDBs are unimportant *in vivo*. In that case, the enzyme is unlikely to be regulated by the modulation of its starch binding capacity. Conversely, if the SBD mutant version of AtGWD cannot restore wildtype starch degradation then this would suggest that the SDBs are important, either for targeting the enzyme to the granule surface or for disrupting the surface structure. In this case the enzyme could potentially be regulated by modulation of its starch binding capacity.

Site mutated	Thought to function as...	Original sequence	New sequence	Name of mutant form used in thesis
Try132 in SBD1	Starch binding residue	EN**W**VL gaaaattgggttcta	EN_VL gaaaat_gttcta	na
Ser161 in SBD1	Phosphorylation site	GN**S**HL gcaattctcacctt	GN**A**HL gcaattGCtacctt	*GWD*^{P}
Lys164	SUMOylation site	L**K**LE cttaaactagag	L**R**LE cttaGactagag	*GWD*^{SUMO}
Try 405 in SBD2	Starch binding residue	GE**W**LD gagaatggttggac	GE_LD gagaa_ttggac	na
His 1004	Phosphorylation site, necessary for catalysis	LS**H**VS ctatctcatgtttct	LS**R**VS ctatctcGtgtttct	*GWD*^{cat}
Cys1019	Part of redox sensitive disulphide bridge	CFAT**C** tgctttgccacatgt	CFAT**S** tgctttgccacaTCt	*GWD*^{redox}

Table 5.1: Mutations made in *AtGWD* and resulting changes in amino acid sequence. na, not available.

5.2 Results

5.2.1 Starch phosphate

I wished to find out whether starch phosphate levels correlated with the rate of starch degradation or changed at all over 24 hours. To do this, I made use of an assay for G6P in which the production of the fluorescent compound resorufin is coupled to the oxidation of G6P. This assay proved to have a good lower limit of detection, allowing measurements in the sub ten nM range (Figure 5.2 A). The dynamic range of the assay was also good, and the assay was linear over three orders of magnitude of G6P concentrations. Starch was purified from *gwd* and Col-0 plants and digested to glucose and glucose phosphates as described in section 2.19.3. Glucose was measured as normal (section 2.16.3) and G6P was assayed with the fluorescence assay (section 2.18.4). *gwd* starch contained 0.098 nmol G6P (μmol glucose)$^{-1}$ while Col-0 starch contains 0.80 nmol G6P (μmol glucose)$^{-1}$ (Figure 5.2 B). Although only based on one sample, these

values are consistent with published data in which *gwd* plants had barely detectable levels of G6P while Col-0 had 0.65 nmol G6P (μmol glucose)$^{-1}$ (Ritte *et al.,* 2006). Together these data indicate that the assay functions well.

Starch phosphate was measured over 24 hours in plants grown in 12 hours light 12 hour dark cycles (Figure 5.2 C). Starch phosphate (mol G6P (mol glucose^{-1})) increased through the middle part of the day, reaching a peak 8 hours after dawn. There was then an almost linear decline in starch phosphate until the end of the night. No starch phosphate measurements were made at the start of the day because of the large numbers of plants required to provide sufficient starch at dawn. If the end of the night value is taken as an estimate of start of the day value, then it seems that starch becomes more phosphorylated over at least the first two thirds of the day.

Given that AtGWD operates at the granule surface, I wished to establish a method to measure starch surface phosphate. Surface glucans were released from the purified starch granules by a 30 min incubation with amyloglucosidase and pullulanase as described in section 2.19.2. Less than 1% of the total glucan present was released by these digests, so the glucans released can be considered a granule surface fraction. The size of this fraction is similar to the 0.3% of total glucan defined as surface glucans by Ritte (2004). G6P was successfully measured in a surface glucan fraction from a sample collected just after the beginning of the night and there was no significant difference (p=0.05) in phosphate levels between the bulk starch and surface starch (Figure 1D). This method may be useful for future studies (see discussion).

Although preliminary, the data presented here show that the balance of phosphorylation and dephosphorylation changes through the diurnal cycle, suggesting that the cycle of phosphorylation is regulated.

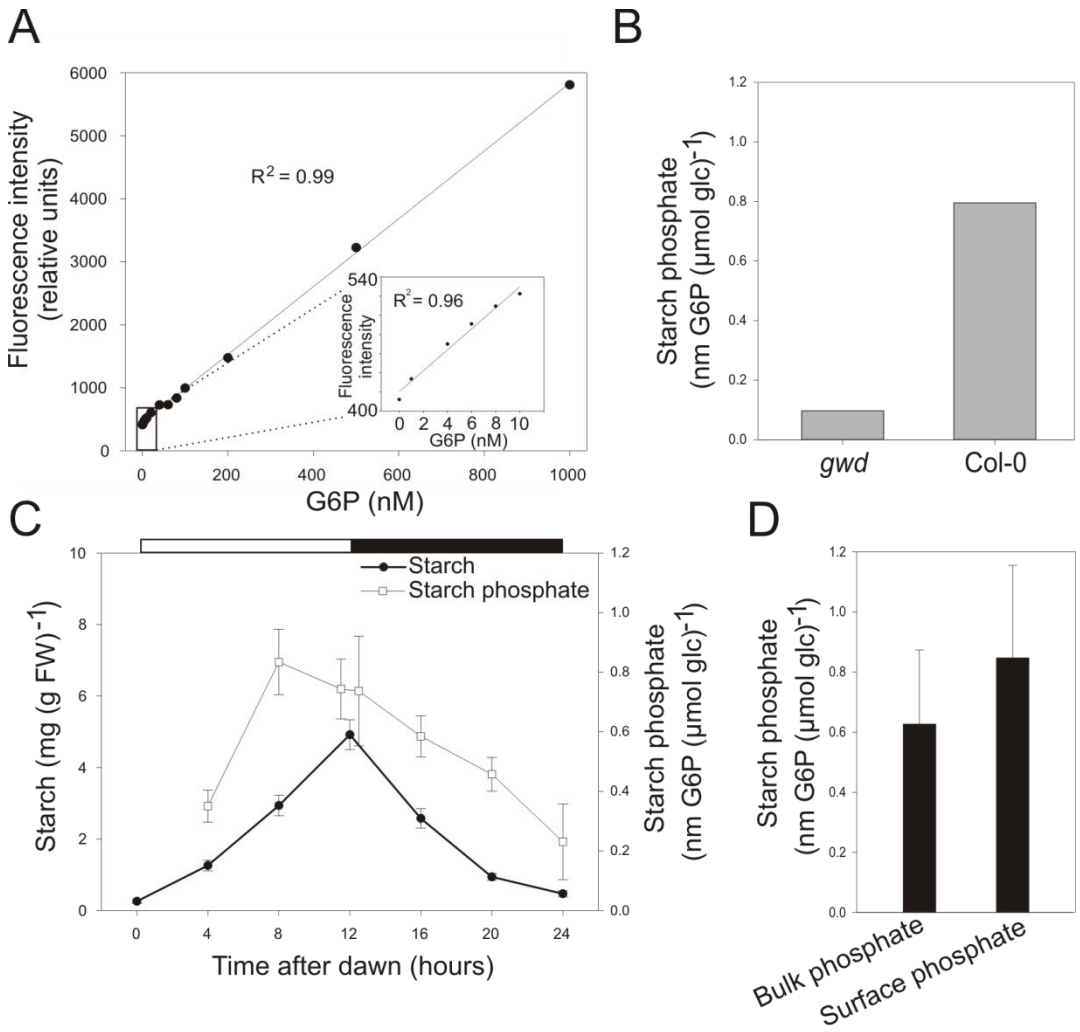

Figure 5.2 Measurements of C6 starch phosphate. **A** Representative glucose-6-phosphate standard curve produced using fluorescence based assay with reazurin. n = 1. Linear regression lines and associated R^2 value are shown on the plots. Insert shows the lower part of the curve at an expanded scale. **B** C6 starch phosphate measured in *gwd* and Col-0. n = 1. **C** Starch (black circles) and bulk C6 starch phosphate (white squares) measured over 24 hours in wildtype plants. For starch measurements n = 5-8 and for starch phosphate measurements n = 3 pools of approximately 20 rosettes each. White bar indicates light period, black bar indicates dark period. **D** C6 starch phosphate measured in rosettes collected 20 min after the onset of darkness in wildtype plants grown in 12 h light, 12 h dark. Both bulk and surface C6 starch phosphate are shown. All error bars are ± SEM.

5.2.2 Selecting transgenic lines.

The *gwd* mutant (SALK_077211) was transformed with the various mutant versions of *AtGWD* by agroinfiltration. The T-DNA contained a gene conferring resistance to the

herbicide BASTA, and transformants were selected on the basis of this resistance. By looking for a 3:1 ratio of BASTA resistant to susceptible plants at the T2 generation, lines with single insertions were selected. These were allowed to self fertilise to produce the T3 generation. T3 homozygous lines were selected on the basis of 100% of individuals displaying resistance to BASTA. Homozygous lines were desirable because each line provides a pool of genetically identical plants which express the protein at consistent levels. Conclusive experiments can thus be performed much more easily than they can on segregating lines. Homozygous lines also represent generationally stable transgenics which can used to produce identical plants for future studies. I isolated multiple independent lines for each construct. This was for two reasons: first, to maximise the chance of finding lines expressing the transgene at a level close to that found in wildtype and second, to ensure that any phenotypes observed in particular lines were independent of T-DNA insertion position. These lines are listed in Table 5.2. T3 lines in the *gwd* background were screened for the presence of the SALK insertion in *AtGWD* to ensure the original mutation remained, and that any restoration of starch turnover was due to the inserted gene (Figure 5.3). Randomly selected T3 homozygotes for each construct were screened for AtGWD protein abundance by immunoblotting with an anti-StGWD antibody (Figure 5.4). On each blot, the protein levels and migration were compared to Col-0 controls.

Construct	**Background**	**Line no.**	**SALK insertion?**	**Protein present?**
Empty vector (pB7FWG2)	*gwd*	98-5	Yes	No
	gwd	97-4	NT	NT
35S_GWD::GFP	*gwd*	2-6	Yes	Yes
	gwd	11-8	Yes	Yes
	gwd	7-7	Yes	Yes
	gwd	132-8	Yes	Yes
	gwd	130-4	Yes	Yes
	gwd	131-2	Yes	Yes
	gwd	6-5	NT	Yes
	gwd	8-9	NT	Yes
	gwd	3-4	NT	NT
	gwd	9-8	NT	NT
	gwd	1-9	NT	NT
	gwd	5-1	NT	NT
NP_GWD	*gwd*	94-4	Yes	Yes
	gwd	85-8	Yes	Yes
	gwd	84-5	Yes	Yes
	gwd	86-8	NT	NT
	gwd	87-7	NT	NT

	gwd	92-1	NT	NT
	gwd	83-2	NT	NT
	gwd	91-6	NT	NT
35S_GWD^{cat}::GFP	*gwd*	26-3	Yes	Yes
	gwd	34-5	Yes	Yes
	gwd	28-4	NT	Yes
	gwd	33-8	NT	NT
	gwd	35-3	NT	NT
	gwd	36-3	NT	NT
35S_GWD^{redox}::GFP	*gwd*	74-2	Yes	Yes
	gwd	76-4	Yes	Yes
	gwd	73-4	Yes	Yes
	gwd	75-8	NT	NT
	gwd	72-1	NT	NT
	gwd	80-3	NT	NT
	gwd	81-4	NT	NT
35S_GWD^{SUMO}::GFP	*gwd*	24-2	Yes	Yes
	gwd	14-3	Yes	Yes
	gwd	17-4	NT	NT
	gwd	15-5	NT	NT
	gwd	18-6	NT	NT
	gwd	20-8	NT	NT
35S_GWD^{P}::GFP	*gwd*	71-4	Yes	Yes
	gwd	63-1	Yes	Yes
	gwd	68-2	Yes	Yes
	gwd	62-9	NT	NT
	gwd	61-4	NT	NT
	gwd	70-3	NT	NT
	gwd	69-9	NT	NT
Empty vector (pB7FWG2)	Col-0	104-7	NT	NT
35S_GWD::GFP	Col-0	123-2	No	Yes
35S_GWD^{cat}::GFP	Col-0	119-6	No	Yes
35S_GWD^{redox}::GFP	Col-0	115-5	NT	Yes
	Col-0	117-4	NT	Yes
	Col-0	114-5	NT	Yes
	Col-0	116-3	NT	NT

Table 5.2: Independent homozygous transformants generated for this thesis. For each line, the construct, the genetic background and the line number are presented as well as whether or not the *gwd* SALK insertion is present (assessed by PCR, see also Figure 1.3) and whether or not the GWD protein is present (assessed by immunoblotting, see also Figure 1.4). All lines described here displayed approximately 3:1 segregation of BASTA resistant : BASTA sensitive plants at T2. They all displayed 100% BASTA resistance at T3. NT = not tested.

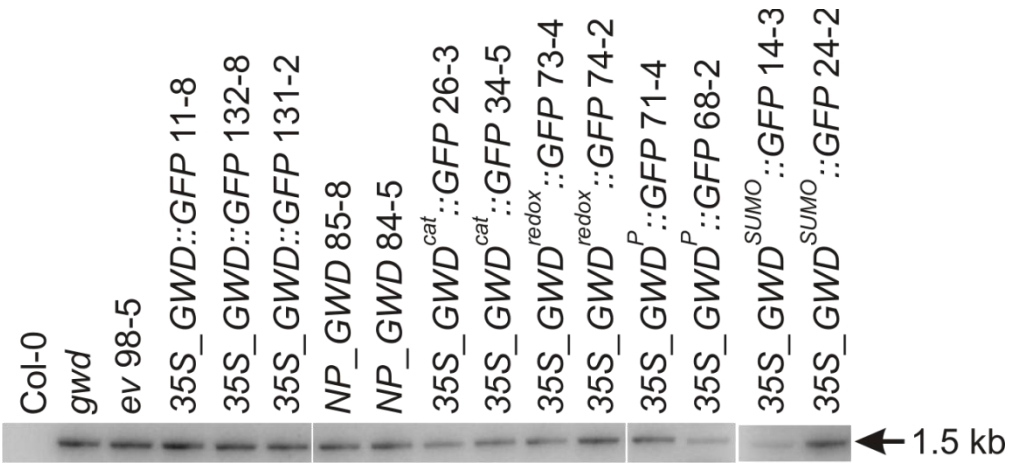

Figure 5.3: Screening of transformed lines for the presence of the SALK insert in *AtGWD*. Agarose gel showing DNA bands stained with ethidium bromide and visualised with UV fluorescence. A band at 1.5 kDa indicates the presence of the SALK insert in *AtGWD*. DNA loaded on the gel was from PCR reactions using primers 10 and 714 (see section 2.9) and DNA extracted from a single plant for the line indicated. The results were confirmed by at least two further PCRs using DNA from different individual plants (data not shown).

Without exception, the transgenic lines had more AtGWD protein than wildtype, Col-0 plants. This was independent of whether expression was driven by the native or the 35S promoter. Immunoblots were performed on dilution series of extracts from *NP_GWD* 85-8 plants. Analysis of the band intensities indicated there was around 16 times more protein in this transgenic line than in wildtype (data not shown). The migration of the protein in SDS-PAGE always matched the expected size of the protein relative to AtGWD in Col-0, taking into account the C-terminal tag (Figure 5.4). Lines expressing untagged AtGWD showed a GWD band on the immunoblot at the same size as the Col-0 band. Lines expressing GFP tagged versions of the protein showed a GWD band somewhat above the Col-0 band. Several lines were also analysed on blots (in addition to those in Figure 5.4) with molecular weight markers (data not shown). Lines expressing GFP tagged AtGWD (132-8, 131-2, 119-6) showed a band a little below the 230 kDa marker on the immunoblot, consistent with a mass of 183 kDa. Line 85-8 showed a band just above the 150 kDa marker, consistent with a mass of 156 kDa. In a few lines expressing AtGWD::GFP (eg *35S_GWD::GFP* 132-8, Figure 5.3), a second

band could be seen on the immunoblot, of the same apparent mass as the AtGWD band in Col-0. This suggests that in some lines a small fraction of the protein is translated without, or otherwise loses, its GFP tag.

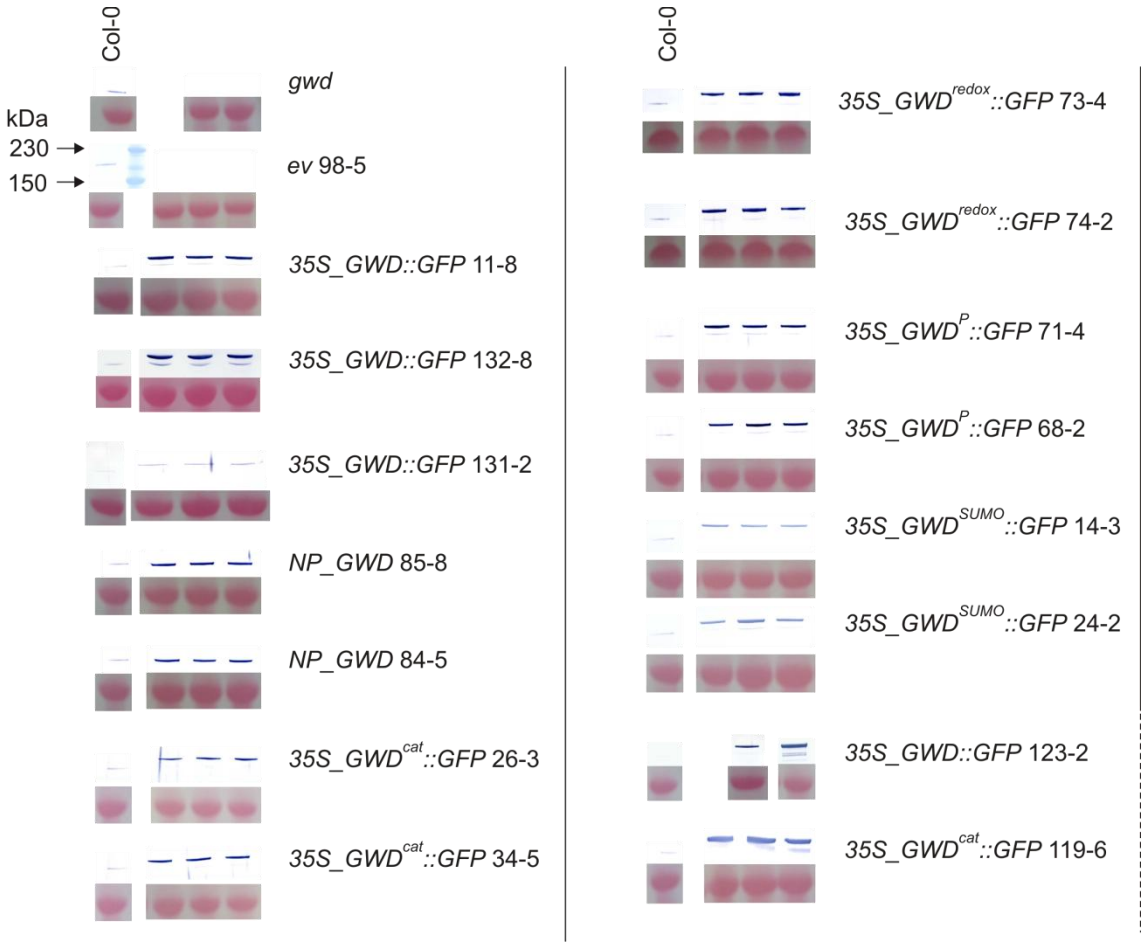

Figure 5.4: Screening transformed lines for AtGWD protein levels. An immunoblot probed with anti-StGWD antibody (upper panels) is displayed for each line (indicated right of blots). Protein on the immunoblot was transferred from SDS-polyacrylamide gels of soluble protein extract. A Ponceau stain of each blot is also displayed (lower panels) indicating the quantity of Rubisco large subunit (55 kDa) as a loading control. Each lane was loaded with extract from a different, individual plant. For each line, a Col-0 control from the same blot is also displayed (left panel). For each line, all four tracks are from the same gel/blot and were developed and photographed identically. The position of the markers is indicated when present. A solid vertical line to the right of the label indicates the line is in the *gwd* background, while a dashed line to the right indicates the line is in the Col-0 background.

On the basis of the above analyses, lines were chosen for detailed characterisation of their starch phenotype. To allow comparison of the effects of the different mutant versions of AtGWD, a set of transgenics was selected which express the introduced protein to similar levels.

5.2.3 Structure of experiments

Transgenic lines were harvested for starch analysis from two large scale experiments conducted in a controlled environment room under identical conditions. For some lines, samples were collected over a 24 h timecourse, and for others samples were only taken at the end of the day and the end of the night. Two replicate 24 h timecourses were collected for Col-0 controls in each experiment. Col-0 behaved almost identically in each replicate, making 6-8 mg starch (g FW)$^{-1}$ by the end of the day and degrading almost all of the starch at night such that less than 0.5 mg (g FW)$^{-1}$ were left at the end of the day. All starch measurements were made on 21 day old plants. In a third experiment, all lines were grown side by side in a semi-randomised design. They were harvested at 28 days and the fresh weight measured.

For clarity, I split the results from the above experiments into three parts. The reader should note that this means the controls are repeated in several figures, to allow comparison with different sets of transgenic lines. First I present the effects of expressing wildtype versions of AtGWD in the *gwd* background (section 5.2.4) and then the effects of expressing mutant forms of AtGWD in the *gwd* background (section 5.2.5). The clearest indications of whether or not a line has been complemented come from end of night starch levels and biomass. Therefore, in each section I first present the end of night starch data for all lines with the biomass data. I then present the more detailed diel starch data separately. Thus the end of night starch values are presented twice, but in different contexts. In section 5.2.6 I describe a separate experiment, in which lines expressing different forms of AtGWD are subject to an unexpectedly early night. In section 5.2.7 I present the final part of the large scale timecourse experiments, examining the effects of expressing different forms of AtGWD in Col-0.

5.2.4 Complementation with wildtype AtGWD

All wildtype versions of *AtGWD* successfully complemented the high starch phenotype of the *gwd* mutant (Figure 5.5). Both *gwd* and the empty vector (*ev*) control contained

very high starch at the end of the night (EON). The *ev* line contained slightly less starch than *gwd*, and although statistically significantly (at $p=10^{-3}$) it was much less significant than differences between the *ev* control and the other transgenics ($p<10^{-6}$). The difference between *gwd* and the *ev* line should be interpreted with caution because there is often a lot of variation in starch content between otherwise identically grown plants with mutations in *GWD*. Lines expressing AtGWD under the 35S promoter with a GFP tag (*35S_GWD::GFP*) contained between 4.5 and 10 fold less starch than the *ev* line at EON. However, none quite attained the very low starch levels of around 0.5 mg $(g\ FW)^{-1}$ found in Col-0 at EON. The constructs under the native promoter and with no tag (*NP_GWD*) provided the best complementation, with EON starch levels very similar to Col-0.

Biomass was essentially inversely correlated with EON starch content (Figure 5.5). Biomass was substantially restored in each transgenic line expressing wildtype AtGWD. All the transgenics had significantly more biomass (at $p=0.05$) than either *gwd* or *ev*. Although some lines expressing AtGWD (eg 11-8, 131-2) seemed a little smaller than Col-0, any differences between these lines and Col-0 were not significant (at $p=0.05$).

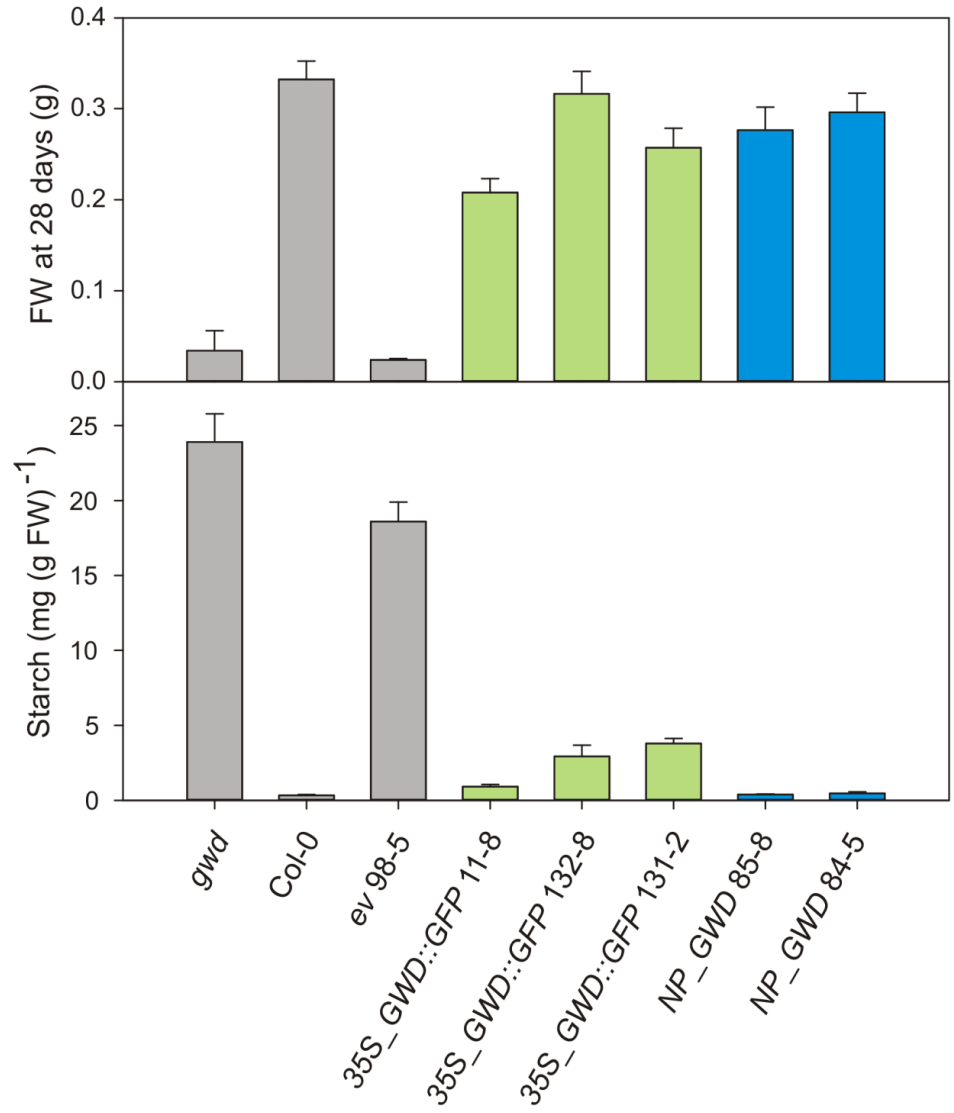

Figure 5.5: Complementation of the *gwd* mutant with wildtype *AtGWD*. Biomass (top) and starch (bottom) measured at the end of the night in Col-0, *gwd* and in homozygous transgenic lines transformed with the empty vector (*ev*) or different wildtype versions of *AtGWD*. All transgenic lines shown are in the *gwd* background. For details of lines see Table 5.1. For starch n = 5 and for biomass n = 15. Error bars are ± SEM. Starch values for the lines: Col-0, 11-8, 132-8, 131-2, 85-8, 84-5 are significantly different from the empty vector ($p < 10^{-5}$). The *gwd* starch value is significantly different from the empty vector at $p = 0.05$. No lines differed significantly in biomass from Col-0 ($p=0.05$) except for the *ev* control and *gwd*. Biomass and starch were measured in separate experiments.

Starch content was characterised in detail over 24 hours in a line expressing AtGWD under the native promoter (*NP_GWD* 85-8), and a line expressing AtGWD under the 35S promoter (*35S_GWD::GFP* 11-8) (Figure 5.6 A). Starch accumulation during the day and depletion at night were essentially linear and total turnover was similar to Col-0. The starch excess relative to Col-0 in the line expressing AtGWD under the 35S promoter is preserved throughout the 24 hour experiment. A line expressing the empty vector in the *gwd* background has high starch throughout the diel cycle without any consistent changes or trends, although there was considerable plant to plant variation.

Starch content at the end of the day and the end of the night was measured in some other lines (Figure 5.6 B). Two additional lines expressing AtGWD under the 35S promoter (132-8, 131-2) displayed similar diurnal starch turnover to wildtype but a greater starch excess phenotype than line 11-8 (Figure 5.6 B). An additional line expressing AtGWD under the native promoter (84-5) displayed EOD and EON starch values essentially indistinguishable from wildtype.

In summary, two lines expressing AtGWD under its own promoter without a GFP tag had starch turnover essentially indistinguishable from wildtype, even though they contained considerably more AtGWD protein than wildtype. In contrast, three lines expressing similarly large amounts of an AtGWD::GFP fusion protein expressed under the 35S promoter displayed higher starch levels than wildtype, although starch turnover was normal.

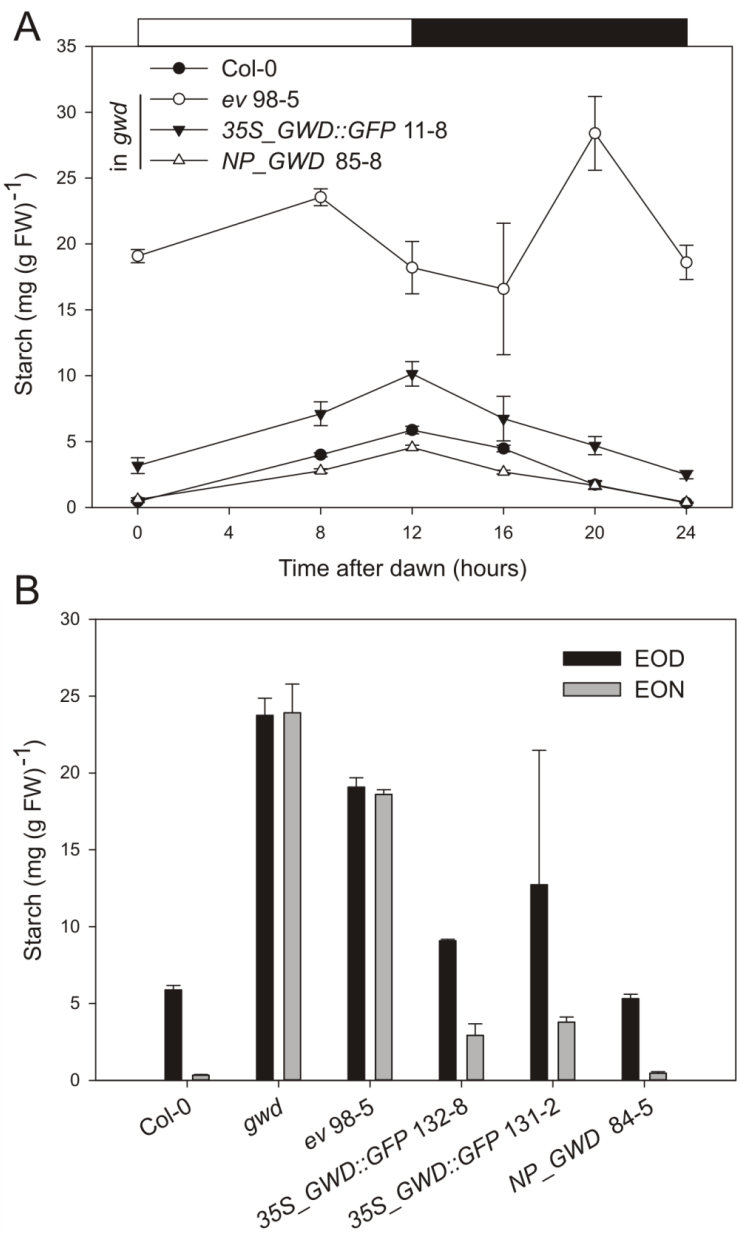

Figure 5.6: Diel patterns of starch accumulation in Col-0, *gwd*, and *gwd* complemented with wildtype versions of *AtGWD*. **A** Starch measured over 24 hours. White bar indicates light period, black bar indicates dark period. **B** Starch measured at the end of the day (EOD, black bars) and the end of the night (EON, grey bars). For details of lines see Table 5.2. n = 4 – 8 and error bars are ± SEM. For each genotype except *gwd* and *ev*, EON starch is significantly different from EOD starch ($p < 0.05$). EON data are the same as used in Figure 5.5.

5.2.5 Complementation with mutant versions of *AtGWD*

End of night starch and biomass were examined in *gwd* mutant plants expressing various mutagenised versions of *AtGWD* (Figure 5.7 A). No complementation of the *gwd* starch excess phenotype was achieved in lines expressing the catalytic mutant of AtGWD (*35S_GWD^{cat}::GFP*). In fact these lines contained 50% more starch at the end of the night than either *gwd* or the *ev* control, but had similar low biomass. In all other lines the mutant phenotype was substantially complemented, although none had end of night starch values as low as wildtype. Two lines expressing the redox insensitive version of AtGWD (*35S_GWD^{redox}::GFP*) had 2 – 4 mg starch (g FW)$^{-1}$ at the end of the night, similar to lines expressing wildtype GWD under the 35S promoter with the GFP tag. Lines expressing the phosphorylation or SUMOylation mutant version of AtGWD (*35S_GWD^{P}::GFP* or *35S_GWD^{SUMO}::GFP*) had slightly more starch at the end of the night (4 – 8 mg (g FW)$^{-1}$). A statistical analysis is presented in the legend to Figure 5.7.

The amount of starch remaining at the end of the night was negatively correlated with biomass (Figure 5.7 B). All lines except those expressing the catalytic histidine mutant had significantly greater biomass than either *gwd* or the *ev* control ($p<0.05$). Both the lines expressing the redox mutant (73-4, 74-2) did not differ significantly in biomass from Col-0 ($p=0.05$) and neither did one of the lines expressing the SUMOylation mutant (14-3) and one of the lines expressing the phosphorylation mutant (68-2). The other lines expressing the SUMOylation mutant (24-2) and the phosphorylation mutant (71-4) had biomass just significantly lower than Col-0 at $p=0.05$.

Figure 5.7: Complementation of the *gwd* mutant with wildtype and altered versions of *AtGWD*. **A** Biomass (top panel) and starch at the end of the night (bottom panel) in Col-0, *gwd* and in homozygous transgenic lines transformed with the empty vector (*ev*) or different wildtype or mutated versions of *AtGWD*. All transgenic lines shown are in the *gwd* background. For details of lines see Table 5.2. For biomass n = 15 and for starch n = 5. Error bars are ± SEM. All starch values are significantly different from the empty vector control ($p < 0.01$). Starch values for all lines are significantly differnt from line 11-8 except for lines 73-4 and 24-2. All lines except *35S_GWD^{cat}::GFP* 26-3 and 34-5 had significantly greater biomass than both *gwd* and the *ev* control line ($p = 0.05$). Biomass was measured in a separate experiment to starch. **B** The relationship between biomass and end of night starch content. Data are the same as used in A.

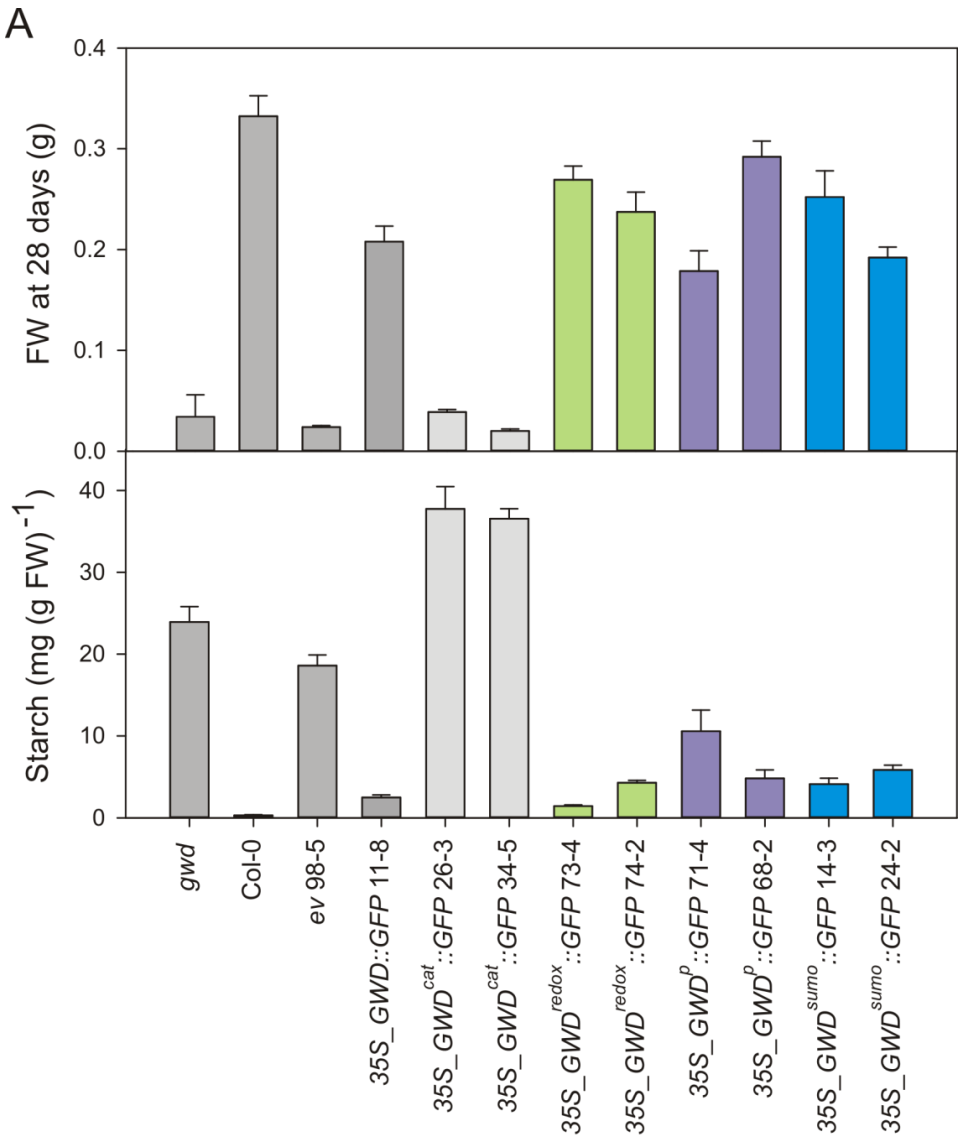
A
FW at 28 days (g)
0.0
0.1
0.2
0.3
0.4
Starch (mg (g FW)-1)
0
10
20
30
40
gwd
Col-0
ev 98-5
35S_GWD::GFP 11-8
35S_GWDcat::GFP 26-3
35S_GWDcat::GFP 34-5
35S_GWDredox::GFP 73-4
35S_GWDredox::GFP 74-2
35S_GWDp::GFP 71-4
35S_GWDp::GFP 68-2
35S_GWDsumo::GFP 14-3
35S_GWDsumo::GFP 24-2

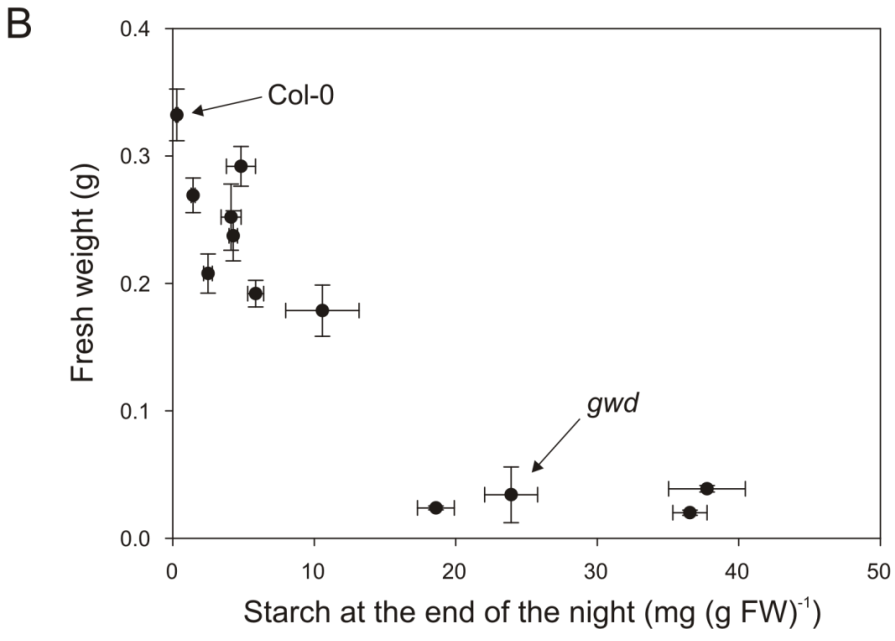
B
Fresh weight (g)
0.0
0.1
0.2
0.3
0.4
Col-0
gwd
0
10
20
30
40
50
Starch at the end of the night (mg (g FW)-1)

One line for each construct was analysed for starch content over over 24 hours (Figure 5.7). Similar to the *ev* control, the catalytic mutant had consistently high starch through the day, with much plant-to-plant variation (Figure 5.8 A, B). Once again, lines expressing the GWD::GFP fusion under the 35S promoter had more starch at all time points than wildtype. This effect was mild in the lines expressing unmutated AtGWD or the redox mutant of AtGWD (Figure 5.8 D, E), but more pronounced in lines expressing the phosphorylation or SUMOylation mutants of AtGWD (Figure 5.8 F, G). All lines displayed pronounced starch turnover with the exception of lines expressing the catalytic mutant of AtGWD, which had essentially no turnover. The magnitude of turnover was similar to Col-0 in all the other lines, except the line expressing the phosphorylation mutant, where it was twice as great as wildtype. However there was considerable plant-to-plant variation in starch content in this line.

End of day and end of night starch content were analysed for several lines in addition to those described above (Figure 5.8 H). The results in each case were similar to those reported above. A further line expressing the catalytic mutant displayed no starch turnover. Starch turnover was similar to or greater that Col-0 in further lines expressing the phosphorylation or SUMOylation mutants versions of AtGWD. Starch content was greater than Col-0 at the end of the day and the end of the night in these lines, but was always much lower than the starch content of the *ev* control.

Figure 5.8: Diel patterns of starch accumulation and degradation in Col-0, and in *gwd* complemented with wildtype and mutated versions of *AtGWD*. Graphs show starch measured over 24 hours in **A** *gwd* transformed with the empty vector (*ev*), **B** *gwd* expressing *35S_GWD^{cat}::GFP*, **C** Col-0, **D** *gwd* expressing *35S_GWD::GFP*, **E** *gwd* expressing *35S_GWD^{redox}::GFP* **F** *gwd* expressing *35S_GWD^{SUMO}::GFP* **G** *gwd* expressing *35S_GWD^{P}::GFP*. White bar indicates light period, black bar indicates dark period. **H** Starch measured at the end of the day (EOD, black bars) and the end of the night (EON, grey bars) for some additional lines. For details of lines see Table 5.2. n = 4 – 8 and error bars are ± SEM. End of night data from these timecourses are the same as those used in Figure 5.6. For each genotype EON values are significantly different to EOD values ($p < 0.05$) except for the empty vector control (A) and the catalytic mutants (26-3, 34-5; B, H).

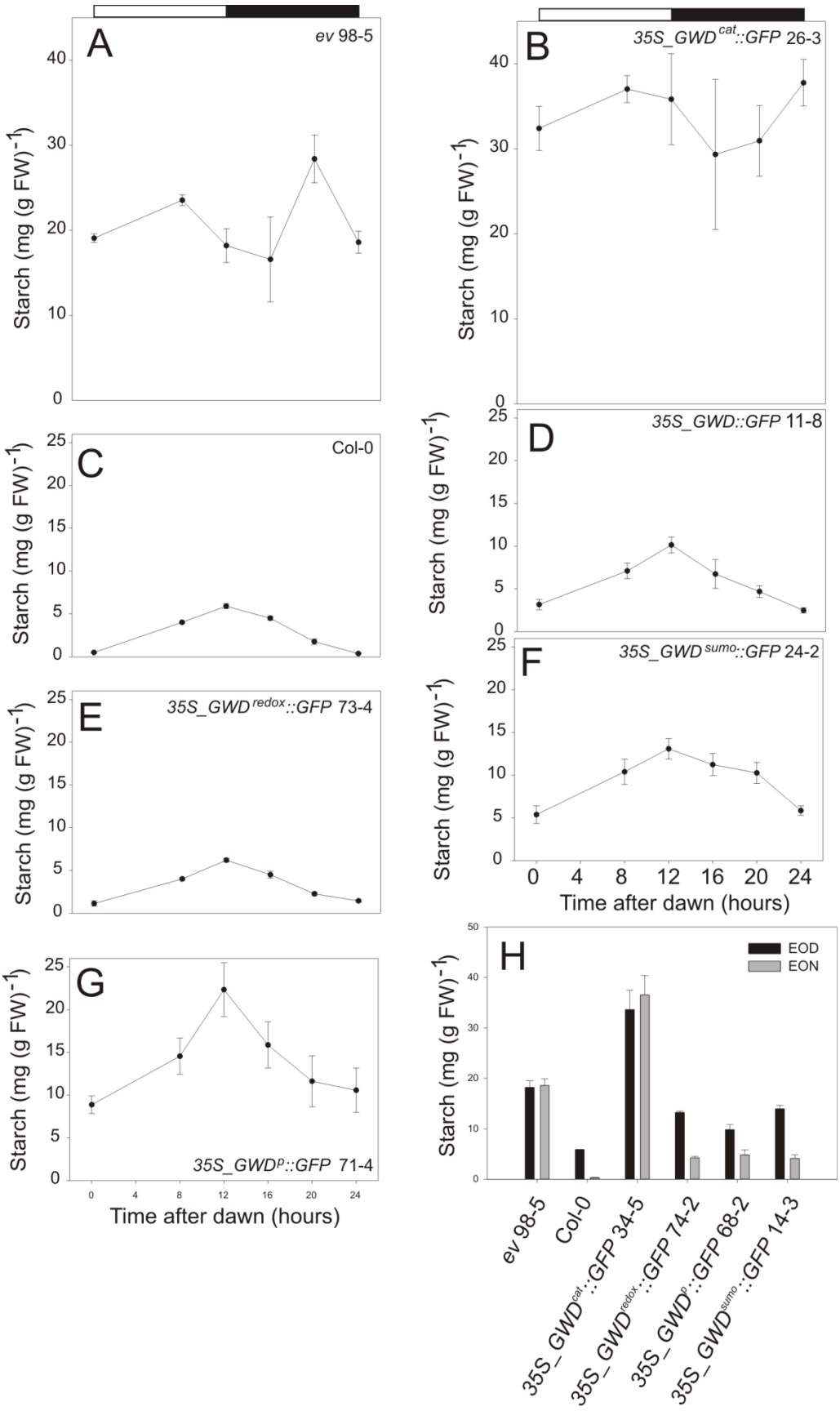
A
ev 98-5
B
35S_GWD cat ::GFP 26-3
C
Col-0
D
35S_GWD::GFP 11-8
E
35S_GWD redox ::GFP 73-4
F
35S_GWD sumo ::GFP 24-2
G
35S_GWD p ::GFP 71-4
H
EOD
EON
Starch (mg (g FW)-1)
Time after dawn (hours)
ev 98-5
Col-0
35S_GWD cat ::GFP 34-5
35S_GWD redox ::GFP 74-2
35S_GWD p ::GFP 68-2
35S_GWD sumo ::GFP 14-3

5.2.6 Response of transgenics to an early night

Starch turnover is restored and EON starch is reduced to near-wildtype levels in many of the transgenics when grown in constant conditions. However this does not mean that they will necessarily adjust their starch metabolism normally when subjected to changing conditions. I wished to test whether *gwd* plants transformed with a redox unresponsive version of AtGWD still adjust the rate of starch degradation when challenged with an early night. Plants were grown in 12 h light, 12 h dark cycles for 21 days and then a subset was transferred to a four h early night. Starch content was measured throughout the diel cycle in plants which were subject to the early night, and a control set that experienced a normal night. As in previous experiments, the lines expressing the *GWD::GFP* fusion from the 35S promoter had higher starch content over the diel cycle than Col-0. Lines expressing GWD under the native promoter without a GFP fusion had starch levels only very slightly greater (by 0.5 – 1 mg $(gFW)^{-1}$) than in Col-0. As previously reported (Lu *et al.*, 2005; Graf *et al.*, 2010), Col-0 displayed a lower rate of starch degradation in the early night as compared to the normal night, timing starch degradation such that reserves were not exhausted before dawn (Figure 5.9 A). Essentially the same behaviour was observed in the transgenic lines expressing wildtype AtGWD, whether the protein was expressed as GFP fusion under the 35S promoter or without a tag under the native promoter (Figure 5.9 B, C). The line expressing the redox mutant version of GWD as a GFP fusion under the 35S promoter also displayed appropriate adjustment of the starch degradation rate to the early night (Figure 5.9 D).

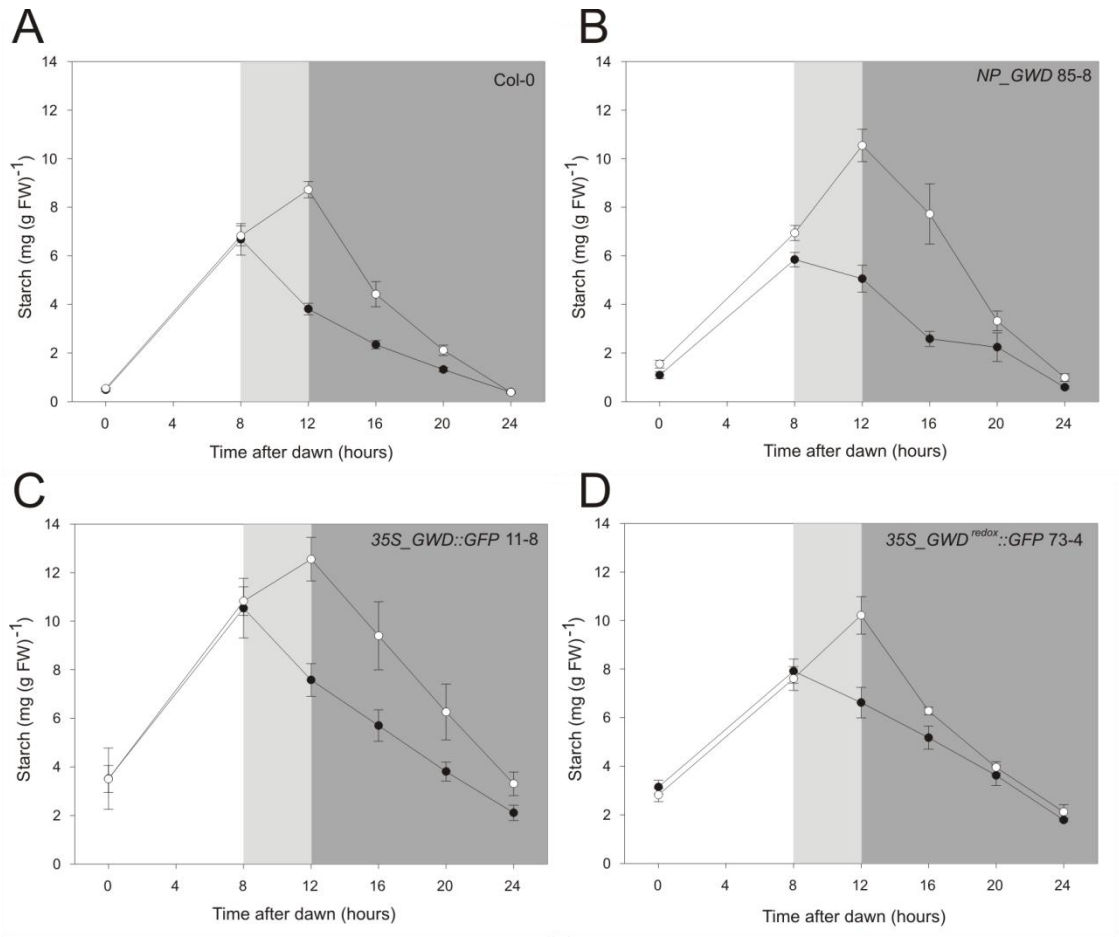

Figure 5.9: The response of starch degradation in Col-0 and transgenic lines to an early night. Plants were grown in 12 hours light, 12 hours dark cycles for 21 days. A set of plants (black circles) for each genotype was transferred to a 4 hour early night (light grey background) while another set (white circles) remained in a normal 12 hour photoperiod (dark grey background). **A** Col-0, **B** *gwd* expressing *NP_GWD*, **C** *gwd* expressing *35S_GWD::GFP*, **D** *gwd* expressing *35S_GWD^{redox}::GFP*. For details of lines see Table 5.2. n = 4 – 8 and error bars are ± SEM.

5.2.7 Effects of overexpression of *AtGWD* in Col-0

Results presented above showed that the catalytic mutant of AtGWD does not restore normal starch turnover to the *gwd* mutant. This result offered me the opportunity to discover whether a catalytically inactive GWD would interfere with starch turnover in a wildtype plant. Accordingly, I expressed wildtype AtGWD and the catalytic mutant form of AtGWD in the Col-0 background. As for transgenics in the *gwd* background, the transgenics in Col-0 expressed AtGWD protein to much higher levels than wildtype. Col-0 expressing the *ev* or the *AtGWD::GFP* fusion on the 35S promoter displayed

patterns of starch turnover very similar to Col-0 (Figure 5.10 A). Neither line differed significantly in EON starch levels from Col-0, although EOD starch levels were slightly depressed in the line overexpressing wildtype AtGWD relative to Col-0. A line expressing the catalytically inactive form of AtGWD in the Col-0 background also showed a diel pattern of starch turnover very similar to Col-0 except it had a slight, but significant, starch excess at the end of the night. It contained over 1 mg $(g\ FW)^{-1}$ as compared to less than 0.5 mg $(g\ FW)^{-1}$ in Col-0. However biomass was not significantly different from Col-0 (Figure 5 B).

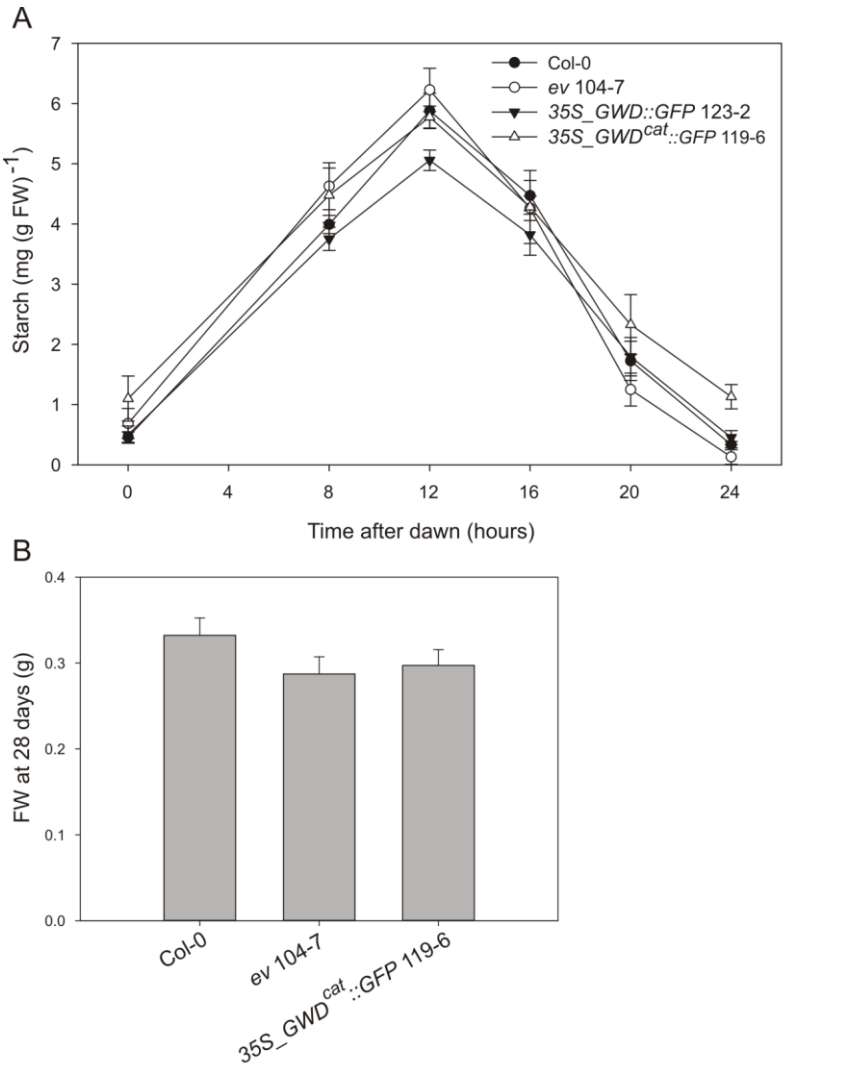

Figure 5.10: Effects of overexpression of *AtGWD* in the Col-0 background. **A** Diel starch accumulation and degradation in Col-0 (black circles), Col-0 transformed with the empty vector (*ev* 104-7, white circles) and Col-0 transformed with wildtype *AtGWD* (*35S_GWD::GFP* 123-2, black triangles) or the catalytic mutant version of *AtGWD* (*35S_GWD^{cat}::GFP* 119-6, white triangles). For details of lines see Table 5.2. n = 4 – 8. At the end of the night (24 h), only the catalytic mutant is significantly different to Col-0 ($p < 0.05$). **B** Biomass of Col-0, Col-0 transformed with the empty vector (*ev*) and Col-0 expressing *35S_GWD^{cat}::GFP*. n=15. None are significantly different from each other (p=0.05). Data for Col-0 expressing *35S_GWD::GFP* were not available. Error bars are ± SEM.

5.3 Discussion

If AtGWD is regulated to change the rate of starch degradation, I have shown that this must be at a post-translational level. Results presented in chapter 3 show that *AtGWD* cannot be regulated at a transcriptional level to cause the rapid changes in starch degradation rates that occur on unexpected changes in the timing of the onset of darkness (Graf *et al.*, 2010). This is because AtGWD is an abundant protein with a long half life, so massive changes in transcription would be required to significantly increase protein levels on short timescales. In addition the protein has a low flux control coefficient for starch degradation, so considerable changes in protein amount would be required to affect starch degradation. In chapter 3 I showed that AtGWD protein levels are essentially invariant over the diurnal cycle, thus the short term control of starch degradation cannot be via transcriptional regulation of AtGWD. In this chapter I test the hypothesis that AtGWD is regulated for the control of starch degradation at the post-translational level.

There is indirect evidence that AtGWD is regulated at a post-translational level. As discussed in chapter 1, AtGWD is likely be regulated to prevent granule hyperphosphorylation and chloroplastic ATP depletion at night. AtGWD also has several properties often associated with post-translational regulation: namely, redox responsiveness, lysine phosphorylation, lysine SUMOylation and the presence of coiled-coil domains (often associated with protein-protein interactions). Additional evidence comes from the biochemistry of the starch granule. On the transition to darkness, an increase of the phosphorylation of starch granule surface glucans is observed (Ritte *et al.*, 2004). These data point to the regulation of AtGWD and/or other enzymes involved in the cycle of phosphorylation and dephosphorylation. In another experiment, the authors supplied exogenous ^{32}Pi to cultures of C*hlamydomnas reinhardtii* and monitored the incorporation of radioactivity into starch. They found that on the onset of darkness, the rate of ^{32}P incorporation transiently increases for around 30 mins before returning to a steady state of no net incorporation. When the ^{32}P label is chased with unlabelled P, substantial turnover of starch phosphate is observed in cultures subject to an hour of darkness, but not in cultures incubated in the light. Thus the cycle of phosphorylation and dephosphorylation clearly operates differently in light and in darkness.

In this chapter I first look for further evidence for the regulation (or not) of the starch phosphorylation cycle. I then select and examine transgenic *gwd* mutant plants expressing mutagenised forms of *AtGWD*. By examining the extent of complementation in these lines, I investigate the relevance of post-translational modifications of AtGWD to starch metabolism *in vivo*.

5.3.1 Preliminary analysis of diel changes in the starch phosphorylation cycle

It is clear from the high starch phenotypes of the *gwd*, *pwd* and *sex4* mutants that the cycle of phosphorylation and dephosphorylation of the starch granule is essential to normal starch degradation. As described above, there is also good evidence that this cycle is regulated. However we do not know how starch phosphate changes over a normal diel cycle in any plant. I have applied a recently developed assay for the measurement of G6P to measure starch phosphate and thereby start to address the above points. The assay is based on the compound reazurin which is transformed into the highly fluorescent resorufin on reduction. In the linear range of the assay, the amount of resorufin produced is equal to the amount G6P present in the sample. The assay is extremely sensitive, and glucose-6-phosphate in the 1-10 nM range can be measured. As a consequence, less plant material is needed to measure starch phosphate than with conventional assays such as that based on malachite green (Hostettler *et al.*, 2011). This means that more data can be collected with a given amount of growth space.

Starch phosphate was measured over 24 h. The general trend observed was of increasing phosphate levels per unit glucose during the day, and decreasing levels during the night. This implies that the later in the day, there is more net starch phosphorylating activity than early in the day such that there is a greater density of starch phosphate in the outer layers of the granule than in the centre. At night, the highly phosphorylated outer layers are progressively removed, so granule phosphate content gradually declines. These observations are intriguing, because they show that a structural property of the starch granule changes over the diel cycle. We know that to adjust the rate of starch degradation appropriately, information regarding the quantity of starch in the chloroplast and the time remaining until dawn is integrated. This information must somehow result in appropriate changes in the activities of the enzymes responsible for starch degradation. Thus any changes in granule properties over the diel cycle could

form part of the process by which time and starch quantity signals combine to determine starch degradation rates.

It is important to note that the above experiment has only been performed once, and that one data point does not fit with the above interpretation. Starch phosphate measured 8 hours after dawn was slightly higher than that measured at dusk, 12 hours after dawn. However, at 16 hours after dawn, starch phosphate was much lower than at 12 hours after dawn. Therefore either starch phosphate was released from within the granule in the early part of the night or one of the data points is not reliable.

There is one previous report which characterised the distribution of phosphate within a starch granule. Blennow *et al.* (2005a) used particle-induced X-ray emission to study the spatial elemental composition of potato tuber starch granules. In contrast to my data, they found that the starch was more highly phosphorylated towards the centre of the granule. However, a tuber starch granule is fundamentally different from a transient leaf starch granule in many ways. For example, the timescales for synthesis are much greater and the granules are much larger. The distribution of starch phosphate may represent another difference between leaf and storage starches.

As far as we know, AtGWD phosphorylates only the granule surface, so I reasoned that any differences in activity with regulatory consequences might be most easily discerned by measuring starch surface phosphate. I began to develop methods to to measure surface phosphate, following ideas from Ritte *et al.* (2004), who used a partial digest of purified starch granules to release surface glucans. In my partial digests, around 1% of the total glucan in the granule was released. The reazurin-based assay was sensitive enough to allow starch phosphate measurements on such relatively small amounts of glucan. It was then possible to compare bulk and surface phosphate levels of granules extracted just after the onset of darkness. From these preliminary measurements, it seemed that surface phosphate broadly reflects bulk phosphate.

In summary, starch phosphorylation does not occur at a constant rate per glucose unit added to the starch, but the rate seems to increase through the morning. This will result in a non-uniform distribution of phosphate within the granule. These data provide further evidence that the cycle of granule phosphorylation and dephosphorylation is

regulated. Such changes in phosphorylation state and phosphate turnover may have consequences for the control of starch degradation.

5.3.2 Selecting transgenic lines

I performed the following checks and controls to validate transgenic lines expressing various forms of AtGWD in either the *gwd* or the Col-0 background. In chapter 4, I described transient expression of the *AtGWD* constructs in *N. benthamiana* to validate the chloroplastic localisation of the protein. Col-0 and *gwd* plants were transformed with these constructs and taken to the T3 generation. T3 homozygous lines were selected on the basis of BASTA resistance, and the presence of the SALK insert in the native *gwd* gene confirmed where relevant. For each line, I confirmed the presence of an AtGWD protein of the expected size given the C-terminal tag encoded in the construct. For each construct, I selected multiple independent T3 lines to so I could make sure that phenotypes observed were independent of the insertional position of the transgene. A set of lines expressing AtGWD to similar levels were selected for detailed analysis.

5.3.3 Complementation of the *gwd* mutant by wildtype AtGWD

The expression of wildtype AtGWD in the *gwd* background successfully complemented the high starch phenotype of the mutant and restored starch turnover. In contrast, the empty vector control did not restore wildtype starch levels. All lines studied vastly overexpressed the AtGWD protein: a typical line contained 16 times more protein than wildtype. The fact that large increases in AtGWD protein had little effect on the flux through starch degradation provides further support for the low flux control coefficient of AtGWD for starch degradation, as calculated in chapter 3. These data also suggest either that the binding of excess amounts of AtGWD to the starch granule has no effect on other enzymes of starch degradation, or that the binding of the enzyme to the surface is regulated such that the total granule-bound AtGWD is unchanged in the overexpressors. It has recently been discovered that AtGWD will hydrolyse ATP and transfer phosphate either to water, AMP or ADP in the absence of any glucan substrate *in vitro* (Hejazi *et al.*, 2012). If this occurs *in vivo*, I might anticipate a deleterious effect of overexpression of catalytically active AtGWD. The fact that several of the transgenic lines have essentially normal starch turnover and biomass despite the high AtGWD levels suggest that this effect is not significant *in vivo*. If AtGWD hydrolysed ATP in an unregulated manner then some negative impact on biomass would probably be anticipated.

The *AtGWD* transgene complemented the *gwd* mutant independent of whether the gene was under control of the 35S or the native promoter. However transgenics expressing *AtGWD* under the 35S promoter, without the 3' UTR and with a GFP tag, tended to have higher starch throughout the diel cycle than Col-0. At the end of the night these lines had 1 – 4 mg $(g\ FW)^{-1}$ compared to less than 0.5 mg $(g\ FW)^{-1}$ in Col-0. In contrast, those transgenics expressing *AtGWD* under control of the native promoter, with the 3' UTR and without a GFP tag, displayed a pattern of starch turnover essentially identical to Col-0. It seems unlikely that the differences in starch metabolism between the types of construct are due to the promoters or 3' UTRs because both types of transgenic contain similarly high AtGWD protein levels. It seems more likely that the presence of a C-terminal tag slightly interferes with the function of AtGWD, resulting in a slight starch excess phenotype. For example, the large GFP tag might prevent the enzyme from accessing more densely packed areas of the granule.

Regardless of the promoter or C-terminal tag used, *gwd* plants complemented with *AtGWD* adjusted starch degradation rates normally. Wildtype Arabidopsis displays a decreased rate of starch degradation when challenged with an unexpectedly early night, such that the plant does not exhaust its reserves before dawn. *gwd* complemented with either AtGWD::GFP fusion protein expressed under the 35S promoter, or the untagged protein expressed under the native promoter, also displayed decreased starch degradation rates in response to an unexpected early night. This supports the view that transcriptional regulation is not important for the short term control of starch degradation. *AtGWD* expressed under the 35S promoter is unlikely to generate oscillations in transcript abundance and the transgenics all expressed AtGWD at much higher levels than wildtype, and yet starch degradation rates adjust normally to an early onset of darkness.

5.3.4 The importance of the granule phosphorylating activity of AtGWD versus other putative functions

gwd mutant plants expressing a version of *AtGWD* mutated in the catalytic histidine retained a severe starch excess phenotype and very low biomass relative to Col-0. This was the expected phenotype from the expression of a version of the enzyme that should completely lack catalytic activity. Thus this construct was successful as a negative

control. The data also demonstrate that the autophosphorylation activity of the enzyme is essential to its function in the plant. In turn this strongly suggests that GWD affects starch degradation through glucan phosphorylation rather than through the interaction of the protein with other partners or via a disruptive effect of the SBDs on granule crystallinity.

There were unexpected effects of the overexpression of the catalytic mutant of AtGWD in *gwd* in that the transgenic lines displayed an even more extreme starch excess phenotype than the *gwd* mutant, although they were no more compromised in growth. The *gwd* mutant I used for transformation was a SALK T-DNA insertion line which lacked the AtGWD protein. Thus it would seem that the presence of a non-catalytic version of AtGWD in vast excess of normal AtGWD levels can exaggerate the *gwd* mutant phenotype. Intriguingly, the overexpression of the catalytic mutant of AtGWD in the Col-0 background had very little effect on either starch or growth. Thus the presence of wildtype AtGWD suppresses the negative effects of GWD^{cat} in the Col-0 background.

There are two possible explanations for these data. The first and most likely is that there is some small amount of starch turnover in *gwd* which is inhibited by the presence of large amounts of the catalytically inactive protein. Evidence that there is some starch turnover in *gwd* comes from analysis of the *gwd*/*mex1* mutant which accumulates maltose, although only to a third of the levels which accumulate in the *mex1* single mutant (Stettler *et al.*, 2009). It is not known how glucan is released from the granule in the *gwd* background. BAM3 can release a small amount of glucose *in vitro* from starch granules purified from a *gwd* mutant, and this release is stimulated by the presence of ISA3 (Edner *et al.*, 2007). It may be that BAM3 and ISA3 are also responsible for the small amount of glucan released in the *gwd* mutant. It is not clear how large amounts of catalytically inactive AtGWD might interfere with the action of BAM3 and ISA3, especially since this form of AtGWD does not interfere with starch degradation in the Col-0 background. Another alternative is that inactive AtGWD interferes with the action of an enzyme not required for normal starch degradation, but that is responsible for release of glucans in the *gwd* background. AMY3 and LDA are candidates for such enzymes. The second possible explanation for the data is that overexpression of inactive AtGWD somehow enhances starch synthesis such that more starch can accumulate. For

example inactive AtGWD might interact with the starch granule or the enzymes of synthesis in such a way that the starch synthesis machinery is less inhibited by the large amounts of starch already in the chloroplast. What these interactions could be is not clear.

Whatever the mechanism resulting in increased starch contents in these lines, it is probable that it requires large amounts of the inactive protein. This is because *gwd* mutants which express the protein at approximately wildtype levels (*sex1-1, sex1-4*) contain less starch than *gwd* mutants which lack the protein entirely (*sex1-2, sex1-3 sex1-5, sex1-6, SALK_077211*) (Yu *et al.*, 2001). Thus it seems that substantial overexpression is required for the inactive protein to have an effect.

5.3.5 The relevance of redox regulation of AtGWD

StGWD has redox responsive properties *in vitro*. Reduction of a disulphide bridge close to the catalytic histidine leads to activation of the enzyme, while oxidation with $CuCl_2$ leads to inactivation (Mikkelsen *et al.*, 2005). The same study demonstrated that the C1008S mutation in StGWD prevents the formation of the disulphide and creates a redox-insensitive enzyme which is active over a large range of redox potentials. I recapitulated this mutation in *AtGWD* and expressed it in the *gwd* mutant plant to examine the relevance of redox regulation *in vitro*.

Two independent transgenic lines expressing the redox-insensitive version of AtGWD in the *gwd* background displayed good complementation of the *gwd* phenotype. End of night starch was restored to near wildtype levels. The slight starch excess observed at the end of the night is probably an effect of the GFP tag on GWD function, as in other lines expressing the GWD::GFP fusion, rather than a specific effect of loss of redox control on enzyme acitvity. Normal starch turnover was restored and starch degradation was timed correctly so that reserves lasted just until dawn. Indeed, when the transgenics were subject to a 4 h early night, starch degradation rates decreased in a similar manner to wildtype, such that reserves again lasted until dawn. Near-wildtype biomass was also restored.

These results demonstrate that the redox regulation of AtGWD through this particular disulphide has no relevance for the daily initiation of starch degradation, or for the

setting of degradation rates in response to anticipated night length. This conclusion is consistent with the fact that the E_m value for AtGWD is so positive that the enzyme is is unlikely to become oxidised and inactivated under normal chloroplastic conditions (Mikkelsen *et al.*, 2005; Edner *et al.*, 2007). The CxxxC motif near the catalytic histidine is conserved in GWD sequences from some species but not others (Table 5.3). The restricted phylogenetic distribution of the motif suggests that is not essential for the normal function of the protein across taxa, in contrast to the catalytic histidine residue, which is absolutely conserved. Thus, even if the disulphide has regulatory importance in some species, different regulatory mechanisms will have evolved in some organisms.

My results do not rule out the possibility that redox regulation plays a role in the regulation of AtGWD. The disulphide bridge investigated here may have relevance in conditions other than those tested so far. There may also be other disulphide bridges in the protein which confer redox responsive properties, but are only effectively reduced/oxidised by specific oxidoreductases *in vivo*, and so have not yet been identified *in vitro*. There are six cysteines in the protein besides the pair studied here: five in the region between SBD2 and the catalytic domain and one in the nucleotide binding domain.

Although it is clear that redox regulation of AtGWD via Cys1019 is not essential for the control of starch degradation, it is still possible that AtGWD is redox regulated as part of a coordinate regulation of enzymes to effect a change in flux. Consider the situation in which many of the enzymes in the pathway, including GWD, have to be upregulated to cause an increase in flux. The GWD^{redox}::GFP version of AtGWD should be permanently in the reduced and active state since the disulphide can no longer form between the cysteines. Thus in conditions in which flux through starch degradation is low (e.g. short days) one might expect *in vivo* GWD activity to be inappropriately high in plants expressing GWD^{redox}::GFP. This will not result in a change in flux, because AtGWD has a low flux control coefficient and control is hypothetically devolved throughout the pathway. However it might result in a detectable increase in granule phosphorylation. If granule phosphorylation is sufficiently stimulated, plant performance might be compromised in conditions under which night-time ATP is likely to be less available, for example in very short days. Thus in the future it will be interesting to examine starch phosphate in lines expressing GWD^{redox}::GFP and also to

evaluate their growth under very short day conditions relative to wildtype and *gwd* expressing GWD::GFP.

5.3.6 The relevance of post-translational modifications within SBD1

My results indicate that neither the phosphorylation nor the SUMOylation modifications reported to occur within SBD1 of AtGWD are of importance for the regulation of starch degradation. *gwd* mutants expressing versions of AtGWD in which the modified sites had been mutated displayed normal initiation of starch degradation and normal starch turnover. This was with the exception of one of the two lines expressing AtGWD mutated at the phosphorylation site, which had greater turnover compared to wildtype. However, all these lines had a pronounced starch excess phenotype at all times of day and night measured. This was not simply the effects of the GFP fusion, because lines expressing the wildtype version of AtGWD or the redox mutant fused to GFP did not show such strong starch excess phenotypes. Thus, although phosphorylation and SUMOylation do not appear to be necessary for the normal control of starch degradation, it may be that mutations in the first SBD of AtGWD are deleterious for the function of the enzyme. This is interesting because it suggests that although low affinity *in vitro* (Glaring *et al.*, 2011), the starch binding domains of GWD may have a role *in vivo*. Further tests of the importance of the starch binding domains will be possible when plants are ready for analysis that express a version of AtGWD in which the tryptophan residues thought to be critical for starch binding have been mutated.

There are eight predicted SUMOylation sites in the AtGWD protein besides the one in SBD1 (Elrouby and Coupland, 2010), all of which could potentially have regulatory roles. In the future it might be interesting to mutate more of these sites, or combinations of sites, and see if the resulting mutant versions of the enzyme can complement the *gwd* phenotype. An alternative strategy would be to examine starch metabolism in Arabidopsis T-DNA lines with insertions in the chloroplastic SUMO proteases. If such lines have no starch phenotype, then it is unlikely that SUMOylation is responsible for the control of starch degradation.

The SBD1 SUMOylation and phosphorylation sites are not universal features of GWD proteins from different plant species (Table 5.3). Indeed some GWD1 proteins, including those of rice, barley and maize, lack SBD1 entirely. Thus, even if

SUMOylation and phosphorylation within SBD1 have some regulatory function in Arabidopsis, this will not be conserved across all species which accumulate leaf starch.

Organism (Sequence no., Uniprot)	Redox (CxxxC)	SUMOylation site in SBD1 (L**K**LE)	Phosphorylation site N**S**HL
Arabidopsis thaliana (Q9SAC6)	✓	✓	✓
Ricinus communis (B9SMZ2)	✓	x	✓
Populus trichocarpa (B9HTV3)	✓	x	✓
Citrus reticulata (Q8LPT9)	✓	✓	✓
Solanum tuberosum (Q9AWA5)	✓	x	✓
Solanum lycopersicum (B5B3R3)	✓	x	✓
Vitis vinifera (A7QP24)	✓	No SBD1	No SBD1
Physcomitrella patens (A9RGK0)	✓	✓	x
Oryza sativa (B8B2U3, B9FTF7)	x	✓	x
Sorgum bicolor (C5Z316)	x	x	✓
Hordeum vulgare (C3W8P1)	x	No SBD1	No SBD1
Triticum aestivum (D7PCT9)	x	No SBD1	No SBD1
Ostreococcus sp. (A4S6H4, AQ00X32)	x	No SBD1	No SBD1
Micromonas sp. (C1MZK9, C1MTG9, C1E487)	x	x	x
Chlamydomonas reinhardtii (A816T5)	x	x	x
Toxoplasma gondii (B0QEA9, B9QNC3, B6KSD6)	x	x	x

Table 5.3: Prevalence of putative regulatory sites across phyla. Tick symbol indicates presence of the site, cross indicates absence. 'No SBD1' indicates the entire first starch binding domain is absent. Sequence data were sourced from Uniprot (www.uniprot.org) and aligned for comparison using MEGA4 (www.megasoftware.net).

5.3.7 Overexpression of AtGWD in Col-0

Overexpression of wildtype or the catalytically inactive form of AtGWD in Col-0 had little effect on starch metabolism. These results are consistent with the low flux control coefficient for AtGWD (chapter 3). This experiment also provides an indirect test of our understanding of how linearity is achieved in starch degradation. The simplest explanation of the observed linear rate of degradation is that granule surface area is never limiting for the rate of degradation, or at least not until near the very end of the night. Alternatively, it would still be possible to achieve linear degradation with partially limiting surface area if the mechanics of starch degradation change through the night to compensate for decreased surface area. For example, regulatory changes in the starch phosphorylation enzymes could result in more surface phosphorylation as the night goes on, allowing the rate of hydrolytic attack to increase.

My results support the simplest hypothesis: one would not expect the overexpression of a catalytically inactive form of AtGWD to have a large effect on the rate of starch degradation if surface area were not limiting for degradation. In contrast, if surface area was limiting for degradation, then one would expect competition for binding sites in the $AtGWD^{cat}$ overexpressor to limit the rate of starch degradation. In this chapter I only characterise a single transgenic line overexpressing the catalytically inactive form of AtGWD in Col-0, so the result must be treated as preliminary. However, starch degradation was almost identical in this line to that in Col-0. The only difference was a slight starch excess in the transgenics at the end of the night. In high time resolution measurements of starch through the night I have previously observed a slight slowing of the rate at the very end of the night in Col-0. This could represent the point at which starch degradation begins to be surface-area limited. If the number of binding sites for active AtGWD is effectively reduced in the line overexpressing the AtGWD catalytic mutant, then one would expect starch degradation to become surface area limited slightly earlier in the night. This might explain the slight starch excess at the end of the night in the $AtGWD^{cat}$ overexpressor.

5.4 Summary

In this chapter I present the first 24 h timecourse of starch phosphate levels. Phosphate is not added at a constant rate per glucose moiety added to the granule, but the rate increases through the morning. This results in a non-uniform distribution of phosphate

through the granule with the outer layers being more densely phosphorylated. Thus the structural and chemical properties of the glucan exposed at the granule surface vary throughout the day and the night, a fact which could have consequences for the regulation of starch degradation.

Transgenics were selected expressing *AtGWD* in the *gwd* background. Complementation of the starch and biomass phenotypes of the mutant was achieved regardless of whether *AtGWD* was expressed under the native or the 35S promoters. This provides further support for the conclusion from chapter 3 that transcriptional regulation is not important for the daily regulation of starch degradation. Transgenic lines contained approximately 16 times more protein than wildtype, and yet starch degradation was normal, supporting the low flux control coefficient of AtGWD as determined in chapter 3. As expected, a non-catalytic version of AtGWD did not complement the *gwd* mutant. This provides confirmation that AtGWD largely affects starch degradation through its glucan phosphorylating activity rather than some other function. Surprisingly however, expression of this non-catalytic mutant enhanced the starch excess phenotype of the *gwd* mutant, although had no effect the biomass. This suggests that large quantities of inactive AtGWD inhibits the activities of enzymes responsible for the small amount of glucan release from starch which occurs in the *gwd* background.

Redox regulation of AtGWD has been widely hailed as a likely mechanism by which starch degradation could be regulated (Kötting *et al.*, 2010; Stitt and Zeeman, 2012). This is based on *in vitro* evidence that AtGWD has redox responsive properties and can be reductively activated by thioredoxins. I found that a redox non-responsive version of AtGWD, lacking a cysteine required to form the redox sensitive disulphide, could complement the *gwd* mutant plant. Starch degradation was initiated as normal, starch turnover was as in wildtype plants, and the rate of starch degradation was correctly adjusted according to the night length. These results demonstrate that under the conditions tested, redox regulation of AtGWD is not important for the control of starch degradation *in vivo*.

Versions of AtGWD lacking residues for phosphorylation or SUMOylation within the first starch binding domain of the enzyme successfully complemented the *gwd* mutant.

Starch turnover was restored indicating that these modifications are not critical for the daily regulation of AtGWD activity. However transgenics expressing these forms of AtGWD were not fully complemented in that they displayed a moderate starch excess phenotype. This indicates that the function of SBD1 may be important for the normal function of the protein.

Finally, I found that overexpression of a catalytic mutant version of AtGWD in Col-0 had little effect on starch turnover. This provides evidence in support of the simplest explanation for the observation that starch is degraded in a linear manner: that granule surface area is far from limiting for starch degradation in a wildtype plant.

6 Summary and Outlook

Starch degradation in Arabidopsis provides the plant with carbon and energy for growth and metabolism each night. The process of nocturnal starch degradation is exquisitely regulated: degradation is linear, providing a constant supply of carbon through the night, and is precisely timed such that reserves run out around dawn. This pattern of degradation is maintained despite acute changes in night length, day irradiance or night temperature (see section 1.4.2). It seems that the amount of starch is divided by the amount of time remaining until dawn to set an appropriate rate of degradation. The circadian clock provides time information to set the rate of degradation (Graf *et al.*, 2010), and we are beginning to understand how the division calculation might occur (see section 1.4.2.3). However we still do not know how starch is measured or how the enzymes of the pathway are regulated. This thesis begins to address this latter question, focusing on the first enzyme in the starch degradation pathway, α-glucan, water dikinase.

In this chapter, I first summarise the main findings of my work and briefly describe the most promising experiments that could be performed to continue the lines of investigation I have begun. I then discuss the particular difficulties associated with the study of the *in planta* control of starch metabolism, and consider ways in which these might be overcome. Finally, I consider the avenues of future research which I think will most improve our understanding of the control of starch degradation.

6.1 Summary of findings and next steps

6.1.1 Transcriptional regulation of AtGWD

The *AtGWD* transcript displays large diel oscillations in abundance with a peak at dusk (Smith *et al.*, 2004). This pattern of transcript accumulation is shared with many other genes involved in starch degradation, but its relevance for regulation of the pathway has been unclear. In chapter 3 I describe a timecourse of the induction of RNAi mediated knockdown of *AtGWD* in a wildtype plant. For a short time, this generates a situation in which the *AtGWD* transcript has been reduced to low levels and yet starch degradation proceeds normally at night. Thus, the presence of the transcript and associated diel oscillations in abundance are not of relevance for the short term, diel regulation of starch metabolism. Indeed, through quantitative proteomic measurements I found that

AtGWD protein abundance changes less than 1.1 fold over the diel cycle. In addition, analysis of the RNAi experiment revealed that AtGWD has a very low flux control coefficient (0.06) for starch degradation. Thus such small changes in protein amounts over the diel cycle will not alter flux through starch degradation. In fact AtGWD protein levels have to drop below 40% of wildtype levels before the flux through starch degradation starts to be affected. This means there is plentiful enzymatic capacity at this step in the starch degradation pathway, and transcriptional regulation and changes in AtGWD protein levels will not be an effective way of regulating starch degradation.

Although AtGWD protein levels are unlikely to be regulated for flux control, regulation of protein amounts is still likely to be important to ensure an efficient use of cellular resources. Using quantitative proteomics, the decay of the AtGWD protein could be followed during the inducible silencing timecourse. Assuming that production of the protein had stopped when the transcript had dropped to low levels, the half life of AtGWD was estimated at two days. This relatively long half life means that any physiologically reasonable change in transcription will not be reflected substantially in protein levels for several days. *AtGWD* has an extremely complex promoter, transcription from which probably reflects an integration of a multitude of external and endogenous signals. Thus the transcriptional system provides environmental sensitivity, while the long protein half life effectively acts as a noise filter, ensuring that protein levels only change when environmental perturbations are sustained.

It turns out that the behaviour of *AtGWD* is not unique: many proteins remain stable over 24 hours although their transcripts oscillate with high amplitude. Diel protein abundance data were collected for 600 proteins in addition to AtGWD. Combining these data with publicly available diel transcript data allowed the prevalence of this behaviour to be tested. When assessed with a statistical criterion of diel rhythmicity I found that in 60% of cases in which the transcript is rhythmic, the protein is not. Indeed, transcript abundance was an extremely poor predictor of protein abundance over the diel cycle. Protein abundance was modelled assuming that the rate of transcription/translation depends only on the amount of transcript, and that degradation rate depends on the amount of protein. If transcript abundance oscillates with time, then we expect protein abundance also to oscillate. However the fold change of the oscillations is damped if protein degradation rates are low. Of course the rates of translation are likely to depend

on factors additional to transcript abundance, and there are also several examples in plants in which protein degradation is controlled by complex mechanisms. I suggest that a detailed knowledge of transcriptional, translational, and protein-degradative processes is required to understand the diel pattern of protein abundance in each specific case.

6.1.2 AtGWD and starch synthesis

Results presented in chapter 3 imply that AtGWD has a previously unrecognised role in starch synthesis. Evidence for this comes from the timecourse of knockdown of *AtGWD*. As AtGWD protein levels decrease, starch progressively accumulates at the end of the night. However starch at the end of the day remains constant, meaning that total starch synthesis is progressively diminished as AtGWD levels fall. Phosphorylation of starch during synthesis has been recognised for some time, but this is the first occasion on which biological significance has been ascribed to the phenomenon. How AtGWD might operate in starch synthesis is unclear. It is possible that phosphorylation of the growing starch granule, and associated structural changes, are necessary for the proper action of the starch synthases and debranching enzymes.

It will be important to follow up the above observation with further experiments. A key experiment will be to begin induction of the RNAi knock-down of *AtGWD* and then transfer the plants to the dark for 24 hours to completely 'de-starch' them. Col-0 plants would be treated identically. When returned to the light, one could then observe whether plants with little AtGWD (the RNAi line) make starch at the same rate as wildtype plants. This experiment permits a direct comparison of starch synthesis in the presence and absence of AtGWD, not confounded by different absolute starch levels.

6.1.3 A putative AtGWD interaction partner: ROC4

Of 600 proteins measured during the inducible knock-down of *AtGWD*, the only protein besides AtGWD to display large and consistent changes in abundance was the cyclophilin and peptidyl prolyl isomerase ROC4 (section 3.2.6). The dynamics of ROC4 decay were remarkably similar to those of AtGWD except that ROC4 did not decay below about 40% of wildtype levels. Given that the ROC4 transcript is unlikely to be affected in this experiment, these data are suggestive of a physical interaction between ROC4 and AtGWD. ROC4 has intriguing links to redox biology. Its expression is highly correlated with that of 2-cysteine peroxiredoxin A, and it will reduce and activate 2-Cys peroxiredoxins *in vitro* (Laxa *et al.*, 2007). The story is complicated by

the fact that ROC4 is not expected to be represented in the data set. This is because only proteins that migrate more slowly than the 100kDa marker on an SDS-PAGE gel were included in the analysis, and yet mature ROC4 is predicted to be 20 kDa. Thus, the quantity measured may not represent ROC4 protein abundance, but could, for example, represent the proportion of ROC4 in some modified state.

The role of ROC4 certainly merits further investigation. First it would be interesting to use an anti-ROC4 antibody to see if the native and modified forms of ROC4 can be identified on an immunoblot. If so, it will be possible to see if the modified form disappears over a timecourse of knockdown of *AtGWD* to confirm the above result. Immunoprecipitation could then be used to discover whether or not AtGWD interacts with ROC4 *in vivo*. Finally, analysis of starch metabolism in a *roc4* knockout line would provide a test of whether ROC4 is required for the normal regulation of starch metabolism in Arabidopsis.

6.1.4 Post-transcriptional regulation of AtGWD

The regulation of starch degradation is highly likely to occur at a post-transcriptional level. This is because degradation rates adjust extremely rapidly to changing conditions, certainly within two hours. In addition, AtGWD has a long half life, meaning that protein levels cannot change rapidly. Several other enzymes of starch degradation do not change in abundance over 24 hours, suggesting they are similarly stable (Smith *et al.*, 2004; Lu *et al.*, 2005; Yu *et al.*, 2005). There is evidence of a role for the cycle of granule phosphorylation and dephosphorylation in the control of starch degradation. For example, on the transition to darkness, starch surface phosphorylation increases and starch phosphate turnover is initiated (Ritte *et al.*, 2004). In chapter 5, I show that starch glucose-6-phosphate per glucose in starch increases during the day and decreases during the night, also pointing to regulation of starch phosphorylation.

AtGWD has many properties often associated with regulation. In particular it is redox responsive *in vitro* and is phosphorylated and SUMOylated *in vivo* (Mikkelsen *et al.*, 2005; Elrouby and Coupland, 2010; Kötting *et al.*, 2010). To test the importance of these modifications I first cloned AtGWD and mutated sites necessary for these post-translational modifications. The process of cloning and mutagenesis was not straight forward and is discussed in chapter 4. These *AtGWD* variants were then expressed in the

gwd background and starch metabolism and biomass examined to assess the degree of complementation of the *gwd* phenotype. Wildtype versions of AtGWD restored starch turnover, growth and the proper adjustment of starch degradation rates in response to an unexpectedly early night in the *gwd* mutant. *AtGWD* mutated in the catalytic histidine did not complement the mutant, indicating that it is the starch phosphorylating activity of AtGWD, rather than some other function of the protein, which is important for normal starch degradation. The redox insensitive *AtGWD* also restored starch turnover, growth and the proper adjustment of starch degradation rates to the *gwd* mutant. This shows that the redox regulation of AtGWD is not important *in vivo*, at least under the conditions tested. Versions of *AtGWD* mutated in SBD1 at the phosphorylation site and in a SUMOylation site, also restored starch turnover to the mutant plant, but gave rise to a significant starch excess at the end of the night. Thus it seems that the SBD1 domain of AtGWD, and possibly phosphorylation or SUMOylation within that domain, are necessary for the proper function of the enzyme.

In the future it will be interesting to characterise starch phosphate levels in some of the transgenic lines. If regulation of the enzyme is affected by the introduced mutations, then one would expect to see changes in starch phosphate, even if there are no associated changes in flux through the pathway. In addition, it may be revealing to analyse plants expressing a version of AtGWD (already prepared) mutated in critical residues for the function of its starch binding domains. This would provide the first indication of the *in vivo* importance of the low affinity starch binding domains associated with several enzymes of starch degradation.

6.2 Prospects for understanding the control of starch degradation

Over the past 20 years, Arabidopsis genetics has revolutionised our understanding of transitory starch degradation. We now know that β-amylases and isoamylases, not α-amylases or phosphorylases as originally assumed, are primarily responsible for starch degradation in leaves. Furthermore, a new and important complement of enzymes responsible for phosphorylating and dephosphorylating the granule surface has been discovered, and novel transporters responsible for the export of carbon from the chloroplast at night have been discovered and cloned. Now the field is beginning to focus on the mechanisms by which flux through the pathway could be regulated. Most work in this area has focused on the *in vitro* properties of the enzymes of degradation.

Although such studies are undoubtedly important, it is essential to test the relevance of any putative mechanism *in vivo* at the earliest possible opportunity. This will ensure that further research is appropriately focussed.

6.2.1 Dealing with complexity

Understanding how metabolism is regulated in a wildtype plant is an especially challenging field of research. Occam's razor states that 'complexity should not be assumed unnecessarily' ('*pluralitas non est ponenda sine necessitate*') (Wildner, 1999). However, when investigating the control of metabolism it is necessary to entertain the possibility that it may be extremely complex. Starch degradation, for example, involves multiple isoforms of many enzymes catalysing a complex network of reactions, which could be responsive to a whole host of input signals from redox, to pH to Ca^{2+} spikes, to kinase cascades. There are very few theoretical tools to help one decide which of the above are likely candidates for regulatory nodes. In addition, the study of a single enzyme is highly unlikely to provide a mechanism for the regulation of a pathway. This is because control is likely to be devolved throughout the pathway, and the properties of one enzyme can only ever be interpreted in the context of the entire pathway. Of course, it is valuable to collect information on the properties of specific enzymes, and if many enzymes are studied then a trend may emerge which suggests how coordinate regulation of the pathway might be achieved. For example, redox responsiveness emerges as a theme from the *in vitro* analysis of many starch degrading enzymes. Although results presented in chapter 5 question the importance of redox regulation *in vivo*, a conclusive test would require the simultaneous *in vivo* manipulation of the redox responsive properties of all the enzymes of degradation.

So what can be done in the face of such potential complexity without adequate theoretical tools to guide us? First, it could be sensible to test hypotheses at the highest level possible. For example, it might be more sensible to test the role of redox regulation by examining mutants in thioredoxins or peroxiredoxins rather than working with each of the potential target enzymes in the pathway. Of course, this is only feasible if other effects of these high level mutations are not too severe. However the approach may be useful for excluding sets of hypotheses. Second, carefully designed forward genetic approaches should be used to uncover novel components and regulatory mechanisms. This latter approach is already being applied in the Smith laboratory (John

Innes Centre), in work designed and conducted by Alex Graf and Doreen Feike. Third, large scale data collection (transciptomics, proteomics, metabolomics) could be applied to look for molecules with different behaviours at, for example, the onset of a normal or an unexpectedly early night. Although this approach is limited to known cellular components that can be measured, it may well provide clues as to how starch degradation is regulated. This is the strategy being pursued by a large EU-funded consortium which includes the Smith laboratory, known as TiMET.

6.2.2 Avenues for future study

In my opinion, there are three key areas in which we need to improve our knowledge to gain a good understanding of starch degradation and its control. First, it is clear that we need a detailed description of the starch granule surface and the processes that operate at this interface. We have very little idea about the molecular organisation of glucans at the surface and how this changes as different enzymes interact with it. Methods to study the surface of a granule, and the dynamics of enzymes at that surface, will be extremely difficult to develop, especially if they are to work on small transitory starch granules such as those found in Arabidopsis. It is probable that a combination of real starch granules and artificial systems will be required. A first step is being taken at the John Innes Centre by Rob Field and colleagues who have developed a thick glucan layer on a surface plasmon resonance chip. This should allow dynamics of protein interactions with a starch-like surface to be monitored in real time. AtGWD, (the purification of which is described in chapter 3) may become one of the first proteins to be studied with this promising new system.

The second area which merits particular study is that of protein-protein interactions. There are several tantalising pieces of evidence to suggest that these are important. First, the non-catalytic proteins, BAM4 and LSF1 are clearly important for normal starch degradation (Fulton *et al.*, 2008; Comparot-Moss *et al.*, 2010). It seems likely that they interact with other proteins and/or the starch granule, and have some regulatory or structural function. Second, the mechanism for dividing the amount of starch by the amount of time until dawn could easily be achieved through protein-protein interactions (see section 1.4.3.2). Third, it is already known that AtGWD interacts with 14-3-3 proteins (Chang *et al.*, 2009), and in chapter 3 I present preliminary evidence that it may also interact with ROC4. These real and putative

protein-protein interactions could be pursued using co-immunoprecipitation or split-YFP type strategies. Such methods are preferred to yeast-2-hybrid or *in vitro* studies, because they better reflect the *in vivo* situation. It would be particularly interesting to see if changes in any interactions correlate with changes in the rate of starch degradation.

A third major advance required is the development of methods to study the importance of particular proteins at different times of day. Much of our knowledge of the pathway of starch degradation originates in the analysis of mutant plants. However, we cannot gain a complete picture from such studies. For example, consider a hypothetical protein thought to be important for starch degradation. In a full mutant, the effects of the absence of the protein on starch degradation may be confounded by effects on starch synthesis, growth rate and other secondary effects which accumulate through the lifetime of the plant. As this thesis demonstrates, the study of inducible mutants may permit the identification of functions of an enzyme which are not apparent from a full mutant. However, inducible knockdown with RNAi cannot be used to study the role of proteins at different times of day unless the protein has a half life of only a few of hours. Therefore we need methods for the inducible inhibition of enzymes, to discover which proteins are required when, and to unambiguously assign functions to enzymes in metabolism. At the end of chapter 3, I discussed engineerable protein degradation and inducible inhibitors based on camelid antibodies. The latter method has already been used to inhibit enzymes in plants (Jobling *et al.*, 2003), and has particular potential when combined with inducible promoters. Such technology could be used to dissect the specific roles of enzymes in different tissues or cells at specific developmental stages and times of day. Alternatively, specific chemical inhibitors of an enzyme identified through *in vitro* studies could be used to test the importance of that enzyme at different times of day. However, this approach relies on the identification of sufficiently specific inhibitors that can diffuse to the cellular compartment of interest,

6.2.3 Applying our knowledge of starch metabolism

What do we stand to gain from an improved knowledge of the regulation of starch metabolism, besides intellectual satisfaction at an intriguing phenomenon understood? One of the aims of plant sciences is to understand the basis of plant productivity such that crop plants can be manipulated to suit our needs. Understanding carbon allocation

in space and time is clearly important step towards achieving that aim. We need to know how photosynthate is partitioned between different parts of the plant: what determines the proportion that ends up in roots, leaves, grain or transitory stores? What are the genetic controls between carbon supply and growth, and to what extent do signals from sinks regulate the supply of carbon by photosynthesis or starch degradation? The study of starch metabolism has, and will continue to, shed light on these and similar questions.

New technologies often have their origins in unexpected scientific discoveries. An excellent example of this is a recent study in which *GWD* was downregulated in wheat endosperm using an RNAi hairpin expressed under an endosperm specific promoter (Ral *et al.*, 2012). Endosperm *GWD* transcript levels were decreased 41% - 72% in the RNAi lines compared to the parent lines, and endosperm starch glucose 6-phosphate was two to three fold lower. α-amylase activity was also increased in the RNAi lines. Remarkably, the RNAi lines displayed increased biomass, seed weight, tiller number, spikelets per head and seed number per spike. The combination of these factors leads to a 29% increase in the grain yield of the RNAi lines compared to the parent. Embryo size was also increased in the RNAi lines. This is intriguing because embryo size is recognised as a key contributor to the vigour of the young plant (LopezCastaneda *et al.*, 1996). It is possible that the increased α-amylase activity provides more carbon for the growth of the developing embryo. However, it is not clear how down regulation of *GWD* could result in the increased α-amylase activity. One might speculate that phosphorylation might result in decreased GWD activity and starch turnover during grain development (if indeed this occurs) and thus better grain filling. We clearly have a lot to learn about the role of starch phosphorylation in the cereal endosperm, but for now it seems that the study of GWD has much to offer, in Arabidopsis and beyond.

Appendix I: Theoretical description of protein oscillations

Solution to integral from section 3.3.2

The rate of change in the amount of a protein, *G*, can be described by the following differential equation, where *t* is time, ε is the translation rate, α is the amplitude of transcript oscillation, ω is the angular frequency of the oscillations, β is the centre of the transcript oscillation and γ is the protein degradation rate:

$$\frac{dG}{dt} = \varepsilon(\alpha \sin(\omega t) + \beta) - \gamma G \tag{i}$$

The solution to equation (i) is as follows:

$$e^{\gamma t}\frac{dG}{dt} + \gamma e^{\gamma t} = e^{\gamma t}\varepsilon(\alpha \sin(\omega t) + \beta)$$

$$e^{\gamma t}\frac{dG}{dt} + \frac{de^{\gamma t}}{dt}G = \varepsilon(\alpha \sin(\omega t) + \beta) - \gamma G$$

$$\frac{d(e^{\gamma t}G)}{dt} = \varepsilon(\alpha \sin(\omega t) + \beta) - \gamma G$$

$$e^{\gamma t}G(t) = \varepsilon \int e^{\gamma t}(\alpha \sin(\omega t) + \beta)\, dt$$

$$e^{\gamma t}G(t) = \varepsilon\alpha \int e^{\gamma t} \sin(\omega t)\, dt + \varepsilon\beta \int e^{\gamma t}\, dt \tag{ii}$$

The first integral on the RHS of equation (ii):

$$\int e^{\gamma t}\sin(\omega t) = \frac{1}{\gamma}e^{\gamma t}\sin(\omega t) - \frac{\omega}{\gamma}\int e^{\gamma t}\cos(\omega t)\, dt \tag{iii}$$

The integral on the RHS of equation (iii):

$$\int e^{\gamma t}\cos(\omega t) = \frac{1}{\gamma}e^{\gamma t}\cos(\omega t) + \frac{\omega}{\gamma}\int e^{\gamma t}\sin(\omega t)\ dt \tag{iv}$$

Substituting (iv) into (iii):

$$\int e^{\gamma t}\sin(\omega t) = \frac{1}{\gamma}e^{\gamma t}\sin(\omega t) - \frac{\omega}{\gamma^2}e^{\gamma t}\cos(\omega t) + \frac{\omega^2}{\gamma^2}\int e^{\gamma t}\sin(\omega t)\ dt$$

Collecting the integrals on the LHS and simplifying:

$$\int e^{\gamma t}\sin(\omega t) = \frac{e^{\gamma t}}{\gamma^2+\omega^2}(\gamma\sin(\omega t) - \omega\cos(\omega t)) + C'$$

Substituting into equation (ii):

$$e^{\gamma t}G(t) = \frac{e^{\gamma t}\varepsilon\alpha}{\gamma^2+\omega^2}(\gamma\sin(\omega t) - \omega\cos(\omega t)) + \varepsilon\beta\int e^{\gamma t}\,dt + C'$$

$$e^{\gamma t}G(t) = \frac{e^{\gamma t}\varepsilon\alpha}{\gamma^2+\omega^2}(\gamma\sin(\omega t) - \omega\cos(\omega t)) + \frac{\beta\varepsilon}{\gamma}e^{\gamma t} + C$$

Finally

$$G(t) = \frac{\varepsilon\alpha}{\gamma^2+\omega^2}(\gamma\sin(\omega t) - \omega\cos(\omega t)) + \frac{\beta\varepsilon}{\gamma} + Ce^{-\gamma t} \qquad \text{(V)}$$

Where C is the constant of integration.

The behaviour of equation (V) with changing protein degradation rates:

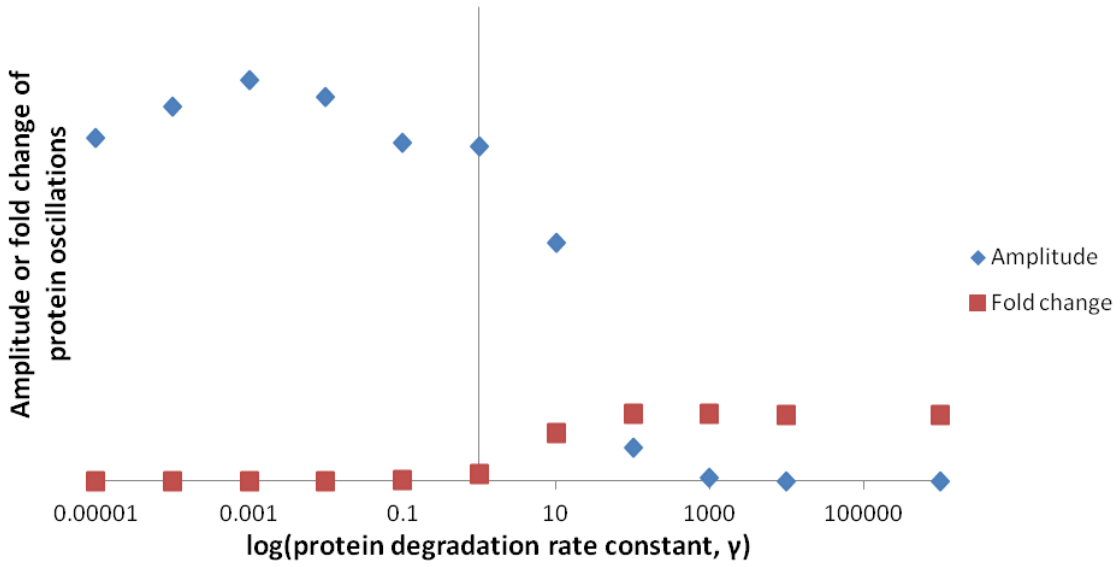

Thus, at high degradation rates the amplitude of protein oscillations is low, while the fold change is high. At low protein degradation rates, the amplitude of protein

oscillations is high while the fold change is low. For a certain range of protein degradation rates, the (logged) protein degradation rate should be approximately negatively related to the amplitude of oscillations and positively related to the fold change. The exact range protein degradation rates for which approximately linear behaviour is found depends on the values of the other parameters in the model.

Predicting the amplitude of AtGWD protein oscillations from the amplitude of transcript oscillations.

As a result of analyses discussed in chapter 5, I know the following information pertinent to the prediction of the amplitude of AtGWD protein oscillations: the fold change in transcript abundance, the period of the transcript oscillations and the protein decay rate. However to predict the amplitude of protein oscillations, I also need to know the absolute amount of transcript and the translation rate. Thus, predicting the amplitude of AtGWD protein oscillations from the transcript data is beyond the scope of this thesis.

Testing the hypothesis that short protein half lives damp oscillations in protein abundance

Below I use the little available pertinent data to test the prediction of equation (v): that the shorter the protein half life, the more damped oscillations in protein abundance will be relative to the oscillations in transcript.

Consider the following differential equation, where G is the average protein amount over the diel cycle; ρ is the average translation rate over the diel cycle and υ is the average protein degradation rate constant over the diel cycle. Protein degradation is assumed to be proportional to the amount of protein (see chapter 5). No additional assumptions are needed beyond those used in equation (i). The rate of change of G is determined by the translation rate and the protein degradation rate:

$$\frac{dG}{dt} = \rho - \upsilon G$$

At steady state:

$$\frac{dG}{dt} = \rho - \upsilon G = 0$$

$$\nu = \frac{\rho}{G}$$

Piques *et al.* (2009) calculated the quantities G and ρ for around 150 proteins in Arabidopsis. In the table below, I report their data for those proteins which also appear in my data set, and estimate a protein degradation rate, υ as ρ/G.

Gene	Protein fold change	Transcript fold change	Protein concentration , G (mol g FW-1)	Translation rate, ρ (mol h-1 g FW-1)	Translation/ protein, υ (h-1)	Transcript fold change/ protein fold change (μ)
AT3G60750	1.25	1.35	1.16E-09	3.58E-12	3.08E-03	1.09
AT3G12780	1.36	1.14	2.32E-09	1.41E-11	6.08E-03	0.84
AT3G54050	1.59	1.16	9.72E-10	6.57E-12	6.75E-03	0.73
AT1G04410	1.28	1.13	9.24E-10	8.59E-12	9.29E-03	0.88
AT5G35630	1.47	1.23	1.16E-09	1.42E-11	1.23E-02	0.84
AT2G42600	1.18	1.52	3.69E-10	4.75E-12	1.29E-02	1.28
AT5G48300	1.82	1.33	1.20E-10	1.91E-12	1.59E-02	0.73
AT2G39730	1.37	1.39	4.54E-09	7.71E-11	1.70E-02	1.01
AT3G55440	1.29	1.17	4.61E-10	8.44E-12	1.83E-02	0.91
AT1G20620	1.32	1.48	3.80E-10	7.11E-12	1.87E-02	1.12
AT1G23310	1.63	1.83	1.07E-09	2.04E-11	1.90E-02	1.12
AT3G26650	1.40	1.27	8.58E-10	1.72E-11	2.00E-02	0.91
AT5G58330	1.11	1.16	1.34E-10	3.05E-12	2.28E-02	1.05
AT2G13360	1.45	1.19	5.29E-10	1.36E-11	2.57E-02	0.82
AT2G21330	1.28	1.77	8.99E-10	2.54E-11	2.83E-02	1.38
AT1G42970	1.37	1.36	5.30E-10	1.58E-11	2.99E-02	0.99
AT5G19220	1.26	1.19	9.24E-11	2.99E-12	3.23E-02	0.94
AT4G38970	1.11	1.23	9.62E-10	3.43E-11	3.57E-02	1.12
AT1G67090	1.20	1.13	6.22E-09	4.34E-10	6.98E-02	0.94
ATCG00490	1.26	2.12	3.89E-09	3.17E-10	8.15E-02	1.68
AT1G37130	1.45	5.60	3.60E-11	8.69E-12	2.41E-01	3.86

Equation (v) predicts that proteins with faster degradation rates will have lower amplitude oscillations and a greater fold change in abundance than proteins with lower degradation rates with the same amplitude oscillations in transcript. In other words, proteins with fast degradation rates (sort half lives) with have lower amplitude protein

oscillations and a greater fold change in abundance relative to the amplitude of the transcript oscillations than proteins with slow degradation rates (long half lives). So the protein degradation rate constant, υ, should be negatively related to the ratio of the fold change in transcript oscillations to the fold change of protein oscillations. In the graph below, it can be seen that this is not the case for this very limited data set:

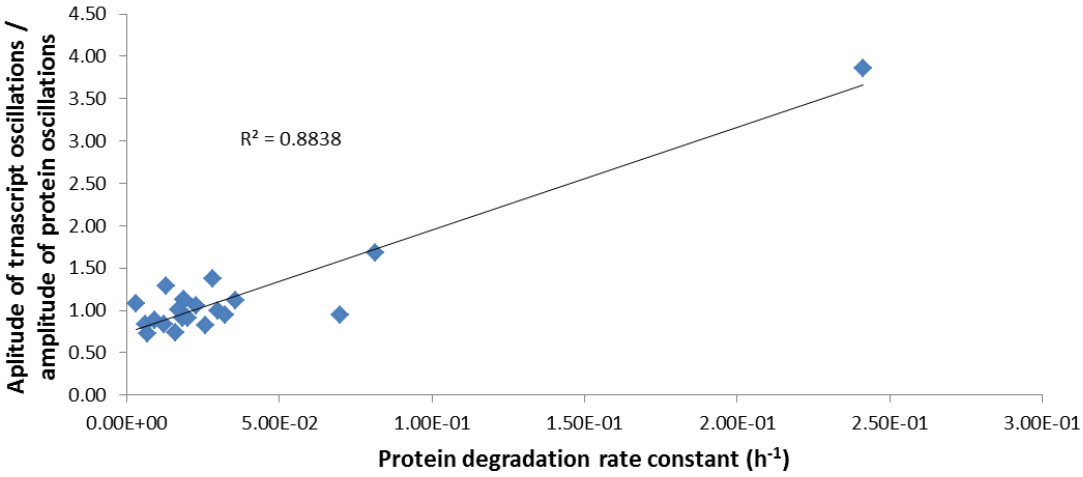

Expanding the bottom left area of this graph, the positive relationship is largely lost:

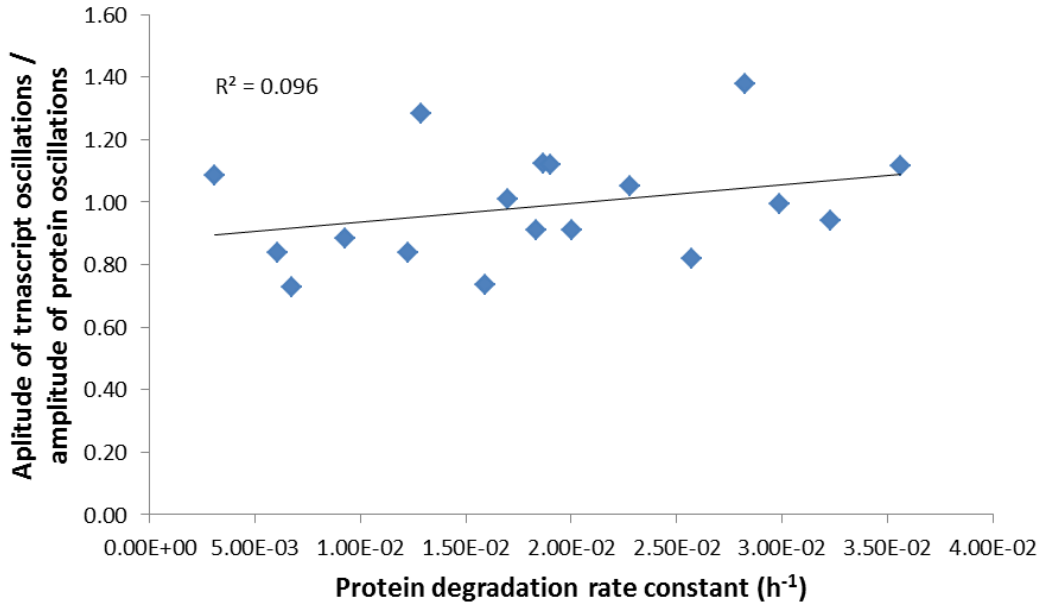

My data on AtGWD provide the possibility to test this relationship further:

The regression line from the first graph has the equation: y = 12.133x + 0.7349

Thus:

$$\frac{amplitude\ transcript\ oscillations}{amplitude\ of\ protein\ oscillations} = 12.133\upsilon + 0.7349$$

Calling the LHS μ:

$$\nu = \frac{\mu - 0.7349}{12.133}$$

For AtGWD, the amplitude of transcript oscillations is 4.8 fold and the amplitude of protein oscillations is 1.01 fold.

Thus

$$\mu = 4.75$$

$$\nu = 0.331\ \mathrm{h}^{-1}$$

υ is related to the half life of the protein as follows:

$$t_{\frac{1}{2}} = \frac{-\ln(0.5)}{\upsilon}$$

Substituting our value of υ:

$$t_{\frac{1}{2}} = \frac{-\ln(0.5)}{\upsilon} = 2.09\ \mathrm{h}$$

Experimentally, I determined the half life of AtGWD to be 46 h, so the relationship determined above does not accurately predict the AtGWD half life. However, the above analysis is based on very little data. In the future it may be possible to extend the analysis to include data from non-plant species to further test the relationship between protein half life and the amplitude of protein oscillations.

Appendix II: Progenesis peptide and protein reports

The CD attached to the back of this thesis contains an excel file named ‘progenesis reports’. This contains the protein mass spectrometry data as exported from Progenesis. There are four worksheets in the file: 24h peptides, 24h proteins, RNAi peptides and RNAi proteins. 24h refers to the 24 hour proteomic timecourse. RNAi refers to the inducible knock down of GWD experiment.

The peptide worksheets contain the following data for each peptide measured and identified:

- HPLC retention time
- Mass
- Mass error
- m/z
- Assigned TAIR accession
- Mascot confidence score for peptide identification (40 was used as lower cut-off)
- Peptide sequence including modifications
- Abundance data for each sample
- Spectral counts per sample

The protein worksheets contain the following data for each protein measured:

- Total peptide count
- Number of peptides used for quantification
- Mascot confidence score for protein identification
- Protein abundance values for each sample

Appendix III: MGF files

The CD attached to the back of this thesis contains folders named ‘24 h MGF’ and ‘RNAi MGF’. These folders contain the RAW mascot files for the 24 h timecourse of protein abundance and the timecourse of knockdown of AtGWD respectively. These files contain the peak list information for the 200 most abundance peaks in each spectrum. MGF files can be read as text files. More details regarding this file format and syntax are available at www.matrixscience.com/help/data_file_help.html.

Adler LN, Gomez TA, Clarke SG, Linster CL (2011) A Novel GDP-D-glucose Phosphorylase Involved in Quality Control of the Nucleoside Diphosphate Sugar Pool in Caenorhabditis elegans and Mammals. Journal of Biological Chemistry **286:** 21511-21523

Alabadi D, Oyama T, Yanovsky MJ, Harmon FG, Mas P, Kay SA (2001) Reciprocal regulation between TOC1 and LHY/CCA1 within the Arabidopsis circadian clock. Science **293:** 880-883

Alberty RA, Goldberg RN (1992) Standard thermodynamic formation properties for the adenosine 5'-triphosphate series. Biochemistry **31:** 10610-10615

ap Rees T, Fuller WA, Wright BW (1977) Measurements of glycolytic intermediates during the onset of thermogenesis in the spadix of *Arum maculatum*. Biochimica et Biophysica Acta **461:** 274-282

Appenroth KJ, Ziegler P (2008) Light-induced degradation of storage starch in turions of Spirodela polyrhiza depends on nitrate. Plant Cell and Environment **31:** 1460-1469

Araujo WL, Nunes-Nesi A, Nikoloski Z, Sweetlove LJ, Fernie AR (2012) Metabolic control and regulation of the tricarboxylic acid cycle in photosynthetic and heterotrophic plant tissues. Plant Cell and Environment **35:** 1-21

Armbruster U, Hertle A, Makarenko E, Zuhlke J, Pribil M, Dietzmann A, Schliebner I, Aseeva E, Fenino E, Scharfenberg M, Voigt C, Leister D (2009) Chloroplast proteins without cleavable transit peptides: rare exceptions or a major constituent of the chloroplast proteome? Molecular Plant **2:** 1325-1335

Arnau J, Lauritzen C, Petersen GE, Pedersen J (2006) Current strategies for the use of affinity tags and tag removal for the purification of recombinant proteins. Protein Expression and Purification **48:** 1-13

Arrivault S, Guenther M, Ivakov A, Feil R, Vosloh D, van Dongen JT, Sulpice R, Stitt M (2009) Use of reverse-phase liquid chromatography, linked to tandem mass spectrometry, to profile the Calvin cycle and other metabolic intermediates in Arabidopsis rosettes at different carbon dioxide concentrations. Plant Journal **59:** 824-839

Baerenfaller K, Grossmann J, Grobei MA, Hull R, Hirsch-Hoffmann M, Yalovsky S, Zimmermann P, Grossniklaus U, Gruissem W, Baginsky S (2008) Genome-scale proteomics reveals *Arabidopsis thaliana* gene models and proteome dynamics. Science **320:** 938-941

Baginsky S, Gruissem W (2009) The chloroplast kinase network: new insights from large-scale phosphoproteome profiling. Molecular Plant **2:** 1141-1153

Ball S, Colleoni C, Cenci U, Raj JN, Tirtiaux C (2011) The evolution of glycogen and starch metabolism in eukaryotes gives molecular clues to understand the establishment of plastid endosymbiosis. Journal of Experimental Botany **62:** 1775-1801

Balmer Y, Koller A, del Val G, Manieri W, Schurmann P, Buchanan BB (2003) Proteomics gives insight into the regulatory function of chloroplast thioredoxins. Proceedings of the National Academy of Sciences of the United States of America **100:** 370-375

Bantscheff M, Schirle M, Sweetman G, Rick J, Kuster B (2007) Quantitative mass spectrometry in proteomics: a critical review. Analytical and Bioanalytical Chemistry **389:** 1017-1031

Barber GA, Hassid WZ (1964) Formation of guanosine diphosphate D-glucose by enzymes of higher plants. Biochimica Et Biophysica Acta **86:** 397-&

Barratt DHP, Derbyshire P, Findlay K, Pike M, Wellner N, Lunn J, Feil R, Simpson C, Maule AJ, Smith AM (2009) Normal growth of Arabidopsis requires cytosolic invertase but not sucrose synthase. Proceedings of the National Academy of Sciences of the United States of America **106:** 13124-13129

Baunsgaard L, Lutken H, Mikkelsen R, Glaring MA, Pham TT, Blennow A (2005) A novel isoform of glucan, water dikinase phosphorylates pre-phosphorylated alpha-glucans and is involved in starch degradation in Arabidopsis. Plant Journal **41:** 595-605

Bell-Pedersen D, Cassone VM, Earnest DJ, Golden SS, Hardin PE, Thomas TL, Zoran MJ (2005) Circadian rhythms from multiple oscillators: Lessons from diverse organisms. Nature Reviews Genetics **6:** 544-556

Bell AW, Deutsch EW, Au CE, Kearney RE, Beavis R, Sechi S, Nilsson T, Bergeron JJM, Grp HTSW (2009) A HUPO test sample study reveals common problems in mass spectrometry-based proteomics. Nature Methods **6:** 423-U440

Belle A, Tanay A, Bitincka L, Shamir R, O'Shea EK (2006) Quantification of protein half-lives in the budding yeast proteome. Proceedings of the National Academy of Sciences of the United States of America **103:** 13004-13009

Biellmann JF, Samama JP, Branden CI, Eklund H (1979) X-Ray studies of the binding of Cibacron Blue F3ga to liver alcohol-dehydrogenase. European Journal of Biochemistry **102:** 107-110

Bigay J, Casella JF, Drin G, Mesmin B, Antonny B (2005) ArfGAP1 responds to membrane curvature through the folding of a lipid packing sensor motif. EMBO Journal **24:** 2244-2253

Binarova P, Cenklova V, Prochazkova J, Doskocilova A, Volc J, Vrlik M, Bogre L (2006) gamma-Tubulin is essential for acentrosomal microtubule nucleation and coordination of late mitotic events in Arabidopsis. Plant Cell **18:** 1199-1212

Biskup B, Scharr H, Fischbach A, Wiese-Klinkenberg A, Schurr U, Walter A (2009) Diel growth cycle of isolated leaf discs analyzed with a novel, high-throughput three-dimensional imaging method is identical to that of intact leaves. Plant Physiology **149:** 1452-1461

Blake MS, Johnston KH, Russell-Jones GJ, Gotschlich EC (1984) A rapid, sensitive method for detection of alkaline-phosphatase conjugated anti-antibody on western blots. Analytical Biochemistry **136:** 175-179

Bläsing OE, Gibon Y, Gunther M, Hohne M, Morcuende R, Osuna D, Thimm O, Usadel B, Scheible WR, Stitt M (2005) Sugars and circadian regulation make major contributions to the global regulation of diurnal gene expression in Arabidopsis. Plant Cell **17:** 3257-3281

Blennow A, Bay-Smidt AM, Olsen CE, Møller BL (1998) Analysis of starch-bound glucose 3-phosphate and glucose 6-phosphate using controlled acid treatment combined with high-performance anion-exchange chromatography. Journal of Chromatography A **829:** 385-391

Blennow A, Bay-Smidt AM, Olsen CE, Møller BL (2000a) The distribution of covalently bound phosphate in the starch granule in relation to starch crystallinity. International Journal of Biological Macromolecules **27:** 211-218

Blennow A, Engelsen SB (2010) Helix-breaking news: fighting crystalline starch energy deposits in the cell. Trends in Plant Science **15:** 236-240

Blennow A, Engelsen SB, Munck L, Moller BL (2000b) Starch molecular structure and phosphorylation investigated by a combined chromatographic and chemometric approach. Carbohydrate Polymers **41:** 163-174

Blennow A, Houborg K, Andersson R, Bidzinska E, Dyrek K, Labanowska M (2006) Phosphate positioning and availability in the starch granule matrix as studied by EPR. Biomacromolecules **7:** 965-974

Blennow A, Sjoland AK, Andersson R, Kristiansson P (2005a) The distribution of elements in the native starch granule as studied by particle-induced X-ray emission and complementary methods. Analytical Biochemistry **347:** 327-329

Blennow A, Wischmann B, Houborg K, Ahmt T, Jorgensen K, Engelsen SB, Bandsholm O, Poulsen P (2005b) Structure function relationships of transgenic starches with engineered phosphate substitution and starch branching. International Journal of Biological Macromolecules **36:** 159-168

Boyes DC, Zayed AM, Ascenzi R, McCaskill AJ, Hoffman NE, Davis KR, Gorlach J (2001) Growth stage-based phenotypic analysis of Arabidopsis: A model for high throughput functional genomics in plants. Plant Cell **13:** 1499-1510

Bozdogan H (1987) Model selection and akaike information criterion (aic) - the general-theory and its analytical extensions. Psychometrika **52:** 345-370

Brown GC (2010) The principle of sufficiency and the evolution of control: using control analysis to understand the design principles of biological systems. Biochemical Society Transactions **38:** 1210-1214

Buléon A, Colonna P, Planchot V, Ball S (1998) Starch granules: structure and biosynthesis. International Journal of Biological Macromolecules **23:** 85-112

Buren S, Ortega-Villasante C, Blanco-Rivero A, Martinez-Bernardini A, Shutova T, Shevela D, Messinger J, Bako L, Villarejo A, Samuelsson G (2011) Importance of post-translational modifications for functionality of a chloroplast-localized carbonic anhydrase (CAH1) in *Arabidopsis thaliana*. Plos One **6**

Buttrose MS (1960) Submicroscopic development and structure of starch granules in cereal endosperms. Journal of Ultrastructure Research **4:** 231-257

Cai W, Ma J, Guo J, Zhang L (2008) Function of ROC4 in the efficient repair of photodamaged photosystem II in Arabidopsis. Photochemistry and Photobiology **84:** 1343-1348

Caspar T, Lin TP, Kakefuda G, Benbow L, Preiss J, Somerville C (1991) Mutants of Arabidopsis with altered regulation of starch degradation. Plant Physiology **95:** 1181-1188

Chang CW (1979) Starch and its component ratio in developing cotton leaves. Plant Physiology **63:** 973-977

Chang I-F, Curran A, Woolsey R, Quilici D, Cushman JC, Mittler R, Harmon A, Harper JF (2009) Proteomic profiling of tandem affinity purified 14-3-3 protein complexes in *Arabidopsis thaliana*. Proteomics **9:** 2967-2985

Chatterton NJ, Silvius JE (1979) Photosynthate partitioning into starch in soybean leaves .1. Effects of photoperiod versus photosynthetic period duration. Plant Physiology **64:** 749-753

Chatterton NJ, Silvius JE (1980) Photosynthate partitioning into leaf starch as affected by daily photosynthetic period duration in six species. Physiologia Plantarum **49:** 141-144

Chia T, Thorneycroft D, Chapple A, Messerli G, Chen J, Zeeman SC, Smith SM, Smith AM (2004) A cytosolic glucosyltransferase is required for conversion of starch to sucrose in Arabidopsis leaves at night. Plant Journal **37:** 853-863

Cho MH, Lim H, Shin DH, Jeon JS, Bhoo SH, Park YI, Hahn TR (2011) Role of the plastidic glucose translocator in the export of starch degradation products from the chloroplasts in *Arabidopsis thaliana*. New Phytologist **190:** 101-112

Cho MJ, Wong LH, Marx C, Jiang W, Lemaux PG, Buchanan BB (1999) Overexpression of thioredoxin h leads to enhanced activity of starch debranching enzyme (pullulanase) in barley grain. Proceedings of the National Academy of Sciences of the United States of America **96:** 14641-14646

Chou IT, Gasser CS (1997) Characterization of the cyclophilin gene family of *Arabidopsis thaliana* and phylogenetic analysis of known cyclophilin proteins. Plant Molecular Biology **35:** 873-892

Clough SJ, Bent AF (1998) Floral dip: a simplified method for *Agrobacterium*-mediated transformation of *Arabidopsis thaliana*. Plant Journal **16:** 735-743

Comparot-Moss S, Kötting O, Stettler M, Edner C, Graf A, Weise SE, Streb S, Lue WL, MacLean D, Mahlow S, Ritte G, Steup M, Chen J, Zeeman SC, Smith AM (2010) A putative phosphatase, LSF1, is required for normal starch turnover in Arabidopsis leaves. Plant Physiology **152:** 685-697

Covington MF, Harmer SL (2007) The circadian clock regulates auxin signaling and responses in Arabidopsis. PLOS Biology **5:** 1773-1784

Covington MF, Maloof JN, Straume M, Kay SA, Harmer SL (2008) Global transcriptome analysis reveals circadian regulation of key pathways in plant growth and development. Genome Biology **9:** Article R130

Craft J, Samalova M, Baroux C, Townley H, Martinez A, Jepson I, Tsiantis M, Moore I (2005a) New pOp/LhG4 vectors for stringent glucocorticoid-dependent transgene expression in Arabidopsis. Plant Journal **41:** 899-918

Craft J, Samalova M, Baroux C, Townley H, Martinez A, Jepson I, Tsiantis M, Moore I (2005b) New pOp/LhG4 vectors for stringent glucocorticoid-dependent transgene expression in *Arabidopsis*. Plant Journal **41:** 899-918

Crevillén P, Ventriglia T, Pinto F, Orea A, Merida A, Romero JM (2005) Differential pattern of expression and sugar regulation of *Arabidopsis thaliana* ADP-glucose pyrophosphorylase-encoding genes. Journal of Biological Chemistry **280:** 8143-8149

Crevillén PN, Ballicora MA, Merida A, Preiss J, Romero JM (2003) The different large subunit isoforms of *Arabidopsis thaliana* ADP-glucose pyrophosphorylase confer distinct kinetic and regulatory properties to the heterotetrameric enzyme. Journal of Biological Chemistry **278:** 28508-28515

Critchley JH, Zeeman SC, Takaha T, Smith AM, Smith SM (2001) A critical role for disproportionating enzyme in starch breakdown is revealed by a knock-out mutation in Arabidopsis. Plant Journal **26:** 89-100

Cross JM, von Korff M, Altmann T, Bartzetko L, Sulpice R, Gibon Y, Palacios N, Stitt M (2006) Variation of enzyme activities and metabolite levels in 24 Arabidopsis accessions growing in carbon-limited conditions. Plant Physiology **142:** 1574-1588

Crumpton-Taylor M, Grandison S, Png KMY, Bushby AJ, Smith AM (2012) Control of starch granule numbers in Arabidopsis chloroplasts. Plant Physiology **158:** 905-916

Czechowski T, Stitt M, Altmann T, Udvardi MK, Scheible WR (2005) Genome-wide identification and testing of superior reference genes for transcript normalization in Arabidopsis. Plant Physiology **139:** 5-17

D'Hulst C, Merida A (2010) The priming of storage glucan synthesis from bacteria to plants: current knowledge and new developments. New Phytologist **188:** 13-21

Dashnau JL, Sharp KA, Vanderkooi JM (2005) Carbohydrate intramolecular hydrogen bonding cooperativity and its effect on water structure. Journal of Physical Chemistry B **109:** 24152-24159

de Marco A (2011) Biotechnological applications of recombinant single-domain antibody fragments. Microbial Cell Factories **10:** article 44

Delatte T, Trevisan M, Parker ML, Zeeman SC (2005) Arabidopsis mutants *Atisa1* and *Atisa2* have identical phenotypes and lack the same multimeric isoamylase, which influences the branch point distribution of amylopectin during starch synthesis. Plant Journal **41:** 815-830

Delatte T, Umhang M, Trevisan M, Eicke S, Thorneycroft D, Smith SM, Zeeman SC (2006) Evidence for distinct mechanisms of starch granule breakdown in plants. Journal of Biological Chemistry **281:** 12050-12059

Delvalle D, Dumez S, Wattebled F, Roldan I, Planchot V, Berbezy P, Colonna P, Vyas D, Chatterjee M, Ball S, Merida A, D'Hulst C (2005) Soluble starch synthase I: a major determinant for the synthesis of amylopectin in *Arabidopsis thaliana* leaves. Plant Journal **43:** 398-412

Denyer K, Barber LM, Burton R, Hedley CL, Hylton CM, Johnson S, Jones DA, Marshall J, Smith AM, Tatge H, Tomlinson K, Wang TL (1995) The isolation and characterization of novel low-amylose mutants of *Pisum sativum* L. Plant Cell and Environment **18:** 1019-1026

Dodd AN, Salathia N, Hall A, Kevei E, Toth R, Nagy F, Hibberd JM, Millar AJ, Webb AAR (2005) Plant circadian clocks increase photosynthesis, growth, survival, and competitive advantage. Science **309:** 630-633

Dominguez-Solis JR, He Z, Lima A, Ting J, Buchanan BB, Luan S (2008) A cyclophilin links redox and light signals to cysteine biosynthesis and stress responses in chloroplasts. Proceedings of the National Academy of Sciences of the United States of America **105:** 16386-16391

Domon B, Aebersold R (2010) Options and considerations when selecting a quantitative proteomics strategy. Nature Biotechnology **28:** 710-721

Dubray G, Bezard G (1982) A highly sensitive periodic acid silver stain for 1,2-diol groups of glycoproteins and polysaccharides in polyacrylamide gels. Analytical Biochemistry **119:** 325-329

Earley KW, Haag JR, Pontes O, Opper K, Juehne T, Song KM, Pikaard CS (2006) Gateway-compatible vectors for plant functional genomics and proteomics. Plant Journal **45:** 616-629

Eden E, Geva-Zatorsky N, Issaeva I, Cohen A, Dekel E, Danon T, Cohen L, Mayo A, Alon U (2012) Proteome half-life dynamics in living human cells. Science **331:** 764-768

Edner C, Li J, Albrecht T, Mahlow S, Hejazi M, Hussain H, Kaplan F, Guy C, Smith SM, Steup M, Ritte G (2007) Glucan, water dikinase activity stimulates breakdown of starch granules by plastidial beta-amylases. Plant Physiology **145:** 17-28

Edwards KD, Anderson PE, Hall A, Salathia NS, Locke JCW, Lynn JR, Straume M, Smith JQ, Millar AJ (2006) FLOWERING LOCUS C mediates natural variation in the high-temperature response of the Arabidopsis circadian clock. Plant Cell **18:** 639-650

Elrouby N, Coupland G (2010) Proteome-wide screens for small ubiquitin-like modifier (SUMO) substrates identify Arabidopsis proteins implicated in diverse biological processes. Proceedings of the National Academy of Sciences of the United States of America **107:** 17415-17420

Engelsen SB, Madsen AO, Blennow A, Motawia MS, Møller BL, Larsen S (2003) The phosphorylation site in double helical amylopectin as investigated by a combined approach using chemical synthesis, crystallography and molecular modeling. FEBS Letters **541:** 137-144

Fernbach A (1904) Quelques observations sur la composition de l'amidon de pommes de terre. Comptes Rendus de l'Académie des Sciences **138:** 428-430

Fettke J, Chia T, Eckermann N, Smith A, Steup M (2006) A transglucosidase necessary for starch degradation and maltose metabolism in leaves at night acts on cytosolic heteroglycans (SHG). Plant Journal **46:** 668-684

Fettke J, Hejazi M, Smirnova J, Hochel E, Stage M, Steup M (2009) Eukaryotic starch degradation: integration of plastidial and cytosolic pathways. J Exp Bot **60:** 2907-2922

Fettke J, Malinova I, Albrecht T, Hejazi M, Steup M (2011) Glucose-1-Phosphate Transport into Protoplasts and Chloroplasts from Leaves of Arabidopsis. Plant Physiology **155:** 1723-1734

Fondy BR, Geiger DR, Servaites JC (1989) Photosynthesis, carbohydrate metabolism and export in *Beta vulgaris* L. and *Phaseolus vulgaris* L. during square and sinusoidal light regimes. Plant Physiology **89:** 396-402

Fox TC, Geiger DR (1984) Effects of decreased net carbon exchange on carbohydrate metabolism in sugar beet source leaves. Plant Physiology **76:** 763

French D (1984) Organisation of starch granules. *In* RL Whistler, JN BeMiller, EF Parshall, eds, Starch, Chemistry and Technology. Academic Press, New York, pp 183-247

Fu YB, Ballicora MA, Leykam JF, Preiss J (1998) Mechanism of reductive activation of potato tuber ADP-glucose pyrophosphorylase. Journal of Biological Chemistry **273:** 25045-25052

Fulton DC, Stettler M, Mettler T, Vaughan CK, Li J, Francisco P, Gil D, Reinhold H, Eicke S, Messerli G, Dorken G, Halliday K, Smith AM, Smith SM, Zeeman SC (2008) Beta-Amylase4, a noncatalytic protein required for starch breakdown, acts upstream of three active beta-amylases in Arabidopsis chloroplasts. Plant Cell **20:** 1040-1058

Gachon CMM, Langlois-Meurinne M, Henry Y, Saindrenan P (2005) Transcriptional co-regulation of secondary metabolism enzymes in Arabidopsis: functional and evolutionary implications. Plant Molecular Biology **58:** 229-245

Gallant DJ, Bouchet B, Baldwin PM (1997) Microscopy of starch: Evidence of a new level of granule organization. Carbohydrate Polymers **32:** 177-191

Gareau JR, Lima CD (2010) The SUMO pathway: emerging mechanisms that shape specificity, conjugation and recognition. Nature Reviews Molecular Cell Biology **11:** 861-871

Gassmann M, Grenacher B, Rohde B, Vogel J (2009) Quantifying Western blots: Pitfalls of densitometry. Electrophoresis **30:** 1845-1855

Geigenberger P (2011) Regulation of starch biosynthesis in response to a fluctuating environment. Plant Physiology **155:** 1566-1577

Geigenberger P, Stitt M, Fernie AR (2004) Metabolic control analysis and regulation of the conversion of sucrose to starch in growing potato tubers. Plant Cell and Environment **27:** 655-673

Geiger DR, Batey JW (1967) Translocation of ^{14}C sucrose in sugar beet during darkness. Plant Physiology **42:** 1743-&

Geiger DR, Servaites JC (1994) Diurnal regulation of photosynthetic carbon metabolism in C-3 plants. Annual Review of Plant Physiology and Plant Molecular Biology **45:** 235-256

Gibon Y, Blaesing OE, Hannemann J, Carillo P, Hohne M, Hendriks JHM, Palacios N, Cross J, Selbig J, Stitt M (2004a) A robot-based platform to measure multiple enzyme activities in Arabidopsis using a set of cycling assays: Comparison of changes of enzyme activities and transcript levels during diurnal cycles and in prolonged darkness. Plant Cell **16:** 3304-3325

Gibon Y, Bläsing OE, Palacios-Rojas N, Pankovic D, Hendriks JHM, Fisahn J, Hohne M, Gunther M, Stitt M (2004b) Adjustment of diurnal starch turnover to short days: depletion of sugar during the night leads to a temporary inhibition of carbohydrate utilization, accumulation of sugars and post-translational activation of ADP-glucose pyrophosphorylase in the following light period. Plant Journal **39:** 847-462

Gibon Y, Pyl ET, Sulpice R, Lunn JE, Hohne M, Gunther M, Stitt M (2009) Adjustment of growth, starch turnover, protein content and central metabolism to a decrease of the carbon supply when Arabidopsis is grown in very short photoperiods. Plant Cell and Environment **32:** 859-874

Gibon Y, Usadel B, Blaesing OE, Kamlage B, Hoehne M, Trethewey R, Stitt M (2006) Integration of metabolite with transcript and enzyme activity profiling during diurnal cycles in Arabidopsis rosettes. Genome Biology **7:** R76

Glaring MA, Baumann MJ, Abou Hachem M, Nakai H, Nakai N, Santelia D, Sigurskjold BW, Zeeman SC, Blennow A, Svensson B (2011) Starch-binding domains in the CBM45 family - low-affinity domains from glucan, water dikinase and alpha-amylase involved in plastidial starch metabolism. FEBS Journal **278:** 1175-1185

Glaring MA, Skryhan K, Kotting O, Zeeman SC, Blennow A (2012) Comprehensive survey of redox sensitive starch metabolising enzymes in *Arabidopsis thaliana*. Plant Physiology and Biochemistry **58:** 89-97

Glaring MA, Zygadlo A, Thorneycroft D, Schulz A, Smith SM, Blennow A, Baunsgaard L (2007) An extra-plastidial alpha-glucan, water dikinase from Arabidopsis phosphorylates amylopectin in vitro and is not necessary for transient starch degradation. Journal of Experimental Botany **58:** 3949-3960

Goldberg RN, Bell D, Tewari YB, McLaughlin MA (1991) Thermodynamics of hydrolysis of oligosaccharides. Biophysical Chemistry **40:** 69-76

Graf A, Schlereth A, Stitt M, Smith AM (2010) Circadian control of carbohydrate availability for growth in Arabidopsis plants at night. Proceedings of the National Academy of Sciences of the United States of America **107:** 9458-9463

Grange RI (1984) The extent of starch turnover in mature pepper leaves in the light. Annals of Botany **54:** 289-291

Haebel S, Hejazi M, Frohberg C, Heydenreich M, Ritte G (2008) Mass spectrometric quantification of the relative amounts of C6 and C3 position phosphorylated glucosyl residues in starch. Analytical Biochemistry **379:** 73-79

Haedrich N, Gibon Y, Schudoma C, Altmann T, Lunn JE, Stitt M (2011) Use of TILLING and robotised enzyme assays to generate an allelic series of Arabidopsis thaliana mutants with altered ADP-glucose pyrophosphorylase activity. Journal of Plant Physiology **168:** 1395-1405

Haedrich N, Hendriks JHM, Koetting O, Arrivault S, Feil R, Zeeman SC, Gibon Y, Schulze WX, Stitt M, Lunn JE (2012) Mutagenesis of cysteine 81 prevents dimerization of the APS1 subunit of ADP-glucose pyrophosphorylase and alters

diurnal starch turnover in *Arabidopsis thaliana* leaves. Plant Journal **70:** 231-242

Hanahan D (1983) Studies on transformation of *Escherichia-coli* with plasmids. Journal of Molecular Biology **166:** 557-580

Hanashiro I, Abe J, Hizukuri S (1996) A periodic distribution of the chain length of amylopectin as revealed by high-performance anion-exchange chromatography. Carbohydrate Research **283:** 151-159

Hansen PI, Larsen FH, Motawia SM, Blennow A, Spraul M, Dvortsak P, Engelsen SB (2008) Structure and hydration of the amylopectin trisaccharide building blocks-synthesis, NMR, and molecular dynamics. Biopolymers **89:** 1179-1193

Hargreaves JA, ap Rees T (1988) Turnover of starch and sucrose in roots of *Pisum sativum* Phytochemistry **27:** 1627-1629

Harmer SL, Hogenesch LB, Straume M, Chang HS, Han B, Zhu T, Wang X, Kreps JA, Kay SA (2000) Orchestrated transcription of key pathways in Arabidopsis by the circadian clock. Science **290:** 2110-2113

Haswell ES, Meyerowitz EM (2006) MscS-like proteins control plastid size and shape in *Arabidopsis thaliana*. Current Biology **16:** 1-11

Hausler RE, Schlieben NH, Schulz B, Flugge UI (1998) Compensation of decreased triose phosphate phosphate translocator activity by accelerated starch turnover and glucose transport in transgenic tobacco. Planta **204:** 366-376

Hazen SP, Schultz TF, Pruneda-Paz JL, Borevitz JO, Ecker JR, Kay SA (2005) LUX ARRHYTHMO encodes a Myb domain protein essential for circadian rhythms. Proceedings of the National Academy of Sciences of the United States of America **102:** 10387-10392

Heazlewood JL, Durek P, Hummel J, Selbig J, Weckwerth W, Walther D, Schulze WX (2008) PhosPhAt: a database of phosphorylation sites in *Arabidopsis thaliana* and a plant-specific phosphorylation site predictor. Nucleic Acids Research **36:** D1015-D1021

Hejazi M, Fettke J, Haebel S, Edner C, Paris O, Frohberg C, Steup M, Ritte G (2008) Glucan, water dikinase phosphorylates crystalline maltodextrins and thereby initiates solubilization. Plant Journal **55:** 323-334

Hejazi M, Fettke J, Kotting O, Zeeman SC, Steup M (2010) The laforin-like dual-specificity phosphatase SEX4 from Arabidopsis hydrolyzes both C6-and C3-phosphate esters introduced by starch-related dikinases and thereby affects phase transition of alpha-glucans. Plant Physiology **152:** 711-722

Hejazi M, Fettke J, Paris O, Steup M (2009) The two plastidial starch-related dikinases sequentially phosphorylate glucosyl residues at the surface of both the A- and B-type allomorphs of crystallized maltodextrins but the mode of action differs. Plant Physiology **150:** 962-976

Hejazi M, Steup M, Fettke J (2012) The plastidial glucan, water dikinase (GWD) catalyses multiple phosphotransfer reactions. FEBS Journal **279:** 1953-1966

Helenius A, Aebi M (2004) Roles of N-linked glycans in the endoplasmic reticulum. Annual Review of Biochemistry **73:** 1019-1049

Hellemans J, Mortier G, De Paepe A, Speleman F, Vandesompele J (2007) qBase relative quantification framework and software for management and automated analysis of real-time quantitative PCR data. Genome Biology **8**

Hellens RP, Edwards EA, Leyland NR, Bean S, Mullineaux PM (2000) pGreen: a versatile and flexible binary Ti vector for Agrobacterium-mediated plant transformation. Plant Molecular Biology **42:** 819-832

Hendriks JHM, Kolbe A, Gibon Y, Stitt M, Geigenberger P (2003) ADP-glucose pyrophosphorylase is activated by posttranslational redox-modification in response to light and to sugars in leaves of Arabidopsis and other plant species. Plant Physiology **133:** 838-849

Hizukuri S (1985) Relationship between the distribution of the chain-length of amylopectin and the crystalline structure of starch granules. Carbohydrate Research **141:** 295-306

Hoege C, Pfander B, Moldovan GL, Pyrowolakis G, Jentsch S (2002) RAD6-dependent DNA repair is linked to modification of PCNA by ubiquitin and SUMO. Nature **419:** 135-141

Hostettler C, Koelling K, Santelia D, Streb S, Koetting O, Zeeman SC (2011) Analysis of starch metabolism in chloroplasts. *In* RP Jarvis, ed, Chloroplast Research in Arabidopsis: Methods and Protocols, Vol 775, pp 387-410

Howitt CA, Rahman S, Morell MK (2006) Expression of bacterial starch-binding domains in Arabidopsis increases starch granule size. Functional Plant Biology **33:** 257-266

Hussain H, Mant A, Seale R, Zeeman S, Hinchliffe E, Edwards A, Hylton C, Bornemann S, Smith AM, Martin C, Bustos R (2003) Three isoforms of isoamylase contribute different catalytic properties for the debranching of potato glucans. Plant Cell **15:** 133-149

Imaizumi T, Kay SA (2006) Photoperiodic control of flowering: not only by coincidence. Trends in Plant Science **11:** 550-558

Imberty A, Chanzy H, Perez S, Buléon A, Tran V (1988) The double-helical nature of the crystalline part of A-starch. Journal of Molecular Biology **201:** 365-378

Imberty A, Perez S (1988) A revisit to the 3-dimensional structure of B-type starch. Biopolymers **27:** 1205-1221

Ishihama Y, Oda Y, Tabata T, Sato T, Nagasu T, Rappsilber J, Mann M (2005) Exponentially modified protein abundance index (emPAI) for estimation of absolute protein amount in proteomics by the number of sequenced peptides per protein. Molecular & Cellular Proteomics **4:** 1265-1272

Jane J, Xu A, Radosavljevic M, Seib PA (1992) Location of amylose in normal starch granules 1. Susceptibility of amylose and amylopectin to cross-linking reagents. Cereal Chemistry **69:** 405-409

Jane JL, Wong KS, McPherson AE (1997) Branch-structure difference in starches of A- and B-type x-ray patterns revealed by their Naegeli dextrins. Carbohydrate Research **300:** 219-227

Jenkins JP, Cameron RE, Donald AM (1993) A universal feature in the structure of starch granules from different botanical sources. Starch-Starke **45:** 417-420

Jeon J-S, Ryoo N, Hahn T-R, Walia H, Nakamura Y (2010) Starch biosynthesis in cereal endosperm. Plant Physiology and Biochemistry **48:** 383-392

Ji Q, Oomen RJF, Vincken JP, Bolam DN, Gilbert HJ, Suurs L, Visser RGF (2004) Reduction of starch granule size by expression of an engineered tandem starch-binding domain in potato plants. Plant Biotechnology Journal **2:** 251-260

Jiang CP, Wechuck JB, Goins WF, Krisky DM, Wolfe D, Ataai MM, Glorioso JC (2004) Immobilized cobalt affinity chromatography provides a novel, efficient method for herpes simplex virus type 1 gene vector purification. Journal of Virology **78:** 8994-9006

Jin JB, Jin YH, Lee J, Miura K, Yoo CY, Kim W-Y, Van Oosten M, Hyun Y, Somers DE, Lee I, Yun D-J, Bressan RA, Hasegawa PM (2008) The SUMO E3 ligase, AtS1Z1, regulates flowering by controlling a salicylic acid-mediated

floral promotion pathway and through effects on FLC chromatin structure. Plant Journal **53:** 530-540

Jobling SA, Jarman C, Teh MM, Holmberg N, Blake C, Verhoeyen ME (2003) Immunomodulation of enzyme function in plants by single-domain antibody fragments. Nature Biotechnology **21:** 77-80

Jossier M, Bouly J-P, Meimoun P, Arjmand A, Lessard P, Hawley S, Hardie GD, Thomas M (2009) SnRK1 (SNF1-related kinase 1) has a central role in sugar and ABA signalling in *Arabidopsis thaliana*. Plant Journal **59:** 316-328

Kacser H, Burns JA (1973) The control of flux. Symposia of the Society for Experimental Biology **27:** 65-104

Kacser H, Burns JA (1981) The molecular basis of dominance. Genetics **97:** 639-666

Kapoor S, Sugiura M (1999) Identificiation of two essential sequence elements in the nonconsensus type II PatpB-290 plastid promoter by using plastid transcription extracts from cultured tobacco BY-2 cells. Plant Cell **11:** 1799-1810

Karimi M, De Meyer B, Hilson P (2005) Modular cloning in plant cells. Trends in Plant Science **10:** 103-105

Kartal O, Mahlow S, Skupin A, Ebenhoh O (2011) Carbohydrate-active enzymes exemplify entropic principles in metabolism. Molecular Systems Biology **7:** Article number: 542

Kitajima A, Asatsuma S, Okada H, Hamada Y, Kaneko K, Nanjo Y, Kawagoe Y, Toyooka K, Matsuoka K, Takeuchi M, Nakano A, Mitsui T (2009) The rice alpha-amylase glycoprotein is targeted from the Golgi apparatus through the secretory pathway to the plastids. Plant Cell **21:** 2844-2858

Kleffmann T, Russenberger D, von Zychlinski A, Christopher W, Sjolander K, Gruissem W, Baginsky S (2004) The *Arabidopsis thaliana* chloroplast proteome reveals pathway abundance and novel protein functions. Current Biology **14:** 354-362

Koenig J, Muthuramalingam M, Dietz K-J (2012) Mechanisms and dynamics in the thiol/disulfide redox regulatory network: transmitters, sensors and targets. Current Opinion in Plant Biology **15:** 261-268

Kolbe A, Tiessen A, Schluepmann H, Paul M, Ulrich S, Geigenberger P (2005) Trehalose 6-phosphate regulates starch synthesis via posttranslational redox activation of ADP-glucose pyrophosphorylase. Proceedings of the National Academy of Sciences of the United States of America **102:** 11118-11123

Kötting O, Kossmann J, Zeeman SC, Lloyd JR (2010) Regulation of starch metabolism: the age of enlightenment? Current Opinion in Plant Biology **13:** 321-329

Kötting O, Pusch K, Tiessen A, Geigenberger P, Steup M, Ritte G (2005) Identification of a novel enzyme required for starch metabolism in Arabidopsis leaves. The phosphoglucan, water dikinase. Plant Physiology **137:** 242-252

Kötting O, Santelia D, Edner C, Eicke S, Marthaler T, Gentry MS, Comparot-Moss S, Chen J, Smith AM, Steup M, Ritte G, Zeeman SC (2009) STARCH-EXCESS4 is a Laforin-like phosphoglucan phosphatase required for starch degradation in *Arabidopsis thaliana.* Plant Cell **21:** 334-346

Kruger NJ, Bulpin PV, ap Rees T (1983) The extent of starch degradation in the light in pea leaves. Planta **157:** 271-273

Kuwabara A, Backhaus A, Malinowski R, Bauch M, Hunt L, Nagata T, Monk N, Sanguinetti G, Fleming A (2011) A shift toward smaller cell size via manipulation of cell cycle gene expression acts to smoothen Arabidopsis leaf shape. Plant Physiology **156:** 2196-2206

Lang K, Schmid FX, Fischer G (1987) Catalysis of protein folding by prolyl isomerase. Nature **329:** 268-270

Lao NT, Schoneveld O, Mould RM, Hibberd JM, Gray JC, Kavanagh TA (1999) An Arabidopsis gene encoding a chloroplast-targeted beta-amylase. Plant Journal **20:** 519-527

Lauwereys M, Ghahroudi MA, Desmyter A, Kinne J, Holzer W, De Genst E, Wyns L, Muyldermans S (1998) Potent enzyme inhibitors derived from dromedary heavy-chain antibodies. Embo Journal **17:** 3512-3520

Laxa M, Koenig J, Dietz K-J, Kandlbinder A (2007) Role of the cysteine residues in *Arabidopsis thaliana* cyclophilin CYP20-3 in peptidyl-prolyl cis-trans isomerase and redox-related functions. Biochemical Journal **401:** 287-297

Lemaire SD, Michelet L, Zaffagnini M, Massot V, Issakidis-Bourguet E (2007) Thioredoxins in chloroplasts. Current Genetics **51:** 343-365

Leustek T, Martin MN, Bick JA, Davies JP (2000) Pathways and regulation of sulfur metabolism revealed through molecular and genetic studies. Annual Review of Plant Physiology and Plant Molecular Biology **51:** 141-165

Ley S, Dolger K, Appenroth KJ (1997) Carbohydrate metabolism as a possible physiological modulator of dormancy in turions of *Spirodela polyrhiza* (L.) Schleiden. Plant Science **129:** 1-7

Li HM, Chiu CC (2010) Protein Transport into Chloroplasts. *In* S Merchant, WR Briggs, D Ort, eds, Annual Review of Plant Biology, Vol 61, Vol 61, pp 157-180

Li J, Francisco P, Zhou W, Edner C, Steup M, Ritte G, Bond CS, Smith SM (2009) Catalytically-inactive beta-amylase BAM4 required for starch breakdown in Arabidopsis leaves is a starch-binding-protein. Archives of Biochemistry and Biophysics **489:** 92-98

Lichty JJ, Malecki JL, Agnew HD, Michelson-Horowitz DJ, Tan S (2005) Comparison of affinity tags for protein purification. Protein Expression and Purification **41:** 98-105

Lillo C (2008) Signalling cascades integrating light-enhanced nitrate metabolism. Biochemical Journal **415:** 11-19

Lin TP, Caspar T, Somerville C, Preiss J (1988) Isolation and characterization of a starchless mutant of *Arabidopsis thaliana* (L) Heynh lacking ADPglucose pyrophosphorylase activity. Plant Physiology **86:** 1131-1135

Lindahl M, Kieselbach T (2009) Disulphide proteomes and interactions with thioredoxin on the track towards understanding redox regulation in chloroplasts and cyanobacteria. Journal of Proteomics **72:** 416-438

Linster CL, Clarke SG (2008) L-Ascorbate biosynthesis in higher plants: the role of VTC2. Trends in Plant Science **13:** 567-573

Linster CL, Gomez TA, Christensen KC, Adler LN, Young BD, Brenner C, Clarke SG (2007) Arabidopsis VTC2 encodes a GDP-L-galactose phosphorylase, the last unknown enzyme in the Smirnoff-Wheeler pathway to ascorbic acid in plants. Journal of Biological Chemistry **282:** 18879-18885

Lippuner V, Chous IT, Scott SV, Ettinger WF, Theg SM, Gasser CS (1994) Cloning and characterization of chloroplast and cytosolic forms of cyclophilin from *Arabidopsis thaliana.* Journal of Biological Chemistry **269:** 7863-7868

Lizotte PA, Henson CA, Duke SH (1990) Purification and characterization of pea epicotyl beta-amylase. Plant Physiology **92:** 615-621

Lohmeier-Vogel EM, Kerk D, Nimick M, Wrobel S, Vickerman L, Muench DG, Moorhead GBG (2008) Arabidopsis At5g39790 encodes a chloroplast-

localized, carbohydrate-binding, coiled-coil domain-containing putative scaffold protein. BMC Plant Biology **8:** 120

Lohrig K, Muller B, Davydova J, Leister D, Wolters DA (2009) Phosphorylation site mapping of soluble proteins: bioinformatical filtering reveals potential plastidic phosphoproteins in *Arabidopsis thaliana*. Planta **229:** 1123-1134

Lomako J, Lomako WM, Whelan WJ (1988) A self-glucosylating protein is the primer for rabbit muscle glycogen biosynthesis. Faseb Journal **2:** 3097-3103

LopezCastaneda C, Richards RA, Farquhar GD, Williamson RE (1996) Seed and seedling characteristics contributing to variation in early vigor among temperate cereals. Crop Science **36:** 1257-1266

Lorberth R, Ritte G, Willmitzer L, Kossmann J (1998) Inhibition of a starch-granule-bound protein leads to modified starch and repression of cold sweetening. Nature Biotechnology **16:** 473-477

Lu Y, Gehan JP, Sharkey TD (2005) Daylength and circadian effects on starch degradation and maltose metabolism. Plant Physiology **138:** 2280-2291

Lu Y, Sharkey TD (2004) The role of amylomaltase in maltose metabolism in the cytosol of photosynthetic cells. Planta **218:** 466-473

Lu Y, Sharkey TD (2006) The importance of maltose in transitory starch breakdown. Plant Cell and Environment **29:** 353-366

Lu Y, Steichen JM, Yao J, Sharkey TD (2006) The role of cytosolic alpha-glucan phosphorylase in maltose metabolism and the comparison of amylomaltase in Arabidopsis and *Escherichia coli*. Plant Physiology **142:** 878-889

Lunn JE, Feil R, Hendriks JHM, Gibon Y, Morcuende R, Osuna D, Scheible WR, Carillo P, Hajirezaei MR, Stitt M (2006) Sugar-induced increases in trehalose 6-phosphate are correlated with redox activation of ADPglucose pyrophosphorylase and higher rates of starch synthesis in *Arabidopsis thaliana*. Biochemical Journal **397:** 139-148

Machovic M, Janecek S (2006) Starch-binding domains in the post-genome era. Cellular and Molecular Life Sciences **63:** 2710-2724

Maitrejean M, Wudick MM, Voelker C, Prinsi B, Mueller-Roeber B, Czempinski K, Pedrazzini E, Vitale A (2011) Assembly and Sorting of the Tonoplast Potassium Channel AtTPK1 and Its Turnover by Internalization into the Vacuole. Plant Physiology **156:** 1783-1796

Marino K, Bones J, Kattla JJ, Rudd PM (2010) A systematic approach to protein glycosylation analysis: a path through the maze. Nature Chemical Biology **6:** 713-723

Matheson NK (1996) The chemical structure of amylose and amylopectin fractions of starch from tobacco leaves during development and diurnally nocturnally. Carbohydrate Research **282:** 247-262

McGinness KE, Baker TA, Sauer RT (2006) Engineering controllable protein degradation. Molecular Cell **22:** 701-707

Michael TP, Mockler TC, Breton G, McEntee C, Byer A, Trout JD, Hazen SP, Shen R, Priest HD, Sullivan CM, Givan SA, Yanovsky M, Hong F, Kay SA, Chory J (2008) Network discovery pipeline elucidates conserved time-of-day-specific cis-regulatory modules. PLOS Genetics **4:** e14

Michalska J, Zauber H, Buchanan BB, Cejudo FJ, Geigenberger P (2009) NTRC links built-in thioredoxin to light and sucrose in regulating starch synthesis in chloroplasts and amyloplasts. Proceedings of the National Academy of Sciences of the United States of America **106:** 9908-9913

Mikkelsen R, Blennow A (2005) Functional domain organization of the potato alpha-glucan, water dikinase (GWD): evidence for separate site catalysis as revealed by limited proteolysis and deletion mutants. Biochemical Journal **385:** 355-361

Mikkelsen R, Mutenda KE, Mant A, Schurmann P, Blennow A (2005) Alpha-Glucan, water dikinase (GWD): A plastidic enzyme with redox-regulated and coordinated catalytic activity and binding affinity. Proceedings of the National Academy of Sciences of the United States of America **102:** 1785-1790

Mikkelsen R, Suszkiewicz K, Blennow A (2006) A novel type carbohydrate-binding module identified in alpha-glucan, water dikinases is specific for regulated plastidial starch metabolism. Biochemistry **45:** 4674-4682

Miura K, Hasegawa PM (2010) SUMOylation and other ubiquitin-like post-translational modifications in plants. Trends in Cell Biology **20:** 223-232

Mizoguchi T, Wheatley K, Hanzawa Y, Wright L, Mizoguchi M, Song HR, Carre IA, Coupland G (2002) *LHY* and *CCA1* are partially redundant genes required to maintain circadian rhythms in Arabidopsis. Developmental Cell **2:** 629-641

Mohammadi A, Perry RJ, Storey MK, Cook HW, Byers DM, Ridgway ND (2001) Golgi localization and phosphorylation of oxysterol binding protein in Niemann-Pick C and U18666A-treated cells. Journal of Lipid Research **42:** 1062-1071

Monnier A, Liverani S, Bouvet R, Jesson B, Smith JQ, Mosser J, Corellou F, Bouget F-Y (2010) Orchestrated transcription of biological processes in the marine picoeukaryote *Ostreococcus* exposed to light/dark cycles. BMC Genomics **11:** 192

Moore I, Samalova M, Kurup S (2006) Transactivated and chemically inducible gene expression in plants. Plant Journal **45:** 651-683

Morita MT (2010) Directional gravity sensing in gravitropism. *In* S Merchant, WR Briggs, D Ort, eds, Annual Review of Plant Biology, Vol 61, pp 705-720

Motohashi K, Kondoh A, Stumpp MT, Hisabori T (2001) Comprehensive survey of proteins targeted by chloroplast thioredoxin. Proceedings of the National Academy of Sciences of the United States of America **98:** 11224-11229

Motohashi K, Koyama F, Nakanishi Y, Ueoka-Nakanishi H, Hisabori T (2003) Chloroplast cyclophilin is a target protein of thioredoxin - Thiol modulation of the peptidyl-prolyl cis-trans isomerase activity. Journal of Biological Chemistry **278:** 31848-31852

Muhrbeck P, Svensson E, Eliasson AC (1991) Effect of the degree of phosphorylation on the crystallinity of native potato starch. Starch-Starke **43:** 466-468

Muhrbeck P, Tellier C (1991) Determination of the phosphorylation of starch from native potato varieties by ^{31}P NMR. Starch-Starke **43:** 25-27

Munoz FJ, Baroja-Fernandez E, Moran-Zorzano MT, Viale AM, Etxeberria E, Alonso-Casajus N, Pozueta-Romero J (2005) Sucrose synthase controls both intracellular ADP glucose levels and transitory starch biosynthesis in source leaves. Plant and Cell Physiology **46:** 1366-1376

Murtas G, Reeves PH, Fu YF, Bancroft I, Dean C, Coupland G (2003) A nuclear protease required for flowering-time regulation in Arabidopsis reduces the abundance of SMALL UBIQUITIN-RELATED MODIFIER conjugates. Plant Cell **15:** 2308-2319

Muthuramalingam M, Seidel T, Laxa M, de Miranda SMN, Gaertner F, Stroeher E, Kandlbinder A, Dietz K-J (2009) Multiple redox and non-redox interactions define 2-Cys peroxiredoxin as a regulatory hub in the chloroplast. Molecular Plant **2:** 1273-1288

Myers AM, Morell MK, James MG, Ball SG (2000) Recent progress toward understanding biosynthesis of the amylopectin crystal. Plant Physiology **122:** 989-997

Nakagawa T, Ishiguro S, Kimura T (2009) Gateway vectors for plant transformation. Plant Biotechnology **26:** 275-284

Nakamura Y, Takahashi J, Sakurai A, Inaba Y, Suzuki E, Nihei S, Fujiwara S, Tsuzuki M, Miyashita H, Ikemoto H, Kawachi M, Sekiguchi H, Kurano N (2005) Some cyanobacteria synthesize semi-amylopectin type alpha-polyglucans instead of glycogen. Plant and Cell Physiology **46:** 539-545

Nanjo Y, Oka H, Ikarashi N, Kaneko K, Kitajima A, Mitsui T, Munoz FJ, Rodriguez-Lopez M, Baroja-Fernandez E, Pozueta-Romero J (2006) Rice plastidial N-glycosylated nucleotide pyrophosphatase/phosphodiesterase is transported from the ER-Golgi to the chloroplast through the secretory pathway. Plant Cell **18:** 2582-2592

Neuhaus HE, Stitt M (1990) Control analysis of photosynthate partitioning - Impact of reduced activity of ADP-glucose pyrophosphorylase or plastid phosphoglucomutase on the fluxes to starch and sucrose in *Arabidopsis thaliana* (L) heynh. Planta **182:** 445-454

Nielsen TH, Wischmann B, Enevoldsen K, Møller BL (1994) Starch phosphorylation in potato tubers proceeds concurrently with de-novo biosynthesis of starch. Plant Physiology **105:** 111-117

Niittylä T, Comparot-Moss S, Lue WL, Messerli G, Trevisan M, Seymour MDJ, Gatehouse JA, Villadsen D, Smith SM, Chen JC, Zeeman SC, Alison MS (2006) Similar protein phosphatases control starch metabolism in plants and glycogen metabolism in mammals. Journal of Biological Chemistry **281:** 11815-11818

Niittylä T, Messerli G, Trevisan M, Chen J, Smith AM, Zeeman SC (2004) A previously unknown maltose transporter essential for starch degradation in leaves. Science **303:** 87-89

Novak B, Tyson JJ (2008) Design principles of biochemical oscillators. Nature Reviews Molecular Cell Biology **9:** 981-991

Oostergetel GT, Vanbruggen EFJ (1993) The crystalline domains in potato starch granules are arranged in a helical fashion. Carbohydrate Polymers **21:** 7-12

Pantin F, Simonneau T, Rolland G, Dauzat M, Muller B (2011) Control of leaf expansion: a developmental switch from metabolics to hydraulics. Plant Physiology **156:** 803-815

Patron NJ, Keeling PJ (2005) Common evolutionary origin of starch biosynthetic enzymes in green and red algae. Journal of Phycology **41:** 1131-1141

Paul M (2007) Trehalose 6-phosphate. Current Opinion in Plant Biology **10:** 303-309

Peltier JB, Cai Y, Sun Q, Zabrouskov V, Giacomelli L, Rudella A, Ytterberg AJ, Rutschow H, van Wijk KJ (2006) The oligomeric stromal proteome of *Arabidopsis thaliana* chloroplasts. Molecular and Cellular Proteomics **5:** 114-133

Pfander B, Moldovan GL, Sacher M, Hoege C, Jentsch S (2005) SUMO-modified PCNA recruits SRS2 to prevent recombination during S phase. Nature **436:** 428-433

Pilling E, Smith AM (2003) Growth ring formation in the starch granules of potato tubers. Plant Physiology **132:** 365-371

Piques M, Schulze WX, Hoehne M, Usadel B, Gibon Y, Rohwer J, Stitt M (2009) Ribosome and transcript copy numbers, polysome occupancy and enzyme dynamics in Arabidopsis. Molecular Systems Biology **5:** Article 314

Piro G, Zuppa A, Dalessandro G, Northcote DH (1993) Glucomannan synthesis in pea epicotyls - the mannose and glucose transferases. Planta **190:** 206-220

Pongratz P, Beck E (1978) Diurnal oscillation of amylolytic activity in spinach chloroplasts. Plant Physiology **62:** 687-689

Pyl E, Piques M, Ivakov A, Schulze W, Ishihara H, Stitt M, Sulpice R (2012) Metabolism and growth in *Arabidopsis* depend on the daytime temperature but are temperature-compensated against cool nights. Plant Cell **24:** 2443-2469

Rakotomala R (2005) TANAGRA: a free sortware for research and academic purposes. Proceedings of extraction et gestion de connaissances **2:** 697

Ral J-P, Bowerman AF, Li Z, Sirault X, Furbank R, Pritchard JR, Bloemsma M, Cavanagh CR, Howitt CA, Morell MK (2012) Down-regulation of glucan, water-dikinase activity in wheat endosperm increases vegetative biomass and yield. Plant Biotechnology Journal **10:** 871-882

Ral JP, Derelle E, Ferraz C, Wattebled F, Farinas B, Corellou F, Buléon A, Slomianny MC, Delvalle D, d'Hulst C, Rombauts S, Moreau H, Ball S (2004) Starch division and partitioning. A mechanism for granule propagation and maintenance in the picophytoplanktonic green alga *Ostreococcus tauri*. Plant Physiology **136:** 3333-3340

Ramamurthi KS, Lecuyer S, Stone HA, Losick R (2009) Geometric cue for protein localization in a bacterium. Science **323:** 1354-1357

Reiland S, Messerli G, Baerenfaller K, Gerrits B, Endler A, Grossmann J, Gruissem W, Baginsky S (2009) Large-scale Arabidopsis phosphoproteome profiling reveals novel chloroplast kinase substrates and phosphorylation networks. Plant Physiology **150:** 889-903

Reimann R, Hippler M, Machelett B, Appenroth KJ (2004) Light induces phosphorylation of glucan water dikinase, which precedes starch degradation in turions of the it duckweed Spirodela polyrhiza. Plant Physiology **135:** 121-128

Reinhold H, Soyk S, Simkova K, Hostettler C, Marafino J, Mainiero S, Vaughan CK, Monroe JD, Zeeman SC (2011) beta-Amylase-like proteins function as transcription factors in Arabidopsis, controlling shoot growth and development. Plant Cell **23:** 1391-1403

Reinhold T, Alawady A, Grimm B, Beran KC, Jahns P, Conrath U, Bauer J, Reiser J, Melzer M, Jeblick W, Neuhaus HE (2007) Limitation of nocturnal import of ATP into Arabidopsis chloroplasts leads to photooxidative damage. Plant Journal **50:** 293-304

Repellin A, Baga M, Chibbar RN (2008) In vitro pullulanase activity of wheat (*Triticum aestivum* L.) limit-dextrinase type starch debranching enzyme is modulated by redox conditions. Journal of Cereal Science **47:** 302-309

Ridout MJ, Gunning AP, Parker ML, Wilson RH, Morris VJ (2002) Using AFM to image the internal structure of starch granules. Carbohydrate Polymers **50:** 123-132

Rieu I, Powers SJ (2009) Real-time quantitative RT-PCR: design, calculations, and statistics. Plant Cell **21:** 1031-1033

Ritte G, Heydenreich M, Mahlow S, Haebel S, Kötting O, Steup M (2006) Phosphorylation of C6- and C3-positions of glucosyl residues in starch is catalysed by distinct dikinases. FEBS Letters **580:** 4872-4876

Ritte G, Lloyd JR, Eckermann N, Rottmann A, Kossmann J, Steup M (2002) The starch-related R1 protein is an alpha-glucan, water dikinase. Proceedings of the National Academy of Sciences of the United States of America **99:** 7166-7171

Ritte G, Lorberth R, Steup M (2000) Reversible binding of the starch-related R1 protein to the surface of transitory starch granules. Plant Journal **21:** 387-391

Ritte G, Scharf A, Eckermann N, Haebel S, Steup M (2004) Phosphorylation of transitory starch is increased during degradation. Plant Physiology **135:** 2068-2077

Roach PJ, Depaoli-Roach AA, Hurley TD, Tagliabracci VS (2012) Glycogen and its metabolism: some new developments and old themes. Biochemical Journal **441:** 763-787

Robin JP, Mercier C, Charbonn R, Guilbot A (1974) Lintnerized starches gel-filtration and enzymatic studies of insoluble residues from prolonged acid treatment of potato starch. Cereal Chemistry **51:** 389-406

Rodriguez S, Wolfgang MJ (2012) Targeted chemical-genetic regulation of protein stability *in vivo.* Chemistry & Biology **19:** 391-398

Roldan I, Wattebled F, Lucas MM, Delvalle D, Planchot V, Jimenez S, Perez R, Ball S, D'Hulst C, Merida A (2007) The phenotype of soluble starch synthase IV defective mutants of *Arabidopsis thaliana* suggests a novel function of elongation enzymes in the control of starch granule formation. Plant Journal **49:** 492-504

Romano PGN, Horton P, Gray JE (2004) The Arabidopsis cyclophilin gene family. Plant Physiology **134:** 1268-1282

Rouhier N, Lemaire SD, Jacquot J-P (2008) The role of glutathione in photosynthetic organisms: Emerging functions for glutaredoxins and glutathionylation. Annual Review of Plant Biology **59:** 143-166

Ruelland E, Miginiac-Maslow M (1999) Regulation of chloroplast enzyme activities by thioredoxins: activation or relief from inhibition? Trends in Plant Science **4:** 136-141

Sai JQ, Johnson CH (2002) Dark-stimulated calcium ion fluxes in the chloroplast stroma and cytosol. Plant Cell **14:** 1279-1291

Sainsbury F, Thuenemann EC, Lomonossoff GP (2009) pEAQ: versatile expression vectors for easy and quick transient expression of heterologous proteins in plants. Plant Biotechnology Journal **7:** 682-693

Sakamoto W (2006) Protein degradation machineries in plastids. *In* Annual Review of Plant Biology, Vol 57, pp 599-621

Salmon MA, Vanmelderen L, Bernard P, Couturier M (1994) The antidote and autoregulatory functions of the f-plasmid CCDa protein - a genetic and biochemical survey Molecular & General Genetics **244:** 530-538

Samol I, Shapiguzov A, Ingelsson B, Fucile G, Crevecoeur M, Vener AV, Rochaix JD, Goldschmidt-Clermont M (2012) Identification of a photosystem II phosphatase involved in light acclimation in Arabidopsis. Plant Cell **24:** 2596-2609

Santelia D, Koetting O, Seung D, Schubert M, Thalmann M, Bischof S, Meekins DA, Lutz A, Patron N, Gentry MS, Allain FHT, Zeeman SC (2011) The phosphoglucan phosphatase Like Sex Four2 dephosphorylates starch at the C3-position in Arabidopsis. Plant Cell **23:** 4096-4111

Scheidig A, Frohlich A, Schulze S, Lloyd JR, Kossmann J (2002) Downregulation of a chloroplast-targeted beta-amylase leads to a starch-excess phenotype in leaves. Plant Journal **30:** 581-591

Schimke RT, Doyle D (1970) Control of enzyme levels in animal tissues. Annual Review of Biochemistry **39:** 929-&

Schindler I, Renz A, Schmid FX, Beck E (2001) Activation of spinach pullulanase by reduction results in a decrease in the number of isomeric forms. Biochimica et Biophysica Acta-Protein Structure and Molecular Enzymology **1548:** 175-186

Schliebner I, Pribil M, Zuehlke J, Dietzmann A, Leister D (2008) A survey of chloroplast protein kinases and phosphatases in *Arabidopsis thaliana*. Current Genomics **9:** 184-190

Schneider A, Hausler RE, Kolukisaoglu U, Kunze R, van der Graaff E, Schwacke R, Catoni E, Desimone M, Flugge UI (2002) An *Arabidopsis thaliana* knock-out mutant of the chloroplast triose phosphate/phosphate translocator is severely compromised only when starch synthesis, but not starch mobilisation is abolished. Plant Journal **32:** 685-699

Schnyder H (1993) The role of carbohydrate storage and redistribution in the source-sink realtions of wheat and barley during grain filling. A review. New Phytologist **123:** 233-245

Schurmann P (2003) Redox signaling in the chloroplast: The ferredoxin/thioredoxin system. Antioxidants & Redox Signaling **5:** 69-78

Schwanhausser B, Busse D, Li N, Dittmar G, Schuchhardt J, Wolf J, Chen W, Selbach M (2011) Global quantification of mammalian gene expression control. Nature **473:** 337-342

Scopes RK (1994) Protein Purification, Principles and Practice, Third Ed. Springer-Verlag, New York

Scott P, Kruger NJ (1995) Influence of elevated fructose-2,6-bisphosphate levels on starch mobilization in transgenic tobacco leaves in the dark. Plant Physiology **108:** 1569-1577

Sehnke PC, Chung HJ, Wu K, Ferl RJ (2001) Regulation of starch accumulation by granule-associated plant 14-3-3 proteins. Proceedings of the National Academy of Sciences of the United States of America **98:** 765-770

Sehnke PC, Henry R, Cline K, Ferl RJ (2000) Interaction of a plant 14-3-3 protein with the signal peptide of a thylakoid-targeted chloroplast precursor protein and the presence of 14-3-3 isoforms in the chloroplast stroma. Plant Physiology **122:** 235-241

Servaites JC, Geiger DR, Tucci MA, Fondy BR (1989) Leaf carbon metabolism and metabolite levels during a period of sinusoidal light. Plant Physiology **89:** 403-408

Shalizi A, Bilimoria PM, Stegmueller J, Gaudilliere B, Yang Y, Shuai K, Bonni A (2007) PIASx is a MEF2 SUMO E3 ligase that promotes postsynaptic dendritic morphogenesis. Journal of Neuroscience **27:** 10037-10046

Shalizi A, Gaudilliere B, Yuan ZQ, Stegmuller J, Shirogane T, Ge QY, Tan Y, Schulman B, Harper JW, Bonni A (2006) A calcium-regulated MEF2 surnoylation switch controls postsynaptic differentiation. Science **311:** 1012-1017

Shapiro J, Machatti.L, Eron L, Ihler G, Ippen K, Beckwith J (1969) Isolation of pure Lac operon DNA. Nature **224:** 768-&

Sicher RC, Harris WG, Kremer DF, Chatterton NJ (1982) Effects of shortened day length upon translocation and starch accumulation by maize, wheat, and pangola grass leaves. Canadian Journal of Botany **60:** 1304-1309

Small JR, Kacser H (1993) Responses of metabolic systems to large changes in enzyme-activities and effectors .1. The linear treatment of unbranched chains. European Journal of Biochemistry **213:** 613-624

Smith AM (2012) Starch in the Arabidopsis plant. Starch-Starke **64:** 421-434

Smith AM, Stitt M (2007) Coordination of carbon supply and plant growth. Plant Cell and Environment **30:** 1126-1149

Smith SM, Fulton DC, Chia T, Thorneycroft D, Chapple A, Dunstan H, Hylton C, Zeeman SC, Smith AM (2004) Diurnal changes in the transcriptome encoding enzymes of starch metabolism provide evidence for both transcriptional and posttranscriptional regulation of starch metabolism in Arabidopsis leaves. Plant Physiology **136:** 2687-2699

Sokolov LN, Dominguez-Solis JR, Allary AL, Buchanan BB, Luan S (2006) A redox-regulated chloroplast protein phosphatase binds to starch diurnally and functions in its accumulation. Proceedings of the National Academy of Sciences of the United States of America **103:** 9732-9737

Sorimachi K, LeGalCoeffet MF, Williamson G, Archer DB, Williamson MP (1997) Solution structure of the granular starch binding domain of *Aspergillus niger* glucoamylase bound to beta-cyclodextrin. Structure **5:** 647-661

Southall SM, Simpson PJ, Gilbert HJ, Williamson G, Williamson MP (1999) The starch-binding domain from glucoamylase disrupts the structure of starch. FEBS Letters **447:** 58-60

Sparla F, Costa A, Lo Schiavo F, Pupillo P, Trost P (2006) Redox regulation of a novel plastid-targeted beta-amylase of Arabidopsis. Plant Physiology **141:** 840-850

Stettler M, Eicke S, Mettler T, Messerli G, Hortensteiner S, Zeeman SC (2009) Blocking the metabolism of starch breakdown products in Arabidopsis leaves triggers chloroplast degradation. Molecular Plant **2:** 1233-1246

Stitt M, Bulpin PV, ap Rees T (1978) Pathway of starch breakdown in photosynthetic tissues of *Pisum sativum*. Biochimica Et Biophysica Acta **544:** 200-214

Stitt M, Sulpice R, Keurentjes J (2010) Metabolic networks: how to identify key components in the regulation of metabolism and growth. Plant Physiology **152:** 428-444

Stitt M, Zeeman SC (2012) Starch turnover: pathways, regulation and role in growth. Current Opinion in Plant Biology **15:** 282-292

Streb S, Delatte T, Umhang M, Eicke S, Schorderet M, Reinhardt D, Zeeman SC (2008) Starch granule biosynthesis in Arabidopsis is abolished by removal of all debranching enzymes but restored by the subsequent removal of an endoamylase. Plant Cell **20:** 3448-3466

Streb S, Egli B, Eicke S, Zeeman SC (2009) The debate on the pathway of starch synthesis: a closer look at low-starch mutants lacking plastidial phosphoglucomutase supports the chloroplast-localized pathway. Plant Physiology **151:** 1769-1772

Szallasi Z, Stelling J, Periwal V (2006) System modeling in cellular biology: from concepts to nuts and bolts. MIT Press, Cambrideg, USA

Szydlowski N, Ragel P, Hennen-Bierwagen TA, Planchot V, Myers AM, Merida A, d'Hulst C, Wattebled F (2011) Integrated functions among multiple starch synthases determine both amylopectin chain length and branch linkage location in Arabidopsis leaf starch. Journal of Experimental Botany **62:** 4547-4559

Szydlowski N, Ragel P, Raynaud S, Lucas MM, Roldan I, Montero M, Munoz FJ, Ovecka M, Bahaji A, Planchot V, Pozueta-Romero J, D'Hulst C, Merida A

(2009) Starch granule initiation in Arabidopsis requires the presence of either Class IV or Class III starch synthases. Plant Cell **21:** 2443-2457

Tabata S, Hizukuri S, Nagata K (1978) Studies on starch phosphate 4. Action of sweet-potato beta-amylase on phosphodextrin of potato starch. Carbohydrate Research **67:** 189-195

Taira T, Uematsu M, Nakano Y, Morikawa T (1991) Molecular identification and comparison of the starch synthase bound to starch granules between endosperm and leaf blades in rice plants. Biochemical Genetics **29:** 301-311

Takaha T, Smith SM (1999) The functions of 4-alpha-glucanotransferases and their use for the production of cyclic glucans. *In* SE Harding, ed, Biotechnology and Genetic Engineering Reviews, Vol 16, pp 257-280

Takeda Y, Hizukuri S (1981) Studies on starch phosphate. Reexamination of the action of sweet-potato beta-amylase on phosphorylated (1,4)-alpha-D-glucan. Carbohydrate Research **89:** 174-178

Taniguchi M, Miyake H (2012) Redox-shuttling between chloroplast and cytosol: integration of intra-chloroplast and extra-chloroplast metabolism. Current Opinion in Plant Biology **15:** 252-260

Teh Y-HA, Kavanagh TA (2010) High-level expression of Camelid nanobodies in *Nicotiana benthamiana.* Transgenic Research **19:** 575-586

Terpe K (2003) Overview of tag protein fusions: from molecular and biochemical fundamentals to commercial systems. Applied Microbiology and Biotechnology **60:** 523-533

Tewari YB, Lang BE, Decker SR, Goldberg RN (2008) Thermodynamics of the hydrolysis reactions of 1,4-beta-D-xylobiose, 1,4-beta-D-xylotriose, D-cellobiose, and D-maltose. Journal of Chemical Thermodynamics **40:** 1517-1526

Thimm O, Bläsing O, Gibon Y, Nagel A, Meyer S, Kruger P, Selbig J, Muller LA, Rhee SY, Stitt M (2004) MAPMAN: a user-driven tool to display genomics data sets onto diagrams of metabolic pathways and other biological processes. Plant Journal **37:** 914-939

Thompson DB (2000) On the non-random nature of amylopectin branching. Carbohydrate Polymers **43:** 223-239

Thompson GA, Okuyama H (2000) Lipid-linked proteins of plants. Progress in Lipid Research **39:** 19-39

Tiessen A, Hendriks JHM, Stitt M, Branscheid A, Gibon Y, Farre EM, Geigenberger P (2002) Starch synthesis in potato tubers is regulated by post-translational redox modification of ADP-glucose pyrophosphorylase: A novel regulatory mechanism linking starch synthesis to the sucrose supply. Plant Cell **14:** 2191-2213

Tikkanen M, Grieco M, Aro EM (2011) Novel insights into plant light-harvesting complex II phosphorylation and 'state transitions'. Trends in Plant Science **16:** 126-131

Trethewey RN, ap Rees T (1994) A mutant of *Arabidopsis thaliana* lacking the ability to transport glucose across the chloroplast envelope. Biochemical Journal **301:** 449-454

Turck CW, Falick AM, Kowalak JA, Lane WS, Lilley KS, Phinney BS, Weintraub ST, Witkowska HE, Yates NA (2007) The association of biomolecular resource facilities proteomics research group 2006 study - relative protein quantitation. Molecular & Cellular Proteomics **6:** 1291-1298

Ulrich HD (2009) Regulating post-translational modifications of the eukaryotic replication clamp PCNA. DNA Repair **8:** 461-469

Usadel B, Blasing OE, Gibon Y, Retzlaff K, Hoehne M, Gunther M, Stitt M (2008) Global transcript levels respond to small changes of the carbon status during progressive exhaustion of carbohydrates in Arabidopsis rosettes. Plant Physiology **146:** 1834-1861

Utsumi Y, Nakamura Y (2006) Structural and enzymatic characterization of the isoamylase1 homo-oligomer and the isoamylase1-isoamylase2 hetero-oligomer from rice endosperm. Planta **225:** 75-87

Utsumi Y, Utsumi C, Sawada T, Fujita N, Nakamura Y (2011) Functional diversity of isoamylase oligomers: The ISA1 homo-oligomer is essential for amylopectin biosynthesis in rice endosperm. Plant Physiology **156:** 61-77

Valerio C, Costa A, Marri L, Issakidis-Bourguet E, Pupillo P, Trost P, Sparla F (2011) Thioredoxin-regulated beta-amylase (BAM1) triggers diurnal starch degradation in guard cells, and in mesophyll cells under osmotic stress. Journal of Experimental Botany **62:** 545-555

Van den Steen P, Rudd PM, Dwek RA, Opdenakker G (1998) Concepts and principles of O-linked glycosylation. Critical Reviews in Biochemistry and Molecular Biology **33:** 151-208

van der Leij FR, Visser RGF, Ponstein AS, Jacobsen E, Feenstra WJ (1991) Sequence of the structural gene for granule-bound starch synthase of potato (*Solanum tuberosum* L.) and evidence for a single point deletion in the *amf* allele. Molecular & General Genetics **228:** 240-248

Van Larebeke N, Zaenen I, Teuchy H, Schell J (1973) Circular DNA plasmids in *Agrobacterium* strains - Investigation of their role in induction of crown-gall tumors. Archives Internationales De Physiologie, De Biochimie Et De Biophysique **81:** 986-986

Vandesompele J, De Preter K, Pattyn F, Poppe B, Van Roy N, De Paepe A, Speleman F (2002) Accurate normalization of real-time quantitative RT-PCR data by geometric averaging of multiple internal control genes. Genome Biology **3:** 0034

Verdaguer D, Ojeda F (2002) Root starch storage and allocation patterns in seeder and resprouter seedlings of two Cape Erica (Ericaceae) species. American Journal of Botany **89:** 1189-1196

Verheesen P, Roussis A, de Haard HJ, Groot AJ, Stam JC, den Dunnen JT, Frants RR, Verkleij AJ, Verrips CT, van der Maarel SM (2006) Reliable and controllable antibody fragment selections from Camelid non-immune libraries for target validation. Biochimica et Biophysica Acta-Proteins and Proteomics **1764:** 1307-1319

Villarejo A, Buren S, Larsson S, Dejardin A, Monne M, Rudhe C, Karlsson J, Jansson S, Lerouge P, Rolland N, von Heijne G, Grebe M, Bako L, Samuelsson G (2005) Evidence for a protein transported through the secretory pathway en route to the higher plant chloroplast. Nature Cell Biology **7:** 1224-1231

Vogel C, Marcotte EM (2012) Insights into the regulation of protein abundance from proteomic and transcriptomic analyses. Nature Reviews Genetics **13:** 227-232

Voinnet O, Rivas S, Mestre P, Baulcombe D (2003) An enhanced transient expression system in plants based on suppression of gene silencing by the p19 protein of tomato bushy stunt virus. Plant Journal **33:** 949-956

Waigh TA, Kato KL, Donald AM, Gidley MJ, Clarke CJ, Riekel C (2000) Side-chain liquid-crystalline model for starch. Starch-Starke **52:** 450-460

Walhout AJM, Temple GF, Brasch MA, Hartley JL, Lorson MA, van den Heuvel S, Vidal M (2000) GATEWAY recombinational cloning: Application to the cloning of large numbers of open reading frames or ORFeomes. Applications of Chimeric Genes and Hybrid Proteins, Pt C **328:** 575-592

Walters RG, Ibrahim DG, Horton P, Kruger NJ (2004) A mutant of Arabidopsis lacking the triose-phosphate/phosphate translocator reveals metabolic regulation of starch breakdown in the light. Plant Physiology **135:** 891-906

Wang Q, Monroe J, Sjolund D (1995) Identification and characterization of a phloem-specific beta-amylase. Plant Physiology **109:** 743-750

Wang SJ, Yeh KW, Tsai CY (2001) Regulation of starch granule-bound starch synthase I gene expression by circadian clock and sucrose in the source tissue of sweet potato. Plant Science **161:** 635-644

Wattebled F, Dong Y, Dumez S, Delvalle D, Planchot R, Berbezy P, Vyas D, Colonna P, Chatterjee M, Ball S, D'Hulst C (2005) Mutants of Arabidopsis lacking a chloroplastic isoamylase accumulate phytoglycogen and an abnormal form of amylopectin. Plant Physiology **138:** 184-195

Wattebled F, Planchot V, Dong Y, Szydlowski N, Pontoire B, Devin A, Ball S, D'Hulst C (2008) Further evidence for the mandatory nature of polysaccharide debranching for the aggregation of semicrystalline starch and for overlapping functions of debranching enzymes in Arabidopsis leaves. Plant Physiology **148:** 1309-1323

Weber A, Servaites JC, Geiger DR, Kofler H, Hille D, Groner F, Hebbeker U, Flugge UI (2000) Identification, purification, and molecular cloning of a putative plastidic glucose translocator. Plant Cell **12:** 787-801

Weise SE, Aung K, Jarou ZJ, Mehrshahi P, Li Z, Hardy AC, Carr DJ, Sharkey TD (2012) Engineering starch accumulation by manipulation of phosphate metabolism of starch. Plant Biotechnology Journal **10:** 545-554

Weise SE, Schrader SM, Kleinbeck KR, Sharkey TD (2006) Carbon balance and circadian regulation of hydrolytic and phosphorolytic breakdown of transitory starch. Plant Physiology **141:** 879-886

Werdan K, Heldt HW, Milovancev M (1975) Role of pH in regulation of carbon fixation in chloroplast stroma - studies on CO_2 fixation in light and dark. Biochimica et Biophysica Acta **396:** 276-292

Werner TP, Amrhein N, Freimoser FM (2005) Novel method for the quantification of inorganic polyphosphate (iPoP) in *Saccharomyces cerevisiae* shows dependence of iPoP content on the growth phase. Archives of Microbiology **184:** 129-136

Wielopolska A, Townley H, Moore I, Waterhouse P, Helliwell C (2005) A high-throughput inducible RNAi vector for plants. Plant Biotechnology Journal **3:** 583-590

Wiese A, Christ MM, Virnich O, Schurr U, Walter A (2007) Spatio-temporal leaf growth patterns of *Arabidopsis thaliana* and evidence for sugar control of the diel leaf growth cycle. New Phytologist **174:** 752-761

Wildner M (1999) In memory of William of Occam. Lancet **354:** 2172-2172

Wischmann B, Blennow A, Madsen F, Jorgensen K, Poulsen P, Bandsholm O (2005) Functional characterisation of potato starch modified by specific in planta alteration of the amylopectin branching and phosphate substitution. Food Hydrocolloids **19:** 1016-1024

Wischmann B, Nielsen TH, Moller BL (1999) In vitro biosynthesis of phosphorylated starch in intact potato amyloplasts. Plant Physiology **119:** 455-462

Witt W, Sauter JJ (1996) Purification and characterization of alpha-amylase from poplar leaves. Phytochemistry **41:** 365-372

Yang ZJ, Midmore DJ (2005) A model for the circadian oscillations in expression and activity of nitrate reductase in higher plants. Annals of Botany **96:** 1019-1026

Yano R, Nakamura M, Yoneyama T, Nishida I (2005) Starch-related alpha-glucan/water dikinase is involved in the cold-induced development of freezing tolerance in arabidopsis. Plant Physiology **138:** 837-846

Yazdanbakhsh N, Fisahn J (2010) Analysis of *Arabidopsis thaliana* root growth kinetics with high temporal and spatial resolution. Annals of Botany **105:** 783-791

Yazdanbakhsh N, Sulpice R, Graf A, Stitt M, Fisahn J (2011) Circadian control of root elongation and C partitioning in *Arabidopsis thaliana*. Plant Cell and Environment **34:** 877-894

Yu TS, Kofler H, Hausler RE, Hille D, Flügge UI, Zeeman SC, Smith AM, Kossmann J, Lloyd J, Ritte G, Steup M, Lue WL, Chen JC, Weber A (2001) The Arabidopsis *sex1* mutant is defective in the R1 protein, a general regulator of starch degradation in plants, and not in the chloroplast hexose transporter. Plant Cell **13:** 1907-1918

Yu TS, Zeeman SC, Thorneycroft D, Fulton DC, Dunstan H, Lue WL, Hegemann B, Tung SY, Umemoto T, Chapple A, Tsai DL, Wang SM, Smith AM, Chen J, Smith SM (2005) Alpha-Amylase is not required for breakdown of transitory starch in Arabidopsis leaves. Journal of Biological Chemistry **280:** 9773-9779

Zeeman SC, Kossmann J, Smith AM (2010) Starch: its metabolism, evolution, and biotechnological modification in plants. *In* S Merchant, WR Briggs, D Ort, eds, Annual Review of Plant Biology, Vol 61, pp 209-234

Zeeman SC, Thorneycroft D, Schupp N, Chapple A, Weck M, Dunstan H, Haldimann P, Bechtold N, Smith AM, Smith SM (2004) Plastidial alpha-glucan phosphorylase is not required for starch degradation in Arabidopsis leaves but has a role in the tolerance of abiotic stress. Plant Physiology **135:** 849-858

Zeeman SC, Tiessen A, Pilling E, Kato KL, Donald AM, Smith AM (2002) Starch synthesis in Arabidopsis. Granule synthesis, composition, and structure. Plant Physiology **129:** 516-529

Zeeman SC, Umemoto T, Lue WL, Au-Yeung P, Martin C, Smith AM, Chen J (1998) A mutant of Arabidopsis lacking a chloroplastic isoamylase accumulates both starch and phytoglycogen. Plant Cell **10:** 1699-1711

Zhang XL, Szydlowski N, Delvalle D, D'Hulst C, James MG, Myers AM (2008) Overlapping functions of the starch synthases SSII and SSIII in amylopectin biosynthesis in Arabidopsis. BMC Plant Biology **8:** 96

Zhu AP, Romero R, Petty HR (2009) An enzymatic fluorimetric assay for glucose-6-phosphate: Application in an in vitro Warburg-like effect. Analytical Biochemistry **388:** 97-101